Title
Bioprocess Development for Production of Polyhydroxyalkanoates from Organic Feedstocks

Author
Wang, Ke

Publication Date
2022

Peer reviewed|Thesis/dissertation

Bioprocess Development for Production of Polyhydroxyalkanoates from Organic Feedstocks

By

KE WANG
DISSERTATION

Submitted in partial satisfaction of the requirements for the degree of

DOCTOR OF PHILOSOPHY

in

Biological Systems Engineering

in the

OFFICE OF GRADUATE STUDIES

of the

UNIVERSITY OF CALIFORNIA

DAVIS

Approved:

_____
Ruihong Zhang, Chair

_____
Bryan M. Jenkins

_____
Chris W. Simmons

Committee in Charge

2022

Abstract

Plastic products are important commodities on a global scale and have been used extensively in almost every aspect of human life. The massive production and use of conventional plastics have created major concerns, including the unsustainable use of fossil carbon feedstocks, the emissions of greenhouse gases in the manufacturing processes, and the disposal of most of the plastic waste and consequent impacts on the natural environment at the end of the lifecycle. As a response to these problems, there has been a global trend towards alternative bioplastic products that are more environmentally friendly than traditional ones. As one popular alternative, polyhydrolxyalkanoates (PHA) are a family of naturally occurring biodegradable plastic materials used as a replacement for the conventional plastics in various applications. Since PHA has similar thermal and mechanical properties to a broad spectrum of different types of conventional plastics, it has been widely used in many applications including packaging, food service, agriculture, medical supplies, consumer products, chemicals, and environmental services. PHA has an established market in recent decades, however, the current bottleneck for the market growth is its high production costs, which are commonly three to four times higher than other bioplastic and traditional plastic products of similar properties and use in the market. There is an urgent need to develop a bioprocessing system to produce PHA with high quality at low cost. Therefore, the goal of this study was to develop an integrated PHA production system utilizing inexpensive feedstocks including food waste and cheese byproducts, which provides high production efficiency and product quality, and low production cost.

Previous studies showed that *Haloferax mediterranei*, a wild-type extreme halophilic archaeon, can be a superior candidate as a microbial PHA producer than freshwater microbes, with regards to the utilization of waste or byproduct feedstocks for PHA production. It can provide robust production of Poly(3-hydroxybutyrate-co-3-hydroxyvalerate) (PHBV), a type of high-value PHA, from various renewable feedstocks. Meanwhile, its high salt tolerance enables natural resistance to contamination introduced by microbes in waste-derived streams, which can reduce the costs from sterilization or pasteurization normally incurred in commercial scale productions. In addition, it offers an easier approach for polymer extraction by salt-free (fresh) water, which consumes less energy and chemicals than current PHA production systems. Food waste and food processing byproducts (such as lactose) have good potentials as feedstocks for PHBV production by *H. mediterranei* because they are rich in sugars and short-chain carboxylates that can be metabolized to PHBV. Pre-treatment processes including anaerobic fermentation, enzymatic hydrolysis, and membrane filtration are required prior to release and to recover those nutrients from the complex macronutrients contained in the feedstocks. The culture of this strain essentially consists of saline medium, carbon source, nitrogen source, phosphorous source, and trace elements. Besides nutrient conditions, a successful cell cultivation process also requires suitable growth conditions including temperature, salinity, pH, and aeration rate.

With the aim of utilizing food waste as low-cost feedstock to produce poly(3-hydroxybutyrate-co-3-hydroxyvalerate) (PHBV) by *Haloferax mediterranei*, the effects of acetate (Ac), propionate (Pr), butyrate (Bu), and the short-chain carboxylates derived from food waste were examined on the microbial growth and PHBV production. Results showed that a mixture of carboxylates yielded a 55% more PHBV than glucose. The food-waste-derived nutrients achieved

yields of 0.41 to 0.54 g PHBV/g Ac from initial loadings of 450 mg/L to 1800 mg/L Ac of total carboxylates. The consumption of individual carboxylate varied among the different compositions of the carbon source.

Based on previous findings, this study further tested the feasibility of using real-world feedstocks which contain different sugars and VFAs as the main carbon sources for PHBV production by the microbes. Four different types of feedstocks including food waste hydrolysate, food waste fermentate, whey sugar (lactose), and delactosed permeate were collected, pretreated with different processes, and utilized as the sole substrate to culture *H. mediterranei*. Before microbial cultivation, food waste hydrolysate and fermentate were processed through microfiltration for the recovery of nutrients and removal of suspended particles. The two cheese processing byproduct streams were subjected to enzymatic hydrolysis to convert lactose into monosaccharides. After pretreatment, each substrate was loaded with two sCOD loadings of 22.5 g/L and 45 g/L to culture *H. mediterranei* and the effects of substrate type and loading on PHBV production were studied. The results show that with the same substrate loading, the substrate derived from food waste fermentate gave higher final cell mass and PHBV concentrations than food waste hydrolysate; and 45 g/L sCOD resulted in the highest PHBV production (3.92 ± 0.08 g/L) within the same culturing time. Comparing substrates derived from whey sugar and delactosed permeate, with 45 g/L sCOD loading, cells grew much faster in whey sugar hydrolysate. Food waste fermentate resulted in higher HV contents than food waste hydrolysate; and substrate loading influenced the HV content of PHBV derived from delactosed permeate, which may be due to the prolonged growth time.

Since food waste fermentate was proven to be one of the better candidates among the four real-world inexpensive feedstocks, more research was conducted to develop an integrated PHBV production system utilizing fermented food waste from commercial anaerobic digesters as feedstock. The effects of feedstock type, substrate loading, and aeration rate were studied and the optimum levels (FWP 1, 40 g/L sCOD, and 2.5 vvm) was determined to yield the highest productions of cell mass and PHBV. A 6-L benchtop bioreactor system has been designed, constructed, and operated to demonstrate the integrated PHA production system from food waste. Through dynamic monitoring of this bioreactor system, the dissolved oxygen level of cell broth was found to drop dramatically to below 20% sat. during the exponential growth phase with a fixed aeration rate. A strategy of maintaining a higher DO level above 50% sat. resulted in faster cell growth but led to lower final cell densities, final PHBV concentration and yield. A novel approach was developed to recycle and reuse the spent salts within the system, should reduce the costs of purchasing raw materials and wastewater treatment and disposal. The spent saline medium (SSM), after the treatment by H_2O_2 and concentrated to a brine solution through rotary evaporation, was successfully reused through four consecutive batches, where both 80% and 90% SSM recycling strategies yielded comparable cell growth and PHA production to the original batch. The PHA production system developed in this study has the potential for practical applications in the current bioplastic industry. The additional revenue from PHA production can help promote the circular economy for the current food system, increase the market share of bioplastics, and create incentives for better practice of organic waste management in general.

In addition to food waste, the study has also developed an integrated PHA production system with utilizing whey sugar from commercial cheese making facilities as feedstock. Through the

dynamic monitoring in a 6-L benchtop bioreactor system, different aeration strategies led to similar results as food waste that with a higher DO level above 50% saturation resulting in faster cell growth, and higher consumption of galactose, but lower final cell densities and PHBV production. The direct reuse of spent saline medium (SSM) was also successfully achieved through four consecutive batches with various substrate loadings, where both 80% and 90% SSM recycling strategies yielded comparable cell growth, PHBV production and PHBV profile to the original batch. This novel PHA production system has the potential of practical applications in the current bioplastic industry; meanwhile, through utilizing whey byproducts and waste streams, an additional revenue can be provided to the dairy industry.

Based on the system design developed here, economic feasibility assessments were conducted to project integrated industrial scale processing. Byproduct streams from a local cheese plant, with an input of 168.7 metric ton/day (MT/day) lactose (186 US ton/day), were used as the feedstock. SuperPro® Designer (Intelligen Inc., USA) was used as the software for the process design and economic modeling. Three scenarios with different processes for the treatments of used enzyme and spent medium were investigated and the major factors that influence the overall economics were identified. The simulated system produces 9700 MT/year PHBV with an assumed PHA yield of 0.2 g PHBV/g lactose and an overall process efficiency of 87%. The breakeven price was found to be more sensitive to the lactose price than enzyme price. The scenario with enzyme reuse and spent medium recycling achieved the lowest breakeven price among the scenarios, which can be less than 4 $/kg PHA based on a delactosed permeate (DLP) unit price of 0.1 $/kg. The study suggests utilizing dairy derived feedstocks has the potential to make PHA competitive in the bioplastic market, which could be beneficial to both the dairy and bioplastic industries.

To

My parents,

Ping-lan Wang and Xiao-tian Wang

And my husband,

Chang Chen

Who support me all the way with their endless encouragement and love

Acknowledgement

First and foremost, I would like to express my most sincere gratitude to my major professor and mentor, Professor Ruihong Zhang, for her wise guidance, generous support and patience during my graduate studies at University of California, Davis. She is my real-life model and has been motivating me to be an innovative thinker, to pursue academic excellence, and to work conscientiously. This dissertation could have not reached to its present form without her consistent encouragement, mentoring and help. I am forever grateful to her invaluable inspiration, mentoring, and care throughout these years.

I would also like to give my sincere gratitude to Professor Bryan M. Jenkins and Professor Chris W. Simmons for serving in my dissertation committee and providing wise guidance to my research. I am more than grateful for their patience and constructive advice during my consultations.

I am also extremely thankful to Professor Jennifer Mullin, Professor Nitin Nitin, and Professor Chris W. Simmons, who have generously offered me the opportunities to gain teaching experience and professional capabilities that are integral to a scientist and engineer. My sincere thanks go to Professor Bryan M. Jenkins, Professor David C. Slaughter, Professor Jennifer Mullin, Professor Chris W. Simmons, and Professor Alissa Kendall who served in my qualifying exam committee.

The experimental work would not have been possible without the help from several colleagues and staff in the Biological and Agricultural Engineering Department: Dr. Hossein Edalati, Dr. Jesus Dionisio Fernandez-Bayo, Professor Tyler Barzee, Dr. Yike Chen, Dr. Cody Yothers,

Professor Hamed El-mashad, Professor Zhongli Pan, Professor Julia Fan, Matthew (Pierce) Mahaffey, Professor Chang Chen, Dr. Shu Cai, Dr. Irving Rabasa, Dr. Xingzhu Wu, Dr. Yi Shen, Weiyi Tao, Dr. Yuting Tang, Alex Hobby, Kameron Chun, Victor, Duraj, Jed Roach, Andy Cobb, and Tom Bell, thank you so much for all your help and invaluable advice in all aspects of my work. My special thanks to Dr. De Wood and Tina Williams from USDA ARS for the technical support on TEM imaging technology. I would also like to thank Professor Xiuzhi (Susan) Sun and Dr. Yizhou Chen from Bio-Materials and Technology Lab in Kansas State University for their help and support on material property analysis.

My dearest thanks also go to all my friends at UC Davis: Xiaoge (Nickie) Liu, Lin Cao, Zhaokun Ning, Allan Chio, Ruoyi (Roy) Liang, Zhi-yu Zhu-ge, Berta Lascuevas Laguna, Alexander Olenskjy, Vivian Voung, Kasey Holbert, Lucia Felix, Clay Swackhamer, Han Zhang, Karry Liang, Yi Wang, Sophie Xu, Josh Peppers, Becky Peppers, Guilerme De Moura Araujo, Alice Dien, Wenlong Cao and Mianfeng Zhang, many thanks to you all for making my life fulfilling, enjoyable, and memorable.

Last but not least, I am extremely grateful and thankful to my husband, Chang Chen, for his constant love, care, and being always by my side. My gratitude also goes to my family, particularly to my parents Ping-lan Wang and Xiao-tian Wang for always being a wise and cool parent and for all the opportunities and unconditional love and support they have given me.

Table of Contents

List of Figures

List of Tables

Chapter 1. Introduction

1.1 Plastic waste as a global issue

As important commodities on a global scale, plastic products are used in almost every aspect of human life. The global plastic production is estimated to be 370 million metric tons (MT) per year, of which 99% are derived from fossil carbon feedstocks (European Bioplastics, 2018). The greenhouse gas (GHG) emissions associated with the manufacturing processes are up to 3 kg CO_2 eq/kg resin produced (Criddle and Frank, 2014), which also contribute to the unsustainability of the petroleum-based plastics. Petroleum-derived plastics are frequently used in food service such as packaging materials for fresh produce, disposable plastic utensils, plastic straws, and beverage bottles. Due to the relatively short shelf life of food, these plastic materials are commonly disposed within a short period of time; however, it can take up to several hundred years to fully decompose these plastic wastes due to their recalcitrance. Around 275 million tons of global plastic wastes are generated annually, of which up to 55% end up in landfills (Geyer et al., 2017). U.S. landfills received 26 million tons of plastics wastes annually, which account for 19% of all landfilled wastes (US EPA, 2019). These persistent plastic debris occupy land, litter oceans and endanger aquatic creatures. The microplastic molecules in water bodies also damage the quality of drinking water and have become a threat to water and food safety. The plastic types commonly found in the natural environment, including but not limited to polyethylene (PE), polypropylene (PP), polyvinyl chloride (PVC), and polycarbonate (PC), are reported to cause severe impacts on human health such as skin diseases, genetic changes, reproductive defects, and cancers (Ilyas et al., 2018). Due to these problems, there has been a global trend towards alternative plastics that are bioderived (from sustainable biological sources rather than petroleum based) and/or biodegradable (will decompose in a short amount of time) (European Bioplastics, 2018). The shift towards bioplastic

production can reduce the use of fossil carbon resources and GHG emissions in manufacturing processes, and become organic compost at disposal.

1.2 Polyhydroxyalkanoates (PHA) as a biodegradable alternative

1.2.1 Definition and categories

There are many research interests and industrial activities on the production of biodegradable plastics as alternatives to conventional petroleum-derived plastics. As a popular alternative, polyhydroxyalkanoates (PHA) is a family of naturally occurring polyesters that can be used as biomaterials in replacement of traditional plastics. PHA has similar properties to conventional thermoplastics and is one of the major materials used for the manufacturing of biodegradable plastics (Reddy et al., 2003). One type of PHA, Poly(3-hydroxybutyrate-co-3-hydroxyvalerate) which is also known as PHBV, in particular can be used as a replacement for high-density polyethylene (HDPE) (Reddy et al., 2003). PHA products can be degraded biologically in the natural environment such as soil and ocean within short periods of time, e.g. 6 months (Queiroz and Collares-Queiroz, 2009). As shown in Figure 1.1, PHA is commonly synthesized and accumulated by certain groups of microbes as intracellular carbon and energy reserves under certain growth stress e.g. limitations on nitrogen or phosphorous nutrients (Anjum et al., 2016). In terms of the chemical structure, PHA is a group of linear head-to-tail polyesters of 3-hydroxy fatty acids, with each monomer connected with ester bonds in between. There are commonly 10^3 to 10^4 monomers in a polyester chain, depending on the specific type of PHA. Based on the number of carbon atoms in the monomers, PHA has been classified into two categories: short-chain-length PHA (SCL PHA) if the number of carbon atoms is no more than 5; and medium-chain-length PHA

(MCL PHA) if the number of carbon atoms is more than 5. The SCL PHA has similar properties to conventional thermoplastics; and the MCL PHA has properties close to rubbers (REHM, 2003).

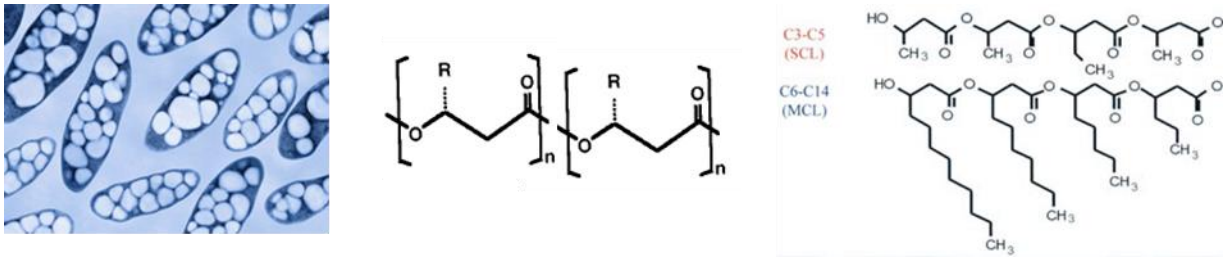

Figure 1. 1 (from left to right) PHA granules (white spheres) within cells; PHA structure; two PHA categories by chain length (Anjum et al., 2016; REHM, 2003)

1.2.2 PHA market and applications

The production of PHA by microbial fermentation has been commercialized since the early 1990s (Chen, 2009). The current applications of PHA are mainly in the fields of packaging, food service, agriculture, medical service, consumer products, chemicals, and environmental service (Cambridge Consultants, 2018). Figure 1.2 shows some common examples of PHA products used for food service, environmental service, and other consumer products. As illustrated in Figure 1.3, the PHA market currently accounts for 1.7 % of global bioplastic market. Given that 58.1% of bioplastic market is from biodegradable plastic products, PHA accounts for around 3.0% of global biodegradable plastic market (European Bioplastics, 2020). The global PHA market size was around $ 72 million in 2020, and is expected to reach $ 121 million by 2025 (Aeschelmann and Carus, 2015). Table 1.1 lists the current PHA manufacturers worldwide with different production scales with up to 50,000 tons/year production (Cambridge Consultants, 2018; Kourmentza et al., 2017).

Figure 1. 2 Various types of PHA products including (from top to bottom) resins, bags, utensils, textile materials and filaments, and food containers (Bluepha, 2019)

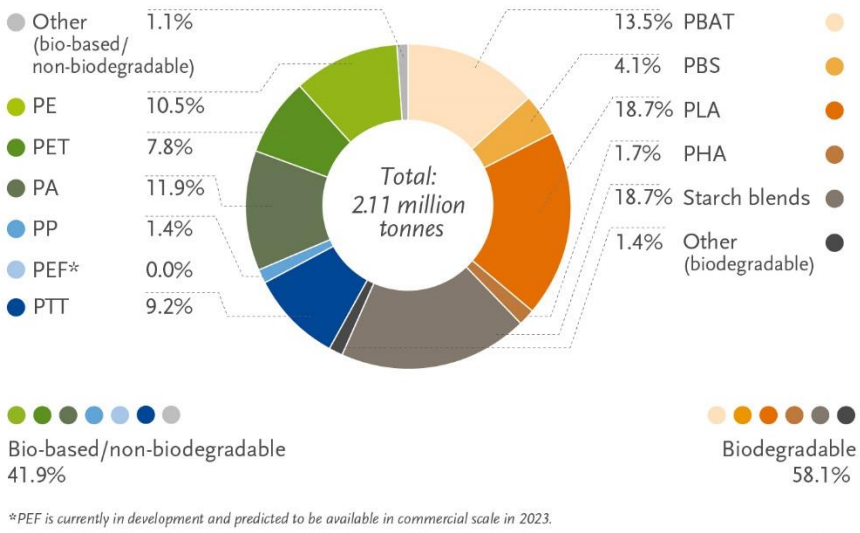

Figure 1. 3 Global bioplastic production capacities 2020 (European Bioplastics, 2020)

Table 1. 1 Pilot and industrial scale PHA manufacturers worldwide modified based on Cambridge Consultants (2018)

Company	Country	Product (Trademark)	Feedstock	Capacity (tons/year)
Genecis Bioindustries Inc	Canada	PHBV	Food waste	3-4
Full Cycle Bioplastics	USA	PHBV	Food waste	Research
Biomatera	Canada	PHA (Biomatera)	Sugar (sucrose)	N/A
Biomer	Germany	PHB (Biomer®)	Sugar beets	N/A
Bio-On Srl.	Italy	PHB, PHBV (minerv®-PHA)	N/A	10,000
Bluepha	China	PHBVHHx, PHV, P3HP3HB, P3HP4HB, P3HP, P4HB	Crops, kitchen waste	N/A
Danimer Scientific	USA	PHA (Nodax® PHA)	Cold pressed canola oil	N/A
Kaneka Corporation	Japan	PHBHHx (AONILEX®)	Plant oils	3500
Newlight Technologies LLC	USA	PHA (AirCarbonTM)	Methane	N/A
PHB Industrial S.A.	Brazil	PHB, PHBV (BIOCYCLE®)	Saccharose	3000
PolyFerm	Canada	PHA (VersaMerTM PHA)	Sugars, vegetable oils	N/A
Shenzhen Ecomann Biotechnology Co. Ltd.	China	PHA (AmBio®)	Sugars	5000
SIRIM Bioplastics	Malaysia	PHA	Palm oil mill effluent	2000
Tepha	USA	P3HB, P3HB4HB, P4HB, PHBV, PHOHH (**T**ephaFLEX®)	N/A	Pilot
TianAn Biologic Materials Co. Ltd.	China	PHB, PHBV (ENMATTM)	Dextrose, corn of cassava	50,000
Tianjin GreenBio Material Co.	China	PHB (Sogreen®)	Sugars	10,000

1.2.3 The current challenge

High production costs limit PHA applications and marketability. The production cost of PHA is around $5.8/kg (Leong et al., 2017); and the production costs are $2/kg for polylactic acid (PLA), the most non-blended bioplastic produced, and $1.1/kg for HDPE (European Bioplastics, 2018, Roland-Holst, 2013). Since PHA and PLA have similar properties, PHA could be used as a replacement in some PLA applications if it were to become cost competitive. Compared to PLA, PHA has more versatile properties with broader ranges of thermoplastic properties including operating temperatures, elasticity, and brittleness, etc. Therefore, PHA could potentially be used in more applications than PLA including high temperature drink cups, drug carriers, and medical materials. Additionally, PHA can decompose in ambient environments including the ocean, while PLA can only break down in industrial composting facilities (Auras et al., 2011; Lingle, 2018). The current feedstocks of PHA production are mainly renewable, e.g. sugars, starch and plant-based oils etc. A recent study reports that the feedstock cost accounts for over 40% of the annual operating cost of PHA production (Leong et al., 2017). Therefore, there is an emerging need to reduce the production cost of PHA through using inexpensive feedstocks, so the PHA products can be more competitive in the plastic market. To address the need, there are many research interests in the utilization of inexpensive carbon sources and organic waste as feedstocks for PHA production in the recent decades.

1.2.4 Inexpensive feedstocks

1.2.4.a Food waste

Food waste is a potential feedstock for PHA production because of its abundancy and high organic content. Excessive food waste has become a global issue. In the US 40% of food produced

ends up uneaten. Food loss occurs in every step of food supply chain, including production, postharvest processing, handling and storage, processing and packaging, retail and consumer levels (Gunders, 2012). Three major categories of the consumer-level food loss in the U.S. are grain (28%), meat (32%), vegetables and fruits (40%) (Buzby et al., 2011). At present, there are 6 million MT of food waste generated annually in California, which accounts for 18% of landfill disposal. The landfilled organic wastes, especially food waste, emit methane gas to the atmosphere, which may cause severe climate consequences. California law (as developed through Senate Bill (SB) 1383 (Senate Bill No. 1383, 2016) targets a 75% reduction of organic waste portion in landfills by 2025 (CalRecycle, 2018). Utilization of food waste for PHA production would promote this goal. Various kinds of waste feedstocks have been researched for PHA synthesis (Reddy et al., 2003). However, major concerns such as low PHA yield and high operating cost are limiting commercial applications. If food waste is utilized as an inexpensive feedstock, it is desirable to obtain high PHA production yield with relatively low operating costs in fermentation and downstream processes.

1.2.4.b Cheese processing byproducts

Besides food waste, food processing byproducts which are currently sold at low prices can also be used as inexpensive feedstocks for PHA production. Whey sugar and delactosed permeate (DLP) are byproduct streams derived from cheese, whey, and lactose manufacturing processes. Whey permeate is the side stream from the separation and concentration of whey protein. Lactose powder is produced from crystalizing the sugars from whey permeate, leaving behind DLP after the recovery of lactose crystals (Oliveira et al., 2019). These byproduct streams are produced in large quantities from cheese-making facilities and contain rich nutrients including sugars, proteins,

amino acids, minerals, and micronutrients. However, whey permeate and DLP are currently sold as low value products including animal feed and, fertilizers, or field spread (Durham, 2009). Converting cheese processing byproducts to PHA can potentially create an additional revenue for dairy processors, while also reducing production costs for PHA, making it more competitive in the bioplastic market. Large cheese manufacturing sites such as Hilmar Cheese Co. (Hilmar, CA) could produce over half the current worldwide PHA capacity of 30,000 MT/year from the lactose contained in DLP and over double of the current worldwide production of PHA from whey permeate. Therefore, utilizing low-value lactose from large dairy manufacturing sites may be a scalable solution for producing PHA. If lactose were taken out of the market for PHA production, it would also increase the value for lactose.

1.2.5 Halophilic PHA producers

Halophiles are a unique class of microbes capable of producing high quality PHA from waste feedstocks. *Haloferax mediterranei* is a well-studied halophile and best PHA producer so far (Kourmentza et al., 2017). It grows and synthesizes the high-value copolymer PHBV in extreme saline aqueous environment with up to 20% total salts. The high salinity facilitates microbial growth in nonsterile environments. This property is promising in terms of reducing costs of pasteurization in commercial production. An additional advantage is that the microbial cells can be lysed by osmotic shock through transfer to salt-free water, which benefits the extraction of PHA polymers. This extraction process may require less energy and chemicals than current production systems (Ghosh et al., 2019).

1.3 Research goal

The goal of this study was to develop efficient and economic systems for the production of PHA using food waste and cheese processing byproducts as inexpensive feedstocks. The main processes addressed in this study are (Figure 1.4): 1) a pre-treatment step where food waste and cheese processing byproducts are converted into nutrients that are ready to use for cell growth and PHA synthesis, and 2) cell cultivation where halophilic microorganisms grow and produce PHA. Saline water recycling is also considered to minimize salt discharge. Compared to conventional processes of PHA production, the proposed system utilizes food waste and cheese byproducts as less costly carbon feedstocks and does not require energy-intensive processes including pasteurization and thermochemical extraction. This research addresses critical issues including reduction of food and plastic wastes, value-added processing of food byproducts, and improved sustainability of food and materials supply chains.

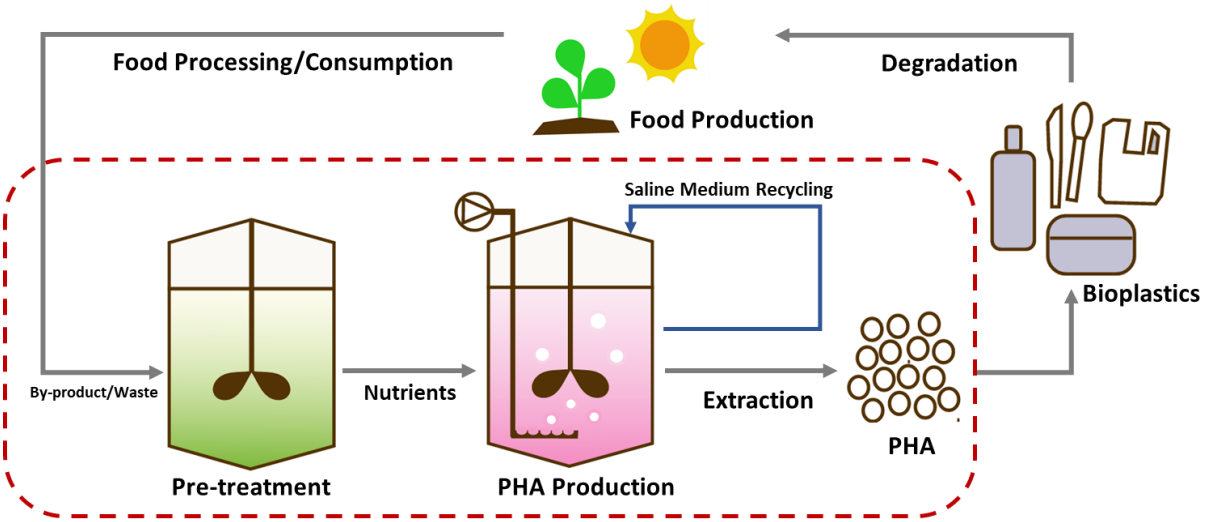

Figure 1. 4 Integrated system of PHA production from inexpensive feedstocks

Chapter 2. Literature Review

2.1 Pre-treatment methods of feedstocks

In most times, the feedstocks from food waste and food processing byproduct streams cannot be utilized directly by *H. mediterranei* for cell growth. In those cases, the macromolecules consisting of insoluble carbohydrates, protein, fat, and other organic particles need to be broken down into smaller molecules, such as monosaccharides, short-chain carboxylates, amino acids, and ammonium, that are the nutrients that can be directly consumed by the microbes. Therefore, the pre-treatment approaches for these feedstocks are important in terms of obtaining the maximum amounts of viable nutrients. This study mainly focuses on two biological pre-treatment methods, anaerobic fermentation, enzymatic hydrolysis, and on nutrient recovery through membrane filtration, as discussed below.

2.1.1 Anaerobic fermentation

Short-chain carboxylates can be produced from food waste and other types of organic waste by anaerobic fermentation. Anaerobic fermentation is a complex system of biochemical reactions where organic macromolecules are converted into soluble nutrients and gases by a mixed consortium of microorganisms under anaerobic conditions. Two major steps are involved: the hydrolysis step where complex organic polymers are broken down to smaller molecules by extracellular enzymes of microbes; and the fermentation step where the reduced compounds are further converted to short-chain carboxylates and other products e.g. ammonium, alcohols, gases of CO_2 and H_2 by the fermentative bacteria (Li et al., 2011). The production outcomes of carboxylates vary between studies; a review reports that the carboxylate yields from organics are between 0.1 and 0.6 g total carboxylate/g COD fed (Arslan et al., 2016). For anaerobic

fermentation in batch systems, the production of carboxylates is influenced by key parameters e.g. substrate, inoculum, pH, temperature, volatile solids (VS) loading, etc. (Lee et al., 2014).

As one of the most important factors, pH influences both hydrolysis and fermentation. A general pattern from literature is that a pH 5 to 6 is optimal for acidogenesis together with hydrolysis (Aehle, 2007). Depending on substrate types, a pH 6 can be optimal for hydrolysis of carbohydrate-rich substrates (Parawira et al., 2005) and carboxylate production from food waste (Jiang et al., 2013); for municipal biowaste, the first order hydrolysis rate constant increases as pH rises from 5 to 7 (Veeken Adrie et al., 2000). A pH below 5 drives carboxylates towards the undissociated forms, which could damage stability of microbial acidogens (Warnecke and Gill, 2005); but it may result in more lactate production because lactic acid bacteria are acid tolerant.

The VS loading is another key factor for carboxylate production. A general principle is that higher VS loadings can give higher concentrations of carboxylates, but concentrations start to level off when the feed loading is above 40 g COD/L (Arslan et al., 2016). By increasing the substrate loading, more organics can be converted to products per unit of reactor working volume, thereby beneficial to reactor economics. However, the overloading of feedstocks may reduce the yield of carboxylates due to substrate inhibition or product toxicity (Arslan et al., 2016). Overloading may also cause unstable operation due to the viscous broth (Lim et al., 2008), e.g. oxygen transfer limitation. Therefore, the pH and VS loading need to be regulated for the optimum carboxylates production of anaerobic fermentation.

2.1.2 Enzymatic hydrolysis

In addition to anaerobic fermentation, another efficient approach to pre-treat feedstocks is enzymatic hydrolysis, which has become a popular method that is used in many applications, such as the production of lactose-free dairy products (Wolf et al., 2018) and bioethanol production from food waste (Moon et al., 2009). Enzymatic hydrolysis is a biochemical process whereby enzymes facilitate the cleavage of the chemical bonds of the parent molecules. Compared to chemical hydrolysis with the aid from strong acids or bases, enzymatic hydrolysis has advantages such as less requirement of inputs of corrosive chemicals, high temperatures and pressures; and less concerns on sugar degradation or generation of toxic compounds (Chaudhary et al., 2012). For the hydrolysis of milk and dairy whey streams, several process parameters including enzyme loading, temperature, and reaction time are essential to the extent of lactose hydrolysis (Dutra Rosolen et al., 2015). Besides, given the complexity of food waste feedstocks, it is necessary to use a mixture of different types of enzymes to decompose various compounds e.g. polysaccharides, proteins, etc. Therefore, several parameters including enzyme type, loading, temperature, and reaction time should be controlled and optimized to achieve the maximum hydrolysis for different types of substrates.

2.1.3 Nutrient recovery through membrane filtration

At the end of pre-treatment processes, the broth becomes rich in sugars, carboxylates and other soluble nutrients which are mixed with residual suspended solids. These solids should be removed from the liquid to prevent any undesired particles introduced to the PHA production system. The majority of the solids naturally precipitate at the reactor bottom so that the upper liquid can be easily recovered by decanting. A secondary filtration step is needed to remove suspended solids and obtain a particle-free solution. Membrane separation is selected for its high efficiency to retain

all soluble nutrients and reject suspended particles from aqueous solution. The membrane filtration process has mainly four types based on the pore sizes (in the order of large to small): microfiltration, 4 to 0.2 microns; ultrafiltration, 0.2 to 0.02 microns; nanofiltration, less than 0.02 microns; and reverse osmosis (RO), less than 0.002 microns (Wagner, 2001). Either micro- or ultra-filtration processes are capable of rejecting suspended particles and insoluble macromolecules, therefore, they are considered as the main processes used for nutrient recovery in this study.

Flux, recovery and rejection are essential indicators of the performance of a membrane filtration process. The permeate flux and solute rejection increase linearly with an increasing feed pressure; a higher feed solute concentration increases osmotic pressure across the membrane and reduces solute rejection (Baker, 2000; Greenlee et al., 2009; Kucera, 2011; Lonsdale et al., 1965). The water flux increases with a rise in temperature; but the solute rejection may decrease due to the more rapid effect of temperature on solute transport (Baker, 2000). Membrane filtration processes have been utilized to recover carboxylates from anaerobic fermentation broth, e.g. up to 95.5% of carboxylates can be retained from anaerobic fermentation broth of kitchen waste (Diltz et al., 2007). The rejection of one species is improved by mixing with other carboxylates (Laufenberg et al., 1996). Different influent pH would result in different concentrations of ionized forms, which influences the extent of their repulsion or attraction at the membrane-solution interphase (Matsuura and Sourirajan, 1973). The rejection of acetate by a membrane material with negatively charged chemical groups increases significantly as pH increases (Ozaki and Li, 2002). Therefore, to efficiently recover soluble nutrients from fermentation liquid, the membrane type, applied pressure and influent pH need to be carefully regulated.

2.2 PHBV and its microbial producer *Haloferax mediterranei*

PHA is a family of head-to-tail linear polyesters of 3-hydroxy fatty acids with typically 1,000 to 10,000 monomers (Suriyamongkol et al., 2007). They are normally synthesized intracellularly by microorganisms including gram-positive and gram-negative bacteria and archaea. PHA in vivo is present as mobile amorphous inclusions (Sudesh et al., 2000). The scarcity of essential growth nutrients, such as deficiency of nitrogen or phosphorous sources, under harsh growth environmental conditions is a typical cause that stimulates microbes to convert excessive carbon source to PHA, and store the polymers in the cytoplasm as carbon and energy reserves (Ganesh Saratale et al., 2021). The halophilic archaeon *H. mediterranei*, however, can synthesize and accumulate PHA under normal growth conditions (Wang and Zhang, 2021). The strain is known for its generation of poly(3-hydroxubutyrate-co-3-hydroxyvalerate) (PHBV), a co-polymer which consists of (R)-3HB and (R)-3HV monomers (Figure 2.1).

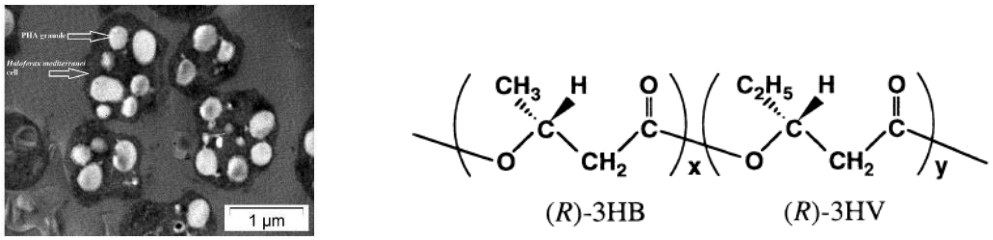

Figure 2. 1 (left) PHBV inclusions in *H. mediterranei* (Bhattacharyya et al., 2015); (right) chemical formula of the copolymer PHBV (Sudesh et al., 2000)

Haloferax mediterranei (ATCC 33500) is an extreme halophilic archaeon that lives in high saline environment (up to 25% w/v of total salts). It is a wild-type strain, which was first isolated

from a seawater evaporation pond near Alicante, Spain. The colonies of this strain have unique light pink color due to the intrinsic pigment from C50 carotenoids (Giani et al., 2021). It can produce and accumulate PHBV polymers intracellularly as carbon and energy stocks along with its cell growth. *H. mediterranei* has been studied for its potential of PHBV production from waste-derived feedstocks. Its high salt tolerance enables natural resistance to contamination introduced by microbes in waste-derived streams. This property is promising in terms of reducing costs from sterilization or pasteurization when waste-derived feedstocks are utilized in commercial production. As an additional advantage of high salt tolerance, the cells can be lysed due to osmotic shock in salt-free water, which facilitates extraction of PHBV polymers. This extraction process consumes less energy and chemicals than current PHA production systems.

2.3 Feedstocks from food waste and food processing byproducts

The property of intrinsic resistance to contamination enables this strain to grow and produce PHBV from nonsterile waste-derived feedstocks. A review of previous research, listed in Table 2.1, suggests the capability of *H. mediterranei* consuming sugar feedstocks derived from food processing byproducts or waste for PHBV production. It generates up to 48.6 wt.% of PHBV when fed with glucose (Don et al., 2006); it can utilize other substrates, such as extruded rice bran and corn starch (Huang et al., 2006), hydrolyzed whey (Koller et al., 2007), high-salinity cheese whey hydrolysate (Pais et al., 2016). VFA-rich wastewater has also been utilized to culture the strain for PHBV production (Alsafadi and Al-Mashaqbeh, 2017). Furthermore, *H. mediterranei* prefers utilizing inorganic nitrogen sources over organic ones (Cui et al., 2017). In light of these, nutrient sources derived from food waste or food processing byproducts can be a suitable feedstock to grow this strain due to the abundant content of sugars and carboxylates as carbon sources and inorganic

and organic nitrogen sources. And further research will add to the understanding of how *H. mediterranei* can metabolize nutrients from food waste or byproduct streams for microbial growth and PHBV production.

Table 2. 1 PHA yield from different feedstocks in literature

Reference	**Cultivation**		**CDM**		**PHA**		
	Substrate (S)	**Reactor**	**g/L**	**g/g S**	**g/L**	**g/g S**	**% CDM**
Alsafadi and Al-Mashaqbeh (2017)	Olive mill wastewater	Batch	10	-	0.2	-	43
Ferre-Guell and Winterburn (2018)	Synthetic short chain fatty acids	Batch, fed-batch	6	0.36 (mol %)	1.2	0.11 (mol %)	19.9
Koller et al. (2007)	Whey sugars	Batch	16.8	0.4	12.2	0.29	72.8
	Whey sugars	Batch	16.8	0.23	14.7	0.2	87.5
Han et al. (2015)	Glucose, valerate	Fed-batch	13.3	-	5.4	-	41
Pais et al. (2016)	Cheese whey hydrolysate	Batch	7.54	0.74	7.92	0.78	53
Lillo and Rodriguez-Valera (1990)	Glucose	Batch	-	-	4.16	0.21	-
	Starch		-	-	6.48	0.324	-
Huang et al. (2006)	Extruded corn starch, rice bran, yeast extract	Fed-batch	140	-	77.8	-	55.6
Cui et al. (2017)	Glucose	Batch	16	1.6	8.6	0.861	36

Waste-derived nutrients are valuable but risky to utilize because of the possible contamination and/or inhibition effects on PHA-producing microbes. Alsafadi and Al-Mashaqbeh (2017) found that up to 25% of olive mill wastewater showed no inhibitory effect on the growth of *H. mediterranei*; in comparison, another PHA-producing strain, *Cupriavidus necator*, cannot survive with the existence of 5% waste stream. *H. mediterranei* can also utilize waste-derived sugar and starch feedstocks, as previous discussed. However, *H. mediterranei* excretes extracellular polymeric substances (EPS) by consuming sugar substrates (Koller et al., 2007; Parolis et al., 1996), which diverts part of carbon-flow from PHA synthesis (Cui et al., 2017b). Short-chain carboxylates are essential carbon sources of cell metabolism and direct precursors of PHA

synthesis, which could potentially be a better candidate of feedstock than sugars. Waste-derived carboxylates have been used as renewable resources to produce PHA by a variety of microorganism (Lee et al., 2014). Carboxylate-rich wastewater has been utilized by *H. mediterranei* (Alsafadi and Al-Mashaqbeh, 2017), however, the mechanism of substrate consumption remains unclear. Large quantities of carboxylates can be generated from food waste through anaerobic fermentation process, where the production of carboxylates can also be controlled and optimized.

2.4 Metabolic pathways for PHBV synthesis by *H. mediterranei*

2.4.1 PHBV synthesis from glucose

Unlike the majority of microbial PHBV producers that require direct precursors such as propionate to form 3-HV units, *H. mediterranei* is well known for its capability to synthesize and accumulate PHBV with more than 10 % 3HV units from unrelated carbon sources including glucose and starch (Han et al., 2013). Figure 2.2 demonstrates the metabolic pathways involved in PHBV synthesis through using glucose as the sole carbon source. The strain can use multiple pathways to synthesize propionyl-CoA, which is an essential precursor of 3-HV monomer. These pathways also release considerable amounts of CO_2, which causes the loss of carbon and reduce the selectivity for PHBV as a product. In addition, previous studies have reported that *H. mediterranei* excretes considerable amounts of extracellular polymeric substances (EPS) when feeding sugars as substrate (Koller et al., 2007; Parolis et al., 1996). The metabolic pathway of glucose by *H. mediterranei* suggests that the formation of EPS diverts part of the carbon-flow towards PHBV production (Cui et al., 2017b). Therefore, this co-product could influence the PHBV yield from sugar-based carbon source.

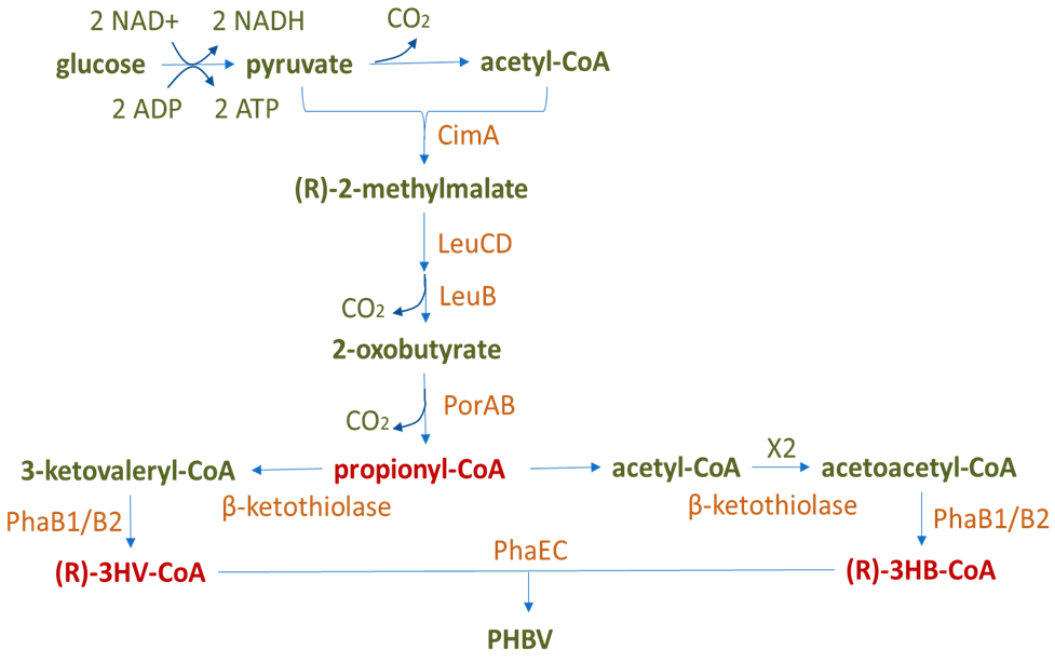

Figure 2. 2 Pathways of PHBV synthesis from glucose by *H. mediterranei* (modified based on Han et al., 2013; KEGG, 2019)

2.4.2 PHBV synthesis from short-chain carboxylates

Short-chain carboxylates, including mainly lactate (La), acetate (Ac), propionate (Pr), butyrate (Bu) and valerate (Va), are essentially soluble nutrients that can be utilized by microorganism. They are also direct building blocks to construct PHA. It is theoretically feasible for *H. mediterranei* to convert carboxylates to PHA due to availability of metabolic enzymes (shown in Figure 2.3). Ac and Bu are the main precursors for 3-hydroxybutyrate (3-HB) monomer, while Pr and Va favor the generation of 3-hydroxyvalerate (3-HV) monomer. The incorporation of 3-HV into 3-HB dominant chains results in the formation of copolymer PHBV, which is more flexible and tougher than PHB in terms of thermoplastic properties (Holmes, 1985). The short-chain

carboxylates can be produced by the anaerobic fermentation of food waste or other types of organic waste; and they normally consist of multiple types. Acetate, butyrate and propionate are the three major types produced from food waste. It is critical to regulate the process of anaerobic fermentation for the optimum production of carboxylates, which can efficiently facilitate the PHA production.

Few studies of *H. mediterranei* have reported the feasibility of feeding short-chain carboxylates or VFA-rich wastewater for PHBV production (Alsafadi and Al-Mashaqbeh, 2017; Ferre-Guell and Winterburn, 2018; Han et al., 2015). Compared to sugars, short-chain carboxylates as carbon source can be directly metabolized towards PHBV synthesis without carbon flow diversion to EPS. Therefore, these sources could potentially be better candidates for higher PHBV yield than sugar-based feedstocks. However, the research is scarce on waste-derived short-chain carboxylate mixtures as carbon sources and the mechanism of PHBV production remains unclear.

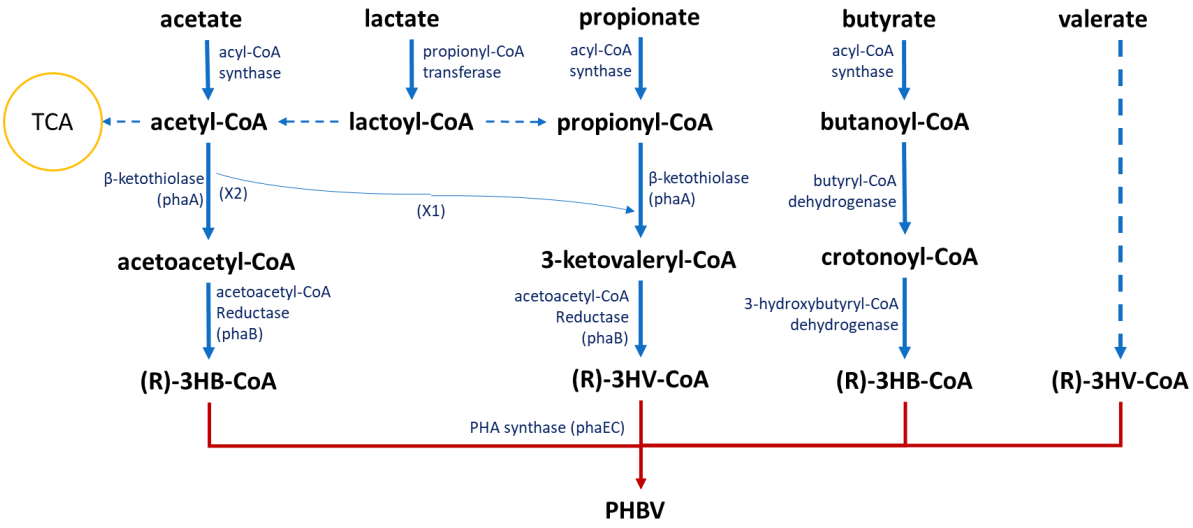

Figure 2. 3 Pathways of PHBV synthesis from short-chain carboxylates by *H. mediterranei* (modified based on Han et al., 2013; KEGG, 2019)

2.5 Essential parameters for culturing *H. mediterranei*

The culture of this strain essentially consists of saline medium, carbon source, nitrogen source, phosphorous source, and trace elements. Besides nutrient conditions, a successful cell cultivation process also requires suitable growth conditions including temperature, salinity, pH, and aeration rate. These key parameters are discussed in the following sessions.

2.5.1 Nutrient conditions

2.5.1.a Major nutrient sources

Carbon, nitrogen, and phosphorous sources are the three major nutrients that can influence the cell growth and PHBV production by *H. mediterranei*. Unlike most PHA-producing microbes, *H. mediterranei* can generate and accumulate PHBV under normal nutrient conditions. However, previous studies found that limitations on nitrogen and phosphorous sources with excessive carbon can stimulate cells to produce and accumulate more PHBV, thus giving higher production (Cui et al., 2017b, 2017d; Lillo and Rodriguez-Valera, 1990). One of the most cited studies (Lillo and Rodriguez-Valera, 1990) has tested the microbial growth and PHA production in various types and loadings of carbon sources including saccharose, glutamate, butyrate, acetate, glycerol, methanol, glucose, and starch; as a result, the researchers found that 2% glucose or starch gave the highest PHA yield among others; however, the acetate and butyrate alone gave very low yield. The same study also reported that phosphorous limitation can increase the PHA production, and the optimal loading was determined to be 0.00375% KH_2PO_4. In terms of nitrogen sources, this study only tested two types including NH_4Cl and yeast extract; the results showed 0.2% NH_4Cl and 0.3% yeast extract gave the highest cell growth and PHA production. Since depletion of nitrogen or

phosphorous would also cause insufficient cell growth, it would be desirable to have these nutrient-limiting conditions to stimulate higher PHBV production after enough cell biomass is obtained. Besides, characterization of carbon, nitrogen and phosphorous sources obtained from food waste and food processing byproduct feedstocks will be critical in terms of incorporating in the PHBV production system.

Additional studies have investigated the effects of nitrogen sources on *H. mediterranei* growth. Esclapez et al. (2014) found that complex medium with yeast extract or casamino acids as nitrogen source provided the greatest growth rate for *H. mediterranei*; among single nitrogen sources, ammonium resulted in higher growth rate than nitrate and some amino acids including glutamine, glutamate, asparagine, and aspartate. Other researchers have reported that *H. mediterranei* cells prefer using inorganic over organic nitrogen (Cui et al., 2017b). Another study compared ammonium and nitrate as the sole nitrogen source and reported that ammonium is the preferred nitrogen source and its assimilation is rapid as it only involves transport into the cell; nitrate can also be consumed after it is converted to ammonium, therefore, the utilization of nitrate is a more energy-demanding process (Martínez-Espinosa et al., 2006). Similarly, it has also been reported by another study that ammonium resulted in higher cell growth than nitrate, but nitrate can led to higher PHBV contents of cell mass than ammonium (Ferre-Guell and Winterburn, 2017).

Some previous studies have also recognized the effect of C/N ratio on microbial growth and PHBV synthesis. (Cui et al., 2017b) found that among four different C/N ratios including 65, 35, 15, and 5, while using glucose and NH_4Cl as modeled C and N source, the maximum cell mass obtained from batch cultivations increased with decreasing C/N, and a C/N of 5 gave the highest

cell mass production. The volumetric production of PHBV was also higher with a C/N of 5 than others; however, the PHBV content of cells was at maximum with a C/N of 35, suggesting that nitrogen limitation may give a significant boost to PHBV synthesis. Another study has investigated more C/N ratios between 5 to 35, which were 8, 17, 25, 34, and found that a C/N ratio of 8 offered the highest cell growth rate, cell mass production and PHA production (Ferre-Guell and Winterburn, 2017). Therefore, a C/N ratio around 8 should be adopted for batch production using ammonium as the nitrogen source.

2.5.1.b Micronutrients and trace elements

Besides the three major nutrient sources, there are certain micronutrients and trace elements that are essential to *H. mediterranei*. The vast majority of published studies use a trace metal solution named SL-6, which contains trace amounts of $ZnSO_4$, $MnCl_2$, H_3BO_3, $CoCl_2$, $CuCl_2$, $NiCl_2$, and Na_2MoO_4 that are comparable to sea water (Ferre-Guell and Winterburn, 2018; Han et al., 2015; Pais et al., 2016). In addition to trace elements, many studies use trace amount of $FeCl_3$ as an essential micronutrient to culture *H. mediterranei* (Cui et al., 2017b; Ferre-Guell and Winterburn, 2017).

2.5.2 Culturing conditions

2.5.2.a Temperature

Several factors including temperature, pH, total salt content, and aeration rate are essential to achieve the massive production of PHBV by *H. mediterranei*. Temperature is an important parameter since temperature difference could potentially influence cell growth kinetics because of its effect on rate constant of a reaction following Arrhenius equation. The effect of temperature on

the productions of cell mass and PHA by *H. mediterranei* was first studied in batch culturing, with different temperature levels of 30, 38, 45, 50 and 55 ℃ (Lillo and Rodriguez-Valera, 1990). The researchers found that the productions of cell mass and PHA increased with temperature from 30 to 45 ℃ and decreased with temperature from 45 to 55 ℃. However, the PHA production and yield from 38 and 45 ℃ were very close and the PHA content decreased from 38 to 45 ℃. Therefore, almost all following studies have used a temperature ranging 37 to 40 ℃ to culture *H. mediterranei*, since it saves energy and costs less compared to higher temperatures above 40 ℃ (Huang et al., 2006). A mesophilic temperature around 40 ℃ is used in this study, which favors both cell growth and energy saving.

2.5.2.b The pH of medium

An initial pH of 7 has commonly been used for culturing *H. mediterranei*. According to a study characterizing *H. mediterranei*, the optimal pH was around 6.5, and there was no growth observed with a pH below 5.0 (Rodriguez-Valera et al., 1983). Ghosh et al. (2019) reported that the pH of culturing medium decreased steadily from 7 to 5 during cell growth in sugar-based medium, which may be due to the accumulation of acids as the metabolites in the cell culturing process. Another study suggested medium containing ammonium as the nitrogen source can yield low cell density which is related to the rapid acidification of the medium during cell growth (Esclapez et al., 2014). Therefore, most studies maintained a stable neutral pH during cell growth and utilized concentrated NaOH or HCl solutions for pH adjustment.

2.5.2.c Salinity or total salts

As a type of extreme halophilic archaea, *H. mediterranei* can survive in the aqueous environment with much higher salinities than sea water. A previous study with a focus on salinity has reported that the optimal salinity for the growth of *H. mediterranei* was in the range of 150 to 200 g/L. A lower salinity (75g/L NaCl) can cause a decrease in cell mass and PHA production but can increase the generation of the red pigment bacterioruberin. An increasing salinity level up to 250 g/L NaCl would result in a higher PHA content of cell, and decrease the carbon diversion towards to synthesis of EPS (Cui et al., 2017a). A lower salinity could reduce feedstock cost on salt medium; however, it would potentially cause unstable cultivation due to breakage of cells facing osmotic shock. Therefore, a universal minimum saline medium (MSM) containing around 20% total salts has been adopted by most investigators for cell cultivation and PHA production by *H. mediterranei* (Ferre-Guell and Winterburn, 2018). The feasibility of recycling and reuse of salt medium will be further investigated to address the issues with salt medium cost reduction and salt effluent treatment.

2.5.2.d Aeration rate and dissolved oxygen level

Aeration rate is also an important parameter for cell cultivation since the high salinity can dramatically reduce the dissolved oxygen (DO) level of the medium. The saturated DO of the MSM medium with around 19% total salts is 2.50 mg/L at 37 ℃, which is only 37% of the saturated DO (6.73 mg/L) in freshwater (DEP, 2021). Therefore, the same aeration level which provides 20% saturated DO in freshwater may not be able to offer sufficient oxygen in MSM medium, which can cause limitations to cell growth. There are no universal guidelines for DO level for culturing *H. mediterranei* in literature, and different aeration rate strategies have been adopted among previous studies. Some studies used shaking flasks with various rotation speeds in

the ambient atmosphere without forced aeration to culture the microbes (Cui et al., 2017b; Ferre-Guell and Winterburn, 2018; Pais et al., 2016). other studies used various sized bioreactors with forced aeration: Lillo and Rodriguez-Valera (1990) provided 100% DO saturation during the entire culturing period; a 50% DO saturation was maintained during balanced cell growth and the DO dropped to 30% for PHA formation process (Koller et al., 2007); another study maintained a DO level above the critical limit which was 20% saturation (Lorantfy et al., 2014); in some other studies, a 20% saturated DO or an oxygen partial pressure at 20% of air saturation was maintained with varying aeration rates and agitation speeds (Koller, 2015; Pais et al., 2016). It is important to determine the aeration level that can avoid DO in the high saline medium from being a growth limiting factor.

2.5.3 Spent saline medium recycling

Halophilic microbes require up to 20% salts for optimum growth and a salt concentration below 10% can cause cell lysis (D'Souza et al., 1997). Apart from the impact on microbial growth, a lower salt concentration can also inhibit PHA synthesis. Decreases in cell biomass production, specific growth rate and PHA content of *H. mediterranei* have been observed when NaCl concentration is reduced to 7.5% (Cui et al., 2017a). Therefore, salinity needs to be consistent in an optimum range to maintain robust PHA production. Previous studies on *H. mediterranei* mostly produce PHA without considering the treatment of saline medium at the end of use. However, wastewater discharge is economically critical to large-scale industrial PHA production. Salts are principal water pollutants which are toxic to freshwater creatures and make water unsafe for drinking, irrigation and other applications (US EPA, 2013). The concentration of chloride ions cannot exceed 1500 mg/L in fresh water bodies (US EPA, 2018). Once into natural water bodies,

the salt ions are hard to remove. Therefore, spent saline water recycling and reuse is critical to the system design, which helps reduce salt cost, maintain high PHA yield and avoid water pollution by excessive wastewater discharge.

Among the few studies that have reported the process of recycling spent saline medium or salts, Bhattacharyya et al. (2014) proposed a method of using a hot solution of decanoic acid to precipitate salts from the spent stillage medium, and the salts were further utilized to culture *H. mediterranei* for PHA production. This method was able to recover and reuse 96% of the salts and the recycled batch had a PHA production close to the original batch with fresh salts. However, the method requires over three days as the processing time, which may add to the operating cost in large-scale productions. Another study using hydrolyzed whey permeate as the substrate reported a direct reuse of the spent saline supernatant resulting in a slower specific cell growth rate and a 68% lower final PHA production than the original batch with fresh salts, which may be due to the inhibitory compounds that formed during the prior pasteurization process (Koller, 2015). Therefore, it is of vital importance to propose an efficient approach to recycle and reuse the spent saline medium with high productivity of PHA and less processing cost.

Previous studies have investigated only one batch with the recycled spent saline medium; therefore, they have not considered the effect of the left-over nutrients that would accumulate in the culturing medium after multiple recycled batches. These accumulating organic compounds can be the residual sugars, short-chain carboxylates, and micronutrients that are not fully consumed by *H. mediterranei*; they can also be cell metabolites that have been produced and accumulated during cell growth, e.g. acetic acid and EPS. Those leftover nutrients can contribute to a significant

amount of COD after multiple batch runs, which can influence cell growth and PHBV production. In that case, pretreatment of the spent saline medium would be necessary to remove the substantial amount of COD resulting from the accumulation. Chemical oxidation using strong oxidizers such as H_2O_2 can be an effective approach to remove COD from the spent saline medium. Chemical oxidation by H_2O_2 has been widely used in the treatment of industrial wastewater for the removal of BOD and COD (Chen et al., 2014; Zaharia et al., 2009). In addition to COD removal, H_2O_2 is known as the oxygen supplier to microorganisms in biological treatment facilities because it can dissociate naturally into oxygen and water (Zaharia et al., 2009). Therefore, chemical oxidation can be a potential approach to treat spent saline medium if there is any inhibitory compound present.

2.6 Conclusions

The literature review provides the foundation of knowledge on PHBV production from inexpensive feedstocks by *H. mediterranei*, and the rationales for the main processes including feedstock pre-treatment and characterization, nutrient recovery, and microbial fermentation. The need of utilizing food waste and food processing byproducts as feedstocks have been identified after exploring the current research area. The essential culturing parameters for the growth and PHBV synthesis by *H. mediterranei* have been determined and their suitable ranges are selected as the basis for the following experimental plans.

Chapter 3. Carbon Sources for Polyhydroxyalkanoates Production by *Haloferax mediterranei*

3.1 Abstract

Given the feasible metabolic pathways of PHBV synthesis from short-chain carboxylates as precursors, in this chapter, the effects of acetate (Ac), propionate (Pr), butyrate (Bu), and the short-chain carboxylates derived from food waste were examined for the microbial growth and PHBV production. A mixture of carboxylates provided a 55% higher PHBV yield than glucose. The food-waste-derived nutrients achieved yields of 0.41 to 0.54 g PHBV/g Ac from initial loadings of 450 mg/L to 1800 mg/L Ac of total carboxylates. The strain was observed to have a different uptake preference on each carboxylate types at various substrate conditions including various composition of carboxylic mixture, and the existence of other soluble nutrients. The present study demonstrates the potential of using food waste as feedstock to produce PHBV by *Haloferax mediterranei*, which can provide economic benefits to the current PHA industry. Meanwhile, it will also help promote organic waste reduction in landfills and waste management in general.

Key words: Polyhydroxyalkanoates, food waste, short-chain carboxylates, *Haloferax mediterranei*

3.2 Introduction

The majority of recent studies have used sugar-based substrates to produce PHBV by *H. mediterranei*: hydrolyzed whey (Koller et al., 2007), extruded rice and corn starch (Huang et al., 2006), ethanol stillage (Bhattacharyya et al., 2014), high-salinity cheese whey hydrolysate (Pais et al., 2016), molasses wastewater (Cui et al., 2017d) and macroalgal hydrolysates (Ghosh et al., 2019) etc. However, *H. mediterranei* excretes extracellular polymeric substances (EPS) when fed

with sugar substrates (Koller et al., 2007; Parolis et al., 1996), which diverts part of carbon-flow from PHA synthesis (Cui et al., 2017b). Short-chain carboxylates are essential carbon sources of cell metabolism and direct precursors of PHA synthesis, which could potentially be the better substrate than sugars. Pure volatile fatty acids (VFAs) can be utilized as the sole carbon source by *H. mediterranei* (Ferre-Guell and Winterburn, 2018). The strain was shown to grow and synthesize PHA in olive mill wastewater containing VFAs (Alsafadi and Al-Mashaqbeh, 2017).

Food waste is a potential feedstock for PHA production because large quantities of carboxylates can be generated through anaerobic fermentation process, where the production of carboxylates can also be controlled and optimized (Zhou et al., 2018). At present, there are 6 million tons of food waste generated annually in California, which accounts for 18% of landfill waste (CalRecycle, 2018a). The landfilled food waste is a major source of methane emissions (Gunders, 2012). The utilization of food waste for PHA production will help reduce organic waste in landfills, and reduce feedstock cost due to the current tipping fees associated with the waste disposal.

The objectives of this research were: (1) to understand the effects of various VFAs as the substrate for the cell growth and PHA production by *H. mediterranei* and (2) to examine the production of PHA using food waste as feedstock through a two-stage process. Food waste was first degraded into carboxylate-rich nutrients through anaerobic fermentation; then the nutrients were utilized by *H. mediterranei* to produce PHBV in the controlled aerobic process. This study demonstrated the feasibility of using food waste as feedstock for PHA production. The two-stage bioconversion process can potentially be employed as an innovative and more environmentally friendly approach in the PHA industry.

3.3 Materials and methods

3.3.1 Culture medium and inoculum preparation

The wild-type strain *H. mediterranei* (ATCC 33500) was used throughout the study. The cells were cultured in ATCC 1176 medium (ATCC, 2020) at 37℃ . At the late exponential growth phase, cells were harvested using centrifugation and resuspended in minimum salt medium (MSM: NaCl, 156 g/L; $MgCl_2.6H_2O$, 13 g/L; $MgSO_4.7H_2O$, 20 g/L; $CaCl_2.6H_2O$, 1 g/L; KCl, 4 g/L; NaBr, 0.5 g/L and $FeCl_3$, 5 mg/L) with trace metal solution (SL-6: $ZnSO_4.7H_2O$, 100 mg/L; $MnCl_2.4H_2O$, 30 mg/L; H_3BO_3, 300 mg/L; $CoCl_2.6H_2O$, 200 mg/L; $CuCl_2.2H_2O$, 10 mg/L; $NiCl_2.6H_20$, 20 mg/L; $Na_2MoO_4.H_2O$, 30 mg/L) according to the prescription of Ferre-Guell and Winterburn (2018) and Tang et al. (2009). The cell suspension was used as inoculum for the following PHA production experiments.

3.3.2 PHA production using pure VFA and glucose

Two types of carbon sources, VFA mixture (containing acetic acid, propionic acid, and butyric acid with a molar ratio of 2:1.33:1) and glucose were used respectively to give the same initial carbon concentration of 4g/L. NH_4Cl was added at 3.06 g/L to give a C/N ratio of 5, which provided excess nitrogen (Cui et al., 2017b). KH_2PO_4 was added at 0.5 g/L to obtain a C/P ratio of 35, which supplied sufficient phosphorous (Ferre-Guell and Winterburn, 2018). MSM and SL-6 were used as the base saline medium. NaOH (10 M) was used to adjust the initial pH of both mediums to 7. Bioreactors with 800-mL working volume were used for the aerobic cultivation. The strain was cultured at 37 ℃ with 100 mL/min aeration. Prior to entering the bioreactors, the air flow passed through a humidifier to reduce water evaporation loss during aeration. The strain was cultured for 144 h until the growth reached stationary phase.

3.3.3 PHA production using carboxylate-rich nutrients derived from food waste

A simulated food waste mixture containing (% w.b.) 28% cooked rice, 32% cooked ground beef and 40% chopped raw cabbage was blended into a slurry using a food processor. The food waste slurry was then anaerobically fermented in 1-L batch reactors with an organic loading of 32 g volatile solids per liter (VS/L) and a food to microorganism (F/M) ratio of 8. A mesophilic sludge collected from a local anaerobic digestion facility was used as the inoculum for anaerobic fermentation. The headspace was purged with argon gas to remove air prior to the start of anaerobic fermentation. All the reactors were housed in an incubator controlled at 37 ℃ and mixed twice per day. The pH of the fermentation broth declined from 6 to 5 and remained 5 ± 0.5 afterwards. The fermentation lasted for three weeks until the concentrations of carboxylates were stabilized. After that, the broth was centrifuged at 5000 rpm for 30 min; the supernatant was then filtered through a 0.2 μm membrane.

The nutrient solution, with carboxylate contents as shown in Table 3.1, was used as the sole carbon source to culture *H. mediterranei*. The nutrient solution was loaded at four levels: 1.06, 2.12, 3.18 and 4.24 g soluble chemical oxygen demand per liter (sCOD/L), with corresponding contents of total carboxylates as 450, 900, 1350, and 1800 mg Ac/L. The base saline medium containing MSM and SL-6, along with sufficient N and P nutrients loadings same to that used in previous experiments. $NaHCO_3$ (30 mM) was used as buffer to maintain pH at 7.0 ± 0.2 for the entire culturing period. The 250-mL bioreactors with 200 mL working volume were used for PHA production. The strain was cultured at 37℃ with 100 mL/min aeration for 144 h until the growth reached stationary phase.

3.3.4 Determination of cell mass and growth kinetics

To monitor cell growth status, 2 mL of cell broth were collected at different time points during the cultivation period and centrifuged at 10000 rpm for 10 min; the cell mass was resuspended in MSM solution, and the optical density (OD) was analysed at 520 nm (Lillo and Rodriguez-Valera, 1990). The cell growth rate was obtained as the slope of ln (OD) versus time. The cell dry mass (CDM) was determined as the volatile suspended solids (VSS) of cell broth: 20 mL of cell broth were sampled and subjected to centrifugation at 8,000 rpm for 20 min. The cell mass was washed with MSM solution twice and measured for VSS (APHA, 2012). The cell growth kinetics were curve-fitted based on the Monod model (Monod, 1949):

$$\mu = \frac{\mu_m S}{K_S + S} \tag{3.1}$$

Where μ is the specific growth rate (h^{-1}), μ_m is maximum specific growth rate (h^{-1}), S is total carboxylate loading (g Ac/L), and *Ks* is the half velocity (g/L).

3.3.5 Recovery and quantification of PHA production

The strain samples were analysed by transmission electron microscopy (TEM) to observe the cell interiors following the method of Lu et al. (2008). The extraction of PHA was achieved following the method of Escalona et al. (1996) with modifications: the 20 mL cell broth was sampled and centrifuged at 8000 rpm and 4℃ for 20 min. The cell mass was washed with 0.1% sodium dodecyl-sulfate (SDS) solution and deionized water. The washed PHA polymers were dried in an oven at 105 ℃ for 4 h and the dry weight measured according to a standard method of total solids (TS) (APHA, 2012). The extracted PHA was dissolved in 2 mL dichloromethane and 2 mL acidic methanol (3% v/v H_2SO_4), with 1g/L benzoic acid as internal standard using the 12 mL culture tubes with rubber lined caps. The tubes with solution were placed in a Hach DRB200 digital reactor block (Hach Corp., Los Angeles) at 105 °C for 4 h and cooled to room temperature.

The solution was mixed with 1 mL deionized water and allow to settle until phase separation was observed. The organic phase was then transferred to a clean vial for quantification. PHBV with 12% hydroxyvalerate (HV) (Sigma-Aldrich, 403105, St. Louis) was used as the standard PHBV chemical. The samples were analysed via gas chromatography using a method developed from the literature (Braunegg et al., 1978; Lemos et al., 1998; Oehmen et al., 2005). A gas chromatograph (GC, Agilent 6890N, Santa Clara) equipped with a flame ionization detector (FID) was employed and a HP-5 capillary column was used with helium carrier gas. Details of this method were: inlet temperature and pressure: 230℃, 16 psi; total flowrate: 30 mL/min; split ratio: 8:1; oven temperature: initial 100℃ for 2 mins; ramping from 100 to 124℃, with a rate of 8℃/min; holding 124℃ for 1 min. FID temperature was 240℃, with 40 mL/min of H_2 flow and 450 mL/min of air flow.

Based on the measured results, the PHBV yield was calculated as the mass of PHBV produced divided by the mass of substrate consumed. Two types of substrate were used in the calculations: glucose and total carboxylates (g Ac/L).

$$Y_{PHBV} = \frac{\Delta m_{PHBV}}{\Delta m_{carbon\ source}} \tag{3.2}$$

The PHBV content of cells was calculated as the percentage of PHBV in the total CDM, described as g VSS:

$$PHBV\% = \frac{m_{PHBV}}{m_{CDM}} * 100\% \tag{3.3}$$

The percentage of HV in PHBV polymer, which indicates the elasticity of the plastic material, was determined based on the mass ratio between HV and the sum of HV and HB units as measured by the GC method described previously:

$$HV(\%) = \frac{m_{HV}}{m_{HB}+m_{HV}} * 100\% \tag{3.4}$$

3.3.6 Measurements of short-chain carboxylates and glucose

To quantify the consumption of the substrates, 2 mL of cell broth was collected at different time points during cultivation and centrifuged at 10,000 rpm for 10 min; the supernatant was then filtered through a 0.22 μm membrane. The filtrate was measured for the content of short-chain carboxylates and glucose by the analytical method reported by Sluiter (2008): a high-performance liquid chromatograph (HPLC) equipped with refractive index detector (RID) and photodiode array detector (PDA) was used for the measurement. Biorad Aminex HPX-87H column was used as the analytical column, where 5 mM H_2SO_4 solution was used as the mobile phase with a flow rate of 0.6 mL/min. The oven temperature was controlled at 60 ℃.

3.4 Results and discussions

3.4.1 Intracellular PHBV generation by *H. mediterranei*

H. mediterranei has a pinkish appearance formed by a group of red carotenoids which naturally exist in the cell membrane (Fang et al., 2010; Tang et al., 2009). During cell cultivation, the pink color was observed on the strain colonies and cell broth, which indicated normal growth of the species. The species is capable of forming PHBV under normal growth conditions (Cui et al., 2017b). The PHBV granules with round and oval shapes in the cell interior were identified by TEM, confirming the presence of PHBV (Figure 3.1). The brittle whitish inclusions in the dried raw PHBV were readily reduced to powder by hand grinding using a mortar and pestle (Figure 3.2).

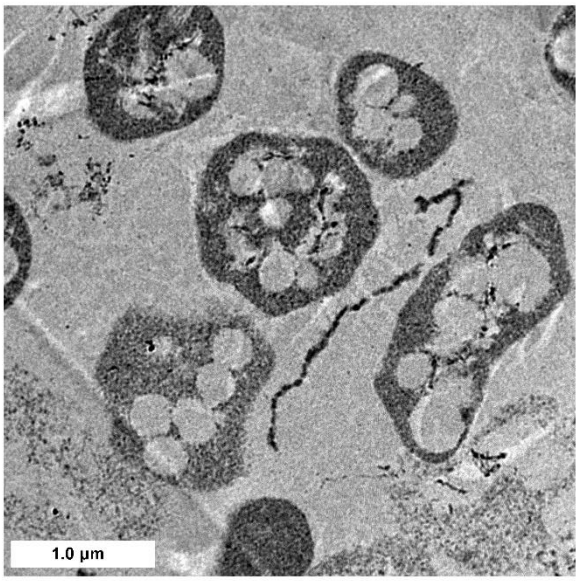

Figure 3. 1 TEM image of *H. mediterranei* cells. The scale bar indicate 1.0 µm.

Figure 3. 2 Dried PHBV samples extracted from *H. mediterranei* cells

3.4.2 Pure VFA and glucose as sole carbon source for PHBV production

3.4.2.a Influence of carbon sources on cell growth and PHBV production

As described in section 2.2, two different types of substrates, pure VFA mixture and glucose, were used individually as the sole carbon sources with the same initial carbon concentration of 4 g/L. The maximum concentrations of cell mass and PHBV obtained from the pure VFA mixture were 2.99 ± 0.29 g/L and 1.57 ± 0.05 g/L, respectively. In comparison, glucose as carbon source gave slightly higher results: 3.59 ± 0.25 g/L of cell mass and 2.17 ± 0.20 g/L of PHBV as shown in Figure 3-3. The growth rate of the species in glucose was 0.032 ± 0.0007 h^{-1}; whereas the growth rate in VFA mixture was 0.024 ± 0.0007 h^{-1}. A previous study reported the μ of *H. mediterranei* by using one or two VFA species as carbon sources to be 0.010 to 0.035 h^{-1} (Ferre-Guell and Winterburn, 2018), and the growth rates in VFA mixture obtained in this study were within the previously reported range. Corresponding to specific growth rate, 96 h were required for cells to reach stationary phase in glucose, shorter than the 144 h of cultivation required for cells grown in the VFA mixture.

The time course monitoring of PHBV production and substrate consumption is shown in Figure 3.3. As pure VFA mixture and glucose were consumed as the sole carbon source, PHBV was generated along with cell growth and a rapid increase of PHBV was observed during the exponential growth phase. The production of PHBV started to decelerate when cell mass was approaching the maximum, and the PHBV concentration remained stable at the stationary phase. For both cases, the PHBV production curve had a very similar trend to the cell growth curve, which suggests the PHBV production was a growth-associated reaction. A similar phenomenon has been observed in previous literature with dominant use of sugar-based feedstocks, e.g. glucose, starch and microalgae hydrolysates (Cui et al., 2017b; Ghosh et al., 2019; Lillo and Rodriguez-Valera, 1990). As far as can be determined from the literature, these present results represent the first time that growth-associated PHBV production was observed when short-chain carboxylates were used

as the sole carbon source by *H. mediterranei*. In addition to sugar-based carbon sources, the species can also accumulate PHBV by consuming VFA under normal growth conditions, an advantage over some other PHA producers which require necessary growth-limiting factors to stimulate PHA accumulation. Such PHBV production that is not limited by cell mass could be beneficial to large-scale industrial production.

Particularly when VFA mixture were used as carbon source, the PHBV generation mostly paralleled that of the cell mass during the entire culturing period. The PHBV content of cell dry mass also remained approximately constant when carboxylic nutrients were consumed. The constant PHBV content may be due to the sufficient supply of nutrients and the preferable C/N ratio that maintained the normal growth of *H. mediterranei* during cell cultivation. Based on the current results, PHBV production under limited growth conditions should be investigated for greater PHA accumulation.

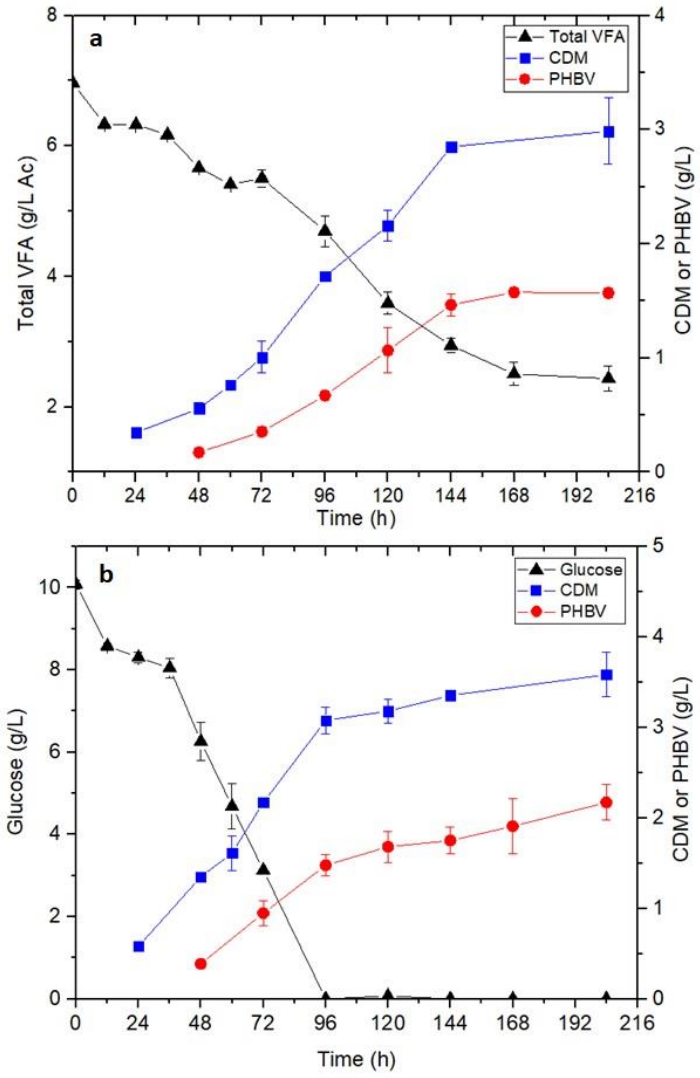

Figure 3. 3 Time course monitoring of PHBV production by *H. mediterranei* by using different carbon sources

3.4.2.b The influence of carbon source on PHBV yield and HV content

As shown in Figure 3.4, PHBV yields were 0.10 ± 0.01 g PHBV/g glucose and 0.13 ± 0.01 g PHBV/g Ac at 48 h and increased with strain growth, becoming stable as approaching the stationary growth phase. The final PHBV yield from pure VFA mixture was significantly higher

than that from glucose: 0.34 ± 0.01 g PHBV/g Ac and 0.22 ± 0.02 g PHBV/g glucose (p-value < 0.05, as shown in Table C.1).

The higher PHBV yield from VFA than glucose may be due to short-chain carboxylates are more direct precursors for the synthesis of PHBV than glucose. Short-chain carboxylates (C2 to C5) can be utilized as the sole carbon source for the polymerization of PHBV (Ferre-Guell and Winterburn, 2018). In the pathways from carboxylates to PHBV, most carbon flows are towards polymer formation, except for those used for energy production and CO_2 evolution in the tricarboxylic acid (TCA) cycle. Meanwhile the metabolic pathways from glucose to PHBV involve more reaction steps than that from carboxylates (Han et al., 2013), which reduces the overall selectivity of PHBV product (Fogler, 2016). Another reason for the lower PHBV yield from glucose is the existence of EPS as a byproduct, which also diverts carbon flows from those towards PHBV generation (Cui et al., 2017b).

Carbon source did influence the HV content of PHBV during cultivation. Under the same carbon loading, the HV content using the pure VFA mixture remained stable between 15% to 18% of PHBV during the entire culturing period; meanwhile the HV content using glucose increased from approx. 12% to 24% of PHBV. Glucose is known to be metabolized into HV precursor with the same molar concentration, while only Pr, accounting for part of VFA mixture, was the HV precursor (Ferre-Guell and Winterburn, 2017). Since a higher HV content results in more elasticity of the plastic material, it should be feasible to direct the HV content through manipulating the VFA composition in future research.

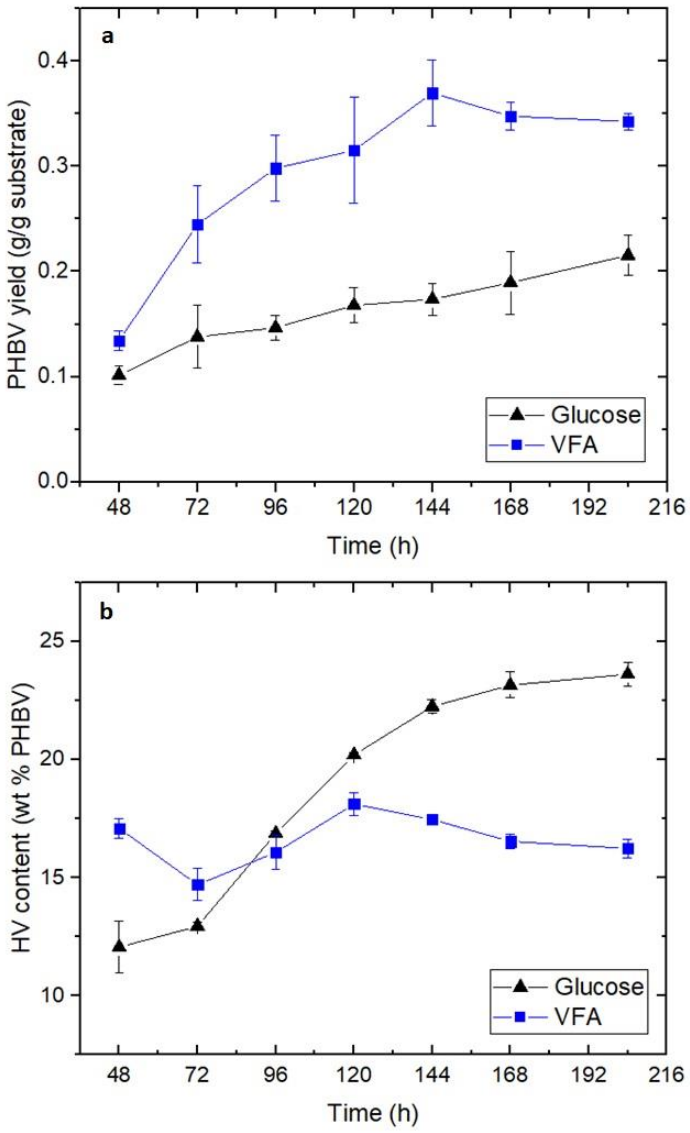

Figure 3. 4 Comparison of PHBV yield and HV content of PHBV polymers by using different carbon sources

3.4.2.c Substrate consumption

There was a small portion of VFA leftover when the concentrations of cell mass and PHBV reached maximum and remained stable. As shown in Figure 3.5, all three VFA species were consumed during cell growth. However, the extent of the consumption differed among species: by

the end of cultivation, Bu was completely consumed, around 81.6% of Pr was consumed, and only 41.6% of Ac was consumed, although all species started with the same mol C% in the mixture. This can be resulted from different substrate uptake rates by *H. mediterranei* for growing and synthesizing PHBV in VFA mixture. The cell growth rate also varies using different VFA species as the single carbon source (Ferre-Guell and Winterburn, 2018). The results suggest that a certain composition of the VFA mixture might give better cell growth and PHBV production by *H. mediterranei*, which could also be investigated in further research.

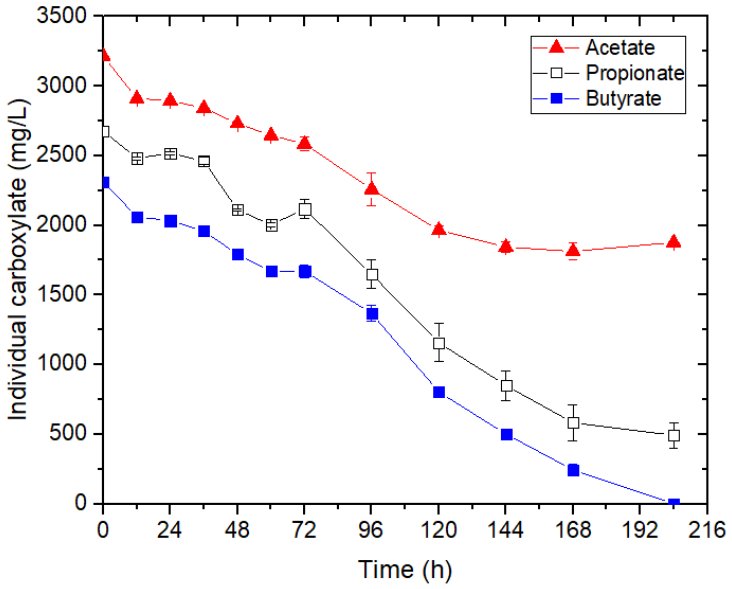

Figure 3. 5 The consumption of individual carboxylate by *H. mediterranei* when using VFA mixture as sole carbon source

3.4.3 PHA production using carboxylate-rich nutrients derived from food waste

3.4.3.a Carboxylates and other nutrients from anaerobically fermented food waste

Approximately 95 ± 2% of total carboxylates were obtained after two weeks of anaerobic fermentation of food waste and the production remained almost constant during the third week.

The average total carboxylate yield was 0.35 g/g VS, which was in the range (0.1 to 0.6 g/g) as previously reported for organic waste (Arslan et al., 2016). Gases consisting of approximately 38% (v/v) H_2 and 62% (v/v) CO_2 were produced and the production of CH_4 gas was not detected, suggesting the process had been well controlled for acid production with no methanogenesis process occurred. The liquid phase of fermented food waste slurry contained over 9 g/L Ac of total carboxylates. The fermentation broth had over 20g sCOD/L, of which about 76% was from carboxylates.

The soluble nutrient composition of the fermentation liquid is shown in Table 3.1. The carboxylates produced from food waste contained approximately 35% Ac, 13% Pr and 46% Bu as the dominant species. This compositional result agreed with previous literature producing carboxylates from different types of food waste through acidogenesis: the mesophilic acidogenic culture obtained 28% Ac, 15% Pr and 57% Bu from dining hall food waste (Shin et al., 2004); and 32% Ac, 10% Pr and 58% Bu were obtained at a pH 5 and mesophilic condition from food waste with a prior heat shock (Kim et al., 2011). Although carboxylate composition varies among studies, Ac, Pr, and Bu are the three major species generated from anaerobic fermentation process.

Table 3. 1 Composition of nutrients derived from food waste

Compound	**Unit**	**Average value (standard deviation)**
sCOD (total)	mg/L	21170 (1598)
sCOD (from carboxylates)	mg/L	17161 (665)
Total nitrogen	mg/L N	24 (0)
Ammonium	mg/L N	20 (4)
Total phosphorous	mg/L PO_4^{3-}	38 (1)
Ash	mg/L	3720 (85)
Total short-chain carboxylates	mg/L Ac	9136 (255)
Ac	mg/L	3982 (142)
Pr	mg/L	1403 (328)
iso-Bu	mg/L	375 (32)
Bu	mg/L	5150 (568)
Iso-Va	mg/L	236 (41)
Va	mg/L	76 (11)
Lactate (La)	mg/L	103 (18)

3.4.3.b Influence of substrate loading on cell growth

The cell growth curves with different substrate loadings (450, 900, 1350, and 1800 mg Ac/L) are illustrated in Figure 3.6. As an indicator of cell number, the OD of cell broth in all substrate loadings increased with time and reached a plateau around 120 h after inoculation. During the stationary growth phase, the final OD increased with higher initial substrate loadings, which were also indicated by the increasing extent of pink color of cell broth. This is reasonable since a higher nutrient concentration would be converted to more cell mass, if the substrate loading did not cause any inhibition effect on cell growth. Besides, indicated by the slope of the growth curve, the μ in

all substrate loadings started to increase rapidly around 24 h after inoculation and remained mostly exponential through 96 h. The μ decreased afterwards, which may be a consequence of nutrient depletion or cell mass loss due to endogenous cell metabolism (Shuler and Kargi, 2008).

Based on the results of OD from 24 h to 96 h when the most rapid growth occurred, μ was calculated to be from 0.014 to 0.025 h^{-1} and increased with higher loadings of total carboxylates. The cell growth rate from waste-derived carboxylic nutrients was very similar to that from pure carboxylic nutrients. As shown in Figure 3.6, the results of experimental μ were used to establish the Monod model through curve-fitting, which reflected the μ as a function of total carboxylate concentration. The cell growth kinetics were also obtained from the Monod model, with an adjusted R^2 of 0.983. The modelled μ_m was 0.0296 ± 0.0007 h^{-1}; the Ks was 383 ± 34 mg/L. The modelled reaction kinetics suggested higher substrate loadings would be possible to obtain higher specific growth rate, which would be beneficial for the steady-state and other continuous production scales. Previous studies have reported the possible inhibition effect of VFA on cell growth of some PHA-producers at high concentrations (Yu et al., 2002); therefore, additional research might investigate possible inhibition effects of high substrate loadings of the waste-derived carboxylic nutrients on the cell growth of *H. mediterranei*.

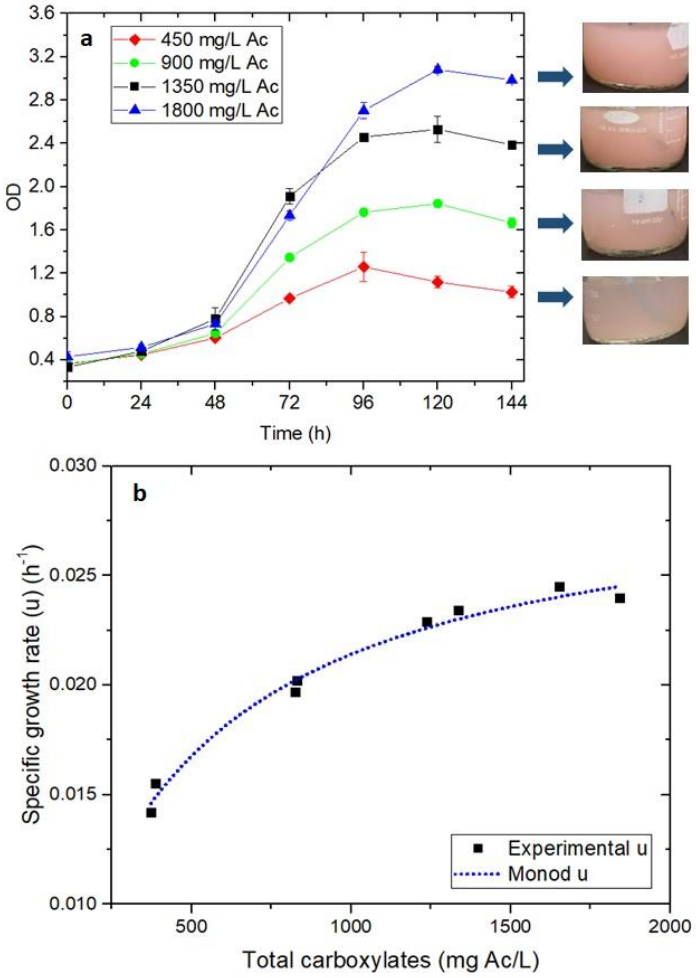

Figure 3. 6 The status of cell growth and growth kinetics of *H. mediterranei* in food waste derived nutrients

3.4.3.c Influence of substrate loading on PHBV production

Like the cell mass production trend, the concentration of PHBV increased with higher loadings of fermented food waste permeate from 450 to 1800 mg Ac/L. As shown in Figure 3.7, the PHBV content of cell biomass was generally stable among different substrate loadings and in the range of 43% to 57% (% CDM). This was the reason for the increasing PHA concentrations with higher cell mass production. Similar results of PHA content in cells have been reported for

H. mediterranei under balanced growth conditions by other studies, as shown in Table 3.2. Apart from this strain, very similar results of PHA content in cells have also been obtained by other PHA-producing microorganisms using VFA as a carbon source. The PHA content can be higher under unbalanced growth conditions, e.g. when nitrogen is limited and C/N ratio is high (Cui et al., 2017b). A similar concept of nutrient limitation is employed when feast-and-famine strategies are used for a mixed consortium of microorganism as the PHA-producer (Korkakaki et al., 2016). Some genetic modifications can also trigger cells to accumulate more PHA intracellularly (Chen, 2009; Madison and Huisman, 1999).

The PHBV yield remained in the range of 0.41 to 0.54 g PHBV/g Ac, with a total carboxylate loading of 450 mg/L to 1800 mg/L Ac. The results suggest that short-chain carboxylates, either pure chemicals or derived from food waste fermentate, can be a good option for the carbon source that achieves high PHBV yield by *H. mediterranei*.

The average HV contents from waste-derived carboxylic nutrients were in the range of 6% to 11% and decreased with higher total carboxylate loadings. Based on current literature, glucose, Pr and Va were found to be the precursors of HV in the PHBV synthesis (Ferre-Guell and Winterburn, 2018; Han et al., 2013). The reason for the lower HV content from carboxylic nutrients may be due to the low concentrations of Pr and Va that were present originally in the substrate. Higher HV content in the PHBV can increase the elasticity and reduce the brittleness of the polymer, which can be desirable for the most common biodegradable plastic applications including plastic films, bags, and containers. Again, additional research could investigate increasing PHBV yields with a high HV content using organic waste streams rich in carboxylic nutrients.

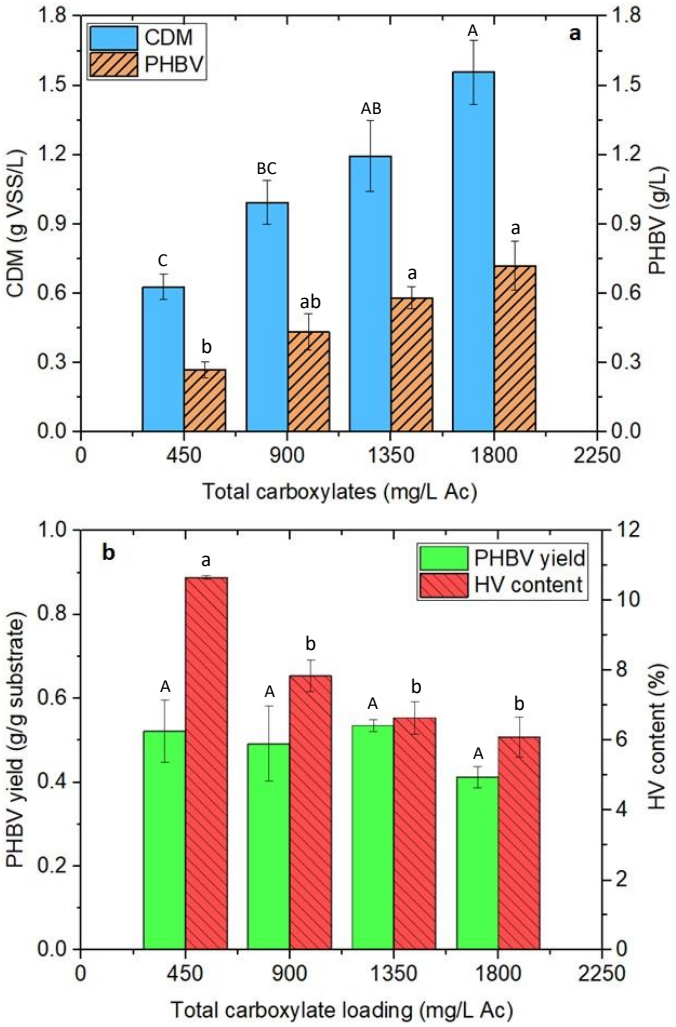

Figure 3. 7 The production and yield of PHBV and the HV content of the polymers produced from food waste derived nutrients

Table 3. 2 Selected results of microbial PHA content

Substrate	Microbial species	CDM	PHA content	PHA yield	HV content	Reference
		g/L	% CDM	g/g	% PHA	
Olive mill wastewater	*H. mediterranei*	0.47	43	-	6.5	(Alsafadi and Al-Mashaqbeh, 2017)
Synthetic VFA	*H. mediterranei*	1.2-7.7	19.9	0.11	-	(Ferre-Guell and Winterburn, 2018)
Glucose and Va	*H.mediterranei* ES1 (EPS gene deleted)	0.4-13.3	41	-	9.1-53.3	(Han et al., 2015)
Cheese whey hydrolysate	*H. mediterranei*	7.5	53	0.78	1.5	(Pais et al., 2016)
Extruded corn starch, rice bran	*H. mediterranei*	140.0	55.6	-	-	(Huang et al., 2006)
Glucose	*H. mediterranei*	1.4-15.8	36	0.86	8.8-12.5	(Cui et al., 2017b)
Synthetic VFA	*H. palleronii*	0.9-1.6	63	0.05	-	(Venkateswar Reddy et al., 2016)
Brewery wastewater	Activated sludge	-	39	0.43	-	(Ben et al., 2016)
Fermented food waste	*H. mediterranei*	0.6-3.0	43-57	0.41-0.54	6.1-10.7	This study

3.4.3.d Substrate consumption

The total carboxylate (as Ac equivalent) consumption with different substrate loadings during the entire culturing period is shown in Figure 3.8. The substrate consumption curves of different substrate loadings had a similar trend: the total carboxylate decreased rapidly from 24 to 96 h and remained stable afterwards. At the end of cell growth and PHBV production, 84% to 88% of the

total carboxylates were consumed (the initial substrate loadings were 450 to 1800 mg Ac/L). This was promising for organic reduction in waste streams. In terms of the consumption of individual carboxylate, almost 100% consumption was achieved for Ac, iso-Bu, Bu, and isovalerate (iso-Va) for all substrate loading levels. However, less than 25% of Pr was consumed at all loading levels, which corresponds to the low HV content of the PHA produced from waste-derived permeates. Most of the Pr was consumed and the majority of Ac was left out when pure carboxylates were used in previous experiment. These results indicate that although all species of short-chain carboxylates are essential carbon sources for microbial growth and PHBV synthesis, the strain might have a different uptake preference on each carboxylate species at various substrate conditions, e.g. when the composition of carboxylic mixture varies, and other soluble nutrients are present in the medium.

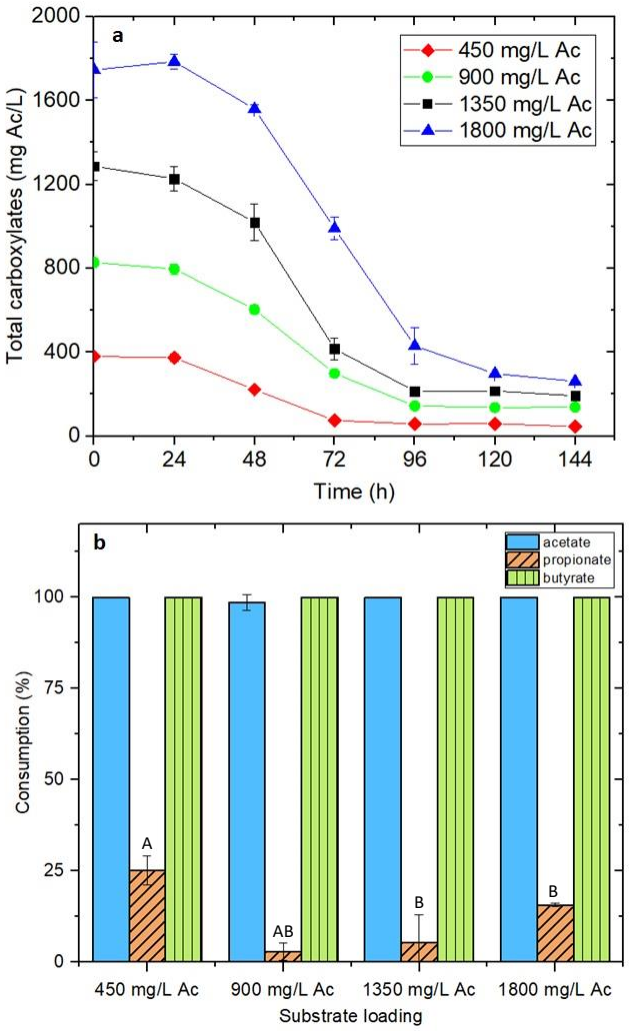

Figure 3. 8 The consumption of short chain carboxylates by *H. mediterranei* with different substrate loadings

3.5 Conclusions

Two sets of experiments were conducted to evaluate the feasibility of utilizing volatile fatty acids (VFA) mixtures as the sole carbon source to produce high-value PHA by *H. mediterranei*. These studies found that *H. mediterranei* can grow and synthesize PHBV from VFA mixtures as the sole carbon source; and a VFA mixture can give a higher PHBV yield than glucose, the common carbon source from the literature. As far as can be identified from the literature, this is

the first time that PHBV synthesis has been found to be a growth-associated process when consuming VFA mixtures. Beyond synthetic VFA substrates, VFA-rich nutrients have also been produced from simulated food waste through anaerobic fermentation and used as the sole substrate to produce PHBV by *H. mediterranei*. PHBV yield from food waste derived VFA nutrients can be up to 0.54 g/g Ac; the higher substrate loadings resulted in more cell mass and PHBV production, though the PHBV contents of cells remain stable within 43% to 57% depending on the composition of the VFA mixtures. The HV content of the PHBV produced from food waste derived VFA nutrients remained within 6% to 11%, due to the low concentrations of HV-precursor including Pr and Va. *H. mediterrranei* can effectively utilize the VFA-rich nutrients with high consumption rates of up to 88% with Ac and Bu completely consumed. This study has successfully proved the concept of robust pure-culture PHBV production from VFA mixtures derived from food waste with very high product yield, cell growth rate, and substrate consumption. The case of making high-value PHA from food waste by halophilic microbes has the potential to accelerate PHA market growth by reducing production cost and providing innovative incentives to food systems through additional revenue from alternative food waste management over the lifecycle. The results may be applicable to other organic waste streams such as agricultural waste, and organic waste effluents from food processing facilities although this remains to be demonstrated through subsequent research.

Chapter 4. The Pretreatment and Utilization of Four Types of Real-world Feedstocks for Polyhydroxyalkanoates Production by *Haloferax mediterranei*

4.1 Abstract

From the previous chapters, sugars and VFAs are proven to be viable carbon sources for cell growth and PHBV production by *H. mediterranei*. This study aimed at testing the feasibility of using the real-world feedstocks which contain different sugars and VFAs as the main carbon sources for PHBV production by the microbes. Four different types of feedstocks including food waste hydrolysate, food waste fermentate, whey sugar (lactose), and delactosed permeate were collected, pretreated with different processes, and utilized as the sole substrate to culture *H. mediterranei*. Before microbial cultivation, food waste hydrolysate and fermentate were processed through microfiltration for the recovery of nutrients and removal of suspended particles. The two cheese processing byproduct streams were subjected to enzymatic hydrolysis to convert lactose into monosaccharides. After pretreatment, each substrate was loaded with two soluble COD (sCOD) loadings of 22.5 g/L and 45 g/L to culture *H. mediterranei* and the effects of substrate type and loading on PHBV production were studied. The results show that with the same substrate loading, the substrate derived from food waste fermentate gave higher final cell mass and PHBV concentrations than food waste hydrolysate; and 45 g/L sCOD resulted in the highest PHBV production (3.92 ± 0.08 g/L) within the same culturing time. Substrates derived from whey sugar and delactosed permeate gave close to the same final cell mass given the same substrate loadings; however, with 45 g/L sCOD loading, cells grew much faster in whey sugar hydrolysate but total PHBV production remained similar. Food waste fermentate resulted in higher HV contents than food waste hydrolysate; and substrate loading had negatively influenced the HV content of PHBV derived from delactosed permeate, which may be due to the prolonged growth time.

Key words: Polyhydroxyalkanoates, food waste, cheese processing byproducts, *Haloferax mediterranei*

4.2 Introduction

The demand for biodegradable plastics is growing worldwide, due to the severe environment burdens caused by conventional plastics. Polyhydroxyalkanaotes (PHA) is a family of microbe-derived and biodegradable thermoplastic materials that has similar properties to common plastics. It can be produced from renewable feedstock, including byproducts and waste streams from food and agricultural systems. PHA has a well-established commercial market, with a market price of $7-10/kg. The PHA market size is projected to reach $ 121 million by 2025 (Aeschelmann and Carus, 2015). PHA has predominant applications in packaging films and plastic containers, and its market is expanding rapidly to other applications e.g. medical implant materials, drug carriers, nutritional supplements and biofuels (Chen, 2009). At present within the PHA industry, most companies utilize costly substrates e.g. sugars, starch and oils for pure culture PHA synthesis at a production cost 3 to 4 times higher than that of conventional plastics (Kourmentza et al., 2017). This high production cost is a bottleneck for the growth of the PHA market. The feedstock cost accounts for over 40% of the total annual operating cost (Leong et al., 2017), therefore, many researchers are developing bioconversion processes to utilize waste streams or industrial byproducts to reduce the production cost.

Food waste is one suitable feedstock, because it can provide essential nutrients for cell growth and direct precursors to PHA synthesis. These nutrients are usually available in many of the commercial anaerobic digesters treating large quantities of food waste. Therefore, it may be

feasible and economically beneficial to add a PHA production facility along with digestion facilities. There are around 6 million tons of food wastes disposed every year in California, which represents nearly 18% of all materials in the landfills (CalRecycle, 2018b). Landfilled organic wastes are one of the largest sources of human-related methane emissions in the US, which contribute over 15% of overall emissions (US EPA, 2016). Therefore, the utilization of food waste for producing PHA can help resolve the negative impacts of landfilled organic waste and promote the concept of waste utilization for value-added products in general.

Another potential feedstock is cheese processing byproducts. Shown in Figure 4.1, whey permeate, whey sugars, and delactosed permeate (DLP) are byproduct streams derived from cheese manufacturing processes. Whey permeate is the side stream from the separation and concentration of whey protein. Lactose powder is produced from crystalizing the sugars from whey permeate, leaving behind DLP after the recovery of lactose crystals (Oliveira et al., 2019). These byproduct streams are produced in large quantities from cheese-making facilities (e.g. 0.5 kg DLP is produced per kg of milk (Liang et al., 2009)) and contain rich nutrients including sugars, protein, amino acids, minerals, and micronutrients. However, whey permeate and DLP are currently sold as low value products including animal feed and fertilizers, or land-applied on fields (Durham, 2009). Converting cheese processing byproducts to PHA can create an additional revenue for dairy processors in California, and potentially reduce high production costs and make PHA more competitive in the bioplastic market.

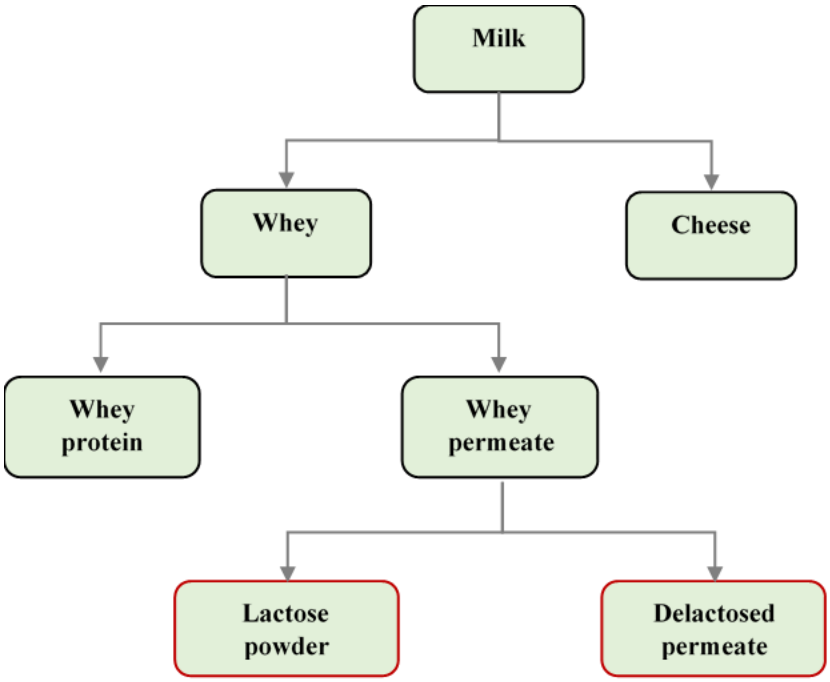

Figure 4. 1 Products in whey processing and sources of LP and DLP feedstocks

Among all types of PHA, poly(3-hydroxybutyrate) (PHB), poly(3-hydroxybutyrate-co-3-hydroxyvalerate) (PHBV), and poly(3-hydroxybutyrate-co-3-hydroxyhexanoate) (PHBH) are the three major PHAs with industrial-scale productions around the world (Chanprateep, 2010). This study focuses on PHBV, which is a type of high value PHA with wide application and commonly seen in the market. As described in previous chapters, an extreme halophilic archaeon, *H. mediterranei*, has been used for synthesizing PHBV by utilizing various types of carbon sources including sugars and short-chain carboxylates, which are commonly present in feedstocks derived from food waste and food processing byproduct streams. Due to the high saline environment for growth, the microbes can grow without any sterilization requirement, which can help reduce the pasteurization or sterilization cost in large scale production. It also facilitates the extraction of PHBV by salt-free water, which can also reduce the cost and the use of toxic chemicals for PHBV extraction as practiced by the current industry.

Focusing on the four types of real-world feedstocks including fermented food waste, food waste hydrolysate, lactose powder (whey sugar powder), and DLP, the objectives of this study were to 1) test the feasibility of using these four different types of feedstocks for cell growth and PHBV production, 2) study the effects of feedstock type and substrate loading on the production and yield of cell biomass and PHBV, and 3) select the representative feedstocks based on improved PHBV yield and HV content, which are to be used for process development in the following chapters.

4.3 Materials and methods

4.3.1 Feedstock collection and characterization

Four types of substrates, including fermented food waste, food waste hydrolysate, lactose powder, and delactosed permeate (DLP), were used to represent feedstocks that contain either VFA or sugars as the major carbon source. The fermented food waste sample was collected from the acidification bioreactor of the Renewable Energy Anaerobic Digesters (READ) located at UC Davis campus. The acidification reactor was operating at 50 to 55 ℃ with a pH at 4 to 5 to facilitate anaerobic fermentation of food waste. The food waste complex consisting of vegetables, and fruits from local grocery stores, along with food scraps from the UC Davis dinning commons, was converted into small molecules including VFA, lactic acid, ammonium, and phosphorous nutrients in the reactor. The fermented food waste sample was taken from the effluent outlet of the reactor after passing through an onsite screw press with 1mm screen to remove larger particles and recover soluble nutrients.

The food waste hydrolysate sample was collected from California Safe Soil LLC, an organics processing business located in McClellan, California. The liquid hydrolysate was produced from a series of enzymatic hydrolysis, pasteurization, and filtration steps to convert food waste including fruits, vegetables, and fish leftovers to sugars, nitrogen and phosphorous nutrients. The food waste hydrolysate was sold as the liquid biofertilizer applied to crop fields.

Whey sugar (lactose powder, LP) and DLP were collected from Hilmar Cheese Co., Hilmar, California. LP and DLP are both byproduct streams from the whey processing units, where LP is the whey sugar crystals that formed during the evaporation process of whey permeate, and DLP is the liquid remaining after the lactose recovery. Both feedstocks have lactose as the main carbon nutrient; DLP has more nutrients of nitrogen, phosphorous, and minerals than lactose powder.

4.3.2 Feedstock pretreatment

4.3.2.a Membrane filtration

The fermented food waste and food waste hydrolysate contained suspended particles which are mainly from the undigested or unhydrolyzed food particles. These suspended particles can introduce impurities to the PHA product in the downstream extraction and purification processes, therefore, they should be removed in the upstream processes to minimize the appearance in the cell broth. Microfiltration was adopted to remove suspended particles from the two types of food waste derived feedstocks. The filtration was facilitated by a benchtop cross-flow ultrafiltration unit (Model 1230060, Sterlitech Co., Auburn, Washington). The unit consists of a heavy-duty pump

(Hydra-Cell^{TM}), a 4 ℃ refrigeration unit, a main filtration chamber with the installation of a 0.22 μm PVDF flat-sheet membrane (Synder), and piping and valves for the liquid transfer of inflow, retentate and permeate streams (shown in Figures 4.2 and 4.3). The fermented food waste and food waste hydrolysate were used as the feed inflow streams and circulated through the filtration chamber. During the process, the suspended particles were concentrated continuously in the retentate stream, and the majority of soluble nutrients were recovered in the outflow of the permeate stream, which was also free of suspended particles. The fermented food waste permeate (FWP) and food waste hydrolysate permeate (FWH) obtained from this process were used as the substrates in the subsequent microbial cultivation and PHA production experiments.

Figure 4. 2 Collection and pre-treatment of fermented food waste feedstock

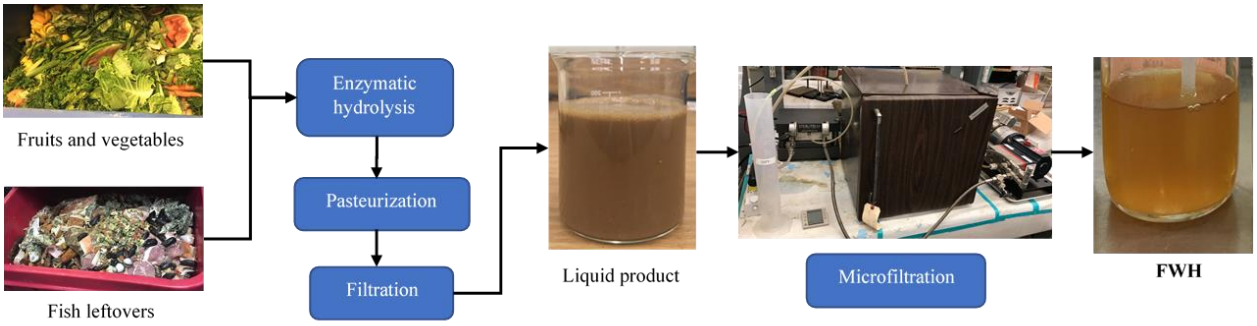

Figure 4. 3 Collection and pre-treatment of food waste hydrolysate feedstock

4.3.2.b Enzymatic hydrolysis

Because *H. mediterranei* cannot utilize lactose directly (Pais et al., 2016), a pretreatment step using lactase enzyme to hydrolyze lactose into monosaccharides was adopted for both cheese process byproduct feedstocks. Prior to enzymatic hydrolysis, lactose powder was dissolved in deionized water to obtain a lactose concentration of 40g/L. The DLP was diluted with deionized water to the same level of lactose concentration. Preliminary experiments were conducted to determine the suitable enzyme loading and reaction time on the two feedstocks: the diluted lactose solution and DLP solution were loaded into 50 mL reactors with 60% as working volume. The reactors were housed in an incubator with a controlled temperature at 40 ℃ and continuous shaking at 180 rpm. The pH of the lactose powder and DLP solutions were around 4 to 5 initially and there was no pH adjustment in the experiments. Lactase (Maxilact® LGi 5000) was added to the solutions with three loadings including 0.005, 0.01, and 0.02 g lactase/g lactose. The hydrolysis reaction was conducted for 0, 1, 2, 3, and 4 hours, and 0.5 mL samples were taken for sugar measurement at each time point of the reaction. The appropriate levels of enzyme loading and reaction time were determined to achieve a lactose conversion rate of at least 90%. After enzymatic hydrolysis, DLP hydrolysate was subjected to microfiltration with the same level as described previously to remove leftover solids in the solution, as shown in Figure 4.4. The enzymatic hydrolysate solutions of lactose powder (LP) and DLP were used respectively as the sole substrate in the subsequent cell cultivation and PHA production experiments. The four feedstocks after pretreatment were characterized for sCOD, total nitrogen, total phosphorous, and individual nutrient profiles.

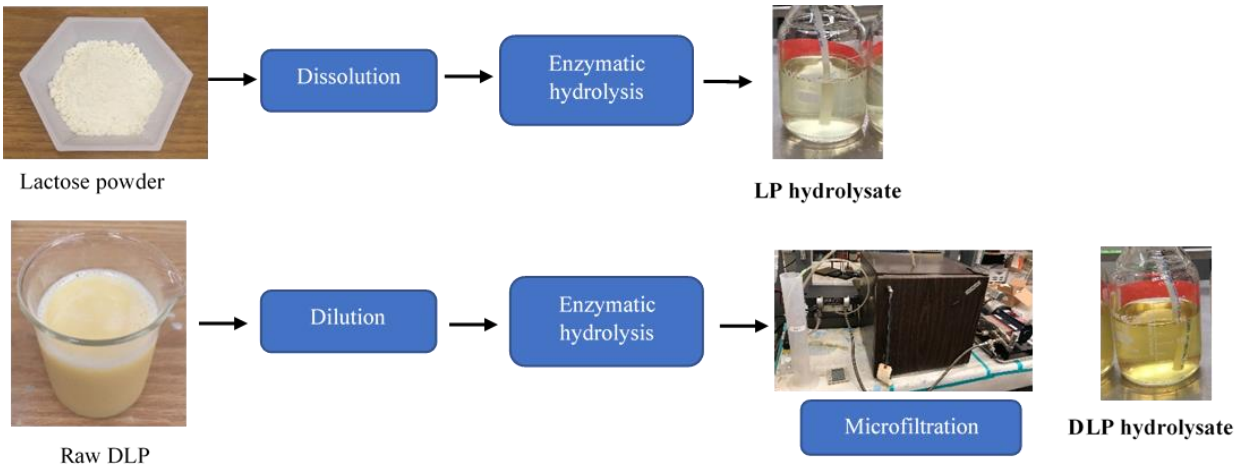

Figure 4. 4 Pretreatment of cheese whey byproducts as feedstocks

4.3.3 Microbial culturing and PHBV production

The four types of pretreated feedstocks (FWP, FWH, LP, and DLP) were used as substrates to culture *H. mediterranei* for PHBV production. Each substrate was loaded at two levels: 22.5 and 45 g/L sCOD to study the effects of substrate type and loading on the cell growth and PHBV production. Minimum saline medium (defined in previous chapter, MSM) was added to the culture medium to provide enough salinity for cell growth. Different from the rest of the feedstocks, DLP by itself has adequate levels of calcium and potassium comparable to MSM; therefore, the salts of these two ions were not added to DLP to eliminate overdosing that may cause precipitation in the medium. There were no additional loadings of nitrogen or phosphorous sources to FWP and FWH because these two substrates naturally contained adequate amounts of the nutrients. Extra amounts of NH_4Cl and KH_2PO_4 were added to LP and DLP to provide sufficient levels of N and P. 50 mM $NaHCO_3$ was added initially as a buffer.

The active cells of *H. mediterranei*, propagated by following the standard procedures described in the previous chapter, were harvested at the late exponential growth phase through centrifugation and resuspended in the MSM solution as the seed solution. The seed was used as the inoculum to give an initial optical density (OD) of around 0.5 for all experiments. Glass bioreactors of 250 mL total volume were used to culture cells with a working volume of 200 mL. The bioreactors were housed in an incubator with controlled temperature at 37 ± 0.5 ℃. Forced aeration was provided for all bioreactors with air humidified by bubbling at a flowrate of 100 mL/min through deionized water prior to the bioreactor. The experimental setup is shown in Figure 4.5. The pH of the cell broth was maintained at around 7 ± 0.2 during the whole cultivation period for each substrate, with the use of 10 M NaOH solution or HCl solution. The microbes were cultured for 216 to 528 h until the OD of the cell broth remained stable at the stationary growth phase.

Figure 4. 5 Experimental setup for cell culturing

4.3.4 Determination of cell mass and growth kinetics

The cell growth was monitored throughout the entire cultivation period by collecting 2 mL of cell broth at different time points. Samples were centrifuged at 10,000 rpm for 10 min, the cell mass was resuspended in MSM solution, and the optical density (OD) was analysed at 520 nm (Lillo and Rodriguez-Valera, 1990). The cell growth rate was obtained as the slope of ln (OD) versus time. The cell dry mass (CDM) was determined as the volatile suspended solids (VSS) of cell broth: 20 mL of cell broth was sampled and subjected to centrifugation at 8,000 rpm for 20 min. The cell mass was washed with MSM solution twice and subjected to VSS measurement (APHA, 2012). The cell growth kinetics were curve-fitted based on the Monod model (Monod, 1949):

$$\mu = \frac{\mu_m S}{K_S + S} \tag{4.1}$$

where, μ is specific growth rate (h^{-1}), μ_m is maximum specific growth rate (h^{-1}), S is total carboxylate loading (g Ac/L), *Ks* is the half velocity constant (g/L).

4.3.5 PHBV extraction and quantification

The extraction of PHA was achieved following a method developed by Escalona et al. (1996) with modifications: the 20 mL cell broth was sampled and centrifuged at 8,000 rpm, 4℃ for 20 min. The cell mass was washed with 0.1% sodium dodecyl sulfate (SDS) solution and deionized water. The washed PHA polymers were dried in an oven at 105 ℃ for 4 h and the dry weight was measured according to a standard method of total solids (TS) (APHA, 2012). The extracted PHA was dissolved in 2 mL dichloromethane and 2 mL acidic methanol (3% v/v H_2SO_4), with 1g/L benzoic acid as internal standard. KIMAX 12 mL culture tubes with rubber lined caps were used

for this preparation. The tubes with solution were placed in a Hach DRB200 digital reactor block (Hach Corp., Loveland, Colorado) at 105 °C for 4 h and cooled to room temperature. The solution was mixed with 1 mL deionized water and settled until complete phase separation was observed. The organic phase was then transferred to a clean vial for quantification. PHBV with 12% hydroxyvalerate (HV) (Sigma-Aldrich) was used as the standard PHBV chemical for analysis. The samples were analysed using a gas chromatograph (GC) method developed based on methods reported in the literature (Braunegg et al., 1978; Lemos et al., 1998; Oehmen et al., 2005) with modifications. The GC (Agilent 6890N, Santa Clara, California) equipped with a flame ionization detector (FID) was employed and a HP-5 capillary column (Agilent, 2016) was used with helium as carrier gas. Details of this method were: inlet temperature and pressure: 230℃, 16 psi; total flowrate: 30 mL/min; split ratio: 8:1; oven temperature: initial 100℃ for 2 mins; ramping from 100 to 124℃, with a rate of 8℃/min; holding 124℃ for 1 min. FID temperature was 240℃, with 40 mL/min of H_2 flow and 450 mL/min of air flow.

Based on the measured results, the PHBV yield was calculated as the mass of PHBV produced divided by the mass of substrate consumed. Two types of substrates were used in the calculations: glucose and total carboxylates (g Ac/L).

$$Y_{PHBV} = \frac{\Delta m_{PHBV}}{\Delta m_{carbon\ source}} \tag{4.2}$$

The cell PHBV content was calculated as the percentage of PHBV in the total CDM, described as g VSS/L:

$$PHBV\ (\%) = \frac{m_{PHBV}}{m_{CDM}} * 100 \tag{4.3}$$

The percentage of HV unit in the PHBV polymer, which indicates the elasticity of the plastic material, was determined based on the mass ratio between HV and the sum of HV and HB units as measured by the GC method described previously:

$$HV(\%) = \frac{m_{HV}}{m_{HB}+m_{HV}} * 100 \quad (4.4)$$

4.3.6 Measurement of substrate properties

The initial and final substrate contents including sCOD, total N, total P, major carbon profiles, and ash content of individual feedstock were measured. Prior to analysis, 2 mL of cell broth was collected and centrifuged at 10,000 rpm for 10 min; the supernatant was then filtered through a 0.22 μm membrane for major particle removal. The filtration samples were measured for the contents of sCOD, total N and total P using standard chemical kits (TNTplus Vial test, Hach Corp., Loveland, Colorado). Lactic acid and VFA were measured by high-performance liquid chromatography (HPLC) following the analytical method described previously (Sluiter, 2008).

4.3.7 Statistical analysis

All the experiments were conducted in triplicates, and the mean value and standard deviation (SD) of each assay were calculated for the triplicates. The final values were presented as mean ± SD. Two-way Analysis of Variance (ANOVA) and Turkey test was performed for the significant levels of the factors and group comparison. The software Origin Pro (OriginLab, 2021) was used for all data analysis in this study.

4.4 Results and discussions

4.4.1 Characterization of feedstocks

As listed in Table 4.1, the four types of feedstocks were characterized for the concentrations of major nutrients. Although both FWP and FWH were derived from similar food waste, they had different types of nutrients due to the treatment processes: FWP was from anaerobic fermentation and contained high amounts of lactate, acetate, propionate, and other VFAs as the soluble nutrients produced from the decomposition of food waste. FWH was produced from enzymatic hydrolysis, so it has various types of sugars including glucose, fructose, maltose, and starch as the major soluble carbon sources, which are the common hydrolytic products derived from mixed food waste (Jinno et al., 2018). The sCOD content of FWH is 50% higher than FWP, which may be due to difference in the commercial food waste treatment facility operations.

As the two feedstocks derived from the same commercial cheese whey processing unit, LP and DLP share similar nutrient types but different concentrations. Lactose is the dominant carbon source in both feedstocks. The dry powder form of LP contains over 98% (wet basis, w.b.) of lactose; the liquid DLP is 12.5% (w.b.) lactose although on a water-free basis the DLP is 66% (w.b.) lactose. DLP has higher contents of crude protein, minerals (ash), and total P due to the greater purification in the precipitation of LP.

Table 4. 1 Characterization of feedstocks in terms of main nutrient profile

FWP	**% (w.b.)**	**FWH**	**% (w.b.)**	**LP**	**% (w.b.)**	**DLP**	**% (w.b.)**
Lactate	2.9	Glucose	7.5	Dry matter	99.7	Dry matter	19.0
Acetate	0.6	Fructose	5.1	Water	0.3	Water	81.0
Propionate	1.1	Lactose	0.2	Lactose	98.1	Lactose	12.5
Butyrate	0.01	Maltose*	2.7	Glucose	0.8	Glucose	0.7
Valerate	0.2	Starch*	1.4	Crude protein	0.5	Crude protein	1.6
Total VFA	2.0	Sucrose	0.04	Ash	0.2	Ash	4.8
Total N	1.3	Total N	1.7	Total N	0.7	Total N	2.3
P	0.16	P	0.35	P	0.05	P	0.46
sCOD**	15.0	sCOD**	22.5	sCOD**	N/A	sCOD**	56.4

*: data obtained from a published analysis on the same feedstock (Jinno et al., 2018)

**: the unit for sCOD is g/L.

4.4.2 Enzymatic hydrolysis of LP and DLP

Because *H. mediterranei* cannot utilize lactose directly, enzymatic hydrolysis was employed to break down lactose into monosaccharides consisting of glucose and galactose. Different levels of lactase enzyme loading and reaction time were tested to determine the appropriate levels of these two parameters to achieve at least 90% hydrolysis of lactose in the lactose powder and DLP. The extent of lactose hydrolysis over time for the two feedstocks is shown in Figure 4.6. For

enzymatic hydrolysis of LP, the hydrolysis increased with reaction time for lower enzyme loadings of 0.005 and 0.01 g/g lactose; and the conversion percentage was 47.3 ± 0.7% and 60.2 ± 0.6% respectively after 4 hours of reaction. With a higher enzyme loading (0.02 g/g lactose), the hydrolysis extent reached and remained around 90% after 2 hours reaction, and the final conversion percentage was 91.6 ± 0.0% after 4 hours. The enzymatic hydrolysis of lactose in DLP suggested a similar trend but achieved a slightly higher conversion percentage for each enzyme loading. With all three enzyme loadings, the hydrolysis extent of lactose in DLP increased with reaction time; and the final conversion percentages after 4 hours of reaction were positively related to the enzyme loading (p-values were 8.99E-6 for LP and 0.0146 for DLP): 57.2 ± 8.4% for 0.005 g enzyme/g lactose, 78.5 ± 0.3% for 0.01 g enzyme/g lactose, and 90.3 ± 0.6% for 0.02 g enzyme/g lactose.

Given the goal to obtain at least 90% conversion of lactose for both LP and DLP, the suitable levels of lactase enzyme loading and reaction time were selected to be 0.02 g/g lactose and 4 hours, for the specific lactase enzyme and controlled temperature at 40 ℃. Therefore, the same conditions were used in preparing the hydrolysates for LP and DLP in the following experiments.

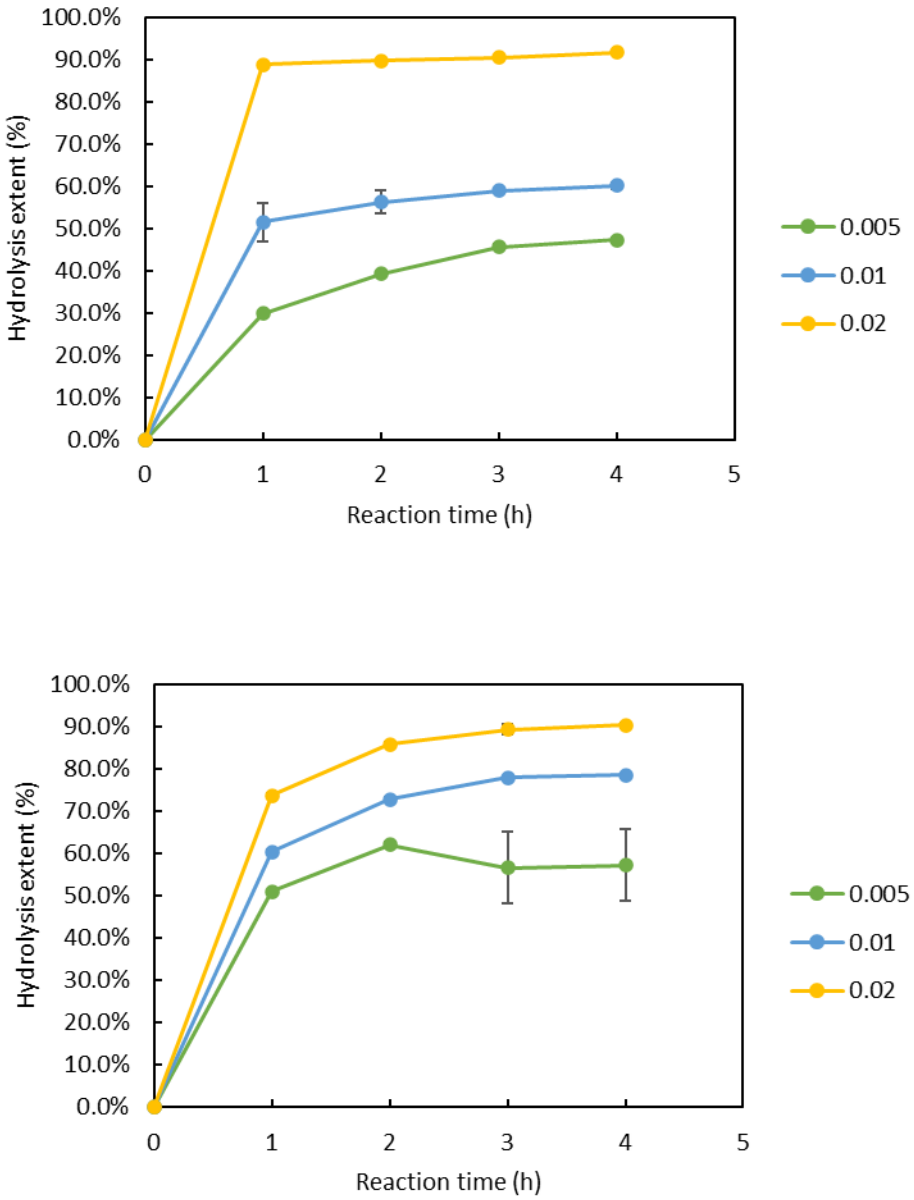

Figure 4. 6 the extent of lactose hydrolysis with different enzyme loadings (0.005, 0.01, and 0.02 g lactase/g lactose) for LP (top) and DLP (bottom)

4.4.3 Cell growth and PHBV production by *H. mediterranei*

4.4.3.a Effects of feedstock type and loading on cell growth and CDM production

H. mediterranei were able to grow in all four types of feedstocks with different substrate loadings. As shown in Figure 4.7, the color of the initial medium varied among feedstocks: brown for FWP, yellow to orange for FWH, light yellow for LP hydrolysate, and yellow for DLP hydrolysate. The color variance was due to the intrinsic color of the soluble components of the feedstocks. After culturing for different amounts of time, the color of all media transitioned to different shades of pink due to the C50 carotenoids present in *H. mediterranei* (Giani et al., 2021).

The time profiles of cell growth (OD vs time) with different feedstocks and loadings were illustrated in Figures 4.8 and 4.9. Compared to FWH, the higher loading of FWP (45 g/L sCOD) achieved the highest OD given the same period of culturing time. When FWP was used as the sole substrate, the final OD of cell broth doubled with a doubling of substrate loading: the final OD from 45 g/L sCOD of FWP was 13.9 ± 0.5 and it was around 7.6 ± 0.1 from 22.5 g/L sCOD of the same feedstock. Different from FWP, the effect of substrate loading was not apparent for FWH because the final cell broth OD from 22.5 g/L sCOD loading was close to that from 45 g/L sCOD loading. However, the OD from 22.5 g/L sCOD of FWH plateaued and remained relatively stable around 8 halfway through the culturing period, while the rest of groups had time-dependent OD increase or decrease throughout the whole culturing time.

As for the cheese byproduct feedstocks, the final cell broth OD from LP was close to that from DLP given the same sCOD loadings, and a higher substrate loading gave a higher final OD for

both substrates: it was around 10 from 22.5 g/L sCOD of LP and DLP; and around 16.5 from 45 g/L sCOD. However, with a higher substrate loading, cells were growing faster in LP than DLP: the total culturing time from 45 g/L sCOD of DLP was more than twice that from the same loading of LP. The prolonged cultivation time may be due to some minerals present in the DLP with high concentrations that may be inhibitory to cell growth of *H. mediterranei*. One example can be a substantial amount of aluminum present in DLP that can be toxic or inhibitory to microbial growth (Piña and Cervantes, 1996). Compared to LP, DLP has a more complex composition of nutrients, which may require cell adaptation.

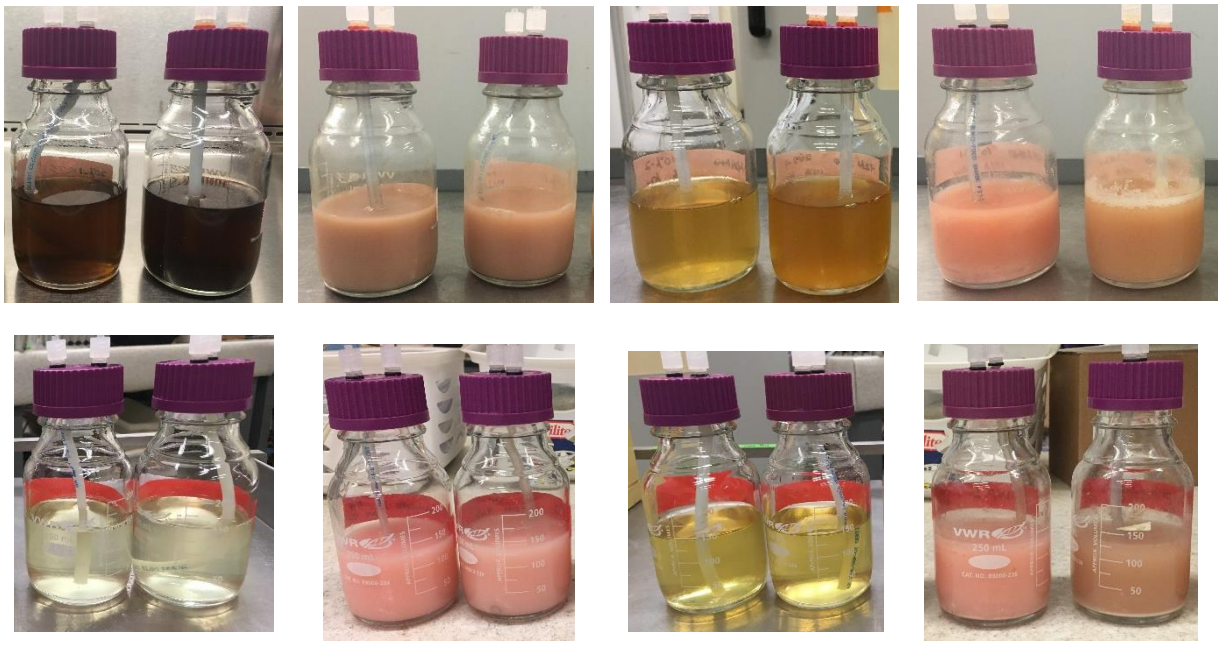

Figure 4. 7 Initial culture medium and final cell broth with two substrate loadings for: FWP (top two left); FWH (top two right); LP (bottom two left); DLP (bottom two right)

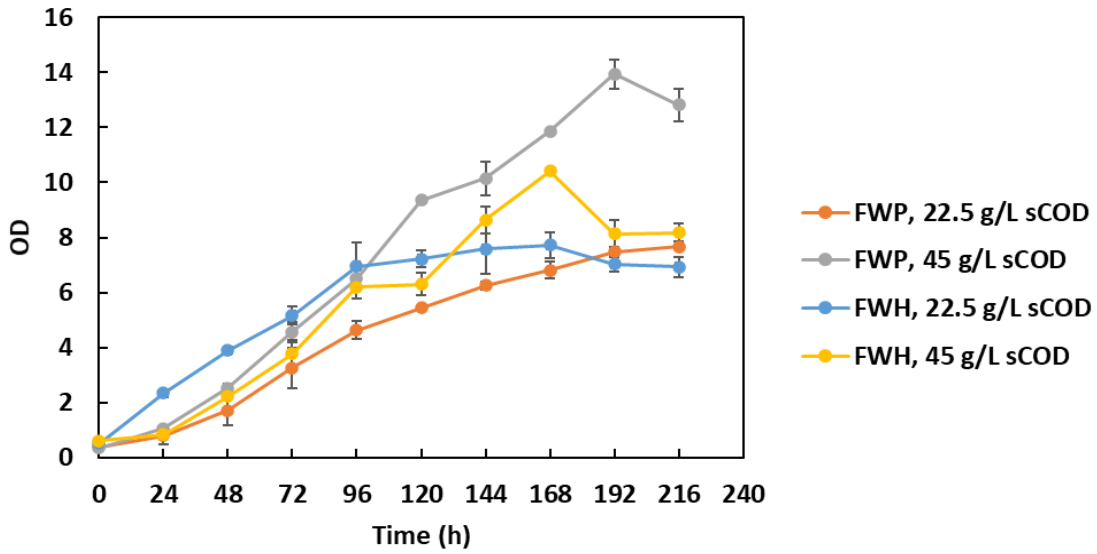

Figure 4. 8 Cell growth curves of *H. mediterranei* with food waste derived substrates

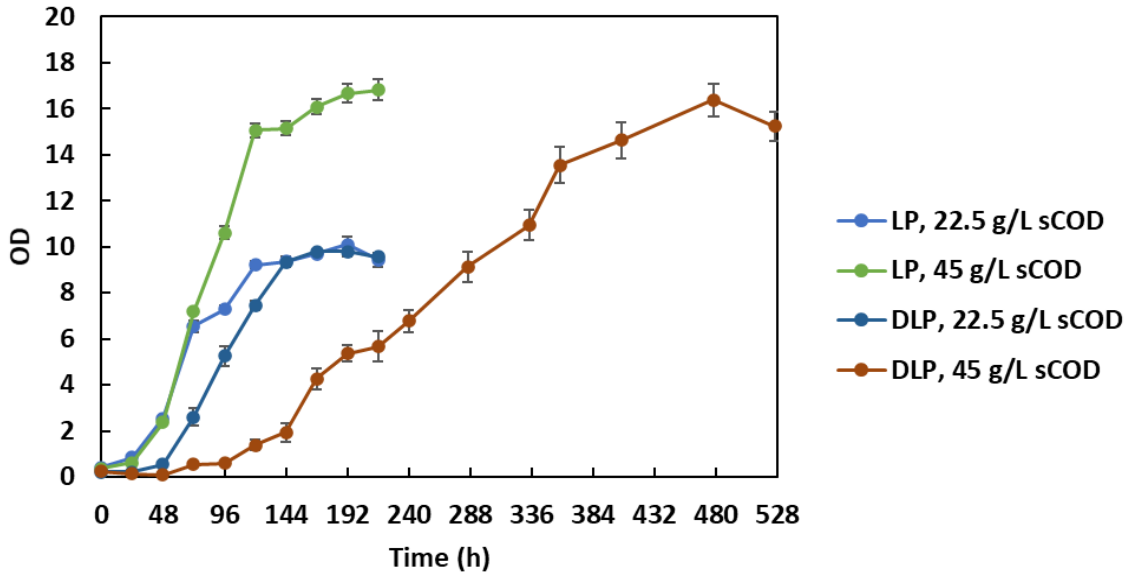

Figure 4. 9 Cell growth curves of *H. mediterranei* with cheese byproducts derived substrates

Corresponding to the final cell broth ODs, the CDM production and yield from different feedstocks with two substrate loadings are shown in Figure 4.10. Among all feedstock types and

loadings, 45 g/L sCOD of FWP and the same loading of LP gave the highest final CDM concentrations (around 6 g/L). The CDM production from 45 g/L sCOD of LP was significantly higher than DLP with both loadings. With the same substrate loading, the CDM production from FWP was not significantly different from FWH. For FWP and LP, the CDM production increased significantly with higher substrate loading, which alligned well with the cell growth curves discussed previously. However, the CDM yields from different loadings were not significantly different for the same substrate except for DLP. The highest CDM yield from food waste derived feedstocks was found to be around 0.36 g/g sCOD from FWH with a loading of 22.5 g/L sCOD; and the highest CDM yield from cheese byproducts feedstocks was around 0.31 g/g sCOD from DLP with a loading of 22.5 g/L sCOD. Statistical analysis results are shown in Appendix C.

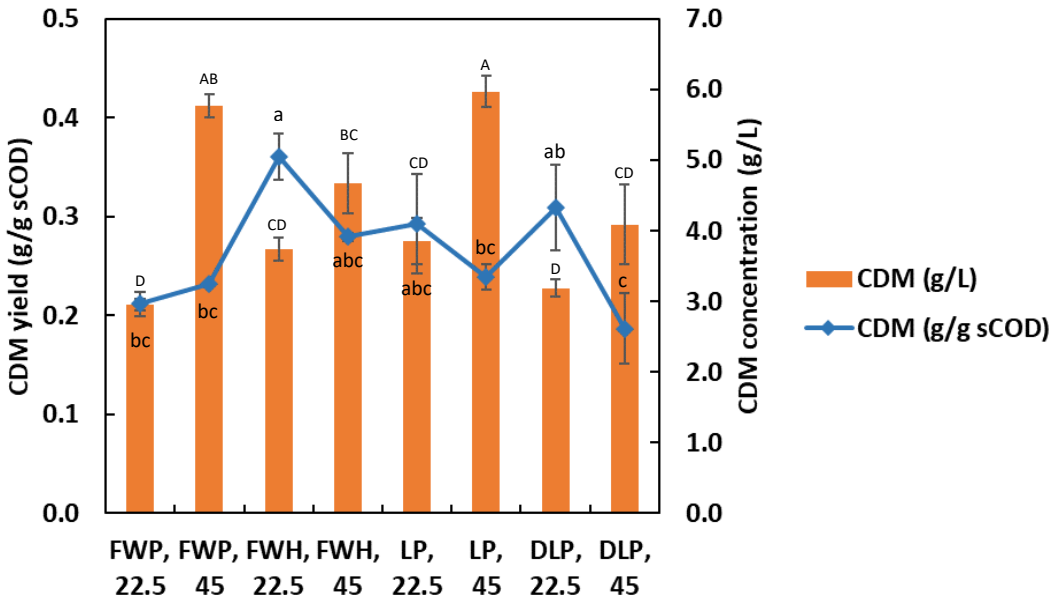

Figure 4. 10 CDM production and yield by *H. mediterranei* with different substrate types and loadings

(Uppercase letters represented group comparison on CDM concentration and lowercase letters represented group comparison on CDM yield; the same letters indicated that the differences were not significant at $p < 0.05$)

4.4.3.b Effects of feedstock type and loading on PHBV production

Figure 4.11 illustrates the production and yield of PHBV with different feedstock types and loadings. For each feedstock, a higher substrate loading gave a significantly higher final PHBV concentration than a lower substrate loading. The highest PHBV production was 3.92 ± 0.08 g/L, which was achieved from FWP with 45 g/L sCOD loading. Feedstocks derived from food waste with 45 g/L sCOD loading resulted in significantly higher final PHBV concentrations than feedstocks derived from cheese processing byproducts. The highest PHBV yield was 0.16 to 0.17 g/g sCOD, which was achieved from 45 g/L sCOD loading of FWP and FWH. As for food waste feedstocks, substrate loading had influenced both the final concentration and yield of PHBV: the final PHBV concentration almost doubled from 22.5 g/L sCOD loading to 45 g/L sCOD loading for both FWP and FWH; and the PHBV yield also increased with a higher substrate loading for both feedstock types. A similar trend was also observed for the PHBV concentrations produced from LP and DLP; however, the effect of substrate loading on the PHBV yield from LP and DLP was not significant. Statistical analysis results are shown in Appendix C.

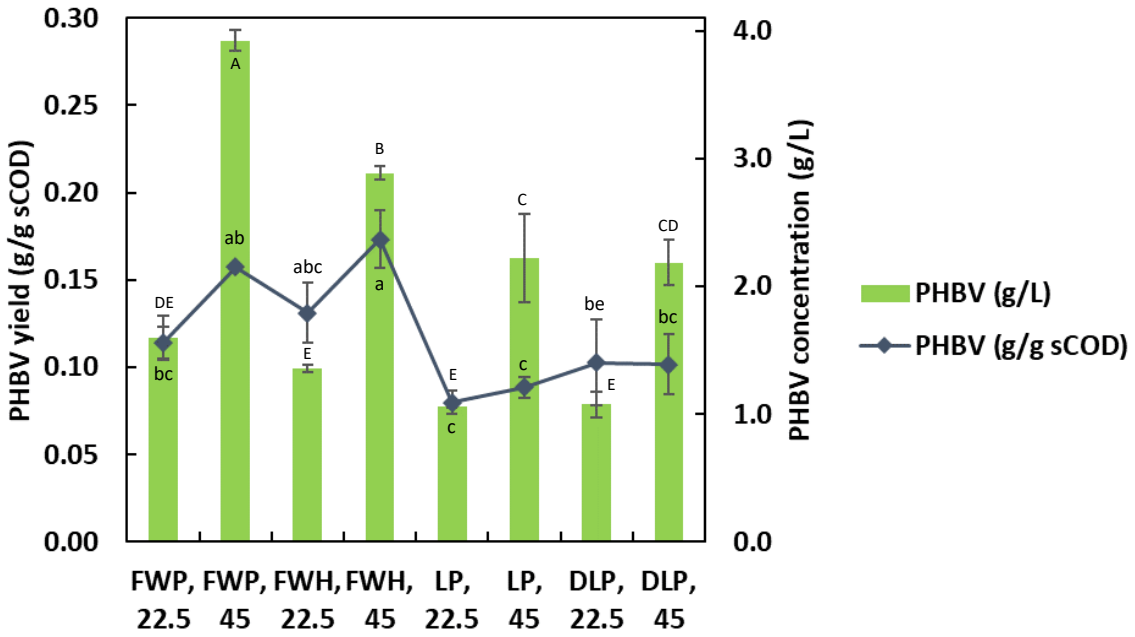

Figure 4. 11 PHBV production and yield by *H. mediterranei* with different substrate types and loadings

(Uppercase letters represented group comparison on PHBV concentration and lowercase letters represented group comparison on PHBV yield; the same letters indicated that the differences were not significant at $p < 0.05$)

As an important indicator of the capability to accumulate PHA by the cells, PHBV in-cell concentration of CDM describes what percentage of the whole cell mass accounts for the PHBV. Figure 4.12 compares the PHBV content of CDM produced from different feedstock types and substrate loadings. Among all groups, FWP and FWH with 45 g/L sCOD loading gave the two highest PHBV contents, which were 68 ±1% and 62 ±1% of CDM, respectively. The higher PHBV content from FWP can be because VFA and lactate are the direct precursors of PHBV synthesis compared with monosaccharides, which leads to more direct carbon flows towards PHBV

formation rather than diverting to the formation of other metabolites such as extracellular polymeric substances (EPS) (Wang and Zhang, 2021). Both as sugar-based substrates, 45 g/L sCOD of FWH gave a significantly higher PHBV content than LP at the same loading. This may be due to the versatile carbon sources (different types of sugars) in FWH which promote the PHBV synthesis than simple carbons sources (glucose and galactose) in LP hydrolysates. For instance, fructose, which is one of the major sugars in FWH, can result in a higher PHBV yield by *H. mediterranei* than galactose (Ghosh et al., 2019). Considering the PHBV contents from cheese byproduct feedstocks, with the same substrate loading, the PHBV content derived from LP was not significantly different from DLP. This may be because both feedstocks share very similar carbon profile where lactose prevails.

The substrate loading did influence the PHBV content of CDM significantly for FWH and DLP; however, the effect was not significant for FWP and LP. When using FWH and DLP as substrate, the PHBV content of cells increased with a higher substrate loading, suggesting that cells of *H. mediterranei* tends to synthesize and accumulate more PHBV when there is more available substrate present in the media. Similar results have been reported by previous studies on different substrates (Ferre-Guell and Winterburn, 2017; Lillo and Rodriguez-Valera, 1990). However, there are also some studies reporting a decrease of PHBV content or production with higher substrate loadings due to substrate inhibition or toxic compounds present in the substrate (Bhattacharyya et al., 2012; Cui et al., 2017b). Therefore, further research interest is needed to determine the substrate loading level for each feedstock to obtain the optimal PHBV content of CDM and compare to the level to achieve the highest PHBV production.

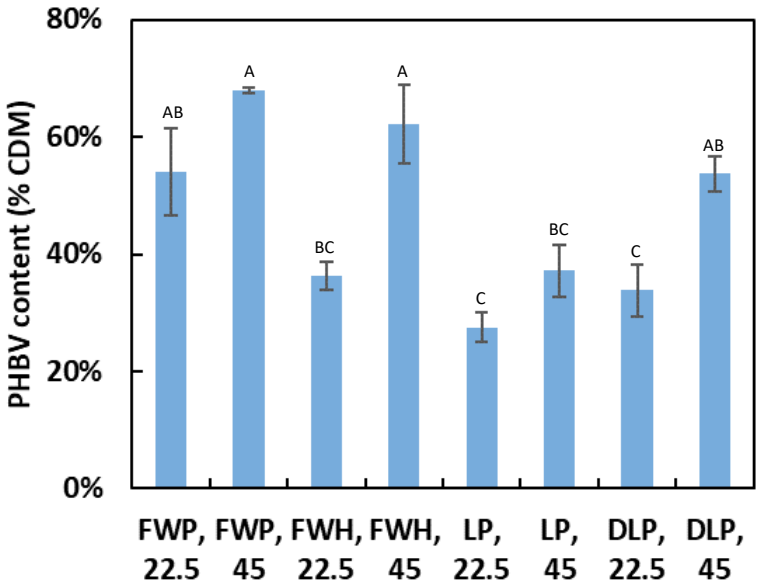

Figure 4. 12 PHBV content of CDM by *H. mediterranei* with different substrate types and loadings

(The same letters indicated that the differences were not significant at $p < 0.05$)

4.4.3.c Effects of feedstock type and loading on PHBV composition

The fraction of 3-hydroxyvalerate (HV) monomers in PHBV polymer directly affects the thermal and mechanical properties of the bioplastic material (Anjum et al., 2016). The 3-hydroxybutyrate (HB) monomers are hardness-expressing units, and the copolymers with high contents of HB are commonly stiff and brittle. The HV monomers are softness-expressing units, which introduce elasticity and flexibility to the copolymer material (Han et al., 2015; Taguchi and

Doi, 2004). Therefore, it is usually desirable to obtain a high percentage of the HV in the PHBV to widen its application as thermoplastic products.

Figure 4.13 compares the HV content of PHBV produced from different feedstock types and loadings. The HV contents derived from FWP with both substrate loadings were significantly higher than FWH. It is probably due to the high content of propionate in FWP (over 50% of total VFAs), which is the direct precursor of HV units in PHBV synthesis. LP hydrolysate (both substrate loadings) and a lower loading of DLP resulted in the second highest HV content, which was around 17% of PHBV. The HV contents derived from FWH and a higher loading of DLP were below 15%. With two different substrate loadings, the HV content of PHBV from FWP, FWH, and LP remained relatively stable; however, a higher loading of DLP caused a decrease in HV content, which may be due to the consumption of HV during the prolonged culturing time.

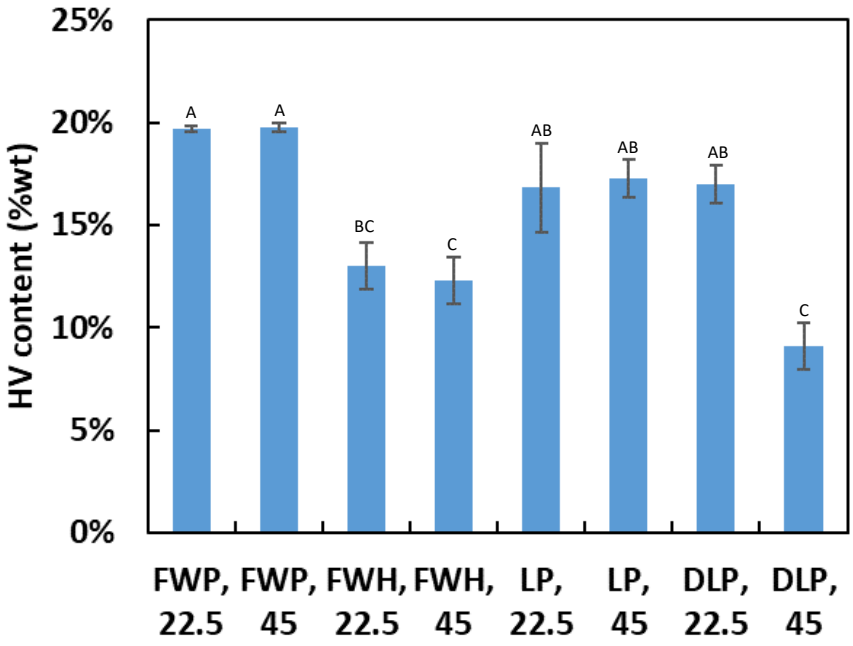

Figure 4. 13 HV contents by *H. mediterranei* with different substrate types and loadings

(The same letters indicated that the differences were not significant at $p < 0.05$)

4.5 Conclusions

Four different types of feedstocks including fermented food waste permeate (FWP), food waste hydrolysate (FWH), whey sugar (lactose) powder (LP), and delactosed permeate (DLP), were pretreated and tested as independent substrates with by *H. mediterranei* for cell growth and Poly(3-hydroxybutyrate-co-3-hydroxyvalerate) (PHBV) production. Cells can grow and synthesize PHBV from all the four feedstocks. With the same substrate loading, fermented food waste permeate (FWP) resulted in a higher production of PHBV containing a higher 3-hydroxyvalerate (HV) content than FWH. Similarly, LP led to faster cell growth, PHBV production and higher HV content than DLP. Substrate loading influences the PHBV production and PHBV content of cell dry mass (CDM) in all feedstock types, and HV content of PHBV in FWP, FWH, and LP. Because of the superior PHBV productivity and composition, FWP and LP were selected as feedstocks for further system analysis and development.

Chapter 5. Process Development of Polyhydroxyalkanoates Production by *Haloferax mediterranei* Utilizing Fermented Food Waste from Commercial Anaerobic Digesters

5.1 Abstract

Production of conventional plastics is unsustainable due to the use of non-renewable fossil carbon feedstocks, the emissions of greenhouse gases, and the massive plastic waste at disposal. Polyhydroxyalkanoates (PHA) are a family of biodegradable plastic materials used as a replacement for conventional plastics in various applications. Renewable PHA is produced through microbial fermentation of renewable feedstocks. The high production cost of PHA, which is mainly due to costly feedstocks, is the current bottleneck for market growth. To reduce the production cost, this study has developed an integrated PHA production system that utilizes fermented food waste from commercial anaerobic digesters as feedstock. The effects of feedstock type, substrate loading, and aeration rate have been studied and the optimum levels (FWP 1, 40 g/L sCOD, and 2.5 vvm) have been determined to yield the highest productions of cell mass and PHA. A 6-L benchtop bioreactor system has been designed, constructed, and operated to demonstrate the integrated PHA production system from food waste. Through the dynamic monitoring by this bioreactor system, it was found that the dissolved oxygen level of cell broth dropped dramatically to below 20% sat. during exponential growth phase with a fixed aeration rate. A strategy of maintaining a higher level above 50% sat. resulted in faster cell growth but led to apparently lower final cell densities and PHBV concentrations. A novel approach has been developed to recycle and reuse the spent salts within the system, which will reduce the costs of purchasing raw materials and wastewater treatment and disposal. The spent saline medium (SSM), after the treatment by H_2O_2 and concentrated to a brine solution through rotary evaporation, has been successfully reused for four consecutive batches, where both 80% and 90% SSM recycling

strategies yielded comparable cell growth and PHA production to the original batch. The PHA production system developed in this study has the potential for practical application in the current bioplastic industry. The additional revenue from PHA production can help promote a circular economy in the food system, increase the market share of bioplastics, and benefits organic waste management in general.

Keywords: Process development, polyhydroxyalkanoates, food waste, spent salts recycling, *Haloferax mediterranei*

5.2 Introduction

Plastic products are important commodities on a global scale, which are frequently used in almost every aspect of our lives. The global plastic production is estimated to be 370 million ton per year, of which around 99% are derived from fossil carbon feedstocks (European Bioplastics, 2018). There are around 275 million tons of plastic waste generated every year in the world, with up to 55% ending up in landfills or the natural environment (Geyer et al., 2017). Since petroleum derived plastics are not readily degraded by microorganisms, plastic wastes have tremendously affected ecosystems and remain a major problem globally.

As an emerging alternative, polyhydroxyalkanoates (PHA) is a family of high-value polyesters with properties of thermoplastics and is one of the major materials used for the manufacturing of biodegradable plastics (Reddy et al., 2003). PHA has been commercialized since early 1990s and widely used in various applications, including packaging films, containers, medical materials, nutritional supplements and biofuels (Chen, 2009). PHA market was estimated to be $ 720 million

in 2020 (Aeschelmann and Carus, 2015). However, one major barrier for the large-scale productions is commonly recognized as the high substrate cost, especially the cost of carbon sources for the microbes that synthesize PHA (Nielsen et al., 2017). Leong et al. (2017) found that feedstock cost contributes over 40% of the total annual production cost through economic modelling. Therefore, many studies have focused on using inexpensive or waste streams as feedstocks to reduce the overall production cost.

Food waste is a potential feedstock for PHA production because of its intrinsically rich organic content and quantity abundance in human society. Approximately 40% of food waste produced in the U.S. is wasted each year (Gunders, 2012). It was also estimated that around 56% of wasted food ended up in landfills, which can cause negative impacts on the natural environment (US EPA, 2017). A pathway towards bioplastic production can potentially create economic benefits by utilizing the massive nutrients in the wasted food; and promote the concept of diverting landfilled food waste to industrial anaerobic digesters for better management. The complex organics in the mixed food waste in general cannot be directly utilized by the PHA-producing microbes, and they often in need of pre-treatment approaches, e.g. hydrolysis and fermentation, to generate precursors for PHA synthesis (Nielsen et al., 2017). One general method that has been used to pre-treat mixed food waste is through acidogenic fermentation, which has been widely applied to those two-stage commercial anaerobic digester facilities. After fermentation, most of studies have endorsed all kinds of mixed microbial consortium (MMC) to produce PHA (Campanari et al., 2017; Colombo et al., 2016; Liu et al., 2008; Shen et al., 2014). However, MMC may have low productivity than pure culture PHA production. Another concern is the possible inhibition effect on microbial growth by the presence of organic acids in fermented food waste (Nielsen et al., 2017). Studies on

utilizing pure culture PHA production from fermented food waste have been scarce. And the development of strategies to increase the productivity is of vital importance.

The fermented food waste, which has rich nutrients e.g. short-chain carboxylates and ammonium, can provide essential carbon, nitrogen and phosphorous sources for microbial cultivation and PHA production (Wang and Zhang, 2020). A well-studied halophilic PHA producer, *Haloferax mediterranei*, was selected for its potential of the economical large scale production using a variety of waste feedstocks (Bhattacharyya et al., 2015; Ferre-Guell and Winterburn, 2018). The saline environment was created to eliminate the need for sterilization and the facilitate an easier PHA extraction process through osmotic shock (Quillaguamán et al., 2010). The PHA produced by *H. mediterranei* has been characterized to be poly (3-hydroxybutyrate-co-3-hydroxyvalerate) (PHBV), which is a type of high-value PHA and have various applications for plastic products. Wang and Zhang (2020) reported that the carboxylate-rich nutrients derived from fermented food waste can provide a yield of up to 0.54 g PHBV/g total acids, suggesting the capability of the strain utilizing fermented food waste as substrate.

The critical parameters involved in cell culturing, including feedstock type, substrate loading and aeration rate, have varied depending on different studies and not been fully understood for the type of halophilic PHA producer. The nutrients derived from fermented food waste can be largely dependent on input feedstocks to the anaerobic digester facilities. The substrate loading can also influence cell growth and PHA production due to possible inhibition effects caused by some organic acid species (Ferre-Guell and Winterburn, 2018) and other compounds such as phenolics and other contaminants in food waste. Wang and Zhang (2020) found that the PHA synthesis was

a growth-associated process when utilizing nutrients derived from fermented food waste. Therefore, it would be reasonable to obtain the maximum cell growth rate to achieve efficient PHA production, which is particularly important for large production scales to have sound economics. Monod (1949) found that the substrate concentration in the culturing media influences the maximum specific growth rate of microbes; in addition, high substrate loadings, with high concentrations of volatile fatty acids (VFA), may as well inhibit cell growth and PHA production (Wang et al., 2010). Ghosh et al. (2019) reported that the substrate loadings of seaweed hydrolysate had significant impacts on cell mass and PHA production by *H. mediterranei*.

The aeration rate, particularly when the saturation dissolved oxygen (DO) level dramatically decreases in the medium with high salinity, can be critical to the growth of halophilic microbes and PHBV synthesis. The saturated DO of the saline medium with around 19% total salts is 2.50 mg/L at 37 ℃, which is only 37% of the saturated DO (6.73 mg/L) in freshwater (DEP, 2021). Therefore, the same aeration level which provides 20% saturated DO in freshwater may not be able to offer sufficient oxygen to *H. mediterranei*, which can cause limitations to cell growth. There are no universal guidelines for DO level for culturing *H. mediterranei* in literature, and different aeration rate strategies have been adopted among previous studies. Some studies used shaking flasks with various rotation speeds in the ambient atmosphere without forced aeration to culture the microbes (Cui et al., 2017b; Ferre-Guell and Winterburn, 2018; Pais et al., 2016). other studies used various sized bioreactors with forced aeration: Lillo and Rodriguez-Valera (1990) provided 100% DO saturation during the entire culturing period; a 50% DO saturation was maintained during balanced cell growth and the DO dropped to 30% for PHA formation process (Koller et al., 2007); another study maintained a DO level above the critical limit which was 20%

saturation (Lorantfy et al., 2014); in some other studies, a 20% saturated DO or an oxygen partial pressure at 20% of air saturation was maintained with varying aeration rates and agitation speeds (Koller, 2015; Pais et al., 2016). It is important to determine the aeration level that can avoid DO in the high saline medium from being a growth limiting factor. Therefore, this study investigated the effects of feedstock type, substrate loading, and aeration rate on cell growth and PHA production with the use of fermented food waste as substrate, which would provide new insights to the current PHA research and make recommendations to large-scale productions.

The halophilic PHA producer, *H. mediterranei*, requires a consistent salinity around 19% salts to maintain robust PHA production. Previous studies on *H. mediterranei* mostly produce PHA without considering the treatment of saline medium at the end of use. However, wastewater discharge is economically critical to large-scale industrial PHA production. Salts are principle water pollutants which are toxic to freshwater creatures and make water unsafe for drinking, irrigation and other applications (US EPA, 2013). The concentration of chloride ions cannot exceed 1500 mg/L in fresh water bodies (US EPA, 2018). Once into natural water bodies, the salt ions are hard to remove. Therefore, spent saline water recycling and reuse is critical to the system design, which helps reduce salt cost, maintain high PHA yield and avoid water pollution by excessive wastewater discharge.

Among the few studies that have reported the process of recycling spent saline medium or salts, Bhattacharyya et al. (2014) proposed a method of using a hot solution of decanoic acid to precipitate salts from the spent stillage medium, and the salts were further utilized to culture *H. mediterranei* for PHA production. This method was able to recover and reuse 96% of the medium

salts and the recycled batch had a close PHA production to the original batch with fresh salts. However, the method requires over three days as the processing time, which may add to the operating cost in large-scale productions. Another study using hydrolyzed whey permeate as the substrate reported a direct reuse of the spent saline supernatant resulted in a slower specific cell growth rate and a 68% lower final PHA production than the original batch with fresh salts, which may be due to the inhibitory compounds that formed during the prior pasteurization process (Koller, 2015). Therefore, it is of vital importance to propose an efficient approach to recycle and reuse the spent saline medium with high productivity of PHA and less processing cost.

Previous studies have investigated only one batch with the recycled spent saline medium; however, they have not considered the effect of the left-over nutrients that would accumulate in the culturing medium after multiple recycled batches. These accumulating organic compounds can be the residual sugars, short-chain carboxylates, and micronutrients that are not fully consumed by *H. mediterranei*; they can also be cell metabolites that have been produced and accumulated during cell growth, e.g. acetic acid and EPS. Those leftover nutrients can contribute to a substantial amount of COD after multiple batch runs, which can influence cell growth and PHBV production. This study proposed to use chemical oxidation with strong oxidizers such as H_2O_2 as an effective approach to remove COD from the spent saline medium. Chemical oxidation by H_2O_2 has been widely used in the treatment of industrial wastewater for the removal of BOD and COD (Chen et al., 2014; Zaharia et al., 2009). In addition to COD removal, H_2O_2 is known as the oxygen supplier to microorganism in biological treatment facilities because it can decompose naturally into oxygen and water (Zaharia et al., 2009). Therefore, chemical oxidation can be a potential approach to treat spent saline medium if there is any inhibitory compound present.

The objectives of this research were: (1) To develop bioconversion processes and determine the optimum processing parameters of PHBV production from fermented food waste collected from commercial anaerobic digestion facilities; (2) To demonstrate the integrated system of PHBV production with spent saline medium recycling.

5.3 Materials and methods

5.3.1 Feedstock collection and pre-treatment

The feedstock used in this study was the fermented food waste collected from the Renewable Energy Anaerobic Digester (READ), which is an anaerobic digestion facility located at UC Davis campus and has been running to treat 20,000 tons of local food waste per year since 2012. READ has a stable source of food waste, including recycled vegetables and fruits from local grocery stores and leftover food scraps from the dining commons at UC Davis. READ employs the two-stage high-solid anaerobic fermentation/digestion processes. The first stage is a thermophilic anaerobic fermentation process running at 50 to 55 ℃ with a pH of 4 to 5, where food waste is decomposed into short-chain carboxylic acids including lactic acid (La), acetic acid (Ac), propionic acid (Pr), butyric acid (Bu) and other volatile fatty acids (VFA), soluble nitrogen, phosphorous sources, and micronutrient. The second stage is a thermophilic anaerobic digestion process running at 55 ℃ with a pH of 7 to 8, where those nutrients from the previous stage are further converted into biogas with a high content of methane (Zhang et al., 2007). The feedstock used in this study was the fermented food waste that was collected from one of the tanks at the first stage. Prior to collection, the feedstock samples were treated by an onsite screw press to pass through a 1-mm screen; as a

result, a thin slurry was recovered after the removal of most of large particles (shown in Figure 5.1).

Figure 5. 1 Collection of fermented food waste at onsite READ facilities; left: food waste; middle: READ facilities; right: thin slurry of fermented food waste

Two feedstock samples with a volume of 45 L each were collected at two different times of a year. The feedstock samples were transported immediately to the lab after collection and stored in a -10 ℃ freezer until further use. For pretreatment, the feedstock samples were processed through a bench-scale crossflow microfiltration unit (Sterlitech Co.) with a 0.22 μm PVDF flat-sheet membrane (Synder). The temperatures of inflow and outflows were maintained around 4 ℃ by a refrigeration unit and ice bath during the filtration process to minimize the loss of volatile solids (shown in Figure 5.2). Obtained from the microfiltration process, an outflow stream free of suspended particles, also known as the fermented food waste permeate (FWP), was used as the sole substrate for the following PHA production experiments, without any other carbon or nitrogen sources for the cell cultivation.

Figure 5. 2 Pre-treatment of fermented food waste feedstock through membrane filtration; left: bench-scale crossflow microfiltration unit; right: fermented food waste permeate after filtration

5.3.2 Microorganism and culture conditions

The wild-type halophilic archaeon, *H. mediterranei* (ATCC 33500) was used as the microbial PHA producer in this study. The strain was firstly grown in the standard seed medium (including NaCl, 156 g/L; $MgCl_2.6H_2O$, 13 g/L; $MgSO_4$, 9.8 g/L; $CaCl_2.6H_2O$, 1 g/L; KCl, 4 g/L; NaBr, 0.5 g/L, yeast extract, 5 g/L, glucose, 10 g/L and $NaHCO_3$, 2.1 g/L) at 37 ℃ until the cells grew to the late exponential growth phase. The seed broth was centrifuged at 2940 g for 20 mins and resuspended in the minimum salt medium (MSM) (containing NaCl, 156 g/L; $MgCl_2.6H_2O$, 13 g/L; $MgSO_4$, 9.8 g/L; $CaCl_2.6H_2O$, 1 g/L; KCl, 4 g/L; NaBr, 0.5 g/L and $FeCl_3$, 5 mg/L with 10 mL/L trace metal solution SL-6, containing $ZnSO_4.7H_2O$, 100 mg/L; $MnCl_2.4H_2O$, 30 mg/L; H_3BO_3, 300 mg/L; $CoCl_2.6H_2O$, 200 mg/L; $CuCl_2.2H_2O$, 10 mg/L; $NiCl_2.6H_20$, 20 mg/L; $Na_2MoO_4.H_2O$, 30 mg/L) (Ferre-Guell and Winterburn, 2018; Tang et al., 2009). The fresh cells resuspended in MSM were used as the inoculum for the following cultivation experiments.

The pretreated permeates of the two feedstock samples, named as FWP 1 and FWP 2, were used as the sole substrate to supply essential sources of carbon, nitrogen and phosphorous for *H. mediterranei* throughout the study. Based on the intrinsic properties of the FWP, there were three

major cultivation parameters including substrate type, substrate loading, and aeration rate studied for their influences on cell growth and PHA production. Two sets of two-factor factorial experiments were conducted: (1) three levels of aeration rate (in air volume per working volume per minute, vvm): 0.5, 1.5, 2.5 and two levels of FWP 1 loading (in g/L COD): 40, 80 in the first set of experiment; (2) two types of substrate: FWP 1, FWP 2 and four levels of substrate loading (in g/L COD): 20, 40, 60, 80 in the second set of experiment. All experiments were conducted using the identical 250-mL glass bioreactors with 80% as working volume. The bioreactors were housed in an incubator with a controlled temperature at around 37 ℃. Forced aeration was applied to all reactors by using air pumps and the aeration rate was adjusted by using air flowmeters. The air was pre-humidified by water to prevent volume loss and salinity change in the reactor during forced aeration (Wang and Zhang, 2020). As fixed conditions, the MSM was added to create a salinity level around 188 parts per thousand (ppt). Same inoculation level was applied for all reactors to give an initial optical density (OD) around 1.0 at 520 nm wavelength. 50 mM $NaHCO_3$ was added as the buffer at the beginning of experiments. The pH of cell broth was maintained at around 7 throughout the cell cultivation. The pH was monitored daily by a pH meter and was adjusted by using either 3M NaOH solution or 3M HCl solution. The dissolved oxygen (DO) levels of cell broth were monitored daily by a DO probe. The experimental set-up is shown in Figure 5.3. The study used triplicates for replication of experiments. The cells were cultured for 120 to 216 hours until cell growth reached the stationary phase.

Figure 5. 3 Experimental set-up of bioreactors with forced and humidified aeration

5.3.3 Batch PHA production

A bench-top bioreactor system was developed for PHA production from FWP. The system consists of a 6-L feeder tank with overhead mixer; a 6-L Bioreactor with controlled aeration (by compressed air, a humidifier, and an inline air flowmeter) and temperature (by water jacket and insolation); a circulating water bath (equipped with internal pumping and heating-cooling components); a tank connected to the bottom outlet of the bioreactor to harvest cell broth; pumps, tubing and controllers for the inflows and outflows of the system; and data logging units of temperature, pH, and DO. All the tanks of the system were made of plastic materials, with an intention to prevent corrosion by the high-saline medium used for cell cultivation. The schematic design and the physical system are demonstrated in Figure 5.4.

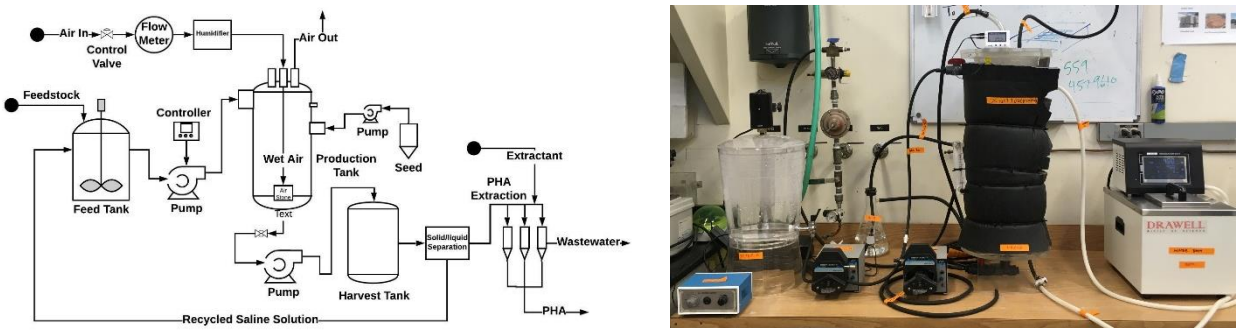

Figure 5. 4 The 6-L benchtop bioreactor system for PHBV production (left: schematic design; right: the actual production system after construction)

Batch production experiments were conducted using the bench-top system. The appropriate cell culture conditions including substrate type, substrate loading, and aeration rate were selected from previous experiments and used for the batch production here. The working volume was 5L. Other culturing conditions were the same to those described in previous sessions. Four production batches were operated with different aeration strategies: the aeration rate was controlled at 2.5 vvm in the first two batches; the DO level of cell broth was controlled above 50% of saturation level in the last two batches with variable aeration rates ranging from 2.5 to 8 vvm. The cell growth, PHA production, substrate consumption, DO level, pH, and temperature were monitored daily during microbial culturing period. The cells were cultured for 132 hours until cell growth reached the stationary phase. Duplicates were prepared for each of the variable conditions.

5.3.4 Spent saline medium (SSM) treatment and recycling

The FWP 1 was used as the substrate to provide a soluble COD of 20 g/L. The 250-mL bioreactors with a working volume of 200 mL were used for cell cultivation experiments. The cell culturing conditions were the same as described previously, and the experimental setup is shown

in Figure 5.3. Triplicates were used for replications in this research. A total of four consecutive batch runs were conducted with the spent salts being recycled and reused for cell cultivation. At the end of each batch run, the cell mass was separated from spent medium through centrifugation at 8000 rpm for 30 min. The spent saline medium was recycled to the following production batch with two mass levels: 80% and 90% of total salt mass. Prior to the next batch, the spent saline medium was processed through rotary evaporation. The evaporation was conducted with applied vacuum and a temperature of 57 ℃ for around 30 mins. The evaporation treatment was stopped exactly when salt crystals started to appear in the brine. The evaporation process removed around 50% water. And the remaining brine solution was about 50% of the original spent saline medium and was then used for cell cultivation in the following batch run.

5.3.5 Treatment of SSM using oxidizing chemicals

Due to the presence of a substantial amount of organic matter in spent saline media (over 12 g/L COD), the cells failed to grow well in the second batch. A novel approach was used to treat the saline media with chemicals to reduce the COD and remove the inhibitory compounds. The spent saline medium of second batch was treated with H_2O_2 by adding aqueous solution containing 50% H_2O_2 to the spend saline medium at 5% of the total volume. After treatment, the spent saline medium was subjected to the same evaporation process as mentioned previously to generate a brine solution, which was reused for the following batch. Same conditions of nutrients and cell cultivation were provided to all batch runs.

5.3.6 Analytical Methods

5.3.6.a Nutrients Characterization

The feedstocks used in this study were characterized for the nutrient composition before and after the microfiltration process. Around 10 mL of samples were collected from the inflow, permeate and retentate streams and characterized for the composition of the major nutrients. The concentrations of short-chain carboxylic acids including La and VFA were measured by a high-performance liquid chromatography (HPLC) following an analytical method described by Sluiter (2008): the HPLC equipped with a refractive index detector (RID) and a photodiode array detector (PDA) was used for the measurement. Biorad Aminex HPX-87H column was used as the analytical column, where 5 mM H_2SO_4 solution was used as the mobile phase with a flow rate of 0.6 mL/min. The oven temperature was controlled at 60 ℃. The contents of chemical oxygen demand (COD), total nitrogen, and reactive phosphorous were measured by standard chemical kits (HACH). The trace elements and micronutrients including K, Ca, Mg, Na, B, Zn, Cu, Mn, Fe, and Ni were measured by UC Davis Analytical Lab following the standard methods.

5.3.6.b Cell Biomass Measurement

Cell growth was monitored daily through collecting 2 mL of strain broth and measuring the optical density (OD) of broth samples with a spectrophotometer at a wavelength of 520 nm (Lillo and Rodriguez-Valera, 1990). The cell dry mass (CDM) of the cells was determined as the volatile suspended solids (VSS) of the cell broth: 10 to 40 mL of cell broth was sampled and subjected to centrifugation at 8000 rpm for 20 mins. The cell pellet was then washed with MSM and measured following a standard method (APHA, 2012). As for the measurement of nutrients, the supernatant from the CDM measurement was filtered through a 0.22 μm membrane. The filtrate was measured

for the COD, total N, and reactive P, and the contents of La and VFA by the methods described in the previous session.

5.3.6.c PHA Extraction and Quantification

PHA was extracted and quantified following a method by Escalona et al.(1996) with modifications: 20 to 40 mL cell broth was collected at designated time points and treated by immediate centrifugation at 8,000 rpm for 30 min. The cell pellet was washed twice with 0.1% sodium dodecyl sulfate (SDS) solution and deionized water. The washed pellet, which was raw PHA, was dissolved in 2 mL dichloromethane and 2 mL acidic methanol (3 % v/v H_2SO_4), with 1g/L benzoic acid as internal standard. The liquid mixture was then heated in Hach DRB200 digital reactor block at 105 °C for 4 h and cooled to room temperature. 1 mL deionized water was added to the solution, mixed and settled until phase separation was observed. The organic phase was then transferred to a clean vial for quantification. Poly (3-hydroxybutyric acid-co-3-hydroxyvaleric acid) with 12% HV (Sigma-Aldrich) was used as the standard PHA chemical. The samples were analysed using a gas chromatograph (GC) method developed based on the methods reported in the literature (Braunegg et al., 1978; Lemos et al., 1998; Oehmen et al., 2005) with modifications. The GC (Agilent 6890N) equipped with a flame ionization detector (FID) was employed and the HP-5 capillary column (Agilent, 2016) was used with helium as carrier gas. Details of this method were: inlet temperature and pressure: 230 ℃, 16 psi; total flowrate: 30 mL/min; split ratio: 8:1; oven temperature: initial 100 ℃ for 2 mins; ramping from 100 to 124 ℃, with a rate of 8 ℃/min; holding 124 ℃ for 1 min. FID temperature was 240 ℃, with 40 mL/min of H_2 flow and 450 mL/min of air flow.

5.3.6.d Physical Properties Analysis

Cell broth from the 6-L batch production experiments was processed to extract PHA following the method described previously. The extracted PHA pellets were dried in an oven with 105 ℃ for 3 to 4 hours until the weight change was less than 4% (APHA, 2012). The dried PHA pellets were then homogenized through a small-scale grinder and yielded a uniform powder. The PHA powder was used for the analysis of thermal, and mechanical properties.

5.3.6.e Film preparation and tensile test

The film preparation and tensile test were conducted following steps in the reference by Ferre-Guell and Winterburn (2018). For each PHBV sample, 0.1g was dissolved in 10 mL of $CHCl_3$, and sonicated for 4 hours in a sonicator (Fisher Scientific FS20H). The films were cut into 5 x 25 mm strips and tested on tensile test machine (Cheminstruments TT-1100) with rate of 25mm/min. Each sample was tested with 3 repeats.

5.3.6.f Thermal properties measurement

The thermal graphs of PHA samples were obtained using differential scanning calorimetry (DSC) Q100 (TA Instruments), following similar procedures described in a previous study (Ferre-Guell and Winterburn, 2018). The samples were tested with 2 cycles of heating and cooling, firstly heated up to 200° at 10 °C/min and maintained for 5 min, then cooled to −20 °C at 10 °C/min, heated up to 200 °C at 10 °C/min, and cooled to −20 °C. The thermogravimetric analysis (TGA) was conducted using TGA Q50 (TA Instruments), the powder samples were heated at 5 °C/min to 500 °C.

5.3.7 Statistical Analysis

All the experiments were conducted in triplicates, and the mean value and standard deviation (SD) of each assay were calculated for the triplicates. The final values were presented as mean ± SD. Two-way Analysis of Variance (ANOVA) and Turkey test was performed for the significant levels of the factors and group comparison. The software Origin Pro (OriginLab, 2021) was used for all data analysis in this study.

5.4 Results and Discussions

5.4.1 Characterization of FWP and other streams

The fermented food waste feedstock collected at READ was pre-treated by microfiltration process to obtain a particle-free FWP. The FWP recovered from the microfiltration process accounted for around 73% (v/v) of the initial feedstock inflow, which was then used as the substrate for cell cultivation and PHA production by *H. mediterranei*. The rest of the inflow come out as the retentate containing the suspended solids which cannot be utilized by the microbes; instead, it could be used as seed culture for anaerobic fermentation of food waste or recycled back to READ facilities for further anaerobic digestion to generate biogas as a source of bioenergy.

Table 5.1 compares the nutrient composition of influent, permeate (FWP), and retentate of the two fermented food waste feedstocks. The three streams of the same feedstock had close contents of short-chain carboxylic acids, however, the concentrations of La, Ac, Pr, and Bu in both permeate and retentate were slightly lower than those in the inflow stream. This may be due to the loss of those volatile organic compounds (VOC) and microbial degradation during the microfiltration process. The loss can be reduced by increasing the filtration flux and shortening the process time.

Among the three filtration streams of each feedstock, inflow and retentate had higher concentrations of COD, total N, reactive P than permeate because it contains only the soluble nutrients of the inflow. The suspended solids of inflow were mainly food waste scraps with a small portion of microbial biomass, which can be further fermented into soluble nutrients and utilized for PHA production. Comparing the permeate from different feedstocks, the permeate 2 (FWP 2) had more La and Ac than the permeate 1 (FWP 1); and FWP 1 had more Pr than FWP 2. The carboxylic acids accounted for 67% of total COD in FWP 1; and it accounted for 92% of total COD in FWP 2. The major species of short-chain carboxylic acids were La, Ac, Pr, and Bu for both permeates, with different composition (% of total carboxylic acids): 41%, 17%, 33%, 7% in FWP 1; and 51%, 23%, 18%, and 6% in FWP 2. FWP 1 had high total N and reactive P contents than FWP 2.

Table 5.2 lists the results of micronutrients and trace elements in the permeate samples, suggesting that FWP 1 and FWP 2 had close contents of those compounds. Compared with the standard medium for cell culture (MSM and SL-6), both permeate samples were able to provide enough nutrients trace elements of K, Ca, B, Zn, Cu, Mn, Fe, and Ni that are required for cell growth. With FWP 1 and FWP 2 as sole substrate for cell culture, only additional Na and Mg salts were needed to provide enough salinity.

Table 5. 1 Comparison of nutrients in the streams of microfiltration process

		Food Waste 1			Food Waste 2		
Compound	**Unit**	**Influent 1**	**Permeate 1**	**Retentate 1**	**Influent 2**	**Permeate 2**	**Retentate 2**
Lactic acid	g/L	24.7 ± 0.9	21.5 ± 1.3	20.4 ± 0.6	37.8 ± 0.4	36.6 ± 0.5	36.0 ± 0.4
Acetic acid	g/L	10.1 ± 0.8	8.7 ± 0.6	8.3 ± 0.4	17.7 ± 0.2	16.8 ± 0.1	15.9 ± 0.1
Propionic acid	g/L	20.0 ± 1.2	17.2 ± 1.1	16.7 ± 0.6	14.1 ± 0.2	12.9 ± 0.2	12.2 ± 0.1
Butyric acid	g/L	4.4 ± 0.3	3.8 ± 0.3	2.8 ± 0.1	4.4 ± 0.1	4.1 ± 0.1	3.6 ± 0.1
Iso-butyric acid	g/L	0.4 ± 0.0	0.4 ± 0.0	0.4 ± 0.0	0.3 ± 0.0	0.3 ± 0.0	0.3 ± 0.0
Iso-valeric acid	g/L	0.7 ± 0.0	0.6 ± 0.0	0.7 ± 0.1	1.0 ± 0.1	0.9 ± 0.1	0.8 ± 0.0
Valeric acid	g/L	0.1 ± 0.0	0.1 ± 0.0	0.3 ± 0.0	0.1 ± 0.0	0.0 ± 0.0	0.0 ± 0.0
Total carboxylic acids	g/L	60.2 ± 3.5	52.4 ± 3.4	49.7 ± 2.8	76.2 ± 0.5	71.6 ± 0.7	68.8 ± 0.4
COD from acids	g/L	82.5 ± 1.5	71.5 ± 1.7	71.1 ± 2.0	96.5 ± 1.0	84.8 ± 0.5	83.9 ± 0.5
Total COD	g/L	232.6 ± 1.5	108.5 ± 2.0	560.3 ± 7.3	108.5 ± 0.8	92.5 ± 1.0	149.8 ± 1.2
Total N	g/L N	4.6 ± 0.3	3.8 ± 0.1	6.7 ± 0.4	3.0 ± 0.2	2.5 ± 0.1	4.3 ± 0.3
Total P	g/L P	3.7 ± 0.1	0.8 ± 0.0	6.5 ± 0.1	2.8 ± 0.1	0.6 ± 0.0	4.8 ± 0.2

Table 5. 2 Nutrient Elements in Fermented Food Waste Permeate

Compound	Unit	Permeate 1	Permeate 2	MSM and SL-6
N	g/L	3.8 ± 0.1	2.5 ± 0.1	0
P	g/L	0.8 ± 0.0	0.6 ± 0.0	0
K	mg/L	2055 ± 7	2072 ± 5	1950
Ca	mg/L	1588 ± 3	1629 ± 6	183
Mg	mg/L	202 ± 0	198 ± 2	5346
Na	mg/L	1579 ± 2	1485 ± 1	61410
B	mg/L	1.69 ± 0.00	1.62 ± 0.01	0.5
Zn	mg/L	3.79 ± 0.01	3.83 ± 0.01	0.25
Cu	mg/L	0.50 ± 0.01	0.38 ± 0.00	0.04
Mn	mg/L	2.81 ± 0.00	2.92 ± 0.01	0.13
Fe	mg/L	30.80 ± 0.71	30.52 ± 0.65	17.3
Ni	mg/L	0.20 ± 0.00	0.18 ± 0.00	0.05

5.4.2 Effect of aeration rate on cell growth and PHA production

Since DO level decreases dramatically with the high salinity present in culture medium, different levels of aeration rate (0.5, 1.5 and 2.5 vvm) have been tested for cell growth, substrate consumption and PHBV production. Shown in Figure 5.5, the cell growth curves, which are represented by Ln(OD) over time, differ apparently with different aeration rates. With the low substrate loading (40 g/L COD), the microbes grew slower with the lowest aeration rate of 0.5 vvm; and the majority of the cell growth curves overlap with the two higher aeration rates of 1.5 and 2.5 vvm. With the high substrate loading (80 g/L COD), the increasing aeration rate resulted in faster cell growth, which indicates that cells may be more sensitive to aeration with a high

substrate loading. Similarly, according to two-way ANOVA analysis on the final OD, the effects of substrate loading and aeration rate were statistically significant (p-values were 0.004 and 0.002).

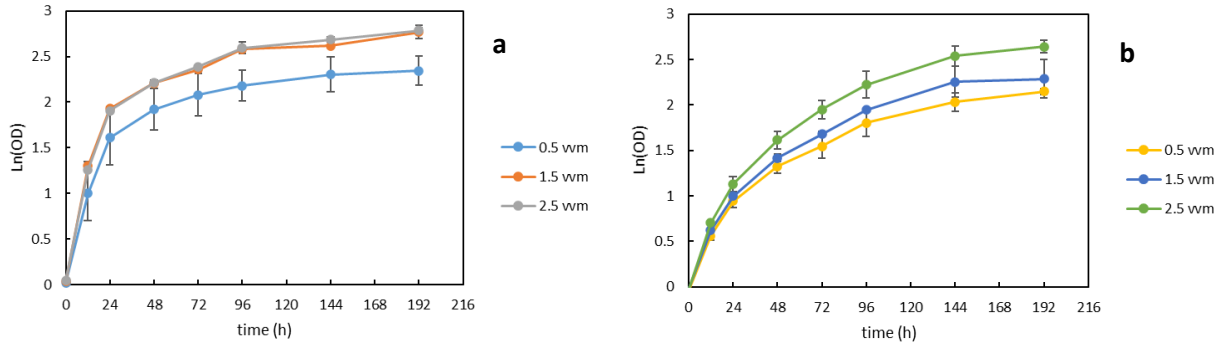

Figure 5. 5 Cell growth curves with different aeration rates; left: with low substrate loading (40 g/L COD); right: with high substrate loading (80 g/L COD)

Figure 5.6 demonstrates the cell mass and PHBV production with different levels of aeration rate and substrate loadings. The statistical analysis by two-way ANOVA suggested that for both CDM and PHBV productions, the levels of substrate loading and aeration rate were significantly different (p-values for CDM were 0.03 and 0.0075, and p-values for PHBV were 0.007 and 0.003), which indicated that these two culturing parameters had significant effects on the CDM and PHBV productions. The interaction between the two factors was not significant. Demonstrated in the means comparisons by Tukey test, with the same aeration rate, the CDM and PHBV productions were not significantly different among the two substrate loadings. The effect of aeration rate was not significant on the CDM production with the same substrate loading.

With the same aeration rate, the effect of substrate loading was not significant on PHBV production. With the same substrate loading, the effect of aeration rate was not significant on

PHBV production either except for between 0.5 and 2.5 vvm with 80 g/L COD loading. The trend of PHBV formation corresponded to cell growth, which can be because PHBV synthesis is a growth-associated reaction when consuming short-chain carboxylates as carbon source (Wang and Zhang, 2021). The highest CDM and PHBV production were 6.7 ± 0.02 g/L VSS and 4.3 ± 0.1 g/L respectively, which were achieved with the highest aeration rate (2.5 vvm) and the lower substrate loading, among others.

The PHBV content of cells and the HV content are shown in Figure 5.7. With the substrate loading of 40 g/L COD, the PHBV content of cell mass remained stably around 62% to 64% among all different aeration rates. And the Tukey comparison results also suggested the aeration rate did not influence the PHBV content of cells significantly. With a higher substrate loading of 80 g/L COD, the PHBV content of cell mass was significantly different (p-value was 0.0048) at the lowest aeration rate (0.5 vvm), but was not significantly different at higher aeration levels. Opposite to the PHBV content, the HV content of the polymer decreased significantly (p-value was 0.013) with a higher aeration rate from 0.5 to 1.5 vvm for 40 g/L COD loading, and from 0.5 to 2.5 vvm for 80 g/L COD loading. Figure 5.8 demonstrates the consumption of short-chain carboxylate species with different growth conditions. Among all carboxylate species, lactate, propionate, and butyrate were the major ones that were consumed by *H. mediterranei* for cell growth and PHBV synthesis. Compared to the high substrate loading, the low substrate loading had more consumption of carboxylates which also corresponds to the higher productions of CDM and PHBV. With low substrate loading, there was more consumption of carboxylates with higher aeration rate from 0.5 to 1.5 vvm, and remained close for 1.5 and 2.5 vvm. With high substrate loading, the effect of aeration rate was not significant on the consumption of carboxylates. The consumption

of acetate was negative in some cases, meaning cells produced and accumulated more acetate during cell growth and PHBV production. This phenomenon was not only observed for FWP as substrate, but also in sugar substrates; as a result, the pH drop below 6 was observed and a pH adjustment was needed during cell culturing. Similar observation on *H. mediterranei* has also be reported by other studies (Ghosh et al., 2019).

These results suggest that an aeration rate of 0.5 to 1.5 vvm, which is normally used in the biotech industry ((Doran, 2013), may not be sufficient for the cell cultivation of *H. mediterranei* or other extreme halophiles. Since the saturated dissolved oxygen level is much lower in high-saline water than freshwater, the oxygen transfer rate can also be lower for cell cultivation (Garcia-Ochoa and Gomez, 2009). Therefore, an aeration rate up to 2.5 vvm is recommended for bioreactors with mild agitation.

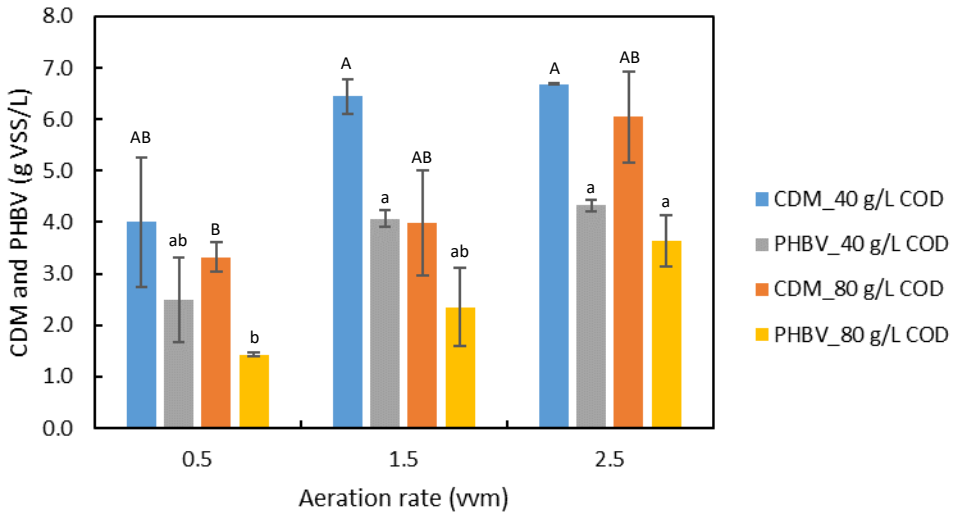

Figure 5. 6 Final concentrations of CDM and PHBV produced with different substrate loadings and aeration rate

(Uppercase letters represented group comparison on CDM and lowercase letters represented group comparison on PHBV; the same letters indicated that the differences were not significant at $p < 0.05$)

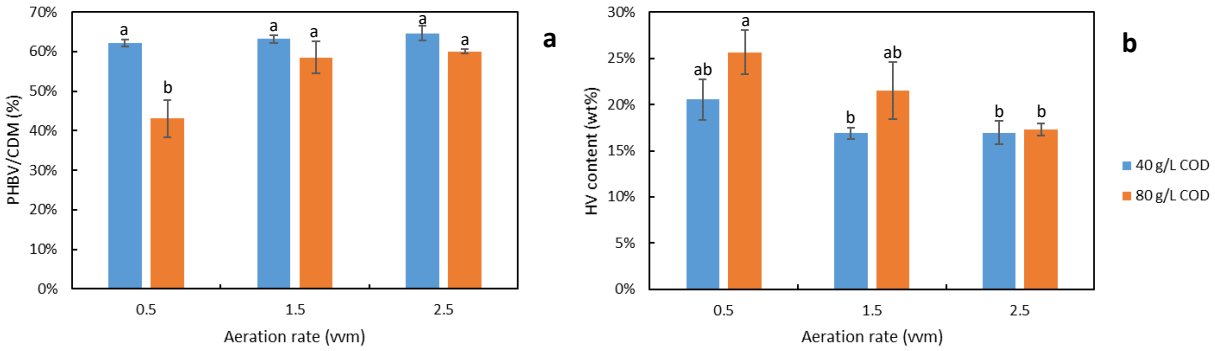

Figure 5. 7 (a) Cell content of PHBV produced with different aeration rates for both substrate loadings; (b) the HV content of PHBV polymers with different aeration rates

(The same lowercase letters indicated that the differences were not significant at $p < 0.05$)

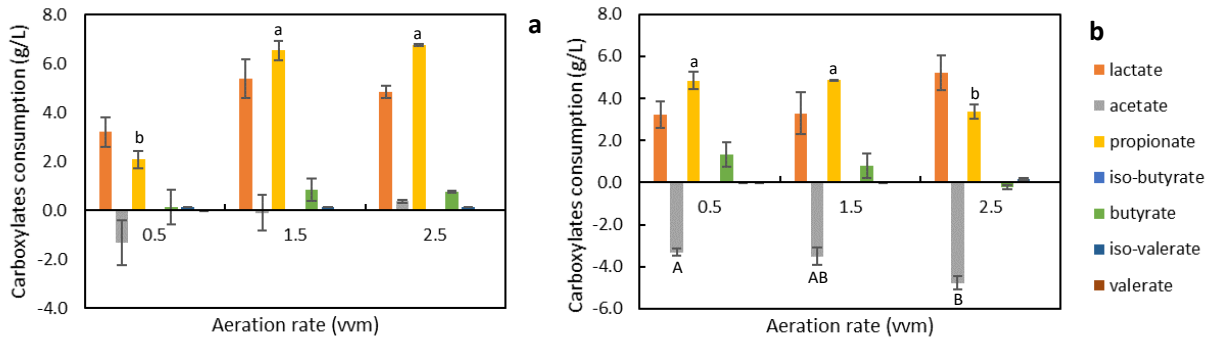

Figure 5. 8 The consumption of short-chain carboxylates with (a) the low substrate loading (40 g/L COD); and (b) the high substrate loading (80 g/L COD)

(The same letters indicated that the differences were not significant at $p < 0.05$)

5.4.3 Effects of substrate loading and type on cell growth and PHA production

The effects of feedstock type and substrate loading were then studied with a fixed aeration rate of 2.5 vvm. Figure 5.9 illustrates the results of final concentrations of CDM and PHBV produced with different substrate loadings for both FWP 1 and FWP 2 as the sole substrate. In terms of feedstock type, although both FWP 1 and FWP 2 were fermented food waste collected at the same digestion facility, they had quite different nutrient compositions of short-chain carboxylates, and they also resulted in different CDM and PHBV productions by *H. mediterranei*. The statistical analysis by two-way ANOVA suggested that for both CDM and PHBV productions, the levels of substrate type and loading were significantly different (p-values for CDM were 1.76E-6 and 3.93E-5, p-values for PHBV were 3.14E-9 and 1.76E-6). The interaction between the two factors was also significant (p-value for CDM was 0.0012 and p-value for PHBV was 5.66E-6). Among all substrate loadings, the CDM produced from FWP 1 was up to 2 times more than that produced from FWP 2; the PHBV yielded from FWP 1 was also much higher than that from FWP 2. This may be due to the total carboxylates account for a higher portion of COD in FWP 2 than FWP 1, which leads to higher loadings of some carboxylic species from FWP 2 than FWP 1 with a fixed COD loading. Some VFA species with high concentrations can be inhibitory to the cell growth of *H. mediterranei* (Ferre-Guell and Winterburn, 2018). Another reason can be the higher contents of other nutrients, including N, P, and the rest of COD besides carboxylates, which may boost up the cell growth and PHBV synthesis.

Substrate loading influenced the cell mass and PHBV production for both feedstocks. A general trend was observed that the CDM and PHBV production firstly increased and later

decreased with higher substrate loadings, which may be due to substrate inhibition when the substrate loading exceeds some threshold. The highest production also differed depending on feedstock types. For FWP 1, the highest CDM and PHBV production were 6.8 ± 0.08 and 4.0 ± 0.05 g/L respectively, which were obtained from a substrate loading of 40 g/L COD. For FWP 2, the highest CDM and PHBV production were 4.4 ± 0.4 and 2.3 ± 0.1 g/L respectively, which were obtained from a substrate loading of 60 g/L COD.

Figure 5.10 demonstrates the PHBV content of cells and HV content of PHBV produced from different feedstocks with four substrate loadings. When FWP 1 was used as the substrate, the loading levels were not significantly different for HV content and PHBV content with 40 to 80 g/L COD loadings. However, the substrate loading levels resulted in significantly different PHBV contents (p-value was 5.36E-6) and HV contents (p-value was 3.45E-4) when FWP 2 was use. Compared with FWP 2, FWP 1 resulted in higher cell contents of PHBV and HV content among all substrate loadings, suggesting FWP 1 is a better candidate as the substrate to culture *H. mediterranei* than FWP 2. A high cell content of PHBV suggests a high mass portion of CDM accounts for PHBV, meaning a good efficiency of PHBV synthesis by the strain. For FWP 1, the cell contents of PHBV were stably around 55% to 60% with all substrate loadings; however, for FWP 2, the cell contents of PHBV increased from 5% to 50% with substrate loading from 20 to 60 g/L COD, and decreased to around 40% with substrate loading of 80 g/L COD. A high HV content of PHBV polymer suggests a high mass ratio of HV monomer versus HB monomer, which would lead to good physical properties of the bioplastic material such as flexibility and elasticity. The HV contents derived from FWP 1 were around 16% to 18% of PHBV among all substrate

loadings; and the HV contents derived from FWP 2 were below 16% of PHBV with all substrate loadings.

The consumption of carboxylates is demonstrated in Figure 5.11. Lactate, propionate, and butyrate were the major carboxylic species consumed during cell growth and PHBV production. Compared to FWP 2, there was more propionate consumed in FWP 1. Since propionate is the direct precursor to synthesize HV units of the PHBV polymer, it can explain why the HV content derived from FWP 1 was higher than FWP 2. It is interesting to see the difference on the consumption of acetate: part of the acetate was consumed in FWP 2 while some acetate in FWP 1 got produced and accumulated. These results above suggest FWP 1 is a better candidate as substrate than FWP 2, because it provides higher CDM and PHBV production, cell content of PHBV, and higher HV content of PHBV polymers. A substrate loading of 40 g/L COD is selected among all other loadings for its higher production yields of CDM and PHBV.

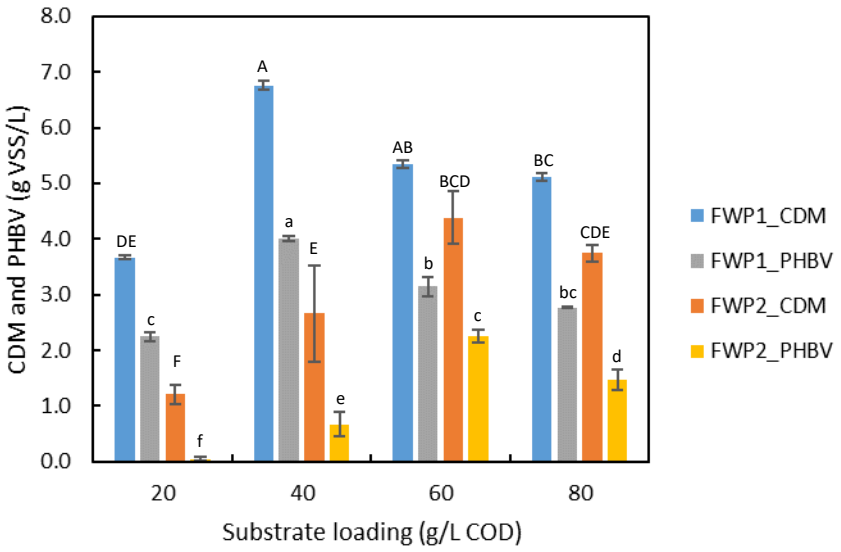

Figure 5. 9 Final concentrations of CDM and PHBV produced with different feedstock type and substrate loadings

(Uppercase letters represented group comparison on CDM and lowercase letters represented group comparison on PHBV; the same letters indicated that the differences were not significant at $p < 0.05$)

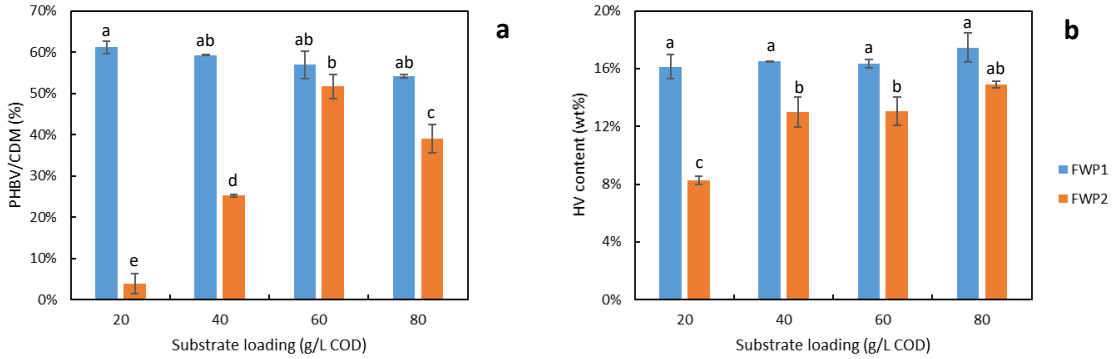

Figure 5. 10 (a) Cell content of PHBV and (b) the HV content of PHBV polymers produced with different feedstock type and substrate loadings

(The same lowercase letters indicated that the differences were not significant at $p < 0.05$)

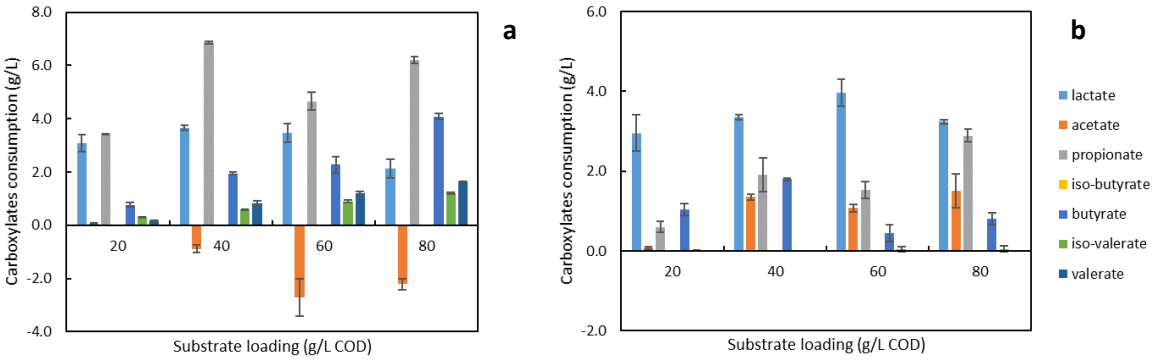

Figure 5. 11 The consumption of short-chain carboxylates with different substrate loadings for (a) FWP 1 as feedstock; and (b) FWP 2 as feedstock

5.4.4 Batch PHA production in 6L bioreactor system

The 6-L bench-top bioreactor system was used for several runs of batch productions to monitor the dynamic profiles of cell growth, PHBV synthesis, and important processing parameters including DO, temperature, and pH etc. The appropriate cell culture conditions used in the productions were based on the findings discussed in previous sessions: (1) feedstock type: FWP1; (2) substrate loading: 40 g/L COD; (3) aeration rate: 2.5 vvm. The temperature and pH were controlled around 40 ℃ and 7 stably during the entire culturing period. Four production batches were operated with different aeration strategies: the aeration rate was controlled at 2.5 vvm in the first two batches; the DO level of cell broth was controlled above 50% of saturation level in the last two batches with variable aeration rates ranging from 2.5 to 8 vvm. As shown in Figure 5.12, the DO of cell broth with a stable aeration rate of 2.5 vvm dropped abruptly from over 80% sat. to less than 20% sat. at the exponential growth phase when the cells were rapidly propagating. The DO increased back to over 60% sat. when cells were approaching stationary phase. With a

different aeration strategy where the aeration rate was adjusted according to the DO level, the DO of cell broth was maintained over 50% sat. during the entire cultivation period.

The curves of cell growth and PHBV synthesis are shown in Figure 5.13, which corresponds to the two different aeration strategies. With a controlled aeration rate at 2.5 vvm, the concentration of CDM reached around 7 g/L VSS within 120 h and remained stable afterwards; and the PHBV concentration in the cell broth increased to around 5 g/L within the same culturing time. The two curves are approximately parallel to each other during the entire production time, which allies with a previous finding that the PHBV synthesis from food waste derived nutrients is a growth-associated reaction by *H. mediterranei* (Wang and Zhang, 2021). With a controlled DO level above 50% sat., the cells were growing in a much faster rate and reached the stationary growth phase within 72 h, which shortens the cultivation period by 2 days with the same substrate loading. The final CDM was around 7 g/L VSS, which is close to the CDM obtained with a controlled aeration rate. Therefore, the second aeration strategy increased the productivity of CDM. However, the final PHBV with a controlled DO level above 50% sat. was around 3 g/L, which is much less than the PHBV produced with a controlled aeration rate at 2.5 vvm. This also suggests that the increase of the aeration rate to maintain a high DO level can decrease the PHBV content of cells, which results in a lower PHBV production within the same batch operation time. The final PHBV yields (g PHBV/g carboxylates consumed) were: 0.28 ± 0.0001 with 2.5 vvm of aeration, and 0.19 ± 0.05 with DO level above 50% sat. This suggests that the increase of aeration rate may reduce the final PHBV yield.

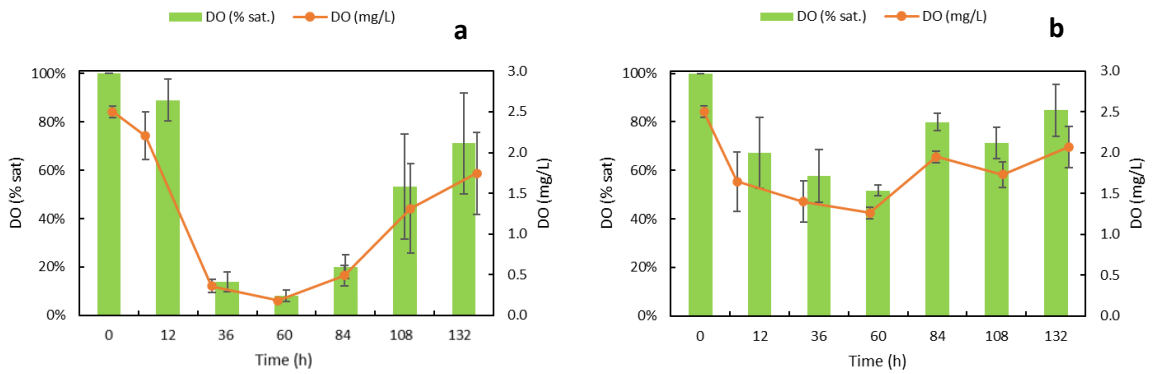

Figure 5. 12 Time profiles of the dissolved oxygen levels of cell broth in 6-L batch: (a) with a controlled aeration rate of 2.5 vvm; (b) with a controlled DO level above 50% sat.

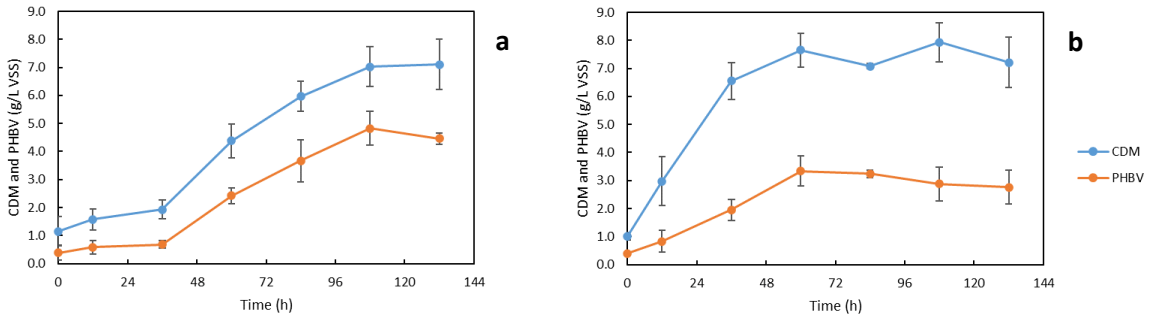

Figure 5. 13 Time profiles of the cell growth and PHBV production in 6-L batch: (a) with a controlled aeration rate of 2.5 vvm; (b) with a controlled DO level above 50% sat.

The time profiles of HV and HB contents of PHBV produced from food waste with different aeration strategies are shown in Figure 5.14. With a controlled aeration rate of 2.5 vvm, the HV content increased from 10% wt. to around 23% wt. during exponential growth phase, and decreased to around 17% wt. at the stationary phase. With a controlled DO level above 50% sat., the HV content showed a similar trend that it increased to around 30% wt. during exponential growth phase and dropped to around 21% wt. in stationary phase. The final HV content obtained

from the batches with the DO above 50% sat. was 21% wt., which is higher than that produced from the batches with lower DO levels during the log phase (15% wt.). Therefore, although higher DO levels cause less PHBV production as discussed previously, it may lead to higher HV content of PHBV, which benefit the thermal and mechanical properties of the bioplastic product.

The consumption of short-chain carboxylates during cell growth is demonstrated in Figure 5.15. The final consumptions of individual carboxylates were (% of initial): 85% lactate, 98% acetate, 84% propionate, 76% butyrate, and 100% valerate in batches with a controlled aeration rate of 2.5 vvm; and 99% lactate, 94% acetate, 77% propionate, 61% butyrate, and 100% valerate in batches with DO levels above 50% sat., respectively. In general, the consumption rates of the major carboxylates including lactate, acetate, propionate, and butyrate were much faster in the batches with DO levels above 50% sat. than those with a controlled aeration rate of 2.5 vvm. Most of the carboxylates were consumed within 108 h for the batches with a controlled aeration rate of 2.5 vvm; and within 60 h for the batches with DO levels above 50% sat. Since the carboxylates account for the majority of carbon sources in FWP, they were quickly utilized for the faster cell growth and PHBV synthesis with higher DO levels, as illustrated in Figure 5.13.

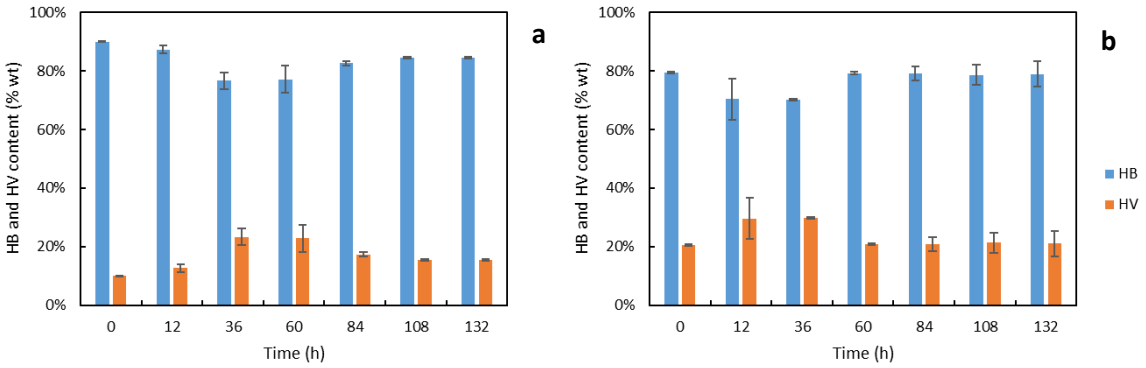

Figure 5. 14 Time profiles of HB and HV contents in the polymer produced from 6-L batch: (a) with a controlled aeration rate of 2.5 vvm; (b) with a controlled DO level above 50% sat.

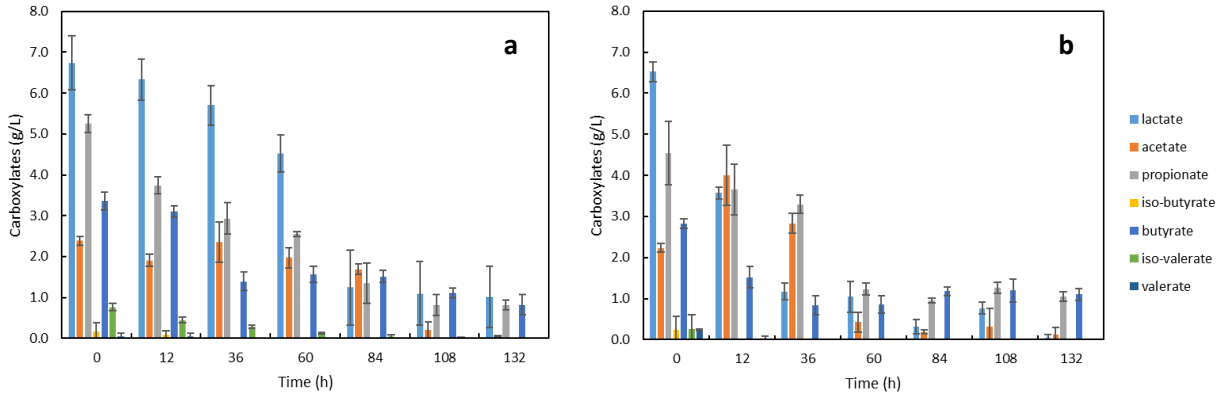

Figure 5. 15 Time profiles of carboxylates in 6-L batch: (a) with a controlled aeration rate of 2.5 vvm; (b) with a controlled DO level above 50% sat.

5.4.5 Physical properties of PHBV

The results of TGA, DSC analysis and tensile tests are shown in Table 5.3. The PHBV produced from food waste has a crystallization temperature (Tc) around 50 ℃, a melting temperature (Tm) around 140 ℃, and decomposition temperatures (T_d) around 245 ℃ and 410 ℃, regardless of with purification process or not. In terms of mechanical properties, the purified and

unpurified PHBV produced from the same food waste feedstock have different results: the PHBV with purification has a lower Young's modulus and a lower tensile strength than the one without purification, suggesting the purification process increased the elasticity and reduced the brittleness of the PHBV. Both purified and unpurified PHBV have similar elongation at break, which means they had similar fracture strain. The thermal and mechanical properties of PHBV produced from food waste fall in the ranges of those that have been reported by other studies on *H. mediterranei* (Ferre-Guell and Winterburn, 2018; Han et al., 2015), and are comparable with the PHA products in the current market (Cambridge Consultants, 2018). These all suggest that PHBV produced in this study has good quality to be manufactured into thermoplastics.

Table 5. 3 Thermal and mechanical properties of PHBV produced from food waste

Feedstock	purification	T_c (ºC)	T_m (ºC)	T_d (ºC)	Young's modulus (MPa)	Tensile strength (MPa)	Elongation at break (%)
Food waste	No	50	140	245, 410	609.78±36.26	12.48±2.54	2.84±0.8
Food waste	Yes	52	145	245, 410	428.76±87.15	8.02±1.62	2.8±0.63

5.4.6 Effect of recycled spent saline medium on cell growth and PHBV production

The cell growth curves of the three consecutive batches with the recycling of SSM after water removal by evaporation are illustrated in Figure 5.16. The SSM from the first batch was used directly as the 80% of saline medium of the second batch without any pre-treatment, but in the third batch, the SSM from the second batch was treated with H_2O_2 before reuse. It was found that the cell growth of the second batch was not as good as the first one. However, after the H_2O_2 treatment of the SSM, the cell growth of the third batch was better than the cell growth of the first batch. And the final cell density of the third batch was around an OD of 12. Figure 5.17 shows the productions of CDM and PHBV from the three recycling batches. The final concentrations of CDM and PHBV allies well with the cell growth curves. The statistical analysis also indicated that

the third batch had significantly higher productions of CDM and PHBV than the previous batches, suggesting that the treatment with H_2O_2 can help with the cell growth and PHBV synthesis when the SSM is reused. Regardless of PHBV production, the contents of HV and HB remained relatively stable among the three recycling batches, which were around 17% and 83% of the PHBV respectively.

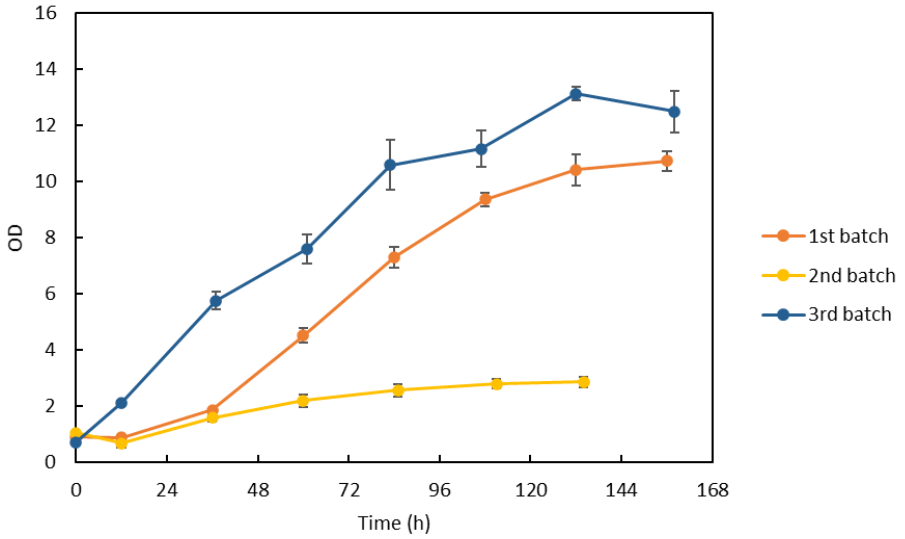

Figure 5. 16 Cell growth curves of three spent salts recycling batch runs: the 2nd batch was without H_2O_2 treatment; the 3rd batch was with H_2O_2 treatment

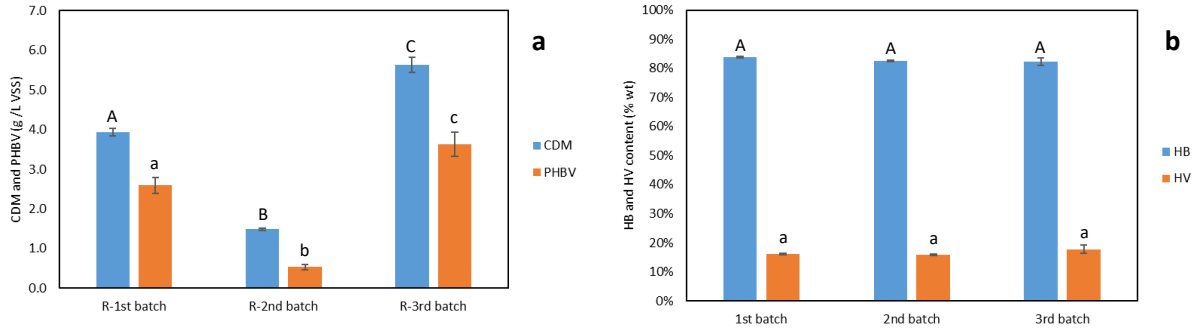

Figure 5. 17 CDM and PHBV productions and compositions of three spent salts recycling batch runs: the 2nd batch was without H_2O_2 treatment; the 3rd batch was with H_2O_2 treatment

(Uppercase letters represented group comparison on CDM or HB content and lowercase letters represented group comparison on PHBV or HV content; the same letters indicated that the differences were not significant at $p < 0.05$)

A following set of experiments was conducted to determine the appropriate loading and reaction time of the H_2O_2 treatment on SSM. As shown in Figure 5.18, among the three loadings of 30% H_2O_2 solution, over 50% COD reduction of SSM was achieved in both 6% and 10% loadings within 8 hours. Although 10% loading resulted in a slightly higher COD reduction than 6% loading, it has a higher chance of causing microbial inhibition due to the accumulation of left-over H_2O_2 during recycling runs over time (McDonnell, 2014). Therefore, a H_2O_2 loading of 6% and a reaction time of 8 h were selected for the SSM treatment. Given the fact that COD of SSM with food waste as feedstock remained relatively within a stable range with the recycling runs in this study, this combination of H_2O_2 loading and reaction time is recommended for the treatment of SSM from food waste. However, the suitable loading and reaction time may vary in practical applications. For example, they may differ depending on feedstock type and substrate loading; and in other circumstances such as left-over COD accumulation over the recycling runs, it would require higher loadings of H_2O_2 and longer reaction time to reduce the COD to an extent where it won't be a growth-limiting factor in the following recycling batches.

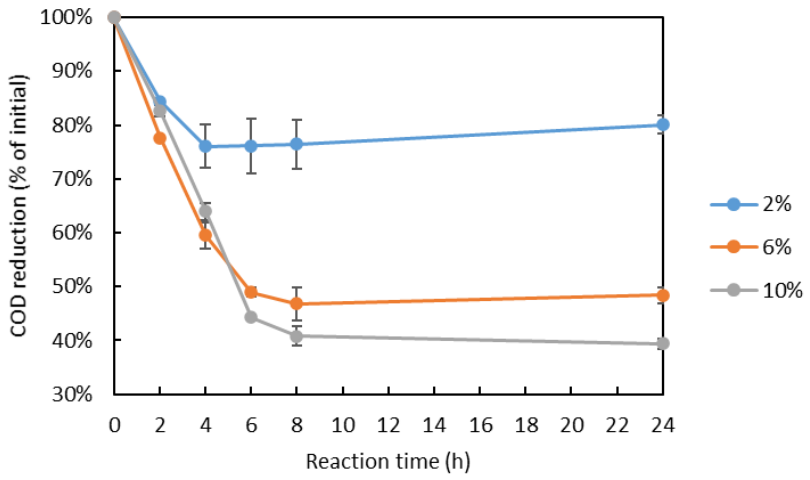

Figure 5. 18 COD reduction of spent saline medium with different loadings of 30% H_2O_2 solution and reaction times

Two series of SSM recycling experiments were conducted with 80% and 90% mass of SSM being recycled after H_2O_2 treatment in four consecutive batches respectively. The cell growth curves shown in Figure 5.19 suggest that cells grew faster and achieved higher final densities in the batches with 80% SSM recycling than the initial batch; and similar growth was found in the batches with 90% SSM recycling except for the second batch. The results of CDM and PHBV productions demonstrated in Figure 5.20 told the same story. With 80% SSM being recycled, the CDM produced in the recycled batches were significantly higher than those of the original batch. Regarding PHBV production, only the second recycling batch was significantly higher than the original batch, and the rest of recycling batches had similar productions to the original one. With the 90% SSM being recycled, the CDM and PHBV productions in the second batch were significantly lower than the original batch; the productions from the third and fourth batches were not significantly different from the first batch. The reason for the lower CDM and PHBV productions in the second batch could be the inhibitory compounds in the H_2O_2-treated SSM such

as leftover COD or H_2O_2 that limited the cell growth; however, it seems that cells were able to acclimate to this condition quickly and back to normal growth and PHBV synthesis in the following recycling batches. The contents of HV and HB units of PHBV, illustrated in Figure 5.21, increased slightly from 16% to around 20% in the batches with 80% SSM being recycled and from 17% to around 22% in the batches with 90% SSM being recycled. With 80% of SSM recycling, the HV contents of the PHBV products were significantly higher in the third and forth batches; and with 90% of SSM recycling, the HV contents were significantly higher in all recycling batches. Therefore, in addition to the relatively stable productions of CDM and PHBV, there are significant evidences that proved the recycling of SSM may increase the HV content of the PHBV products. The higher HV content of PHBV can introduce more flexibility and elasticity to the thermoplastic material, which can help broaden the product applications.

Both 80% and 90% SSM recycling experiments suggest a promising potential of employing the H_2O_2 pretreatment strategy on the SSM to maintain normal cell growth and PHBV synthesis from food waste with the use of spent salts. The recycling of SSM can provide economic and environmental advantages due to the major savings of purchasing new salts and the costly treatment and disposal of high-saline wastewater. Another advantage is the possibility of achieving a better product quality through significant increase of HV content of PHBV. Based on the findings of this study, a further research interest can be the optimization of chemical treatment and recycling conditions in a pilot to commercial production scale, and demonstrate the feasibility and economic efficacy for the practical applications.

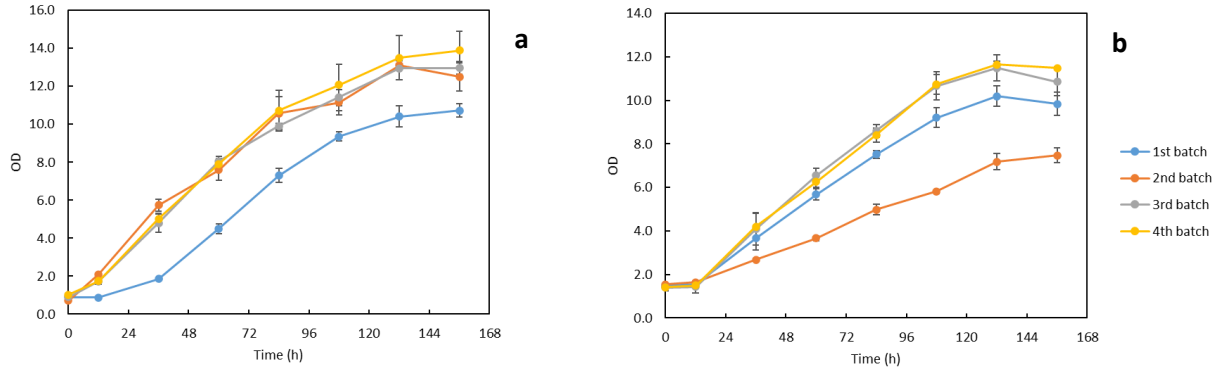

Figure 5. 19 Cell growth curves of four batches with spent salts recycling after H_2O_2 treatment: (a) with 80% spent salts recycled and; (b) with 90% spent salts recycled

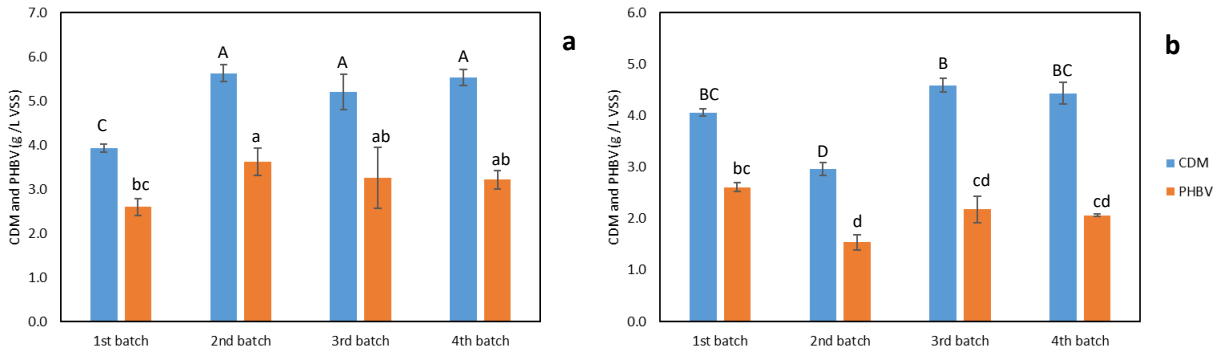

Figure 5. 20 CDM and PHBV productions of four batches with spent salts recycling after H_2O_2 treatment: (a) with 80% spent salts recycled and; (b) with 90% spent salts recycled (Uppercase letters represented group comparison on CDM and lowercase letters represented group comparison on PHBV; the same letters indicated that the differences were not significant at $p < 0.05$)

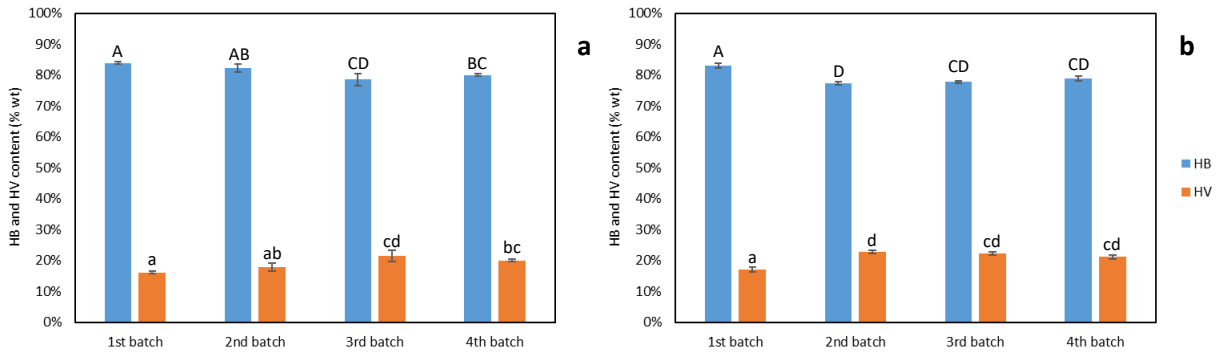

Figure 5. 21 HB and HV contents of PHBV from four batches with spent salts recycling after H_2O_2 treatment: (a) with 80% spent salts recycled and; (b) with 90% spent salts recycled (Uppercase letters represented group comparison on HB content and lowercase letters represented group comparison on HV content; the same letters indicated that the differences were not significant at $p < 0.05$)

5.5 Conclusions

A production system of PHBV synthesis by *H. mediterranei* with utilizing fermented food waste from commercial anaerobic digestors has been developed in this study. Main processes including feedstock collection and pre-treatment, microbial production, and spent saline medium treatment and recycling are demonstrated on a bench scale. The important processing parameters including feedstock type, substrate loading, and aeration rate have been determined to achieve the highest production. The main processes consist of feedstock pre-treatment, robust PHA production by *Haloferax mediterranei*, and spent salts recovery and recycling have been demonstrated through benchtop bioreactor systems. The dynamic dissolved oxygen levels throughout microbial cultivation were found to be critical to PHA synthesis. The recycling of spent saline medium has been successfully achieved for four consecutive batches after the treatment by H_2O_2. The

demonstrated production system in this study has the potential to apply to practical production scenarios, which can help promote the circular economy of the current food system by adding an additional revenue from food waste. At the same time, it can help reduce the production cost of bioplastics, which help penetrate the conventional plastic market and mitigate the environmental pollution and health threat caused by plastic waste.

Chapter 6. Process Development of Polyhydroxyalkanoates Production by *Haloferax mediterranei* Utilizing Whey Sugar from Commercial Cheese Manufacturing Facilities

6.1 Abstract

Production of conventional plastics is unsustainable due to the use of non-renewable fossil carbon feedstocks, the emissions of greenhouse gases, and the massive generation of non-degradable plastic waste. Polyhydroxyalkanoates (PHA) are a family of biodegradable plastic materials used as a replacement for conventional plastics in various applications. PHA are produced through microbial fermentation of renewable feedstocks. The high production cost of PHA, which is mainly due to use of high value feedstocks, is the current bottleneck for market growth. To reduce the production cost, this study has developed an integrated PHA production system that utilizes whey sugar from commercial cheese making facilities as feedstock. The effect of substrate loading has been studied on the final batch productions of cell mass and PHBV. Through dynamic monitoring in a 6-L benchtop bioreactor system, the dissolved oxygen (DO) level of cell broth dropped dramatically to below 20% saturation during the exponential growth phase with a fixed aeration rate. Two aeration strategies were compared, and the strategy of maintaining a DO level above 50% saturation resulted in faster cell growth, and higher consumption extent of galactose, but led to lower final cell densities and PHBV concentration. The direct reuse of spent saline medium (SSM), after a concentration step by rotary evaporation, was successfully achieved for four consecutive batches with various substrate loadings, where both 80% and 90% SSM recycling strategies yielded comparable cell growth, PHBV production and PHBV profile to the original batch. This novel PHA production system has the potential for practical use in the current bioplastic industry. Moreover, by utilizing whey sugar or other byproduct and waste

streams, this process can also create opportunities for waste valorization and additional revenue in the dairy industry.

Keywords: Process development, polyhydroxyalkanoates, whey sugar, spent salts recycling, *Haloferax mediterranei*

6.2 Introduction

As important commodities on a global scale, plastic products are used frequently in many aspects of human life. The global plastic production is estimated to be 370 million tons per year, of which 99% are derived from fossil carbon feedstocks (European Bioplastics, 2018). The greenhouse gas (GHG) emissions associated with the manufacturing processes generate up to 3 kg CO_2 eq/kg resin produced (Criddle and Frank, 2014), which also contribute to the unsustainability of petroleum-based plastics. Moreover, around 275 million tons of global plastic wastes are generated annually, of which up to 55% end up in landfills or the environment (Geyer et al., 2017). U.S. landfills received 26 million tons of plastics wastes annually, which account for 19% of all landfilled wastes (US EPA, 2019). This persistent plastic debris occupies land, litters oceans and endangers aquatic creatures. Microplastic molecules in water bodies also damage the quality of drinking water and have become a threat to water and food safety (Andrady, 2011).

There are many research endeavors and industrial activities to advance the production of biodegradable plastics as alternatives to the conventional ones. Polyhydroxyalkanoates (PHA) is a family of high-value polyesters with similar properties to conventional thermoplastics and is one of the major materials used for the manufacturing of biodegradable plastics (Reddy et al., 2003).

PHA products can be degraded biologically in the natural environment (Queiroz and Collares-Queiroz, 2009). Utilizing renewable feedstocks, the production of PHA by microbial fermentation approaches has been commercialized since early 1990s (Chen, 2009). The current applications of PHA are mainly packaging films, plastic containers, and other applications such as medical implant materials, drug carriers, nutritional supplements and biofuels. To reduce the production cost, there are many research interests in utilizing processing byproducts or waste streams as feedstock for PHA production.

Whey sugar, generally known as lactose, is one of the byproduct streams derived from cheese manufacturing. Whey permeate is the side stream from the separation and concentration of whey protein. Whey sugar is produced from crystalizing the sugars from whey permeate, leaving behind delactosed permeate (DLP) after the recovery of lactose crystals (Oliveira et al., 2019). Whey sugar is produced in large quantities from cheese-making facilities and contain other nutrients besides lactose including crude protein, minerals, and micronutrients. Converting cheese processing byproducts such as whey sugar to PHA can create an additional revenue for dairy processors, and potentially reduce high production cost and make PHA more competitive in the bioplastic market.

Haloferax mediterranei is an extreme halophilic archaeon that can maintain robust pure microbial culture in unsterile conditions. It has been extensively studied for its capability of producing Poly(3-hydroxybutyrate-co-3-hydroxyvalerate) (PHBV), a type of high-quality PHA. Previous studies have reported the feasibility of using cheese whey hydrolysates (Pais et al., 2016),

which contain the monosaccharides hydrolysed from lactose, as the substrate to culture this strain for PHBV synthesis. In Chapter 4 of this study, the enzymatic hydrolysate of whey sugar (lactose) gave faster cell growth and similar PHBV yields as compared with DLP, which also suggests that the whey sugar can be a good candidate as the substrate. The biorefinery system involving this strain as the PHBV producer and whey sugar as feedstock has not been extensively studied, especially when it comes to the fate of the spent brine. As discussed in Chapter 5, among the few studies that have reported the process of recycling spent saline medium or salts, it remains unclear on whether the direct use of spent brine would influence the production of cell mass or PHBV. Besides, none of the previous studies have researched the effect of multiple recycling batches. Apart from the spent salt recycling, the process design of the production system would also be different from the systems using freshwater PHA producers and mixed cultures, mainly on the fermentation, downstream PHA extraction and purification processes, as well as the wastewater treatment.

Therefore, the objectives of this research were: (1) To develop bioconversion processes and determine the optimum processing parameters for PHBV production from whey sugar collected from commercial cheese making facilities; (2) to demonstrate the integrated system of PHBV production with spent saline medium recycling.

6.3 Materials and methods

6.3.1 Feedstock collection and characterization

Whey sugar (powder form) was collected from Hilmar Cheese Co. It was the lactose crystals that formed during the evaporation process of whey permeate, as one of the byproduct streams from the whey processing units. The feedstock had lactose as the main carbon nutrient; and nutrients of nitrogen, phosphorous, and minerals. After collection, the feedstock was stored in a cool and ventilated cabinet to preserve. The feedstock was characterized for the contents of lactose, dry matter, crude protein, and minerals including calcium (Ca), chloride (Cl), magnesium (Mg), phosphorous (P), potassium (K), sodium (Na), sulfur (S), aluminum (Al), boron (B), cupper (Cu), iron (Fe), manganese (Mn), zinc (Zn) by Denele Analytical, Inc, Turlock, CA.

6.3.2 Enzymatic hydrolysis

The whey sugar contains lactose as the main carbon source. Since *H. mediterranei* cannot utilize lactose directly (Pais et al., 2016), a pretreatment step using lactase enzyme to hydrolyze lactose into monosaccharides was adopted for both cheese process byproduct feedstocks. Prior to enzymatic hydrolysis, lactose powder was dissolved in deionized water to obtain a lactose concentration of 40g/L. The optimum enzyme loading and reaction time to obtain at least 90% lactose conversion had been determined previously and demonstrated in Chapter 4, which were 0.02 g/g lactose and 4 hours, for the specific lactase enzyme and controlled temperature at 40 ℃. Therefore, the same conditions were used in preparing the whey sugar hydrolysate in this study. After enzymatic hydrolysis, lactose hydrolysate was used as the sole substrate in the following cell cultivation and PHA production experiments. The substrate was characterized for the soluble

chemical oxygen demand (sCOD), total nitrogen, total phosphorous, and individual nutrient profiles.

6.3.2 Microorganism and culture conditions

The wild-type halophilic archaeon, *H. mediterranei* (ATCC 33500) was used as the microbial PHA producer in this study. The fresh and active seed of the strain was prepared according to the procedures described in previous chapter. The hydrolysate of whey sugar was used as the sole substrate to supply essential sources of carbon, nitrogen and phosphorous for *H. mediterranei* throughout the study. There were three substrate loadings including 20, 40, and 60 g/L sCOD to study the effect of substrate loading on cell growth and PHBV production. The experimental setup was the same as what was described in Chapter 5. All experiments were conducted using the identical 250-mL glass bioreactors with 80% working volume. The bioreactors were housed in an incubator with a controlled temperature at 37 ± 0.5 ℃. Forced aeration was applied to all reactors by using air pumps and the aeration rate was adjusted by using valved air flowmeters. The air was pre-humidified by bubbling through distilled water to prevent liquid volume loss and salinity change in the reactor during forced aeration (Wang and Zhang, 2020). As fixed conditions, the aeration rate was controlled at 2.5 volumes per volume per minute (vvm), which was selected based on results of Chapter 5. The minimum saline medium (MSM) was added to create a salinity level around 188 parts per thousand (ppt). The same inoculation level was used for all reactors to give an initial optical density (OD) 1.0 ± 0.2 at 520 nm wavelength. 50 mM $NaHCO_3$ was added as the buffer at the beginning of experiments. The pH of cell broth was maintained at around 7 throughout the cell cultivation. The pH was monitored daily by a pH meter and was adjusted by using either 3M NaOH solution or 3M HCl solution. The study used triplicates for replication of

experiments. The cells were cultured for 168 to 240 hours until cell growth reached the stationary phase.

6.3.3 Batch PHA production

As described in Chapter 5, the same 6-L benchtop bioreactor system was used for batch PHA production from whey sugar hydrolysate. The appropriate level of substrate loading was selected from previous experiments and used for the batch production here. The working volume was 5L. Other culturing conditions were the same to those described in previous sections. Four production batches were operated with different aeration strategies: the aeration rate was controlled at 2.5 vvm in the first two batches; the DO level of cell broth was controlled above 50% of saturation level in the last two batches with variable aeration rates ranging from 2.5 to 8 vvm. The cell growth, PHA production, substrate consumption, DO level, pH, and temperature were monitored daily during microbial culturing period. The cells were cultured for 132 hours until cell growth reached the stationary phase. Duplicates were prepared for each of the variable conditions.

6.3.4 Spent saline medium (SSM) treatment and recycling

The hydrolysate of whey sugar was used as the sole substrate with three loadings including 20, 40, and 60 g/L sCOD. The 250-mL bioreactors with a working volume of 200 mL were used for cell cultivation experiments. The cell culturing conditions and experimental setup were the same as described previously. Triplicates were used for replications in this research. A total of four consecutive batch runs were conducted with the spent salts being recycled and reused for cell cultivation. At the end of each batch run, the cell mass was separated from spent medium through centrifugation at 8000 rpm for 30 min. The spent medium was recycled to the following production

batch with two mass levels: 80% and 90% of total salt mass. Prior to the next batch, the spent medium was processed through rotary evaporation. The evaporation was conducted with applied vacuum and a temperature of 57 ℃ for 25 ± 5 mins. The evaporation treatment was stopped upon any appearance of salt crystals started in the brine. The evaporation process removed around 50% water, and the remaining brine solution was about 50% of the original SSM and was then used for cell cultivation in the succeeding batch run.

6.3.5 Analytical Methods

6.3.5.a Nutrients Characterization

The concentrations of lactose, glucose and galactose were measured by high-performance liquid chromatography (HPLC) following an analytical method described by Sluiter (2008). Chemical oxygen demand (COD), total nitrogen, and reactive phosphorous were measured by standard chemical kits (HACH). Trace elements and micronutrients including K, Ca, Mg, Na, B, Zn, Cu, Mn, Fe, and Ni were measured by Denele Analytical Inc., Turlock, CA, following the standard methods.

6.3.5.b Cell Biomass Measurement

Cell growth was monitored daily through collecting 2 mL of strain broth and measuring the optical density (OD) of broth samples by a spectrophotometer at a wavelength of 520 nm (Lillo and Rodriguez-Valera, 1990). The cell dry mass (CDM) was determined as the volatile suspended solids (VSS) of the cell broth: 10 to 40 mL of cell broth was sampled and subjected to centrifugation at 8000 rpm for 20 mins. The cell pellet was then washed with MSM and measured following a standard method (APHA, 2012). As for the measurement of nutrients, the supernatant

from the CDM measurement was filtered through a 0.22 μm membrane. The filtrate was measured for COD, total N, and reactive P, and the contents of sugars by the methods described in the previous section.

6.3.5.c PHA Extraction and Quantification

PHA was extracted and quantified following a method by Escalona et al.(1996) with modifications: 20 to 40 mL cell broth was collected at designated time points and treated by immediate centrifugation at 8,000 rpm for 30 min. The cell pellet was washed twice with 0.1% sodium dodecyl sulfate (SDS) solution and deionized water. The washed pellet, which was raw PHA, was dissolved in 2 mL dichloromethane and 2 mL acidic methanol (3 % v/v H_2SO_4), with 1g/L benzoic acid as internal standard. The liquid mixture was then heated in a Hach DRB200 digital reactor block at 105 °C for 4 h and cooled to room temperature. 1 mL deionized water was added to the solution, mixed and settled until phase separation was observed. The organic phase was then transferred to a clean vial for quantification. Poly (3-hydroxybutyric acid-co-3-hydroxyvaleric acid) with 12% HV (Sigma-Aldrich) was used as the standard PHA chemical. The samples were analysed using a gas chromatograph (GC) method developed based on the methods reported in the literature (Braunegg et al., 1978; Lemos et al., 1998; Oehmen et al., 2005) with modifications. The GC (Agilent 6890N) equipped with a flame ionization detector (FID) and the HP-5 capillary column (Agilent, 2016) was used with helium as carrier gas. Details of this method were: inlet temperature and pressure: 230 °C, 16 psi; total flowrate: 30 mL/min; split ratio: 8:1; oven temperature: initial 100 °C for 2 mins; ramping from 100 to 124 °C, with a rate of 8 °C/min; holding 124 °C for 1 min. FID temperature was 240 °C, with 40 mL/min of H_2 flow and 450 mL/min of air flow.

6.3.5.d Physical Properties Analysis

Cell broth from the 6-L batch production experiments was processed to extract PHA following the method described previously. The extracted PHA pellets were dried in an oven at 105 ℃ for 3 to 4 hours until the weight change was less than 4% of previous weight. The dried PHA pellets were then homogenized through a small-scale grinder and to yield a uniform powder. The PHA powder was used for the analysis of thermal and mechanical properties.

6.3.5.e Film preparation and tensile test

Film preparation and tensile testing were conducted following steps in Ferre-Guell and Winterburn (2018). For each PHBV sample, 0.1g was dissolved in 10 mL of $CHCl_3$, and sonicated for 4 hours (Fisher Scientific FS20H sonicator). The films were cut into 5 x 25 mm strips and tested on a tensile test machine (Cheminstruments TT-1100) with an extension rate of 25mm/min. Each sample was tested in triplicate.

6.3.5.f Thermal properties measurement

Thermograms of PHA samples were obtained using differential scanning calorimetry (DSC) Q100 (TA Instruments), following similar procedures described in a previous study (Ferre-Guell and Winterburn, 2018). The samples were tested with 2 cycles of heating and cooling, firstly heated to 200° at 10 °C/min and maintained for 5 min, then cooled to −20 °C at 10 °C/min, heated up to 200 °C at 10 °C/min, and cooled to −20 °C. Thermogravimetric analysis (TGA) was conducted using a TGA Q50 (TA Instruments, New Castle, DE); the powder samples were heated at 5 °C/min to 500 °C.

6.3.6 Statistical Analysis

All the experiments were conducted in triplicate, and the mean value and standard deviation (SD) of each assay were calculated. The final values were presented as mean ± SD. Two-way Analysis of Variance (ANOVA) and Turkey test were performed for the significant levels of the factors and group comparison. The software Origin Pro (OriginLab, 2021) was used for all data analysis in this study.

6.4 Results and Discussions

6.4.1 Characterization of whey sugar feedstock

As shown in Table 6.1, the whey sugar feedstock has 99.7% dry matter, of which 99.5% was lactose. Besides lactose, there was less than 1% crude protein and trace amounts of minerals. Given an estimate nitrogen-to-protein factor of 6.25 (Mariotti et al., 2008), the carbon-to-nitrogen (C/N) ratio of whey sugar was calculated to be 521.7, which is much higher than the recommended C/N ratio (around 10) (Ferre-Guell and Winterburn, 2017) for the normal growth of *H. mediterranei* cells. The carbon-to-phosphorous (C/P) ratio of feedstock was around 834.6, which was also much higher than the desired C/P ratio for the microbial growth (35) (Ferre-Guell and Winterburn, 2017). Therefore, additional nitrogen and phosphorous sources such as NH_4Cl and KH_2PO_4 were added to the culture medium. Some other byproduct streams from cheese making processes including whey permeate and DLP can have higher nitrogen and phosphorous contents, which would reduce the costs from external nutrient sources.

Table 6. 1 Characterization of whey sugar

	dry matter	crude protein	lactose	Ca	Cl	Mg	P	K	Na	S	Al	B	Cu	Fe	Mn	Zn
Unit	%	%	% DM	%	%	%	%	%	%	%	ppm	ppm	ppm	ppm	ppm	ppm
Feedstock	99.7	0.5	99.5	0.05	0.09	0.06	0.05	0.08	0.06	0.02	22.0	0.0	2.3	63.8	0.0	0.0

The results of enzymatic hydrolysis of whey sugar were previously discussed in Chapter 4, where 90% lactose conversion was achieved with the optimum levels of enzyme loading and reaction time. Therefore, 90% of COD in hydrolysate of whey sugar were glucose and galactose, and 10% was leftover lactose.

6.4.2 Effect of substrate loading on cell growth and PHBV production

The effect of substrate loading was studied with fixed levels of other culturing conditions. Figure 6.1 illustrates the results of cell growth and PHBV synthesis in batch production with whey sugar hydrolysate as the substrate. As shown in Figure 6.1 (a), the cell growth curves from three substrate loadings overlapped at the exponential growth phase, which suggests that the microbes had close specific growth rates among the three substrate loadings. It took similar culturing times of around 168 h for cells to reach the stationary growth phase with loadings of 20 and 40 g/L COD. The cells required much longer time, which was around 240 h, to reach the stationary phase for 60 g/L COD loading. The final cell densities (represented by OD) were significantly different among three substrate loadings (p-value was 0.003). The results of CDM, shown in Figure 6.1 (b), agree well with the OD. The final PHBV productions also increased with the substrate loadings, which were 1.90 ± 0.64, 3.85 ± 0.11, and 5.89 ± 0.65 g/L produced with 20, 40, and 60 g/L COD loadings respectively. As intracellular polymers, the PHBV produced with different substrate loadings accounted for approximately 50% of CDM.

As shown in Figure 6.1 (c), the HV content, which influences the flexibility and elasticity of the thermoplastic material, increased slightly from 15% to 21% of PHBV which higher substrate loadings. The HV contents produced from whey sugar hydrolysate were higher than the 10% from previous studies using whey or similar dairy byproduct streams to produce PHBV by *H. mediterranei* (Koller et al., 2007; Koller, 2015), and close to studies using other sugar-based feedstocks (Cui et al., 2017b; Han et al., 2013). As discussed in previous chapters, a high HV content of the PHBV polymer is desirable to increase elasticity and flexibility and reduce the brittleness and stiffness of the plastic material; therefore, it can be manufactured into more types of products and help broaden the commercial applications of PHBV. The yields of CDM and PHBV which were the final productions divided by the substrate consumption, as illustrated in Figure 6.1 (d), remained similar among all substrate loadings. The yields of CDM and PHBV from whey sugar hydrolysate were around 0.8 g CDM/g COD and 0.4 g PHBV/g COD respectively, which are on the higher ends of what have been reported in literature (Ferre-Guell and Winterburn, 2018; Han et al., 2013; Koller et al., 2007; Pais et al., 2016). To summarize, the substrate loading of whey sugar hydrolysate influenced the final cell mass and PHBV concentrations in the batch production, but it did not influence the yields of CDM and PHBV, or the PHBV profile.

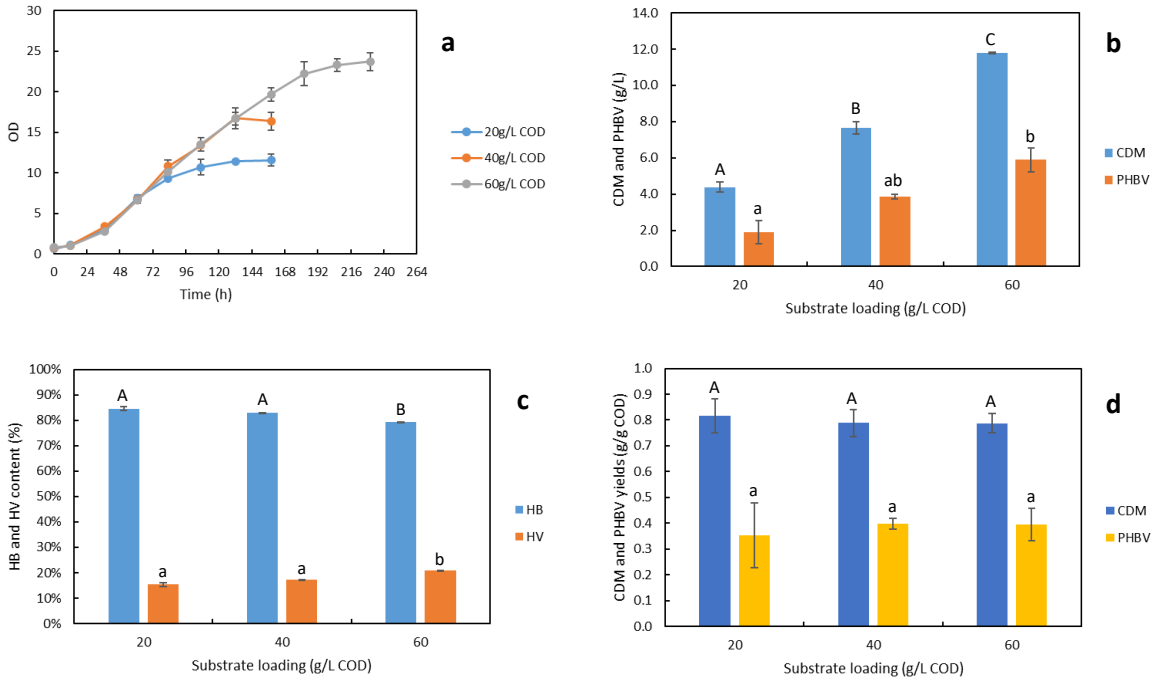

Figure 6. 1 (a) cell growth curves; (b) final concentrations of CDM and PHBV in batch production; (c) HV and HB contents of PHBV; and (d) yields of CDM and PHBV which were produced with different substrate loadings of whey sugar hydrolysate

(The same letters indicated that the differences were not significant at $p < 0.05$)

6.4.3 Batch PHA production in 6L bioreactor system

The 6-L bench-top bioreactor system was used for several runs of batch productions to monitor the dynamic profiles of cell growth, PHBV synthesis, and important processing parameters including DO, temperature, and pH etc. The substrate loading was 40 g/L COD. The temperature and pH were controlled at 40 ± 2 ℃ and 7 ± 0.2 during the entire culturing period. Four production batches were operated with different aeration strategies: the aeration rate was controlled at 2.5 vvm in the first two batches; the DO level of cell broth was controlled above 50% of saturation level in the last two batches with variable aeration rates ranging from 2.5 to 8 vvm.

As shown in Figure 6.2, the DO of cell broth with a stable aeration rate of 2.5 vvm dropped abruptly from over 80% sat. to less than 20% sat. at the exponential growth phase when the cells were rapidly propagating. The DO increased back to over 60% sat. when cells were approaching stationary phase. A similar phenomenon was observed in Chapter 5 where food waste was used as substrate to culture *H. mediterranei* in 6-L batches. With a different aeration strategy where the aeration rate was adjusted according to the DO level, the DO of cell broth was maintained over 50% sat. during the entire cultivation period.

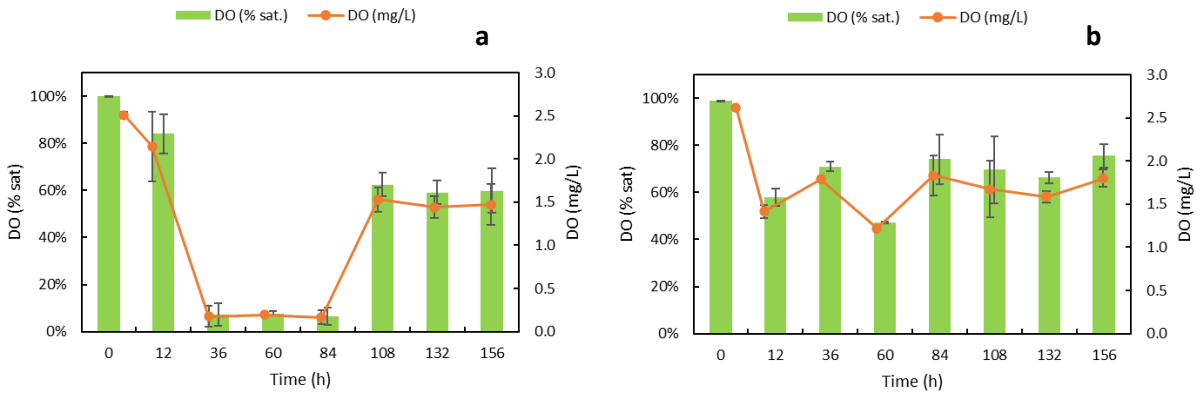

Figure 6. 2 Time profiles of the dissolved oxygen levels of cell broth in 6-L batch: (a) with a controlled aeration rate of 2.5 vvm; (b) with a controlled DO level above 50% sat.

The time profiles of cell growth and PHBV synthesis are demonstrated in Figure 6.3, corresponding to the two different aeration strategies. With a controlled aeration rate at 2.5 vvm, the concentration of CDM reached around 7 g/L VSS within 120 h and remained stable afterwards; and the PHBV concentration in the cell broth increased to around 3 g/L within the same culturing time. With a controlled DO level above 50% sat., the cells were growing at a much faster rate and reached the stationary growth phase within 84 h, which shortens the cultivation period by almost 2 days with the same substrate loading. The final CDM was slightly above 7 g/L VSS, which is

close to the CDM obtained with a controlled aeration rate. Therefore, a higher DO level of cell broth through the second aeration strategy increased the productivity of CDM. However, the final PHBV with a controlled DO level above 50% sat. was around 2 g/L, which is less than the PHBV produced with a controlled aeration rate at 2.5 vvm. This also suggests that the increase of the aeration rate to maintain a high DO level can decrease the PHBV content of cells, which results in a lower PHBV production within the same batch operation time. This may be due to more carbon flows directed towards cell growth and metabolism rather than PHBV synthesis. A similar result was also observed when food waste was used as the feedstock to produce PHBV by the same strain, which has been extensively described in previous chapter. The final PHBV yields (g PHBV/g sugars consumed) were: 0.17 ± 0.01 with 2.5 vvm of aeration, and 0.08 ± 0.03 with DO level above 50% sat. This suggests that the increase of aeration rate may reduce the final PHBV yield.

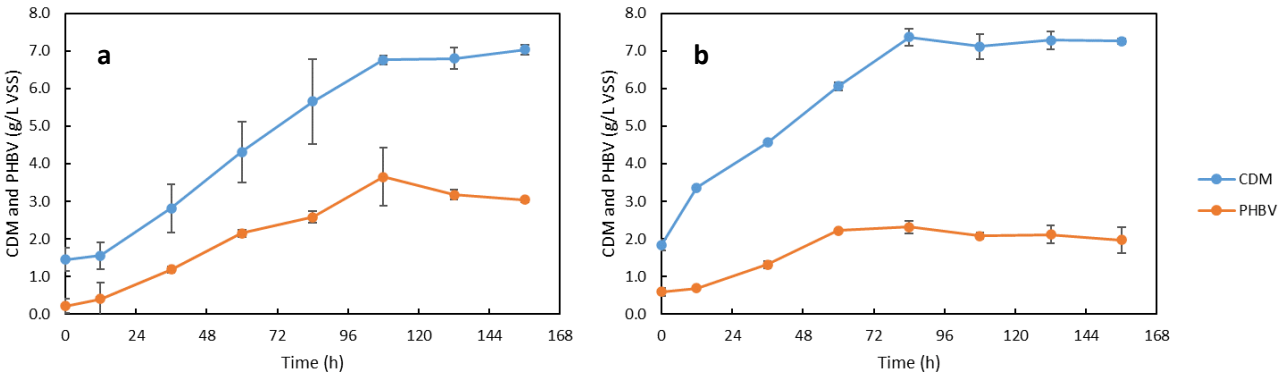

Figure 6. 3 Time profiles of the cell growth and PHBV production in 6-L batch: (a) with a controlled aeration rate of 2.5 vvm; (b) with a controlled DO level above 50% sat.

The dynamic profiles of HV and HB contents of PHBV produced from whey sugar hydrolysate with different aeration strategies are shown in Figure 6.4. With a controlled aeration

rate of 2.5 vvm, the HV content increased from 11% wt. to around 25% wt. during exponential growth phase, and decreased slightly to around 24% wt. at the stationary phase. With a controlled DO level above 50% sat., the HV content showed a similar trend in that it increased to around 26% wt. during the exponential growth phase and maintained similar levels in the stationary phase. The final HV content obtained from the batches with the DO above 50% sat. was 27% wt., which is higher than that produced from the batches with lower DO levels during the log phase (24% wt.). Therefore, although higher DO levels cause less PHBV production as discussed previously, it may lead to higher HV content of PHBV, which benefit the thermal and mechanical properties of the bioplastic product.

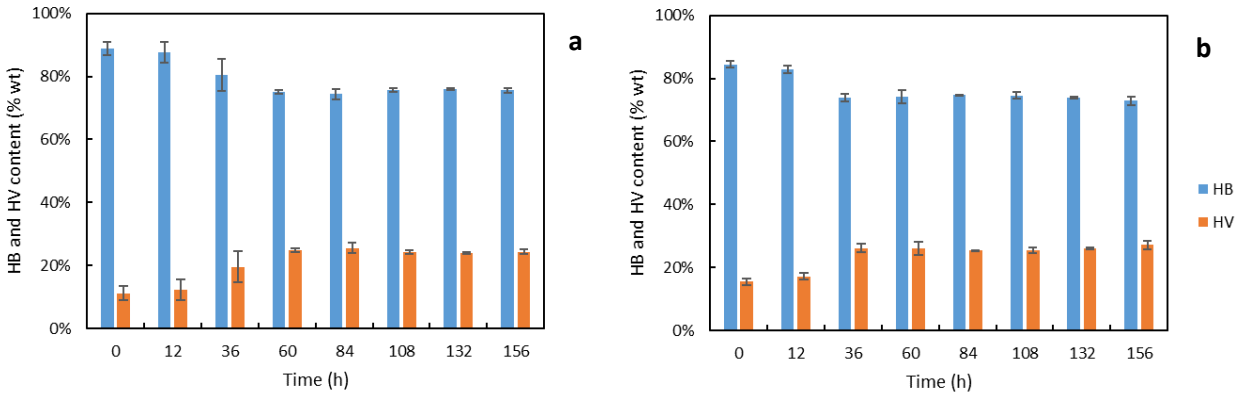

Figure 6. 4 Time profiles of HB and HV contents in the polymer produced from 6-L batch: (a) with a controlled aeration rate of 2.5 vvm; (b) with a controlled DO level above 50% sat.

The consumption of sugars including glucose, galactose, and lactose during cell growth is demonstrated in Figure 6.5. The final consumptions of individual sugars were (% of initial): 96% glucose, 49% galactose, and 4% lactose in batches with a controlled aeration rate of 2.5 vvm; and 99% glucose, 85% galactose, and 9% lactose in batches with DO levels above 50% sat.,

respectively. In general, the consumption rates of glucose and galactose were much faster in the batches with DO levels above 50% sat. than those with a controlled aeration rate of 2.5 vvm. Most of the glucose was consumed within 108 h for the batches with a controlled aeration rate of 2.5 vvm; and within 60 h for the batches with DO levels above 50% sat. Since the glucose and galactose account for the majority of carbon sources in whey sugar hydrolysate, they were quickly utilized for the faster cell growth and PHBV synthesis with higher DO levels, as illustrated in Figure 6.5. It is interesting to notice that the higher DO levels of cell broth actually promoted the consumption extent of galactose from 49% to 85% of initial level. Previous studies on similar dual-carbon substrates, consisting of both glucose and galactose, have reported that *H. mediterranei* usually starts to consume galactose after glucose is almost completely consumed (Koller et al., 2007; Pais et al., 2016; Saleh, 2012). The second aeration strategy increased the DO levels of cell broth during the exponential growth phase, where glucose was completed in a much faster rate, which resulted in an earlier start of galactose consumption. Therefore, galactose can be utilized to a higher extent with a higher DO level during rapid cell growth.

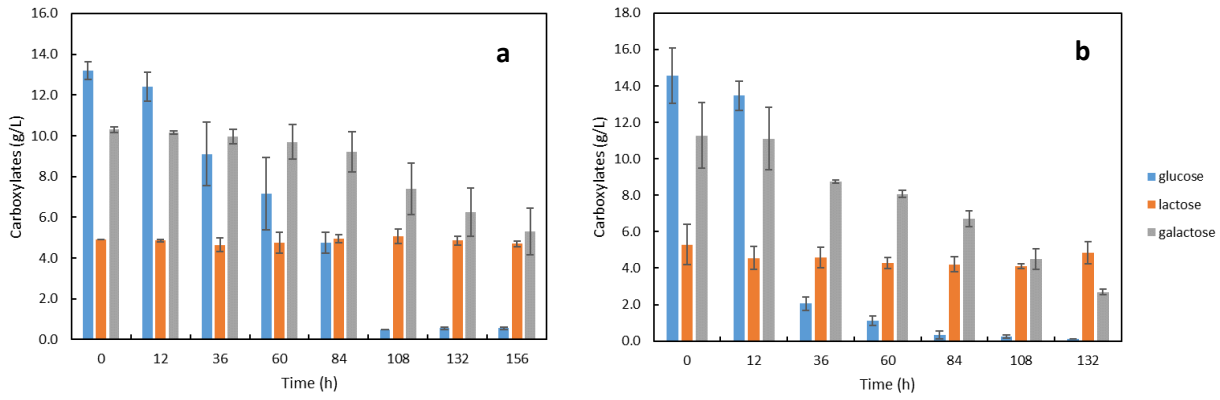

Figure 6. 5 Time profiles of sugars in 6-L batch: (a) with a controlled aeration rate of 2.5 vvm; (b) with a controlled DO level above 50% sat.

6.4.4 Physical properties of PHBV

The results of TGA, DSC analysis and tensile tests are shown in Table 6.2. The PHBV produced from whey sugar has a crystallization temperature (Tc) around 50 ℃, a melting temperature (Tm) around 130 ℃, and decomposition temperatures (T_d) around 300 ℃, regardless of whether purified or not. Those temperature parameters were different from the PHBV produced from food waste, which has been discussed in Chapter 5. In terms of mechanical properties, the purified and unpurified PHBV produced from the same whey sugar feedstock have different results: the PHBV with purification has a higher Young's modulus and a slightly higher tensile strength than the one without purification, suggesting the purification process may decrease the elasticity and increase the brittleness of the PHBV. The unpurified PHBV had a higher elongation at break, which means the purification process can decrease the fracture strain of the sample. The thermal and mechanical properties of PHBV were different from the ones produced from food waste, which has been discussed in Chapter 5. This suggests the feedstock type alone can influence the quality of the PHBV product. The thermoplastic properties of PHBV produced from whey sugar fall in the ranges of those that have been reported by other studies on *H. mediterranei* (Ferre-Guell and Winterburn, 2018; Han et al., 2015), and are comparable with the PHA products in the current market (Cambridge Consultants, 2018). These all suggest that PHBV produced in this study has good quality to be manufactured into thermoplastics.

Table 6. 2 Thermal and mechanical properties of PHBV produced from whey sugar

Feedstock	purification	T_c (ºC)	T_m (ºC)	T_d (ºC)	Young's modulus (MPa)	Tensile strength (MPa)	Elongation at break (%)
Lactose	No	55	125	295	565.68±64.43	15.84±3.39	8.09±2.03
Lactose	Yes	48	130	300	1140.56±351.3	17.27±7.72	4.82±0.47

6.4.5 Effect of recycled spent saline medium on cell growth and PHBV production

The cell growth curves of the four consecutive batches with the recycling of SSM after water removal by evaporation are illustrated in Figure 6.6. With 20 g/L COD loading, the recycling of 80% and 90% spent salts resulted in similar cell growth among the four consecutive batches, as illustrated by the Figure 6.6 (a) and (b). The final cell densities of the recycled batches were around an OD of 12, which were close to the final OD of the original batch production. Comparing Figure 6.6 (b), (c), and (d), which were the cell growth curves with different substrate loadings, the recycling of 90% spent salts resulted in similar cell growth among the four consecutive batches with 20 and 40 g/L COD loadings. However, for 60 g/L COD loading, the recycling of 90% spent salts decreased cell growth with a greater number of batch runs, which may be due to the inhibiting effect caused by the accumulation of leftover nutrients and cell metabolites.

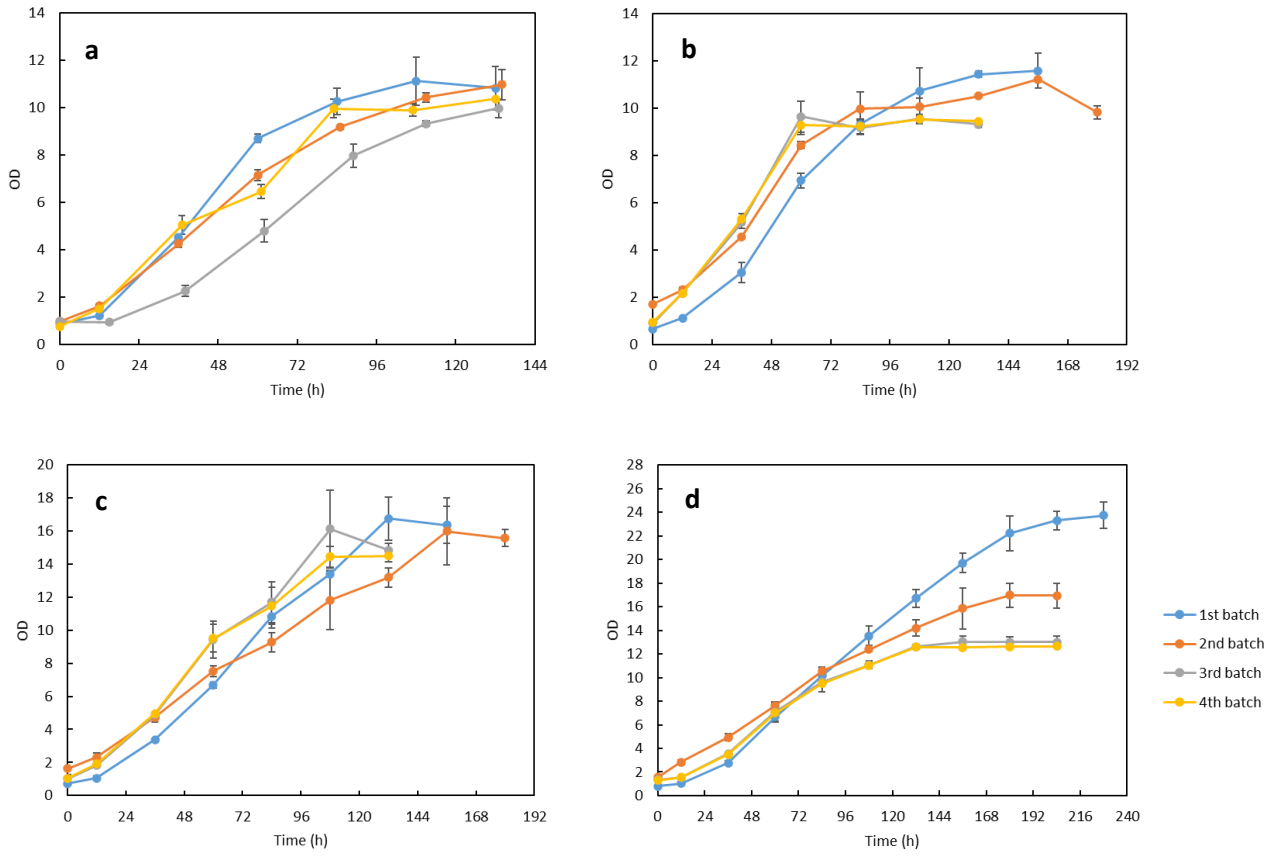

Figure 6. 6 Cell growth curves of four spent salts recycling batch runs with different substrate loading (g/L COD) and percentage of salts being recycled (% wt.): (a) 20, 80%; (b) 20, 90%; (c) 40, 90%; (d) 60, 90%

The results of CDM and PHBV productions of the recycling batches demonstrated in Figures 6.7 and 6.8 agree well with the cell growth curves. As suggested by the statistical results shown in Figure 6.7, the productions of PHBV in four consecutive recycling batch runs with the same substrate loading (20 g/L COD) were not significantly different with two different mass percentages of salts being recycled. And the productions of CDM from the four recycling batches were also very close. These results indicate that a higher mass percentage of the recycled salts can achieve similar productions compared to the lower mass percentage, and maintain robust

productions of PHBV among the four consecutive batches. With a 10% higher saving of salts, the cost reductions on purchasing new salts and high-saline wastewater treatment can help with overall economics in commercial-scale productions.

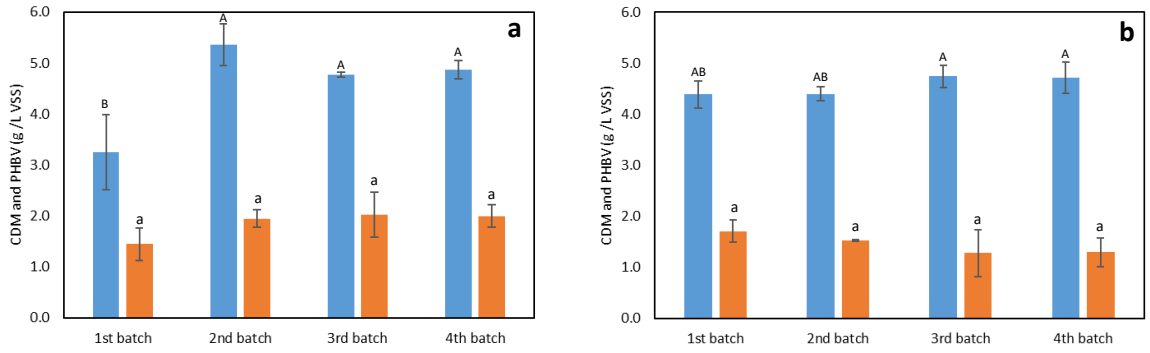

Figure 6. 7 CDM and PHBV productions in four spent salts recycling batch runs with the substrate loading of 20 g/L COD and different percentages of salts being recycled (% wt.): (a) 80%; (b) 90%

(Uppercase letters represented group comparison on CDM and lowercase letters represented group comparison on PHBV; the same letters indicated that the differences were not significant at $p < 0.05$)

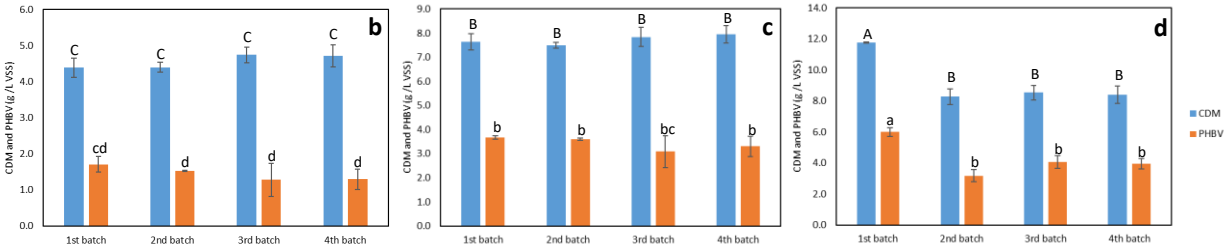

Figure 6. 8 CDM and PHBV productions in four spent salts recycling batch runs with different substrate loading (g/L COD) and 90% wt. of salts being recycled: (b) 20, 90%; (c) 40, 90%; (d) 60, 90%

(Uppercase letters represented group comparison on CDM and lowercase letters represented group comparison on PHBV; the same letters indicated that the differences were not significant at $p < 0.05$)

Given the statistical similarities of productions from the two mass percentages of recycled salts, the higher percentage (90% wt.) was then selected, and production results from recycling batches with three different substrate loadings are illustrated in Figure 6.8. The results of (b), (c), and (d) suggest that similar CDM and PHBV productions were obtained among the four recycling batches with 20 and 40 g/L COD loadings. However, with 60 g/L COD loading, the recycling of 90% spent salts had lower final CDM and PHBV productions with more recycling runs. Compared to the lowest substrate loading (20 g/L COD), the productions of CDM and PHBV with the higher loadings (40 and 60 g/L COD) were significantly higher among all four consecutive batches. However, the productions from 60 g/L COD loading were not significantly different from those derived from 40 g/L COD loading. These results indicate that an increase in substrate loading to some extent can help increase the PHBV productions among the recycling batches; however, to a greater extent, the substrate may be overloaded to cause an inhibition to cell growth and PHBV production. The effect of substrate inhibition can also be exacerbated due to the accumulation of leftover nutrients with more recycling runs. In terms of the PHBV profiles in the recycling runs, as shown in Figures 6.9 and 6.10, the HV and HB contents remained stable at around 20% and 80% of PHBV respectively among the four consecutive recycling batches, regardless of the substrate loadings of whey sugar hydrolysate or the mass percentages of the spent salts being recycled. This result suggests that the recycling of the spent salts did not influence the product quality of PHBV, which is promising for large-scale productions.

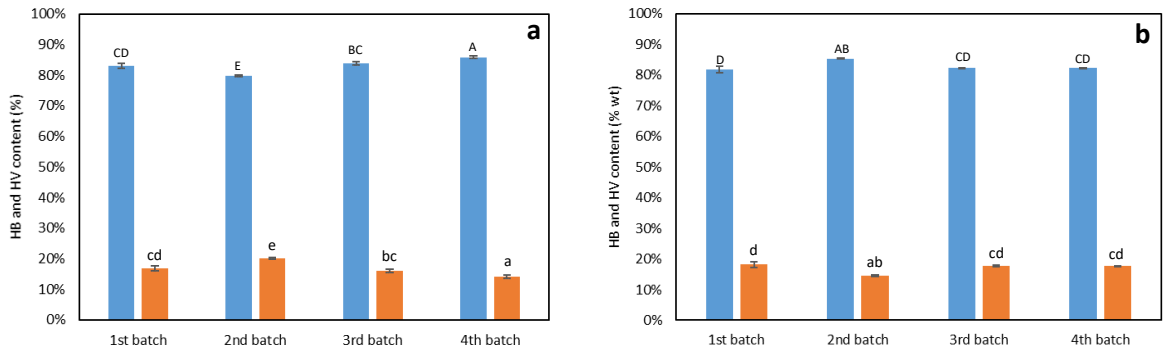

Figure 6. 9 HV and HB contents of PHBV produced from four spent salts recycling batch runs with the substrate loading of 20 g/L COD and different percentage of salts being recycled (% wt.): (a) 80%; (b) 90%

(Uppercase letters represented group comparison on HB content and lowercase letters represented group comparison on HV content; the same letters indicated that the differences were not significant at $p < 0.05$)

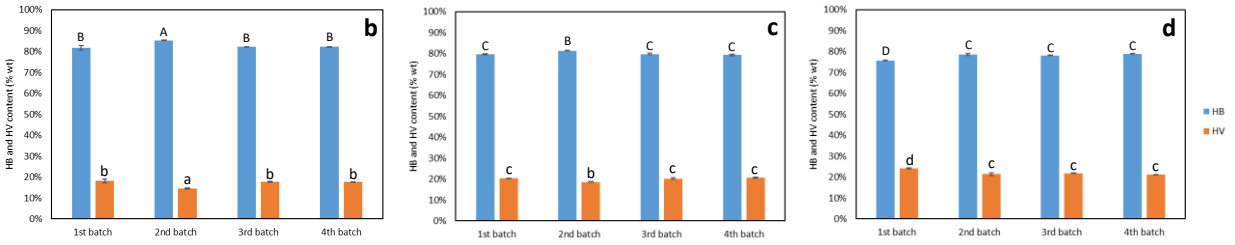

Figure 6. 10 HV and HB contents of PHBV produced from four spent salts recycling batch runs with different substrate loading (g/L COD) and 90% wt. of salts being recycled: (b) 20, 90%; (c) 40, 90%; (d) 60, 90%

(Uppercase letters represented group comparison on HB content and lowercase letters represented group comparison on HV content; the same letters indicated that the differences were not significant at $p < 0.05$)

6.5 Conclusions

The bioprocesses of PHBV production system utilizing whey sugar from commercial cheese making facilities as feedstock was developed. Major unit operations of the production system consisting of feedstock pretreatment through enzymatic hydrolysis, microbial fermentation, and spent salts recovery and recycling are demonstrated on a bench scale through 6L bioreactor systems. The dissolved oxygen (DO) levels of cell broth especially during the exponential growth phase were influential in that a higher DO level above 50% saturation. increased the microbial growth rate and the consumption extent of galactose, but reduced the final PHBV production. The direct recycling of spent brine after an evaporation step was successfully conducted for four consecutive batches with different substrate loadings, and the 90% recycling of spent salts resulted in stable productions of cell mass and PHBV for both 20 and 40 g/L sCOD loadings. The production system illustrated in this study has the potential of commercial bioplastic applications, suggests a feasible and environmental-friendly approach, and can be beneficial to the current dairy industry by providing a source of additional revenue.

Chapter 7. Techno-economic Analysis of An Industrial-scale System for Producing Polyhydroxyalkanoates from Cheese Byproducts by Halophiles

7.1 Abstract

Polyhydroxyalkanoates (PHA) are a family of biodegradable plastics used as an environmentally friendly alternative for conventional plastics in various applications. PHA can be produced through microbial fermentation of renewable feedstocks, including low-cost byproducts and waste streams from food processing plants. In this study, an industrial-scale PHA production system using cheese byproducts as feedstock was designed and analyzed for the material flows and economics. *Haloferax mediterranei* was utilized as the PHA-producer. Poly(3-hydroxybutyrate-co-3-hydroxyvalerate) (PHBV), a type of high-quality PHA, was the target product. Byproduct streams from a local cheese plant, with an input of 168.7 metric ton/day (MT/day) lactose, were used as the feedstock. SuperPro Designer was used as the software for the process design and economic modeling. Three scenarios with different processes for the treatments of used enzyme and spent medium were investigated and the major factors that influence the overall economics were identified. The simulated system produces 9700 MT/year PHBV with assumed PHA yield of 0.2 g PHBV/g lactose and an overall process efficiency of 87%. The breakeven price was found to be more sensitive to the lactose price than enzyme price.. The scenario with enzyme reuse and spent medium recycling achieved the lowest breakeven price among others, which can be less than 4 $/kg PHA based on the delactosed permeate (DLP) unit price. The study suggests utilizing dairy derived feedstocks has the potential to make PHA competitive in the bioplastic market, which could be beneficial to both dairy and bioplastic industries.

Keywords: Cheese byproducts, economic analysis, extreme halophiles, polyhydroxyalkanoates, whey streams.

7.2 Introduction

PHA is a group of 3-hydroxy fatty acid polyesters derived naturally from various types of microbes. It has thermoplastic properties and ecological characteristics, such as renewable origins and is biodegradable in the natural environment. Therefore, PHA has been an emerging bioplastic material in recent decades and has become a popular alternative for conventional petroleum-based plastics (Koller, 2018). PHA has a well-established commercial market and has been made into various products, e.g. packaging films, plastic containers, medical implant materials, drug carriers, nutritional supplements and biofuels, etc. PHA is produced globally at industrial scale, for example, 50,000 MT/a by ADM, USA (with Metabolix), 10,000 MT/a by Bio-On, Italy and 10,000 MT/a by Tianjin Green Bio-Science, China (Chen, 2009). The PHA market is around $0.72 billion in 2020 (Aeschelmann and Carus, 2015). The production cost of PHA is usually 3 to 4 times higher than that of petroleum-based plastic resins (Kourmentza et al., 2017). Reducing the production cost has been a bottleneck for the market expansion. The feedstock cost is one of the main contributors and accounts for over 40% of the total annual operating cost (Leong et al., 2017). Therefore, many researchers are developing bioconversion processes to utilize waste streams or industrial byproducts.

Whey permeate, lactose powder, and delactosed permeate (DLP) are byproduct streams derived from cheese, whey, and lactose manufacturing processes. Whey permeate is the side stream from the separation and concentration of whey protein. Lactose powder is produced from crystalizing the sugars from whey permeate, leaving behind DLP after the recovery of lactose

crystals (Oliveira et al., 2019). These byproduct streams are produced in large quantities from cheese-making facilities and contain rich nutrients including sugars, protein, amino acids, minerals, and micronutrients. However, whey permeate and DLP are currently sold as low value products including animal feed, fertilizers, field spread (Durham, 2009). Converting cheese processing byproducts to PHA can create an additional revenue for dairy processors, and potentially reduce high production cost and make PHA more competitive in the bioplastic market.

Haloferax mediterranei is an extreme halophilic archaeon that can maintain robust pure microbial culture in unsterile conditions. It has been extensively studied for its capability of producing Poly(3-hydroxybutyrate-co-3-hydroxyvalerate) (PHBV), a type of high-quality PHA, from various waste feedstocks, including ethanol stillage (Bhattacharyya et al., 2014), molasses wastewater (Cui et al., 2017d), cheese whey hydrolysates (Pais et al., 2016), olive mill wastewater (Alsafadi and Al-Mashaqbeh, 2017), macroalgal hydrolysates (Ghosh et al., 2019) and fermented food waste (Wang and Zhang, 2020). The biorefinery system involving this strain as the PHBV producer has several benefits over other freshwater microbes, which includes (1) a cheaper feedstock cost due to the use of waste/byproduct streams; (2) less energy consumption as sterilization and/or pasteurization is unnecessary; (3) less downstream process inputs due to the novel extraction process facilitated by osmotic shock. Correspondingly, the process design of the production system would be different from the systems using freshwater PHA producers and mixed cultures, mainly on the fermentation, downstream PHA extraction and purification processes, as well as the wastewater treatment.

The production system of PHA from cheese processing byproducts involves several essential

steps, including upstream feedstock pretreatment, fermentation for PHA production, and downstream processes for PHA extraction, purification, and drying. Several economic aspects involved in these processes, including direct capital cost, annual operating cost, revenue, etc. are studied in this research. The substrate cost varies among different types of cheese processing byproducts, and the price of the same type can also fluctuate depending on the market. Since *H. mediterranei* cannot use lactose directly (Pais et al., 2016), there is an essential step to hydrolyze lactose into its monosaccharides constituents, glucose and galactose, before the PHA production. Enzymatic hydrolysis is an environmentally friendly approach, which does not require as much mass and energy inputs as acid-catalyzed hydrolysis (El-Zawawy et al., 2011). The enzyme cost may be high depending on its price and usage in the hydrolysis. However, the cost can be saved through enzyme reuse or immobilization, which are viable in the lactose hydrolysis process (Gänzle et al., 2008; Wolf et al., 2018). The cultivation of *H. mediterranei* also requires around 18% total salts to maintain a suitable growth environment. The massive salt input involved in the fermentation step is another important factor which may influence the overall economics of the system. The recycling of the spent salts can reduce the costs of salts and high-saline wastewater treatment, and is also found to be feasible on *H. mediterranei* through many strategies by a previous study (Koller, 2015).

The objectives of this study were to: (1) develop a techno-economic model for an industrial-scale PHA production system and analyze the economics with focus on production cost and breakeven price; (2) identify potential pitfalls and aspects that would have major influence on the systematic economics; and (3) based on the former findings, provide suggestions on the primary targets of research and development before the actual construction and operation of PHA

production facilities.

7.3 Materials and Methods

7.3.1 Process design and analysis tool

The techno-economic model of PHA production systems using cheese whey byproduct streams was developed, and the process flows and operations were demonstrated using SuperPro Designer software v12.0 (Intelligen Inc., USA). Three types of byproducts, lactose powder, whey permeate, and DLP, were utilized as the carbon source in the model. An industrial scale of production was employed for the model. The cheese processing byproduct feedstock was simplified as 168.7 MT/day of lactose, which was a feasible scale for a local cheese processing facility. Shown in Figure 7.1, the generic flowsheet of the production system consists of 10 essential unit operations, which are operated to convert the three types of cheese whey byproduct streams into the dry PHA powder as the target product. The essential unit operations involved in the model were (in the order of process flows): hydrolysis, blending, fermentation, storage, centrifugation 1, extraction, centrifugation 2, wash, centrifugation 3, and spray drying. Depending on the process design, the additional unit operations were ultrafiltration (after hydrolysis), and evaporation (after centrifugation 1). As the general description of the system, the lactose in the byproduct streams was first hydrolyzed into glucose and galactose with appropriate amount of lactase enzyme in the hydrolysis tank. The hydrolysate streams were then mixed with salts and other nutrients in a blending process and fed into a fermentation tank where the microbe *H. mediterranei* was inoculated to produce PHA polymers intracellularly. The fermentation was designed to be operated in a staggered mode with 5 fermenters with a retention time of 5 days. At the end of fermentation, the cell broth was transferred into a storage tank and further processed through centrifugation to separate the cells from spent medium. The cells were then subjected to

an extraction process via water addition that caused osmotic shock and cell lysis to release PHA polymers. The PHA was then processed through consecutive runs of centrifugation and wash to improve purity. The washed PHA was finally processed with a spray dryer which yielded a dry PHA powder with less than a 5% moisture content (MC).

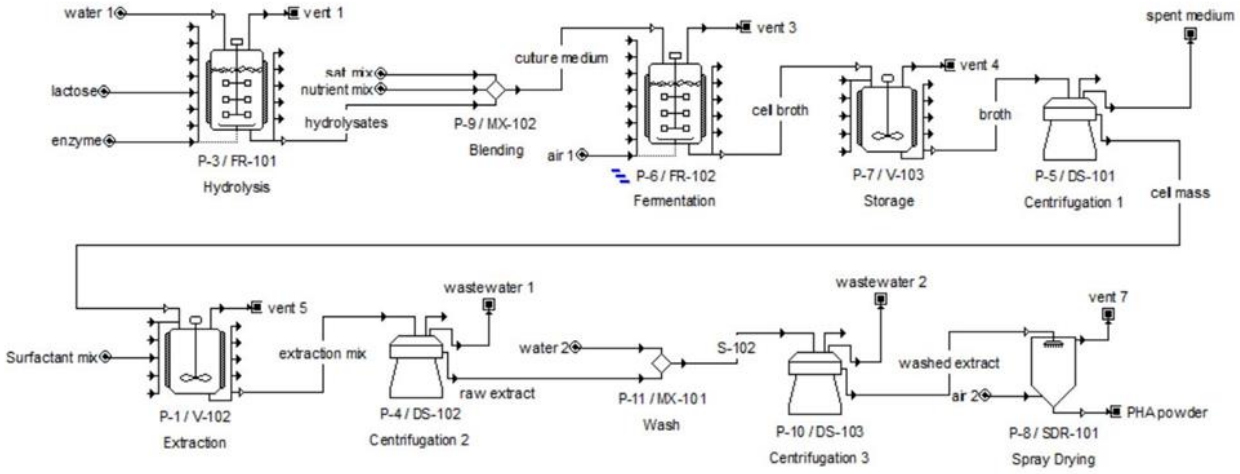

Figure 7. 1 Process flowsheet of PHA production model (Scenario 1)

Three scenarios (shown in Figures 7.1, 7.2 and 7.3) were compared in the model: Scenario 1 without enzyme reuse or spent salt recycling; Scenario 2 with enzyme reuse but without spent salt recycling; Scenario 3 with both enzyme reuse and spent salt recycling. In Scenario 2, an ultrafiltration unit was added right after the hydrolysis tank to concentrate and reuse the enzyme separated from the hydrolysate streams. This may not only save costs for purchasing new enzymes, but also minimize the influence of enzyme accumulation in the following processes. Based on the Scenario 2, Scenario 3 added an evaporation process after the centrifugation 1, where the spent saline medium (SSM) was further concentrated to yield a brine concentrate and water condensate. The brine concentrate was then recycled back to the fermentation process, and the water

condensate went into the hydrolysis process. The recycling of the spent brine concentrate is designed in a way where 90% salts were reused with 10% discharged as high-saline wastewater. In that case, there wouldn't be salt accumulation in each batch run; instead, there was additional fresh salts needed for each batch, which is designed as equivalent to the loss of the 10% salts.

The SSM recovery and water reclamation strategies were developed to reduce the raw material input and minimize salt discharge to the environment, making this biorefinery system more environmentally friendly.

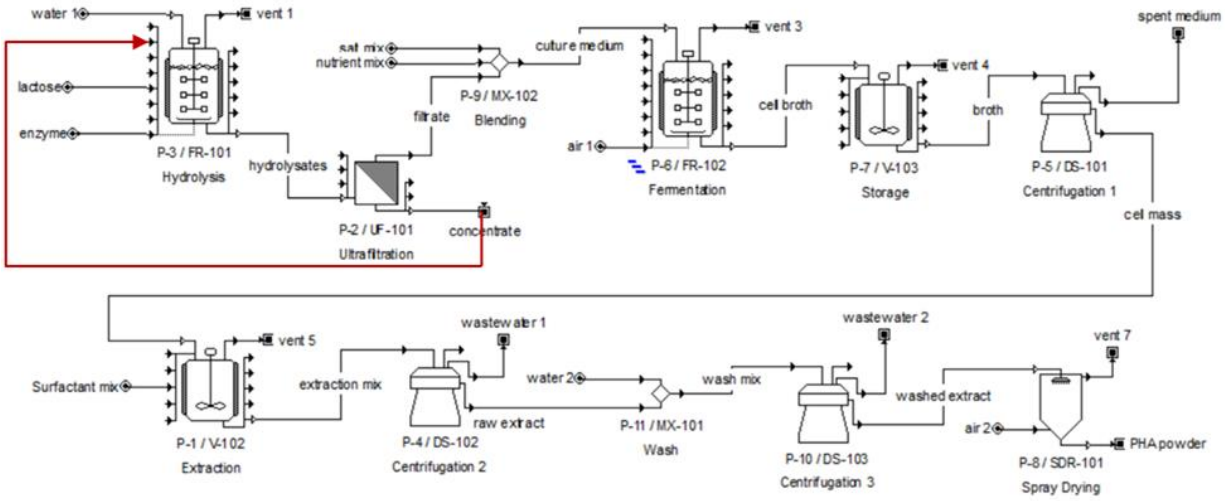

Figure 7. 2 Process flowsheet of PHA production model with enzyme reuse (Scenario 2)

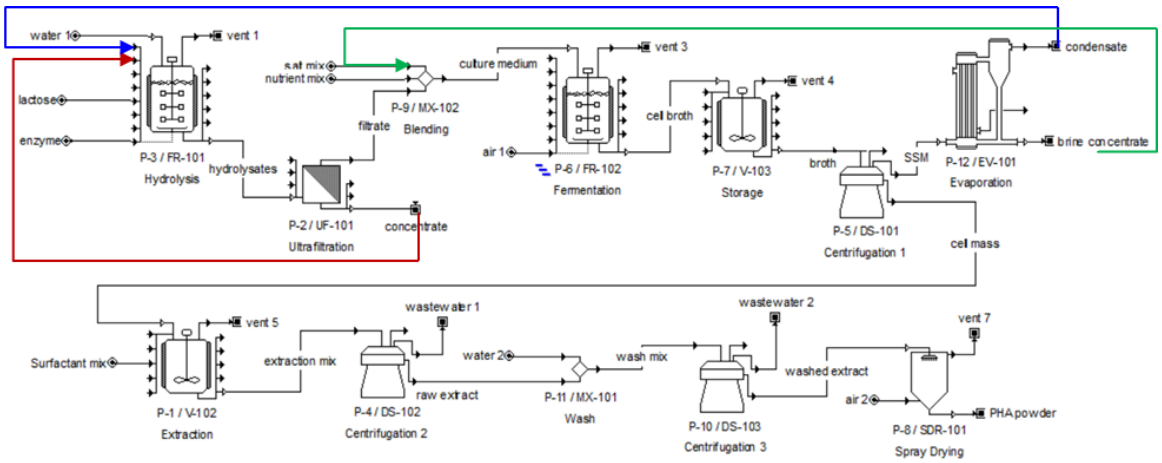

Figure 7. 3 Process flowsheet of PHA production model with enzyme reuse and spent brine recycling (Scenario 3)

7.3.2 Scenario unit operations

7.3.2.a Hydrolysis

The process starts with the hydrolysis operation. During this process, the lactose of the feedstock is broken down into monosaccharides through enzymatic hydrolysis. The input streams of this unit operation are: (1) lactose, 168.7 MT/day; (2) water, 744.7 MT/day (calculated based on the density of a solution with 20% lactose (McDonald and Turcotte, 1948); (3) lactase enzyme, 0.53 MT/day. The operational conditions of hydrolysis are set to be: charge 1: water, 2500 gal/min, 79.1 min; charge 2: lactose, 560 MT/h, 20 min; charge 3: enzyme, 15 min; agitation: 12h; heating: 37 ºC, 12h; hydrolysis: 12h, 80% maximum working volume, 95% reaction extent. The stoichiometric equation of hydrolysis (with mass coefficients) is:

$$342.30\ lactose + 18.02 water \xrightarrow{lactase} 180.16\ glucose + 180.16\ galactose. \quad (7.1)$$

Right after the reaction, 100% vessel volume is transferred out with a flow rate of 2500 gal/min for 96.2 min. The compounds of output stream (hydrolysates) are water, 736.3 MT/batch; glucose, 84.4 MT/batch; galactose, 84.4 MT/batch; lactose, 8.4 MT/batch; and enzyme, 0.53 MT/batch.

7.3.2.b Blending

Following the hydrolysis step, the hydrolysates stream is then blended with the salts and nutrient mix before feeding into the next fermentation tank. A mixed salt stock named minimum saline medium (MSM) is registered with the composition as follows: NaCl, 156 g/L; $MgCl_2.6H_2O$, 13 g/L; $MgSO_4.7H_2O$, 20 g/L; $CaCl_2.6H_2O$, 1 g/L; KCl, 4 g/L; NaBr, 0.5 g/L and $FeCl_3$, 5 mg/L (Wang and Zhang, 2020). The salinity of MSM was measured to be 18.8 parts per thousand (ppt), correspondingly the salt water density is around 1.13 kg/L (McDonald and Turcotte, 1948). The mass input of MSM is calculated as 172 MT/batch based on this density. The hydrolysate from the previous unit operation is used as the carbon source for the fermentation. An additional nutrient mix including mostly 16.9 MT/batch of ammonium chloride is used to provide essential nutrients besides the carbon source.

7.3.2.c Fermentation

The fermentation process is the main unit operation of the system, where *H. mediterranei* is cultured for PHBV production using the hydrolysates derived from cheese whey byproduct streams. The input streams of fermentation are culture medium coming out of the previous blending process, which consist of cheese whey hydrolysates, MSM, nutrient mix, etc. Forced aeration is provided with a flow rate of 1 volume per volume per minute (vvm). There are 5

identical fermentation tanks operated in a staggered batch mode in the system. One tank is filled with culture medium and started the fermentation each day, while another tank is emptied and cleaned to prepare for the next day fermentation. The fermentation time for each batch is assumed to be 5 days. Each batch fermentation adopts the same operational conditions: continuous agitation, heating (37 ºC), venting. The PHBV yield is assumed as 0.2 g/g sugar, which was obtained from experiments. The PHBV content is assumed to be around 60% cell dry mass (CDM) (Pais et al., 2016). Both reactions are set to have 95% conversion efficiency. After fermentation, 90% of cell broth is transferred out to downstream processes for PHBV production, meanwhile 10% of cell broth is left in the fermentation tank to be used as the seed for the following batch production. The output streams in the cell broth are: PHBV (contained in the cells), 31.8 MT/batch; residual biomass, 20.1 MT/batch; MSM, 155.1 MT/batch; glucose, 3.8 MT/batch; galactose, 3.8 MT/batch; lactose, 7.6 MT/batch; ammonium chloride, 0.7 MT/batch; enzyme, 0.5 MT/batch; water, 691.5 MT/batch. After each fermentation batch, the harvested cell broth is temporarily stored in a storage tank for downstream processes.

7.3.2.d Cell mass separation through centrifugation

The centrifugation 1 is used to proceed solid and liquid separation on the harvested cell broth. The duration is set to be 4 h. Through centrifugation, 98% (m/m) of solids which are cells containing PHBV granules are separated from the cell broth. And 2% (m/m) of cell solids are left in the spent medium. Additionally, 10% (v/v) of cell broth is assumed to be the cell solids slurry, which would then go to downstream PHBV production processes, and 90% (v/v) of cell broth is the supernatant from the centrifugation process, which contains the majority of salts, sugars, and other leftover nutrients from the spent medium. The output streams of centrifugation 1 are: (1) cell

mass stream containing PHBV, 31.1 MT/batch; residual biomass, 19.8 MT/batch; Spent MSM, 15.5 MT/batch; glucose, 0.38 MT/batch; galactose, 0.38 MT/batch; lactose, 0.76 MT/batch; ammonium chloride, 0.07 MT/batch; enzyme, 0.05 MT/batch; water, 103.7 MT/batch; (2) spent medium stream containing PHBV, 0.64 MT/batch; residual biomass, 0.36 MT/batch; spent MSM, 139.6 MT/batch; glucose, 3.4 MT/batch; galactose, 3.4 MT/batch; lactose, 6.8 MT/batch; ammonium chloride, 0.7 MT/batch; enzyme, 0.5 MT/batch; water, 587.8 MT/batch. The mass compositions of cell mass stream and spent medium stream are 60.4% and 79.1% respectively. The cell mass stream then proceeds to downstream processes, and the spent medium stream is disposed of as high salinity wastewater in the Scenario 1 and 2. The spent medium stream is subjected to an additional unit operation of evaporation for salt recycling in Scenario 3.

7.3.2.e PHA extraction, purification and drying

The concentrated cell mass stream from centrifugation 1 is then fed into a tank to extract PHBV granules from cells. 0.1% (m/m) of Sodium dodecyl chloride (SDS) water solution is used as the surfactant to facilitate the unique extraction process for *H. mediterranei* (Escalona et al., 1996). The extraction process is conducted with continuous agitation and heating at 37 ºC for 4 h. After extraction, 100% vessel working volume with 80.2% (m/m) water is transferred out to another centrifugation process (centrifugation 2) to concentrate the PHBV extract from the mixed solution. The process duration of centrifugation 2 is set as 2 h. The recovery efficiencies of mass and volume in this process are assumed to be the same as centrifugation 1. The output raw extract stream consists of PHBV, 30.5 MT/batch; residual biomass, 2.0 MT/batch; MSM, 1.5 MT/batch; glucose, 0.04 MT/batch; galactose, 0.04 MT/batch; lactose, 0.07 MT/batch; ammonium chloride, 0.007 MT/batch; enzyme, 0.005 MT/batch; and water, 55.1 MT/batch (61.7% m/m). The supernatant from the centrifugation 2 is subjected to wastewater treatment with the local sewer

price.

The raw extract stream is then processed through a wash run, where it is mixed with 89.3 MT/batch of water to remove most of the soluble compounds and purify the PHBV extract. After the wash run, the streams are centrifuged again in the centrifugation 3 step, where the recovery efficiencies of mass and volume in this process are assumed to be the same to centrifugation 1 and 2. The output purified extract stream contains PHBV, 29.8 MT/batch; residual biomass, 0.2 MT/batch; MSM, 0.2 MT/batch; glucose, 4 kg/batch; galactose, 4 kg/batch; lactose, 8 kg/batch; ammonia chloride, 0.8 kg/batch; enzyme, 0.5 kg/batch; and water, 43.3 MT/batch (59% m/m). Finally, the purified extract stream is treated by a spray dryer to yield dry PHBV powder with less than 5% MC, as the final product stream of the system. The dryer is operated at 70 ^{o}C for 12 h to achieve a final loss on drying (LOD) of 5%.

7.3.3 Additional unit operations involved in the Scenario 2 and Scenario 3

7.3.3.a Ultrafiltration for enzyme reuse

Based on the processes of Scenario 1, an additional ultrafiltration unit is added in Scenario 2 immediately after the hydrolysis operation. In the ultrafiltration process, it is assumed that 100% enzyme is rejected (rejection factor =1) and permeate stream is 80% (v/v) of feed stream (concentration factor =5). The duration of the process is set to be 8 hours per batch. The membranes used in this process are Dft membranes with a pore size of 0.45 micron, and the replacement frequency of the membranes is once per every 5000 operating hours. The filtrate from the process containing hydrolysates goes to the next fermentation process for cell cultivation and PHBV production. The concentrate stream containing mostly spent enzyme goes to the next hydrolysis

batch run, where 80% of spent enzyme with 20% fresh enzyme are used.

7.3.3.b Evaporation for spent brine recycling

Additional to Scenario 2, an evaporation unit is added after centrifugation 1 in Scenario 3 to further process the spent saline medium from cell broth. The evaporation process takes 6 hours per batch. It is assumed that 50% (m/m) water is evaporated from the spent medium, and 100% vapor gets condensed and is reused in the following hydrolysis batch run. After evaporation, the spent medium turns into a brine concentrate stream, where all of the salts from spent medium are reclaimed. The model assumed that 90% of the brine concentrate is reused in the following fermentation batch run, and the leftover 10% is treated as the high saline wastewater.

7.3.4 Economic evaluations

The economic analysis was conducted based on the technical process design and mass and energy balances of the production system. All costs were given with 2021 pricing in US dollars ($). The prices of major raw materials, utilities, consumable materials, and waste treatment services were listed in Table 7.1. The cost of labor was based on an adjusted basic rate of 35.65$/h and a lumped rate of 25$/h. The labor rates were adjusted based on the assumption of four operators a shift at 30$/h, 24h/day, and 320 day/year; and an engineer at 50$/h and 2080 h/year; and a manager at 50$/h, 40h/week, and 52 week/year to maintain the year-round operation of the production system. The price of PHBV product was assumed as 10$/kg.

Table 7. 1 Prices of raw materials, utility, consumable materials, and waste treatment services

Raw materials price				Utility and consumable materials rate			
Item	Price	Unit	Source	Item	Price	Unit	Source
$CaCl_2$	0.15	$/kg	(Alibaba Group, 2021a, p. 2)	Steam	12	$/MT	Default values from SuperPro Designer (Intelligen, Inc., 2021)
KCl	0.3	$/kg	(Statista, 2021)	Cooling water	0.05	$/MT	
$MgCl_2$	0.1	$/kg	(Alibaba Group, 2021b, p. 2)	Chilled water	0.4	$/MT	
$MgSO_4$	0.35	$/kg	(Alibaba Group, 2021c, p. 4)	Glycol	0.35	$/MT	
NaBr	0.4	$/kg	(Alibaba Group, 2021d)	Standard electricity	0.063	$/MT	
NaCl	0.04	$/kg	(Alibaba Group, 2021e)	Filtration membranes	400	$/$m^2$	
$NaHCO_3$	0.2	$/kg	(Alibaba Group, 2021f, p. 3)	Cleaning powder	4.91	$/kg	
NH_4Cl	0.2	$/kg	(Alibaba Group, 2021g)	lubricant	1.84	$/L	
SDS	0.8	$/kg	(Alibaba Group, 2021h)	Wastewater treatment rate			
water	0.0017	$/kg	(California Water Service, 2021)	Item	Price	Unit	Source
PHBV	10	$/kg	(Leong et al., 2017)	Wastewater	0.002	$/L	(Gryczko et al., 2021)
				High-saline wastewater	0.041	$/L	Personal communication[b]

[b] The rate of high-saline wastewater treatment service was determined from a personal communication with a local food business based on the treatment rate of a specific type of wastewater with similar high salinity to this study.

The economic analysis of the study focused on the direct fixed capital cost (DCC), and annual operating cost (AOC). The professional estimates from business vendors were considered for major equipment selection, sizing, and cost. Table 7.2 lists the cost items and calculation factors involved in the capital investment estimation. The coefficients were obtained as the default values of the SuperPro built-in database (Intelligen, Inc., 2021), which have been compared against other sources from literature with similar sizes PHA production systems (Leong et al., 2017), as well as personal communications with industrial partners for quality assurance. The breakdown of AOC included raw materials cost (RMC) and other major costs of labor, facility, consumables, waste treatment/disposal, and utilities.

Table 7. 2 Capital investment estimation of the economic model

Cost item	Estimation factor	Cost item	Estimation factor
Total plant direct cost (TPDC)		Total plant indirect cost (TPIC)	
Equipment cost (EC)		Engineering	0.25 × TPDC
Unlisted equipment cost	0.20 × EC	Construction	0.35 × TPDC
Installation	0.36 × EC		
Process piping	0.35 × EC	Total plant cost (TPC)	TPDC+TPIC
Instrumentation	0.40 × EC		
Insulation	0.03 × EC	Other cost (OC)	
Electrical facilities	0.10 × EC	Contractor's fee	0.05 × TPC
Building	0.45 × EC	Contingency	0.10 × TPC
Yard improvement	0.15 × EC		
Auxiliary facilities	0.40 × EC	Direct fixed capital cost (DCC)	TPC+OC

The economic feasibility of the model was analyzed for a 20-year economic lifetime with an annual interest or discount rate of 7%. The breakeven price (BP, $/kg) of PHBV was calculated and compared for the three scenarios in this study. The BP is the cutoff selling price of the product that makes the net annual worth (NAW, $/year) zero, based on the following equations (7.1) through (7.4). The taxes and depreciation were neglected because of no profit or net income above cost present in the annual cash flow.

$$-(A + AOC) + BP * MP = NAW = 0 \tag{7.2}$$

$$BP = \frac{A+AOC}{MP} \tag{7.3}$$

$$A = DCC * \frac{i(1+i)^n}{(1+i)^n-1} \tag{7.4}$$

Where,

A = level cash flow of capital investment ($/year), which is the equivalent annualized capital cost with escalation over the life of the project;

DCC = direct capital cost ($), the total fixed capital investment assumed to occur all at time zero;

AOC = level annual operating cost ($/year), assumed constant over the life of the project;

MP = main product production and sales rate (kg/year), assumed constant over the life of the project;

i = annual interest or discount rate (%), constant at 7% over the lifetime of the project;

n = project economic lifetime (years), assumed as 20 years.

7.3.5 Sensitivity analysis

Sensitivity analysis was conducted to understand the influence of major factors on the overall economic model and make recommendations to optimize process parameters for better economic purposes. Two price items including feedstock price (described as lactose price) and the lactase enzyme price, which were identified as the major factors influencing the operating cost, were analyzed with the feasible price ranges in the market: 0.04 to 2.20 $/kg lactose and 1 to 120 $/kg lactase enzyme, respectively. Given the price ranges, the breakeven price of selling the main product PHA was calculated based on Equations (2) and (3). The different responses of breakeven price to the two factors were then compared among the three production scenarios to identify which scenario can give the lowest breakeven price. The breakeven price was also examined based on the median prices of different types of cheese processing byproducts including lactose powder (0.77 $/kg lactose), whey permeate (0.37 $/kg lactose), and DLP (0.13 $/kg lactose).

7.4 Results and Discussions

7.4.1 Mass and energy flows in the model

The model aimed at converting the daily input of feedstock into PHBV dry powder within the

same time frame. Therefore, the operating schedule was designed to fit the time frame by adopting the staggered operation mode for the main production tanks, which resulted in a faster recipe cycle time of 24 h than the recipe batch time of 123 h. The annual operating time was assumed to be 7899 h in the model, and there were 325 batch runs per year. These values were considered for the calculations of materials and energy flows of the system, and equipment sizing. Figures 7.1 through 7.3 show the schematic flow diagrams of the three scenarios. The mass and energy balance was determined in the model. Table 7.3 presents the major material flows in the three scenarios.

Table 7. 3 The mass of input and output streams of Scenarios 1 through 3[a]

Input (MT/batch)	Scenario 1	Scenario 2	Scenario 3	Output (MT/batch)	Scenario 1	Scenario 2	Scenario 3
Water	834.0	834.0	286.4	PHBV	31.8	31.8	31.8
Lactose	168.7	168.7	168.7	SSM	743.2	743.2	44.3
Enzyme	0.5	0.1	0.1	Wastewater	359.6	359.6	359.6
Salt mix	172.4	172.4	46.7	Vent	9631.5	9631.5	9631.5
Nutrient mix	16.9	16.9	16.9				
Air	9499.5	9499.5	9499.5				
Extraction mix	0.3	0.3	0.3				

[a] Scenario 1: PHA production base model; Scenario 2: PHA production model with enzyme reuse; Scenario 3: PHA production model with enzyme reuse and spent brine recycling

All scenarios have the same inputs of cheese byproduct feedstock (represented by lactose), nutrient mix, air, and extraction mix, and outputs of main product PHBV, wastewater, and vent, because of the mass balance achieved for the same production target per batch. The target product stream (PHBV) is 31.8 MT/batch, which corresponds to an overall yield of 18.8% from lactose input. The major wastewater streams are SSM and wastewater. The wastewater is the sum of normal-salinity wastewater 1 and wastewater 2 streams derived from PHA extraction and wash operations. The SSM is treated as high-salinity wastewater, which costs considerably more than normal-salinity wastewater in terms of treatment and disposal. The vent stream output contains air and biogenic CO_2 emitted from various tanks. The input enzyme in Scenario 2 and 3 is 0.1

MT/batch, which is only 20% of that in Scenario 1, since it was assumed that the enzyme was separated from the hydrolysates stream through an ultrafiltration unit and 80% of spent enzyme was reused in the following batch. Additionally, since there is an evaporation unit in the Scenario 3 for salt and water recovery and recycling, the input amounts of salt mix and water are 46.7 and 286.4 MT/batch respectively, which are around 27% and 34% of those materials used in Scenario 1 and 2. The output amount of SSM in Scenario 3 is 44.3 MT/batch, which is only 6% of that in the former two scenarios. The reductions of input and output materials in Scenario 3 can lead to economic benefits of the production system. Since Scenario 3 also has much less output of SSM, it can help minimize the energy consumption and environmental concerns regarding high-saline wastewater treatment and disposal.

Table 7.4 shows the consumptions of standard electricity, steam, and cooling water in different scenarios. According to the energy balance conducted in the model, Scenarios 1 and 2 have the same consumptions of utilities. The utility steam in Scenario 3 is 1.4E+5 MT, which is about 5 times that in the other two scenarios. This high consumption of steam is due to the additional evaporation unit. Table 7.5 summarizes the major equipment and specifications used in the three scenarios, which were used to estimate equipment cost (EC). The material and energy balances of the model is used to determine the size and the operational throughput of each piece of equipment. The vessel volumes of the tanks are estimated based on the volumes of input and output streams and the assumption that 85% of vessel volume is working volume and the remaining 15% is used as headspace surge capacity. The throughputs of centrifuges are adjusted in a way that the total processing time of the three centrifuges is less than the cycle time (24h), so that the downstream processes of PHA extraction, purification and drying can be completely within the same batch

time. The unit costs of tanks are estimated based on a rate of 793$/m^3.

Table 7. 4 Utility consumption in Scenarios 1 through 3[a]

Scenario No.	Electricity (thousand MW-h/year)	Steam (thousand MT/year)	Cooling water (million MT/year)
1	164	28	19.6
2	165	28	19.6
3	165	140	19.3

[a] Scenario 1: PHA production base model; Scenario 2: PHA production model with enzyme reuse; Scenario 3: PHA production model with enzyme reuse and spent brine recycling

Table 7. 5 The specifications of major equipment used in Scenarios 1 through 3[a]

Equipment	Label	Scenarios[a]	Quantity/ Staggered	Description	Unit cost ($)
Fermenter	FR-101	1,2,3	1/0	Vessel Volume = 1025 m^3	636,000
Fermenter	FR-102	1,2,3	1/5	Vessel Volume = 1129 m^3	619,000
Blending tank	V-103	1,2,3	1/0	Vessel Volume = 939 m^3	552,000
Disk-Stack centrifuge	DS-101	1,2,3	1/0	Throughput = 211 m^3/h	310,000
Blending tank	V-102	1,2,3	1/0	Vessel Volume = 376 m^3	141,000
Disk-Stack centrifuge	DS-102	1,2,3	1/0	Throughput = 169 m^3/h	200,000
Disk-Stack centrifuge	DS-103	1,2,3	1/0	Throughput = 90 m^3/h	100,000
Spray Dryer	SDR-101	1,2,3	1/0	Dryer Volume = 35 m^3	150,000
Ultrafilter	UF-101	2,3	1/0	Membrane Aera = 5575 m^2	1,000,000
Evaporator	EV-101	3	1/0	Evaporation Aera = 111 m^2	491,000

[a] Scenario 1: PHA production base model; Scenario 2: PHA production model with enzyme reuse; Scenario 3: PHA production model with enzyme reuse and spent brine recycling

7.4.2 Economic analysis: comparison on equipment cost, direct capital cost and annual operating cost

The economic analysis has been conducted in the model for all three scenarios based on the material and energy flows. The important factors of model economics including EC, DCC, and AOC have been compared among the three scenarios, as shown in Figure 7.4. EC and DCC increase from Scenario 1 to 3, mainly due to more unit operations in scenarios 2 and 3. The DCC of the system starts at a little more than 40 million $ to 55 million $, which is a comparable capital size of a full scale production plant to previous studies (Bhattacharyya et al., 2015; Choi et al.,

2010). The EC is around 10 million $, which can be reduced by many operational strategies, e.g. maximizing the occupancy time per batch by using the same centrifuge for multiple unit processes without compromising overall productivity; and reducing equipment sizes by a continuous operating schedule. Opposite to the EC and DCC, the AOC has a descending order among the three scenarios, which is from around 56 million to 40 million $.

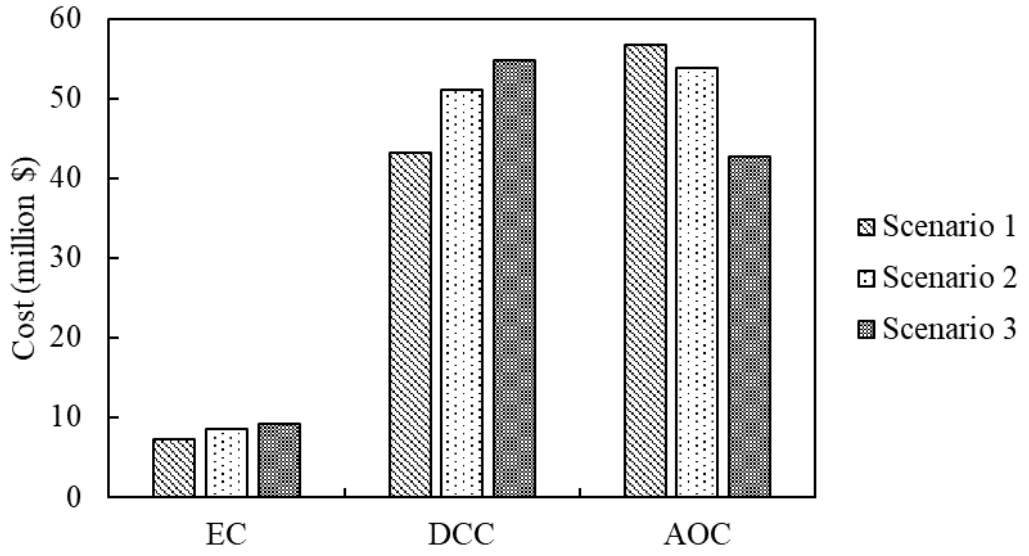

Figure 7. 4 EC, DCC and AOC of Scenarios 1 through 3 (the lactose price of 0.22 $/kg and enzyme price of 40 $/kg were used for all scenarios)

Scenario 1: PHA production base model; Scenario 2: PHA production model with enzyme reuse; Scenario 3: PHA production model with enzyme reuse and spent brine recycling

Taking a closer look at the AOC of the three scenarios, as shown in Figure 7.5, the RMC is the largest share of the AOC in all scenarios, which is similar to previous findings on the PHA production systems (Choi and Lee, 1997; Leong et al., 2017). The RMC in Scenario 1 is 24.7 million $, which accounts for 43% of AOC. The RMC in Scenario 2 is 19.2 million $, and in

Scenario 3 it is 15.9 million $. The lower RMC in the latter scenarios is due to the savings of enzyme, salt mix and water through enzyme reuse and SSM recycling. The cost of utilities is the second largest share of AOC, which is 11.6 million $ in Scenario 1 and 2, and 13.0 million $ in Scenario 3. The additional utility cost from the evaporator accounts for the total utility increase in Scenario 3. The facility-dependent cost also accounts for 8.2 to 10.2 million $ in the AOC, which is estimated based on the direct fixed capital and used for annual maintenance, depreciation, and miscellaneous expenses of the facilities. It is worth noting that the cost for waste treatment/disposal is around 10 million $ in the first two scenarios, but it is only 0.2 million $ in Scenario 3. This is because the SSM, which has been treated as the costly high-saline wastewater, is recycled and reused in Scenario 3. The accumulation of salts or other nutrients have been avoided in the process design by the addition or the reduction of the feed streams: for instance, given 90% of spent brine concentrate is recycled, the feed of new salt mix in the following batch operation has been reduced to 10% of its original input amount to achieve the salt balance of the system. Moreover, the cost of consumables in Scenario 1 is almost 0, but it is 1.2 million $ in the latter two scenarios. This results from the need for frequent changes of filtration membranes (twice per year) of the ultrafilter, which accounts for 97% of the total consumable cost. The labor-dependent cost is 2.3 million $ in all scenarios, which is reasonable for an assumption that the operation of the whole plant requires the same number of operating and management personnel for all capacities considered.

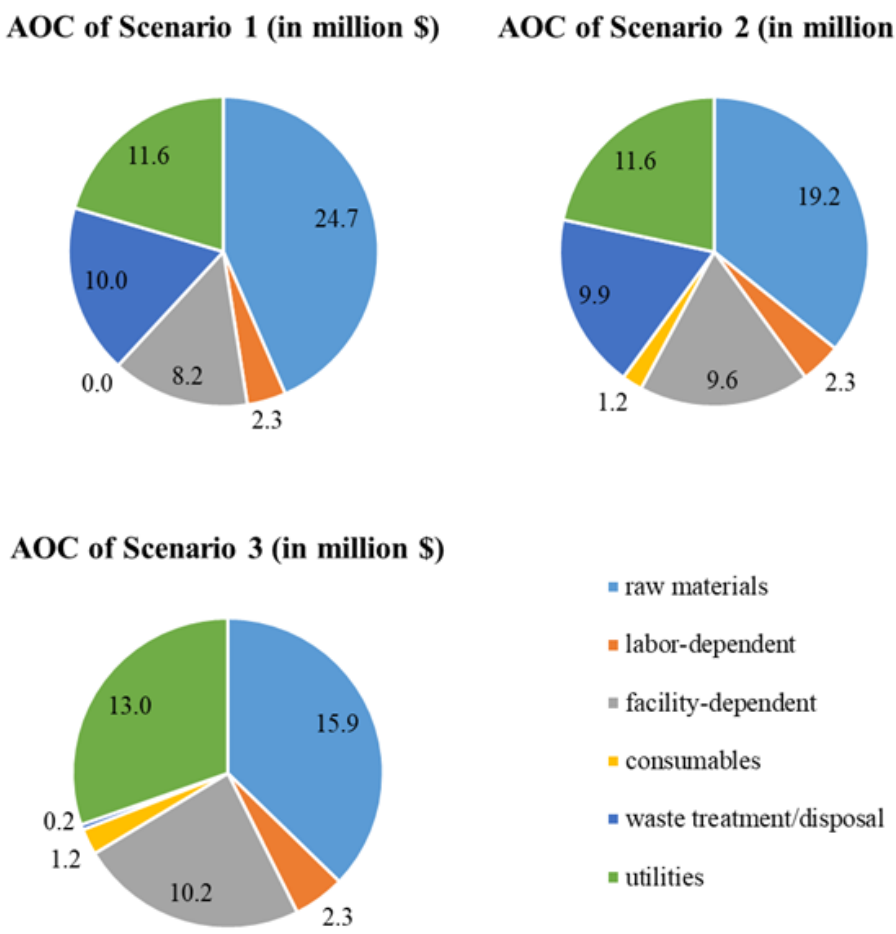

Figure 7. 5 Breakdown of AOC in Scenarios 1 through 3 (the lactose price of 0.22 $/kg and enzyme price of 40 $/kg were used for all three scenarios)

Scenario 1: PHA production base model; Scenario 2: PHA production model with enzyme reuse; Scenario 3: PHA production model with enzyme reuse and spent brine recycling

7.4.3 Economic analysis: break-down of raw materials cost

Since the RMC accounts for the largest portion of AOC in all scenarios, it is worthwhile to investigate the break-down of the RMC to determine the important factors that have influence on AOC and overall economics. Shown in Figure 7.6, the largest portion of RMC is the cost of lactose

(12 million $), which accounts for 49% of RMC in Scenario 1, 63% in Scenario 2, and 76% in Scenario 3. The lactose cost depends on the input mass and the lactose price. Therefore, with a larger feedstock input than is defined in the base model (168.7 MT/day), and with a higher lactose price (the price range is commonly 0.1 to 2.2 $/kg from local cheese companies), the portion of lactose cost in RMC would possibly increase, which can influence the overall economics.

The cost of enzyme is the second largest share in Scenario 1, which accounts for 28% of RMC. However, it is reduced by 86% in Scenario 2 and 3, which is a result of enzyme recycling. Although enzyme loading is only 0.3% of lactose input, the high enzyme price (40$/kg) makes the enzyme cost an important parameter of RMC. In that case, technologies to recycle enzyme in the hydrolysis step of the production system are necessary for the benefits of overall economics. Another important factor is the cost of the salt mix, which is $ 4 million in Scenario 1 and 2, and $ 1 million in Scenario 3. The system requires a large amount of salt mix input due to the high salinity requirement of *H. mediterranei* in this case. High salt is advantageous in helping eliminate the energy-intensive pasteurization or sterilization operations; however, the costs to purchase salts and treat/dispose of high-saline wastewater would become an issue for this type of production (Zhao et al., 2020). Therefore, the recycling of SSM using an evaporation-condensation process is necessary for financial and environmental benefits. These results of RMC breakdown indicate that the prices and input mass of raw materials, particularly feedstocks, are the major factors that can influence the overall economics of the PHA production system.

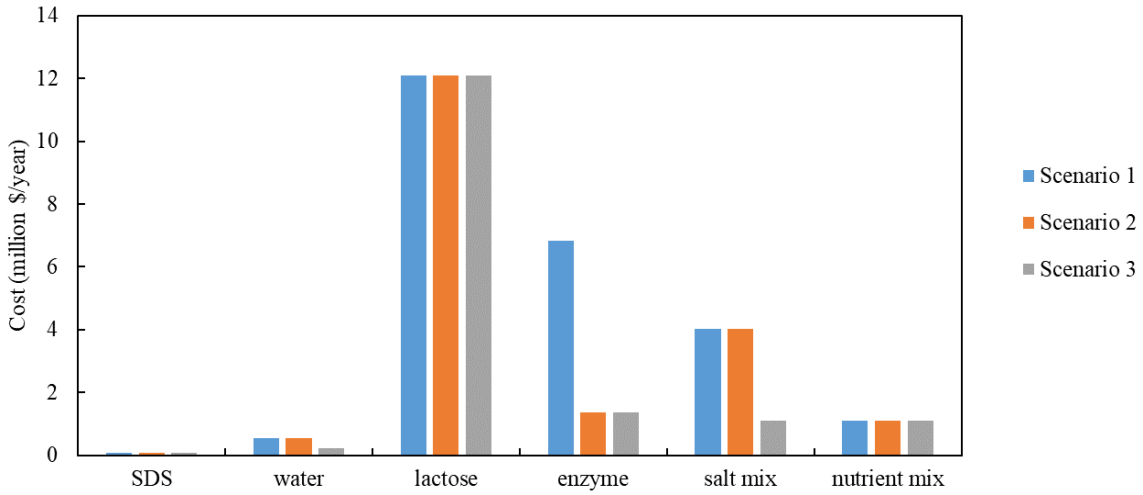

Figure 7. 6 The breakdown of RMC in Scenarios 1 through 3 (the lactose price of 0.22 $/kg and lactase enzyme price of 40 $/kg were used for all three scenarios)

Scenario 1: PHA production base model; Scenario 2: PHA production model with enzyme reuse; Scenario 3: PHA production model with enzyme reuse and spent brine recycling

7.4.4 Sensitivity analysis

Since the previous results suggest the cost of lactose and lactase enzyme are the most important factors that influence the RMC and AOC, a further analysis was conducted to determine how sensitive the breakeven price (BP) of the main product (PHA) is to these factors. Figures 7.7 and 7.8 illustrate the sensitivity analysis for the three scenarios. Shown in Figure 7.7, given a lactose price range of 0.04 to 2.2 $/kg, the breakeven price increases from 5 to 16.4 $/kg PHA in Scenario 1, from 4.7 to 16.2 $/kg PHA in Scenario 2, and from 3.7 to 15.2 $/kg PHA in Scenario 3. Table 7.6 lists the slopes of the lines in the sensitivity analysis for all scenarios. The BP increases by 5.3 $/kg for each 1$/kg increase of lactose price. Since the slopes of the three lines are nearly the same, the BP is approximately equally sensitive to the changing lactose price in all three scenarios. Given the same selling price of PHBV around 10 $/kg, Scenario 3 has the lowest BP

with greater potential for profitability among the other scenarios.

As shown in Figure 7.8, with a lactase enzyme price of 1 through 120 $/kg, the BP increases from 5.2 to 7.2 $/kg PHA in Scenario 1, from 5.5 to 5.9 $/kg PHA for Scenario 2, and from 4.5 to 4.9 $/kg PHA in Scenario 3. The slope of the line of Scenario 1 is steeper than the other two scenarios and the BP is more sensitive to the enzyme price in Scenario 1 than others. This is because 80% of used enzyme is recycled in the latter two scenarios, making the enzyme cost a less influential factor than Scenario 1. It is worth noting that the BPs in Scenario 1 are lower than Scenario 2 when the enzyme prices are less than 20 $/kg, indicating the enzyme recycling strategy does not benefit the economics with inexpensive enzyme. This is because the costs added to DCC and AOC from the ultrafiltration unit cause an overspend even with the savings from enzyme reuse. Moreover, since the slope of BP to the enzyme price is 0.017 to 0.0033 and is much less than the slope of BP to the lactose price (5.3), the BP is less sensitive to the lactase enzyme price than lactose price. This corresponds to the previous finding of this study that the lactose cost is a much larger share than enzyme cost in the breakdown of RMC.

Depending on the type of cheese processing byproduct streams, the feedstock has different unit prices based on lactose: for lactose powder, the price is often around 0.77 $/kg lactose; for whey permeate, the price is around 0.37 $/kg lactose; and for DLP, the price can be as low as 0.13 $/kg lactose. The vertical dash lines with different colours on Figure 7.7 represent the unit prices of different cheese whey byproduct streams and their corresponding BPs. Compared to other byproduct streams, the price of DLP results in the lowest BP, which can be around 4 $/kg PHA in Scenario 3. The BP for whey permeate is around 5 to 6 $/kg PHA, and the higher one is around 6

to 8 $/kg PHA when lactose powder is used as the feedstock. The results indicate that the BP of PHA can be largely influenced by the type and price of cheese byproduct feedstock. Apart from these findings, there are potentially other cheaper dairy byproducts and wastewater streams, e.g. organic-rich effluents from milk, cream and butter processing units, that can result in better economics for PHA production (Amaro et al., 2019; Shete and Shinkar, 2013).

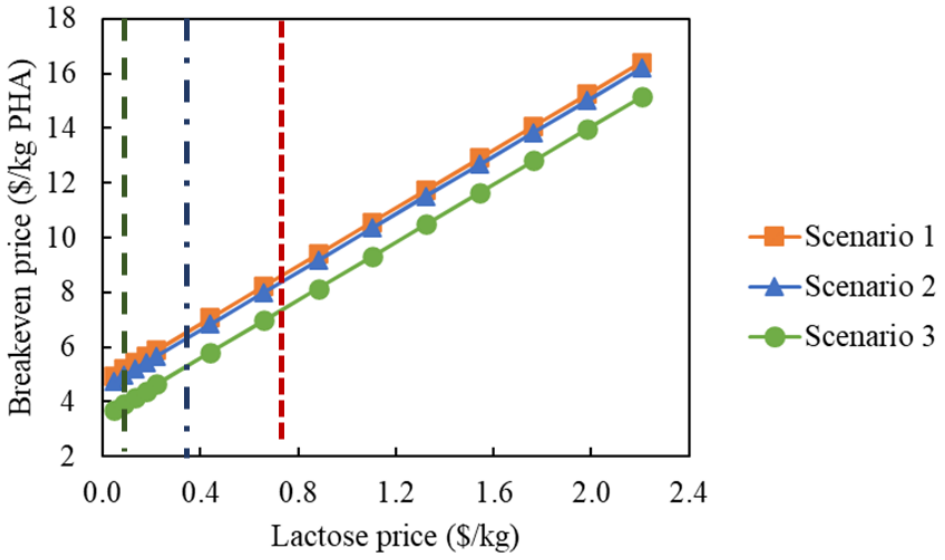

Figure 7. 7 Sensitivity analysis of the changing lactose price on the BP of PHA for Scenarios 1 through 3 (the lactase enzyme price of 40 $/kg was used for all scenarios)

Scenario 1: PHA production base model; Scenario 2: PHA production model with enzyme reuse; Scenario 3: PHA production model with enzyme reuse and spent brine recycling

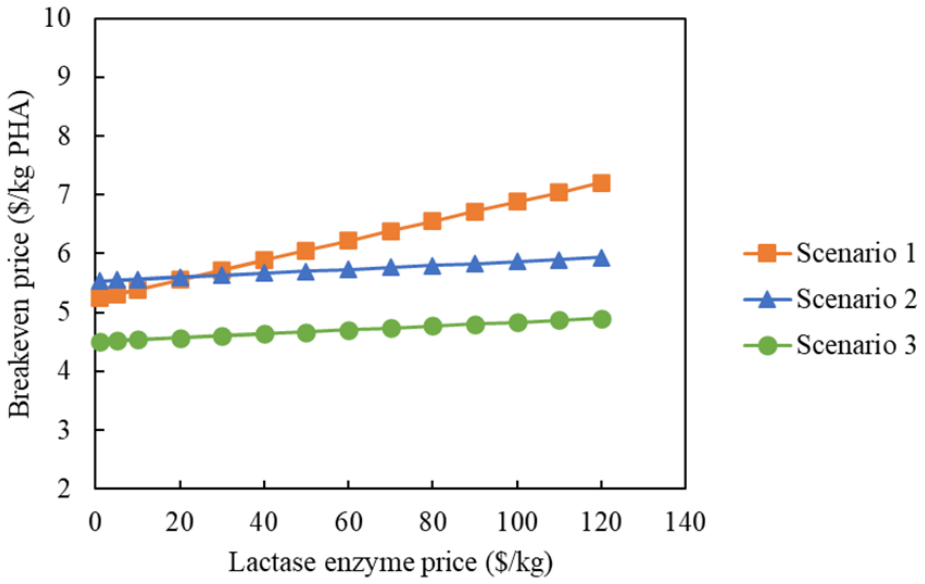

Figure 7. 8 Sensitivity analysis of the changing lactase enzyme price on the BP of PHA for Scenarios 1 through 3 (the lactose price of 0.22 $/kg was used for all scenarios)

Scenario 1: PHA production base model; Scenario 2: PHA production model with enzyme reuse; Scenario 3: PHA production model with enzyme reuse and spent brine recycling

Table 7. 6 The slopes of the sensitivity lines in Scenarios 1 through 3[a]

Scenario No.	BP/lactose price	BP/enzyme price
1	5.30	0.017
2	5.30	0.0033
3	5.30	0.0033

[a] Scenario 1: PHA production base model; Scenario 2: PHA production model with enzyme reuse; Scenario 3: PHA production model with enzyme reuse and spent brine recycling

7.5 Conclusions

A techno-economic analysis study has been conducted on the PHA production system by using cheese processing byproduct streams as feedstock. Three scenarios with different unit operations

have been compared for materials and energy flows, major equipment cost (EC), direct capital cost (DCC) and annual operating cost (AOC), and sensitivity analysis. Due to the additional unit operations in Scenario 2 and 3, the energy consumption, EC and DCC are higher than Scenario 1. However, since those additional units lead to savings of major inputs including salt mix, water, enzyme, and output of costly wastewater, the latter two scenarios, particularly Scenario 3, have less AOC than Scenario 1. Given that feedstock cost is found to be the largest portion of total raw materials cost (RMC), the breakeven price of PHA is equally sensitive to changes in lactose price for all scenarios. The breakeven price is less sensitive to lactase enzyme price than lactose price, and an enzyme recycling strategy may not be economically beneficial with inexpensive enzyme below $20/kg. However, a failure to recycle or reuse enzyme may cause excessive nitrogen discharge to water bodies, which would require additional costs to mitigate the relevant environmental impacts. Scenario 3 is the most profitable case among the three, and the use of DLP as feedstock results in the lowest breakeven price which can be less than 4 $/kg PHA. The low breakeven price enables PHA to be economically competitive with conventional plastics and common bioplastics. This can be beneficial to the dairy industry by adding an additional revenue stream to dairy byproducts. The case of making PHA from cheese byproducts can be applied to other dairy byproducts and waste streams such as organic effluents from milk, cream, and butter processing. Therefore, PHA production from dairy derived byproducts has the potential to grow dairy markets into non-food products, which also offers a business case with economic feasibility for the bioplastic industry.

Chapter 8. Conclusions and Future Research

The production and use of the conventional petroleum-based plastics are unsustainable due to the emissions of greenhouse gases during manufacturing processes, and massive plastic waste that end up in the environment. As one resolution to this issue, opportunities exist for the increased production of more sustainable bioplastics in replacement of traditional plastics. Polyhydroxyalkanoates (PHA) is a family of naturally occurring polyester materials that share similar properties with conventional thermoplastics and are biodegradable. PHA has an established market but the current bottleneck for market growth is the high production cost. Therefore, the motivations of this research were to address the global issues of conventional plastics and develop efficient and economical techniques to produce high-value PHA at lower costs than the current PHA industry.

Efficient and economic systems to produce PHA using food waste and cheese processing byproducts as inexpensive feedstocks were developed and evaluated during this study. Pretreatment processes were developed corresponding to different feedstocks to recover nutrients. The effects of major culturing parameters on cell growth, PHA synthesis and PHA profiles were determined and optimum levels identified. PHA production was demonstrated with dynamic monitoring through a 6-L benchtop bioreactor system. A novel process of salt recovery and recycling was designed to minimize salt discharge in the system. Below are the conclusions from this research as well as suggestions for future research.

8.1 Conclusions

8.1.1 The feasibility of volatile fatty acids (VFA) as carbon sources for PHA production by *Haloferax mediterranei*

This part of study found that *H. mediterranei* can grow and synthesize PHBV from VFA mixture as the sole carbon source with higher PHBV yield than the standard carbon source, glucose. This appears to be the first time PHBV synthesis has been found to be a growth-associated process when consuming a VFA mixture. Besides synthetic VFA substrates, PHBV yield from food waste derived VFA nutrients was found to be up to 0.54 g/g acetate and the higher substrate loadings resulted in more cell mass and PHBV production though the PHBV cell contents remained largely stable within 43% to 57%. The HV content of the PHBV produced from food waste derived VFA nutrients remained within 6% to 11% by weight, due to the low existence and consumption of HV-precursor including propionate and valerate. *H. mediterrranei* can effectively utilize the VFA-rich nutrients with high consumption rates of up to 88%, where acetate and butyrate were consumed completely. This study successfully proved the concept of robust pure-culture PHBV production from VFA mixtures derived from food waste, with very high product yield, cell growth rate, and substrate consumption. High-value PHA from food waste by halophilic microbes has the potential to accelerate the PHA market growth by reducing production cost and provides innovative incentives to food life-cycle systems by an additional revenue from food waste management in general. The process can be applied to other organic waste streams such as agricultural residues and organic waste effluents from food processing facilities.

8.1.2 Pretreatment and utilization of four types of real-world feedstocks for PHA production

Four different types of real-world feedstocks, including fermented food waste permeate (FWP), food waste hydrolysate (FWH), whey sugar (lactose) powder (LP), and delactosed permeate (DLP), were pretreated and tested for utilization by *H. mediterranei* as the sole substrate for cell growth and PHBV production. The results showed that the cells can grow and synthesize PHBV from all four feedstocks. With the same substrate loading, FWP resulted in a higher production of PHBV and a higher HV content than FWH, LP led to faster cell growth, PHBV production and higher HV content than DLP. Substrate loading influenced the PHBV production, PHBV content of CDM in all feedstock types, and HV content of PHBV in FWP, FWH, and LP. Because of the superior PHBV productivity and composition, FWP and LP were selected as representative feedstocks for further system development.

8.1.3 Process development of PHA production utilizing fermented food waste from commercial anaerobic digesters

A production system of PHBV synthesis by *H. mediterranei* utilizing fermented food waste from commercial anaerobic digestors was developed. The main processes including feedstock collection and pre-treatment, microbial production, and spent saline medium treatment and recycling were demonstrated on a bench scale. Important processing parameters achieving the highest production included feedstock type, substrate loading, and aeration rate were determined. The dissolved oxygen levels throughout microbial cultivation were found to be critical to PHA synthesis. The recovery and recycling of spent saline medium were successfully achieved through four consecutive batches after the treatment by H_2O_2. The demonstrated production system in this

study has application to practical production scenarios, that can help promote a circular economy within the food system by adding additional revenue from food waste; and at the same time, help reduce the production cost of bioplastics, to increase market penetration and mitigate the environmental pollution and health threats caused by plastic waste.

8.1.4 Process development of PHA production utilizing whey sugar from commercial cheesing manufacturing facilities

A PHBV production system utilizing whey sugar from commercial cheese making facilities as feedstock was also developed. Major unit operations of the production system consisting of feedstock pretreatment through enzymatic hydrolysis, microbial fermentation, and spent salts recovery and recycling were demonstrated on a bench scale through 6L bioreactor systems. The dissolved oxygen (DO) levels of cell broth especially during the exponential growth phase were influential with a DO level above 50% sat. increasing the microbial growth rate and the consumption of galactose, but reducing the final PHBV production. The direct recycling of spent brine after an evaporation step was successfully conducted through four consecutive batches with different substrate loadings, and 90% recycling of spent salts resulted in stable productions of cell mass and PHBV for both 20 and 40 g/L sCOD loadings. The production system illustrated in this study has the potential of commercial bioplastic applications, poses a feasible and environmental-friendly approach, and can be beneficial to the current dairy industry by providing additional revenue.

8.1.5 Techno-economic analysis on an industrial-scale production system of PHA from cheese byproducts

A techno-economic analysis study was conducted on the PHA production system assuming cheese processing byproduct streams as feedstock. Three scenarios with different unit operations (Scenario 1: base model; Scenario 2: base model + enzyme recycling; Scenario 3: base model + enzyme and spent salts recycling) were compared for materials and energy flows, major equipment cost (EC), direct capital cost (DCC) and annual operating cost (AOC). Sensitivity analysis was also conducted. Due to the additional unit operations in Scenario 2 and 3, the energy consumption, EC and DCC are higher than Scenario 1. However, since those additional units lead to savings of major inputs including salt mix, water, enzyme, and output of costly wastewater, the latter two scenarios, particularly Scenario 3, have lower AOC than Scenario 1. Given that feedstock cost is found to be the largest portion of total raw materials cost (RMC), the breakeven price of PHA is equally sensitive to changes in lactose price for all scenarios. The breakeven price is less sensitive to lactase enzyme price than lactose price, and an enzyme recycling strategy may not be economically beneficial with inexpensive enzyme below $20/kg. However, a failure to recycle or reuse enzyme may cause excessive nitrogen discharge to water bodies, which would require additional costs to mitigate the relevant environmental impacts. Scenario 3 is the most profitable case among the three, and the use of delactosed permeate (DLP) as feedstock results in the lowest breakeven price which can be less than $4/kg PHA. The low breakeven price enables PHA to be economically competitive with conventional plastics and common bioplastics. This can be beneficial to the dairy industry by adding an additional revenue stream to dairy byproducts. The case of making PHA from cheese byproducts can be applied to other dairy byproducts and waste streams such as organic effluents from milk, cream, and butter processing. Therefore, PHA

production from dairy derived byproducts has the potential to grow dairy markets into non-food products, which also offers a business case for the bioplastic industry.

8.2 Future research

Through this research, suggested future investigations are identified as follows:

(1) As one promising inexpensive feedstock, food waste has variable sources, compositions and qualities, even for those collected from a same food waste processing facility. These variables introduce uncertainty and instability to the PHA production processes, which does not meet the requirements of good manufacturing practice in commercial-scales production. Therefore, it is necessary to identify the influence of food waste complexity on PHA production and optimize the feedstock through technically viable and economical approaches.

(2) Another issue with regard to the food waste feedstock is the uncertainty of the short-chain carboxylates derived from anaerobic fermentation process. As the precursors to PHBV synthesis, the profile of carboxylates can significantly influence the product yield and quality. Therefore, further research is needed to find ways to manipulate the anaerobic fermentation process so as to give the optimum carboxylate profile for PHA production.

(3) Regarding batch demonstration of the production system, further research is needed to establish efficient process control through effective kinetic models of microbial growth, PHBV synthesis and nutrient decay, heat and mass transport, and other scaling effects.

(4) Techno-economic analysis finds that whey permeate and DLP as primary feedstocks may give lower breakeven price than whey sugar. However, these substrates may have similar quality issues to food waste due to the inconsistency of composition among different sources. Therefore, the influence of feedstock complexity including source, composition, physical and chemical properties should also be studied, and the production process should be further characterized and optimized.

(5) Success in batch demonstration through 6-L benchtop bioreactor system is a very first step and there are more steps of demonstration needed towards the commercialization of the system. One is to investigate the scaling-up effect through pilot-scale batch demonstration such as with a 2000 L capacity. Another investigation is the economic effects that are important to longer term commercialization decisions in augmenting the PHA markets through new systems to use currently lower cost feedstocks.

References

Aehle, W., 2007. Enzymes in industry: production and applications. John Wiley & Sons.

Aeschelmann, F., Carus, M., 2015. Biobased Building Blocks and Polymers in the World: Capacities, Production, and Applications–Status Quo and Trends Towards 2020. Industrial Biotechnology 11, 154–159. https://doi.org/10.1089/ind.2015.28999.fae

Alibaba Group, 2021a. Cacl2 Water Purification Calcium Chloride Bulk Agent Calcium Chloride [WWW Document]. URL https://www.alibaba.com/product-detail/Cacl2-Cacl2-CaCl2-Water-Purification-Calcium_1600206332554.html?spm=a2700.galleryofferlist.normal_offer.d_title.70b5593bA8wM5V&s=p (accessed 7.27.21).

Alibaba Group, 2021b. Industrial Grade 6h2o 46% Purity Mgcl2 Magnesium Chloride Hexahydrate Flakes [WWW Document]. URL https://www.alibaba.com/product-detail/Mgcl2-Mgcl2mgcl2-Industrial-Grade-6h2o-46_1600252529812.html?spm=a2700.galleryofferlist.normal_offer.d_title.363d1b71w3FSll&s=p (accessed 7.27.21).

Alibaba Group, 2021c. High Purity White Powder Anhydrous Mgso4 Magnesium Sulphate Magnesium Sulfate Anhydrou 99% 14168-73-1 [WWW Document]. URL https://www.alibaba.com/product-detail/Mgso4-Mgso4-High-Purity-White-Powder_1600280791324.html?spm=a2700.galleryofferlist.normal_offer.d_title.7c842baaZJs5Xp&s=p (accessed 7.27.21).

Alibaba Group, 2021d. Industrial Grade High Purity Sodium Bromide (nabr) [WWW Document]. URL https://www.alibaba.com/product-detail/Industrial-grade-high-purity-sodium-

bromide_60377614864.html?spm=a2700.galleryofferlist.normal_offer.d_title.725c4f6eJciUZh (accessed 7.27.21).

Alibaba Group, 2021e. 94.5% Raw Sea Salt Bulk Sea Salt Price Nacl - Buy Raw Sea Salt,Nacl,Bulk Sea Salt Product on Alibaba.com [WWW Document]. URL https://www.alibaba.com/product-detail/Nacl-Nacl-Nacl-94-5-Raw_60286953075.html?spm=a2700.galleryofferlist.normal_offer.d_title.26747c45R7ZfF5&s=p (accessed 7.27.21).

Alibaba Group, 2021f. High Quality Heavy Alkali Sodium Bicarbonate Nahco3 3144-55-8 Sodium Bicarbonate [WWW Document]. URL https://www.alibaba.com/product-detail/Nahco3-Nahco3-High-Quality-Heavy-Alkali_1600257570258.html?spm=a2700.galleryofferlist.normal_offer.d_title.d8d1215fFXiDsD&s=p (accessed 7.27.21).

Alibaba Group, 2021g. Amonium Chloride / Nh4cl / Ammonium Chloride 99.5%/feed Or Industrial Grade/good Price [WWW Document]. URL https://www.alibaba.com/product-detail/Nh4cl-Nh4cl-Ammonium-Chloride-Industrial-Amonium_60586402024.html?spm=a2700.galleryofferlist.normal_offer.d_title.538b7818y6cZX4&s=p (accessed 7.27.21).

Alibaba Group, 2021h. Sodium Dodecyl Sulfate Sds K12,95%/93% /92% Powder,Cas 151-21-3 [WWW Document]. URL https://www.alibaba.com/product-detail/Sodium-Dodecyl-Sulfate-Sodium-Dodecyl-Sulfate_1600266362204.html?spm=a2700.galleryofferlist.normal_offer.d_title.44495c65X95ddT&s=p (accessed 7.27.21).

Alsafadi, D., Al-Mashaqbeh, O., 2017. A one-stage cultivation process for the production of poly-3-(hydroxybutyrate-co-hydroxyvalerate) from olive mill wastewater by Haloferax mediterranei. New Biotechnology 34, 47–53. https://doi.org/10.1016/j.nbt.2016.05.003

Amaro, T.M.M.M., Rosa, D., Comi, G., Iacumin, L., 2019. Prospects for the Use of Whey for Polyhydroxyalkanoate (PHA) Production. Front Microbiol 10, 992. https://doi.org/10.3389/fmicb.2019.00992

Andrady, A.L., 2011. Microplastics in the marine environment. Marine Pollution Bulletin 62, 1596–1605. https://doi.org/10.1016/j.marpolbul.2011.05.030

Anjum, A., Zuber, M., Zia, K.M., Noreen, A., Anjum, M.N., Tabasum, S., 2016. Microbial production of polyhydroxyalkanoates (PHAs) and its copolymers: A review of recent advancements. International Journal of Biological Macromolecules 89, 161–174. https://doi.org/10.1016/j.ijbiomac.2016.04.069

APHA, 2012. Standard methods for the examination of water and wastewater. American public health association.

Arslan, D., Steinbusch, K.J.J., Diels, L., Hamelers, H.V.M., Strik, D.P.B.T.B., Buisman, C.J.N., Wever, H.D., 2016. Selective short-chain carboxylates production: A review of control mechanisms to direct mixed culture fermentations. Critical Reviews in Environmental Science and Technology 46, 592–634. https://doi.org/10.1080/10643389.2016.1145959

ATCC, 2020. Haloferax mediterranei (Rodriguez-Valera et al.) Torreblanca et al. AT [WWW Document]. URL https://www.atcc.org/products/all/33500.aspx#culturemethod (accessed 1.4.20).

Auras, R.A., Lim, L.-T., Selke, S.E.M., Tsuji, H., 2011. Poly(lactic acid): Synthesis, Structures, Properties, Processing, and Applications. John Wiley & Sons.

Baker, R.W., 2000. Membrane technology and applications, McGraw-Hill professional engineering. McGraw-Hill, New York.

Ben, M., Kennes, C., Veiga, M.C., 2016. Optimization of polyhydroxyalkanoate storage using mixed cultures and brewery wastewater. Journal of Chemical Technology & Biotechnology 91, 2817–2826. https://doi.org/10.1002/jctb.4891

Bhattacharyya, A., Jana, K., Haldar, S., Bhowmic, A., Mukhopadhyay, U.K., De, S., Mukherjee, J., 2015. Integration of poly-3-(hydroxybutyrate-co-hydroxyvalerate) production by Haloferax mediterranei through utilization of stillage from rice-based ethanol manufacture in India and its techno-economic analysis. World Journal of Microbiology and Biotechnology 31, 717–727. https://doi.org/10.1007/s11274-015-1823-4

Bhattacharyya, A., Pramanik, A., Maji, S.K., Haldar, S., Mukhopadhyay, U.K., Mukherjee, J., 2012. Utilization of vinasse for production of poly-3-(hydroxybutyrate-co-hydroxyvalerate) by Haloferax mediterranei. AMB Expr 2, 34. https://doi.org/10.1186/2191-0855-2-34

Bhattacharyya, A., Saha, J., Haldar, S., Bhowmic, A., Mukhopadhyay, U.K., Mukherjee, J., 2014. Production of poly-3-(hydroxybutyrate-co-hydroxyvalerate) by Haloferax mediterranei using rice-based ethanol stillage with simultaneous recovery and re-use of medium salts. Extremophiles 18, 463–470. https://doi.org/10.1007/s00792-013-0622-9

Bluepha, 2019. PHA Bioplastic [WWW Document]. Bluepha - a synthetic biology company from China, with leading technologies for low-cost production of PHAs. URL http://en.bluepha.com/pha-bioplastic (accessed 9.4.21).

Braunegg, G., Sonnleitner, B., Lafferty, R.M., 1978. A rapid gas chromatographic method for the determination of poly-?-hydroxybutyric acid in microbial biomass. European Journal of Applied Microbiology and Biotechnology 6, 29–37. https://doi.org/10.1007/BF00500854

Buzby, J.C., Hyman, J., Stewart, H., Wells, H.F., 2011. The Value of Retail- and Consumer-Level Fruit and Vegetable Losses in the United States. Journal of Consumer Affairs 45, 492–515. https://doi.org/10.1111/j.1745-6606.2011.01214.x

California Water Service, 2021. Home [WWW Document]. California Water Service. URL https://www.calwater.com/ (accessed 7.27.21).

CalRecycle, 2018a. Food Recovery in California [WWW Document]. URL https://www.calrecycle.ca.gov/Organics/SLCP/FoodRecovery (accessed 1.22.22).

CalRecycle, 2018b. Preventing Food from Reaching the Landfill [WWW Document]. Preventing Food from Reaching the Landfill. URL https://www.calrecycle.ca.gov/organics/food (accessed 6.17.20).

Cambridge Consultants, 2018. Polyhydroxyalkanoates: Plastic the way nature intended? (White Paper).

Campanari, S., Augelletti, F., Rossetti, S., Sciubba, F., Villano, M., Majone, M., 2017. Enhancing a multi-stage process for olive oil mill wastewater valorization towards polyhydroxyalkanoates and biogas production. Chemical Engineering Journal 317, 280–289. https://doi.org/10.1016/j.cej.2017.02.094

Chanprateep, S., 2010. Current trends in biodegradable polyhydroxyalkanoates. Journal of Bioscience and Bioengineering 110, 621–632. https://doi.org/10.1016/j.jbiosc.2010.07.014

Chaudhary, G., Singh, L.K., Ghosh, S., 2012. Alkaline pretreatment methods followed by acid hydrolysis of Saccharum spontaneum for bioethanol production. Bioresource Technology 124, 111–118. https://doi.org/10.1016/j.biortech.2012.08.067

Chen, G.-Q., 2009. A microbial polyhydroxyalkanoates (PHA) based bio- and materials industry. Chemical Society Reviews 38, 2434–2446. https://doi.org/10.1039/B812677C

Chen, Y., Liu, C., Nie, J., Wu, S., Wang, D., 2014. Removal of COD and decolorizing from landfill leachate by Fenton's reagent advanced oxidation. Clean Techn Environ Policy 16, 189–193. https://doi.org/10.1007/s10098-013-0627-1

Choi, D., Chipman, D.C., Bents, S.C., Brown, R.C., 2010. A Techno-economic Analysis of Polyhydroxyalkanoate and Hydrogen Production from Syngas Fermentation of Gasified Biomass. Appl Biochem Biotechnol 160, 1032–1046. https://doi.org/10.1007/s12010-009-8560-9

Choi, J., Lee, S.Y., 1997. Process analysis and economic evaluation for Poly(3-hydroxybutyrate) production by fermentation. Bioprocess Engineering 17, 335–342. https://doi.org/10.1007/s004490050394

Colombo, B., Pepè Sciarria, T., Reis, M., Scaglia, B., Adani, F., 2016. Polyhydroxyalkanoates (PHAs) production from fermented cheese whey by using a mixed microbial culture. Bioresource Technology 218, 692–699. https://doi.org/10.1016/j.biortech.2016.07.024

Criddle, C.S., Frank, C.W., 2014. Renewable Bioplastics and Biocomposites From Biogas Methane and Waste-Derived Feedstock: Development of Enabling Technology, Life Cycle Assessment, and Analysis of Costs.

Cui, Y.-W., Gong, X.-Y., Shi, Y.-P., Wang, Z. (Drew), 2017a. Salinity effect on production of PHA and EPS by *Haloferax mediterranei*. RSC Advances 7, 53587–53595. https://doi.org/10.1039/C7RA09652F

Cui, Y.-W., Shi, Y.-P., Gong, X.-Y., 2017b. Effects of C/N in the substrate on the simultaneous production of polyhydroxyalkanoates and extracellular polymeric substances by Haloferax

mediterranei via kinetic model analysis. RSC Advances 7, 18953–18961. https://doi.org/10.1039/C7RA02131C

Cui, Y.-W., Zhang, H.-Y., Ji, S.-Y., Wang, Z.-W., 2017d. Kinetic Analysis of the Temperature Effect on Polyhydroxyalkanoate Production by Haloferax mediterranei in Synthetic Molasses Wastewater. Journal of Polymers and the Environment 25, 277–285. https://doi.org/10.1007/s10924-016-0807-2

DEP, 2021. DO Saturation Calculator | Florida Department of Environmental Protection [WWW Document]. URL https://floridadep.gov/dear/water-quality-standards-program/documents/do-saturation-calculator%C2%A0 (accessed 9.24.21).

Diltz, R.A., Marolla, T.V., Henley, M.V., Li, L., 2007. Reverse osmosis processing of organic model compounds and fermentation broths. Bioresource Technology 98, 686–695. https://doi.org/10.1016/j.biortech.2006.01.022

Don, T.-M., Chen, C.W., Chan, T.-H., 2006. Preparation and characterization of poly(hydroxyalkanoate) from the fermentation of Haloferax mediterranei. Journal of Biomaterials Science, Polymer Edition 17, 1425–1438. https://doi.org/10.1163/156856206778937208

Doran, P.M., 2013. Bioprocess Development, in: Bioprocess Engineering Principles. Elsevier, pp. 3–11. https://doi.org/10.1016/B978-0-12-220851-5.00001-0

D'Souza, S.E., Altekar, W., D'Souza, S.F., 1997. Adaptive response of Haloferax mediterranei to low concentrations of NaCl (< 20%) in the growth medium. Archives of Microbiology 168, 68–71. https://doi.org/10.1007/s002030050471

Durham, R.J., 2009. Modern approaches to lactose production, in: Dairy-Derived Ingredients: Food and Nutraceutical Uses. pp. 103–144.

Dutra Rosolen, M., Gennari, A., Volpato, G., Volken de Souza, C.F., 2015. Lactose Hydrolysis in Milk and Dairy Whey Using Microbial β -Galactosidases. Enzyme Research 2015, 1–7. https://doi.org/10.1155/2015/806240

El-Zawawy, W.K., Ibrahim, M.M., Abdel-Fattah, Y.R., Soliman, N.A., Mahmoud, M.M., 2011. Acid and enzyme hydrolysis to convert pretreated lignocellulosic materials into glucose for ethanol production. Carbohydrate Polymers 84, 865–871. https://doi.org/10.1016/j.carbpol.2010.12.022

Escalona, A.M., Varela, F.R., Gomis, A.M., 1996. Procedure for extraction of polyhydroxyalkanoates from halophilic bacteria which contain them. US5536419A.

Esclapez, J., Bravo-Barrales, G., Bautista, V., Pire, C., Camacho, M., Bonete, M.J., 2014. Effects of nitrogen sources on the nitrate assimilation in Haloferax mediterranei: growth kinetics and transcriptomic analysis. FEMS Microbiology Letters 350, 168–174. https://doi.org/10.1111/1574-6968.12325

European Bioplastics, 2020. Market. European Bioplastics e.V. URL https://www.european-bioplastics.org/market/ (accessed 9.7.21).

European Bioplastics, 2018. Bioplastic Market Data. European Bioplastics e.V. URL https://www.european-bioplastics.org/market/ (accessed 6.24.19).

Fang, C.-J., Ku, K.-L., Lee, M.-H., Su, N.-W., 2010. Influence of nutritive factors on C50 carotenoids production by Haloferax mediterranei ATCC 33500 with two-stage cultivation. Bioresource Technology 101, 6487–6493. https://doi.org/10.1016/j.biortech.2010.03.044

Ferre-Guell, A., Winterburn, J., 2018. Biosynthesis and Characterization of Polyhydroxyalkanoates with Controlled Composition and Microstructure. Biomacromolecules 19, 996–1005. https://doi.org/10.1021/acs.biomac.7b01788

Ferre-Guell, A., Winterburn, J., 2017. Production of the copolymer poly(3-hydroxybutyrate-co-3-hydroxyvalerate) with varied composition using different nitrogen sources with Haloferax mediterranei. Extremophiles 21, 1037–1047. https://doi.org/10.1007/s00792-017-0964-9

Fogler, H.S., 2016. Elements of chemical reaction engineering, Fifth edition. ed. Prentice Hall, Boston.

Ganesh Saratale, R., Cho, S.-K., Dattatraya Saratale, G., Kadam, A.A., Ghodake, G.S., Kumar, M., Naresh Bharagava, R., Kumar, G., Su Kim, D., Mulla, S.I., Seung Shin, H., 2021. A comprehensive overview and recent advances on polyhydroxyalkanoates (PHA) production using various organic waste streams. Bioresource Technology 325, 124685. https://doi.org/10.1016/j.biortech.2021.124685

Gänzle, M.G., Haase, G., Jelen, P., 2008. Lactose: Crystallization, hydrolysis and value-added derivatives. International Dairy Journal, MILESTONE ACHIEVEMENTS IN DAIRY SCIENCE RESEARCH AND THEIR CURRENT AND FUTURE INDUSTRIAL APPLICATIONS 18, 685–694. https://doi.org/10.1016/j.idairyj.2008.03.003

Garcia-Ochoa, F., Gomez, E., 2009. Bioreactor scale-up and oxygen transfer rate in microbial processes: An overview. Biotechnology Advances 27, 153–176. https://doi.org/10.1016/j.biotechadv.2008.10.006

Geyer, R., Jambeck, J.R., Law, K.L., 2017. Production, use, and fate of all plastics ever made. Science Advances 3, e1700782. https://doi.org/10.1126/sciadv.1700782

Ghosh, S., Gnaim, R., Greiserman, S., Fadeev, L., Gozin, M., Golberg, A., 2019. Macroalgal biomass subcritical hydrolysates for the production of polyhydroxyalkanoate (PHA) by Haloferax mediterranei. Bioresource Technology 271, 166–173. https://doi.org/10.1016/j.biortech.2018.09.108

Giani, M., Montero-Lobato, Z., Garbayo, I., Vílchez, C., Vega, J.M., Martínez-Espinosa, R.M., 2021. Haloferax mediterranei Cells as C50 Carotenoid Factories. Marine Drugs 19, 100. https://doi.org/10.3390/md19020100

Greenlee, L.F., Lawler, D.F., Freeman, B.D., Marrot, B., Moulin, P., 2009. Reverse osmosis desalination: Water sources, technology, and today's challenges. Water Research 43, 2317–2348. https://doi.org/10.1016/j.watres.2009.03.010

Gryczko, S., Alexander, J., Heinig, A., 2021. Wastewater Rate Studies | City of Davis, CA [WWW Document]. URL https://www.cityofdavis.org/city-hall/public-works-utilities-and-operations/wastewater/wastewater-rate-studies (accessed 7.27.21).

Gunders, D., 2012. Wasted: How America Is Losing Up to 40 Percent of Its Food from Farm to Fork to Landfill. NRDC 26.

Han, J., Hou, J., Zhang, F., Ai, G., Li, M., Cai, S., Liu, H., Wang, L., Wang, Z., Zhang, S., Cai, L., Zhao, D., Zhou, J., Xiang, H., 2013. Multiple Propionyl Coenzyme A-Supplying Pathways for Production of the Bioplastic Poly(3-Hydroxybutyrate- *co* -3-Hydroxyvalerate) in Haloferax mediterranei. Applied and Environmental Microbiology 79, 2922–2931. https://doi.org/10.1128/AEM.03915-12

Han, J., Wu, L.-P., Hou, J., Zhao, D., Xiang, H., 2015. Biosynthesis, Characterization, and Hemostasis Potential of Tailor-Made Poly(3-hydroxybutyrate- *co* -3-hydroxyvalerate) Produced by *Haloferax mediterranei*. Biomacromolecules 16, 578–588. https://doi.org/10.1021/bm5016267

Holmes, P.A., 1985. Applications of PHB - a microbially produced biodegradable thermoplastic. Physics in Technology 16, 32–36. https://doi.org/10.1088/0305-4624/16/1/305

Huang, T.-Y., Duan, K.-J., Huang, S.-Y., Chen, C.W., 2006. Production of polyhydroxyalkanoates from inexpensive extruded rice bran and starch by Haloferax mediterranei. Journal of Industrial Microbiology & Biotechnology 33, 701–706. https://doi.org/10.1007/s10295-006-0098-z

Ilyas, M., Ahmad, W., Khan, H., Yousaf, S., Khan, K., Nazir, S., 2018. Plastic waste as a significant threat to environment – a systematic literature review. Reviews on Environmental Health 33, 383–406. https://doi.org/10.1515/reveh-2017-0035

Intelligen, Inc., 2021. SuperPro Designer. Intelligen, Inc, US.

Jiang, J., Zhang, Y., Li, K., Wang, Q., Gong, C., Li, M., 2013. Volatile fatty acids production from food waste: Effects of pH, temperature, and organic loading rate. Bioresource Technology 143, 525–530. https://doi.org/10.1016/j.biortech.2013.06.025

Jinno, C., He, Y., Morash, D., McNamara, E., Zicari, S., King, A., Stein, H.H., Liu, Y., 2018. Enzymatic digestion turns food waste into feed for growing pigs. Animal Feed Science and Technology 242, 48–58. https://doi.org/10.1016/j.anifeedsci.2018.05.006

KEGG, 2019. KEGG PATHWAY: Butanoate metabolism [WWW Document]. URL https://www.genome.jp/kegg-bin/show_pathway?ko00650 (accessed 4.11.19).

Kim, D.-H., Kim, S.-H., Jung, K.-W., Kim, M.-S., Shin, H.-S., 2011. Effect of initial pH independent of operational pH on hydrogen fermentation of food waste. Bioresource Technology, Special Issue : Biofuels-III: Biohydrogen 102, 8646–8652. https://doi.org/10.1016/j.biortech.2011.03.030

Koller, M., 2018. A Review on Established and Emerging Fermentation Schemes for Microbial Production of Polyhydroxyalkanoate (PHA) Biopolyesters. Fermentation 4, 30. https://doi.org/10.3390/fermentation4020030

Koller, M., 2015. Recycling of Waste Streams of the Biotechnological Poly(hydroxyalkanoate) Production by Haloferax mediterranei on Whey. International Journal of Polymer Science 2015, e370164. https://doi.org/10.1155/2015/370164

Koller, M., Hesse, P., Bona, R., Kutschera, C., Atlić, A., Braunegg, G., 2007. Biosynthesis of High Quality Polyhydroxyalkanoate Co- and Terpolyesters for Potential Medical Application by the ArchaeonHaloferax mediterranei. Macromolecular Symposia 253, 33–39. https://doi.org/10.1002/masy.200750704

Korkakaki, E., Mulders, M., Veeken, A., Rozendal, R., van Loosdrecht, M.C.M., Kleerebezem, R., 2016. PHA production from the organic fraction of municipal solid waste (OFMSW): Overcoming the inhibitory matrix. Water Research 96, 74–83. https://doi.org/10.1016/j.watres.2016.03.033

Kourmentza, C., Plácido, J., Venetsaneas, N., Burniol-Figols, A., Varrone, C., Gavala, H.N., Reis, M.A.M., 2017. Recent Advances and Challenges towards Sustainable Polyhydroxyalkanoate (PHA) Production. Bioengineering 4, 55. https://doi.org/10.3390/bioengineering4020055

Kucera, J., 2011. Reverse Osmosis: Industrial applications and processes. Wiley.

Laufenberg, G., Hausmanns, S., Kunz, B., 1996. The influence of intermolecular interactions on the selectivity of several organic acids in aqueous multicomponent systems during reverse osmosis. Journal of Membrane Science 110, 59–68. https://doi.org/10.1016/0376-7388(95)00231-6

Lee, W.S., Chua, A.S.M., Yeoh, H.K., Ngoh, G.C., 2014. A review of the production and applications of waste-derived volatile fatty acids. Chemical Engineering Journal 235, 83–99. https://doi.org/10.1016/j.cej.2013.09.002

Lemos, P.C., Viana, C., Salgueiro, E.N., Ramos, A.M., Crespo, J.P.S.G., Reiszcorr>, M.A.M., 1998. Effect of carbon source on the formation of polyhydroxyalkanoates (PHA) by a phosphate-accumulating mixed culture. Enzyme and Microbial Technology 22, 662–671. https://doi.org/10.1016/S0141-0229(97)00243-3

Leong, Y.K., Show, P.L., Lan, J.C.-W., Loh, H.-S., Lam, H.L., Ling, T.C., 2017. Economic and environmental analysis of PHAs production process. Clean Techn Environ Policy 19, 1941–1953. https://doi.org/10.1007/s10098-017-1377-2

Li, Y., Park, S.Y., Zhu, J., 2011. Solid-state anaerobic digestion for methane production from organic waste. Renewable and Sustainable Energy Reviews 15, 821–826. https://doi.org/10.1016/j.rser.2010.07.042

Liang, B., Bund, R.K., Hartel, R.W., 2009. Effect of composition on moisture sorption of delactosed permeate. International Dairy Journal 19, 630–636. https://doi.org/10.1016/j.idairyj.2009.04.010

Lillo, J.G., Rodriguez-Valera, F., 1990. Effects of Culture Conditions on Poly(3-Hydroxybutyric Acid) Production by Haloferax mediterranei. APPL. ENVIRON. MICROBIOL. 56, 5.

Lim, S.-J., Kim, B.J., Jeong, C.-M., Choi, J., Ahn, Y.H., Chang, H.N., 2008. Anaerobic organic acid production of food waste in once-a-day feeding and drawing-off bioreactor. Bioresource Technology 99, 7866–7874. https://doi.org/10.1016/j.biortech.2007.06.028

Lingle, R., 2018. PHA bioplastics a ‘tunable’ solution for convenience food packaging [WWW Document]. plasticstoday.com. URL https://www.plasticstoday.com/packaging/pha-bioplastics-tunable-solution-convenience-food-packaging (accessed 9.5.21).

Liu, H.-Y., Hall, P.V., Darby, J.L., Coats, E.R., Green, P.G., Thompson, D.E., Loge, F.J., 2008. Production of Polyhydroxyalkanoate During Treatment of Tomato Cannery Wastewater. Water Environment Research 80, 367–372. https://doi.org/10.2175/106143007X221535

Lonsdale, H.K., Merten, U., Riley, R.L., 1965. Transport properties of cellulose acetate osmotic membranes. Journal of Applied Polymer Science 9, 1341–1362. https://doi.org/10.1002/app.1965.070090413

Lorantfy, B., Seyer, B., Herwig, C., 2014. Stoichiometric and kinetic analysis of extreme halophilic Archaea on various substrates in a corrosion resistant bioreactor. N Biotechnol 31, 80–89. https://doi.org/10.1016/j.nbt.2013.08.003

Lu, Q., Han, J., Zhou, L., Zhou, J., Xiang, H., 2008. Genetic and Biochemical Characterization of the Poly(3-Hydroxybutyrate-co-3-Hydroxyvalerate) Synthase in Haloferax mediterranei. Journal of Bacteriology 190, 4173–4180. https://doi.org/10.1128/JB.00134-08

Madison, L.L., Huisman, G.W., 1999. Metabolic Engineering of Poly(3-Hydroxyalkanoates): From DNA to Plastic. Microbiol Mol Biol Rev 63, 21–53.

Mariotti, F., Tomé, D., Mirand, P.P., 2008. Converting Nitrogen into Protein—Beyond 6.25 and Jones' Factors. Critical Reviews in Food Science and Nutrition 48, 177–184. https://doi.org/10.1080/10408390701279749

Martínez-Espinosa, R.M., Richardson, D.J., Butt, J.N., Bonete, M.J., 2006. Respiratory nitrate and nitrite pathway in the denitrifier haloarchaeon Haloferax mediterranei. Biochemical Society Transactions 34, 115–117. https://doi.org/10.1042/BST0340115

Matsuura, T., Sourirajan, S., 1973. Reverse osmosis separation of organic acids in aqueous solutions using porous cellulose acetate membranes. Journal of Applied Polymer Science 17, 3661–3682. https://doi.org/10.1002/app.1973.070171210

McDonald, E.J., Turcotte, A.L., 1948. Density and refractive indices of lactose solutions. U. S. Department of Commerce National Bure au of Standards 6.

McDonnell, G., 2014. The Use of Hydrogen Peroxide for Disinfection and Sterilization Applications, in: PATAI'S Chemistry of Functional Groups. John Wiley & Sons, Ltd, pp. 1–34. https://doi.org/10.1002/9780470682531.pat0885

Monod, J., 1949. The Growth of Bacterial Cultures. Annual Review of Microbiology 3, 371–394. https://doi.org/10.1146/annurev.mi.03.100149.002103

Moon, H.C., Song, I.S., Kim, J.C., Shirai, Y., Lee, D.H., Kim, J.K., Chung, S.O., Kim, D.H., Oh, K.K., Cho, Y.S., 2009. Enzymatic hydrolysis of food waste and ethanol fermentation. International Journal of Energy Research 33, 164–172. https://doi.org/10.1002/er.1432

Nielsen, C., Rahman, A., Rehman, A., Walsh, M., Miller, C., 2017. Food waste conversion to microbial polyhydroxyalkanoates. Microbial Biotechnology 10. https://doi.org/10.1111/1751-7915.12776

Oehmen, A., Keller-Lehmann, B., Zeng, R.J., Yuan, Z., Keller, J., 2005. Optimisation of poly-β-hydroxyalkanoate analysis using gas chromatography for enhanced biological phosphorus removal systems. Journal of Chromatography A 1070, 131–136. https://doi.org/10.1016/j.chroma.2005.02.020

Oliveira, D., Puri, R., Fenelon, M.A., O'Mahony, J.A., 2019. Delactosed permeate as a dairy processing co-product with major potential value: a review. International Journal of Food Science & Technology 54, 999–1008. https://doi.org/10.1111/ijfs.14064

Ozaki, H., Li, H., 2002. Rejection of organic compounds by ultra-low pressure reverse osmosis membrane. Water Research 36, 123–130. https://doi.org/10.1016/S0043-1354(01)00197-X

Pais, J., Serafim, L.S., Freitas, F., Reis, M.A.M., 2016. Conversion of cheese whey into poly(3-hydroxybutyrate-co-3-hydroxyvalerate) by Haloferax mediterranei. New Biotechnology 33, 224–230. https://doi.org/10.1016/j.nbt.2015.06.001

Parawira, W., Murto, M., Read, J.S., Mattiasson, B., 2005. Profile of hydrolases and biogas production during two-stage mesophilic anaerobic digestion of solid potato waste. Process Biochemistry 40, 2945–2952. https://doi.org/10.1016/j.procbio.2005.01.010

Parolis, H., Parolis, L.A.S., Bo, I.F., Rodriguez-Valera, F., Manta, M.C., Jansson, P.-E., Sutherland, I.W., 1996. The structure of the exopolysaccharide produced by the halophilic Archaeon Haloferax mediterranei strain R4 (ATCC 33500). Carbohydrate Research 10.

Piña, R.G., Cervantes, C., 1996. Microbial interactions with aluminium. Biometals 9, 311–316. https://doi.org/10.1007/BF00817932

Queiroz, A.U.B., Collares-Queiroz, F.P., 2009. Innovation and Industrial Trends in Bioplastics. Polymer Reviews 49, 65–78. https://doi.org/10.1080/15583720902834759

Quillaguamán, J., Guzmán, H., Van-Thuoc, D., Hatti-Kaul, R., 2010. Synthesis and production of polyhydroxyalkanoates by halophiles: current potential and future prospects. Applied Microbiology and Biotechnology 85, 1687–1696. https://doi.org/10.1007/s00253-009-2397-6

Reddy, C.S.K., Ghai, R., Rashmi, Kalia, V.C., 2003. Polyhydroxyalkanoates: an overview. Bioresource Technology 87, 137–146. https://doi.org/10.1016/S0960-8524(02)00212-2

REHM, B.H.A., 2003. Polyester synthases: natural catalysts for plastics. Biochemical Journal 376, 15–33. https://doi.org/10.1042/bj20031254

Rodriguez-Valera, F., Juez, G., Kushner, D.J., 1983. Halobacterium mediterranei spec, nov., a New Carbohydrate-Utilizing Extreme Halophile. Systematic and Applied Microbiology 4, 369–381. https://doi.org/10.1016/S0723-2020(83)80021-6

Roland-Holst, D., 2013. Bioplastics in California: Economic Assessment of Market Conditions for PHA/PHB Bioplastics Produced from Waste Methane 82.

Saleh, H.E.-D.M., 2012. Polyester. BoD – Books on Demand.

Senate Bill No. 1383, 2016. Bill Text - SB-1383 Short-lived climate pollutants: methane emissions: dairy and livestock: organic waste: landfills. [WWW Document]. URL https://leginfo.legislature.ca.gov/faces/billNavClient.xhtml?bill_id=201520160SB1383 (accessed 1.16.22).

Shen, L., Hu, H., Ji, H., Cai, J., He, N., Li, Q., Wang, Y., 2014. Production of poly(hydroxybutyrate–hydroxyvalerate) from waste organics by the two-stage process: Focus on the intermediate volatile fatty acids. Bioresource Technology 166, 194–200. https://doi.org/10.1016/j.biortech.2014.05.038

Shete, B., Shinkar, N.P., 2013. Dairy industry wastewater sources, characteristics & its effects on environment. Int. J. Curr. Eng. Technol. 3, 1611–1615.

Shin, H.-S., Youn, J.-H., Kim, S.-H., 2004. Hydrogen production from food waste in anaerobic mesophilic and thermophilic acidogenesis. International Journal of Hydrogen Energy 29, 1355–1363. https://doi.org/10.1016/j.ijhydene.2003.09.011

Shuler, M.L., Kargi, F., 2008. Bioprocess engineering: basic concepts, 2. ed., 14. print. ed, Prentice Hall PTR international series in the physical and chemical engineering sciences. Prentice Hall PTR, Upper Saddle River, NJ.

Sluiter, A., 2008. Determination of Sugars, Byproducts, and Degradation Products in Liquid Fraction Process Samples: Laboratory Analytical Procedure (LAP); Issue Date: 12/08/2006. Technical Report 14.

Statista, 2021. Potassium chloride price forecast 2015-2035 [WWW Document]. Statista. URL https://www.statista.com/statistics/469705/potassium-chloride-price-forecast/ (accessed 7.27.21).

Sudesh, K., Abe, H., Doi, Y., 2000. Synthesis, structure and properties of polyhydroxyalkanoates: biological polyesters. Progress in Polymer Science 25, 1503–1555. https://doi.org/10.1016/S0079-6700(00)00035-6

Suriyamongkol, P., Weselake, R., Narine, S., Moloney, M., Shah, S., 2007. Biotechnological approaches for the production of polyhydroxyalkanoates in microorganisms and plants — A review. Biotechnology Advances 25, 148–175. https://doi.org/10.1016/j.biotechadv.2006.11.007

Taguchi, S., Doi, Y., 2004. Evolution of Polyhydroxyalkanoate (PHA) Production System by "Enzyme Evolution": Successful Case Studies of Directed Evolution. Macromolecular Bioscience 4, 145–156. https://doi.org/10.1002/mabi.200300111

Tang, S.-L., Tarasov, V., Athanasopoulos, V., Bath, C., Wendoloski, D., Ferrer, C., Pfeiffer, M., Pohlschroder, M., Santos, F., Allers, T., Eichler, J., Camakaris, H., McAlpine, T., Burns, D., Porter, K., Cukalac, T., Russ, B., 2009. The Halohandbook 144.

US EPA, 2019. Plastics: Material-Specific Data | Facts and Figures about Materials, Waste and Recycling | US EPA [WWW Document]. URL https://www.epa.gov/facts-and-figures-about-materials-waste-and-recycling/plastics-material-specific-data (accessed 6.19.19).

US EPA, 2018. Chapter 62-302: Surface Water Quality Standards 84.

US EPA, O., 2017. Food: Material-Specific Data [WWW Document]. US EPA. URL https://www.epa.gov/facts-and-figures-about-materials-waste-and-recycling/food-material-specific-data (accessed 2.17.21).

US EPA, O., 2016. Basic Information about Landfill Gas [WWW Document]. US EPA. URL https://www.epa.gov/lmop/basic-information-about-landfill-gas (accessed 6.22.20).

US EPA, O., 2013. Indicators: Salinity [WWW Document]. US EPA. URL https://www.epa.gov/national-aquatic-resource-surveys/indicators-salinity (accessed 4.15.19).

Veeken Adrie, Kalyuzhnyi Sergey, Scharff Heijo, Hamelers Bert, 2000. Effect of pH and VFA on Hydrolysis of Organic Solid Waste. Journal of Environmental Engineering 126, 1076–1081. https://doi.org/10.1061/(ASCE)0733-9372(2000)126:12(1076)

Venkateswar Reddy, M., Mawatari, Y., Yajima, Y., Satoh, K., Venkata Mohan, S., Chang, Y.-C., 2016. Production of poly-3-hydroxybutyrate (P3HB) and poly(3-hydroxybutyrate-co-3-hydroxyvalerate) P(3HB-co-3HV) from synthetic wastewater using Hydrogenophaga palleronii. Bioresource Technology 215, 155–162. https://doi.org/10.1016/j.biortech.2016.03.025

Wagner, J., 2001. Membrane Filtration Handbook Practical Tips and Hints 129.

Wang, J., Yue, Z.-B., Sheng, G.-P., Yu, H.-Q., 2010. Kinetic analysis on the production of polyhydroxyalkanoates from volatile fatty acids by Cupriavidus necator with a consideration of substrate inhibition, cell growth, maintenance, and product formation. Biochemical Engineering Journal 49, 422–428. https://doi.org/10.1016/j.bej.2010.02.005

Wang, K., Zhang, R., 2021. Production of Polyhydroxyalkanoates (PHA) by Haloferax mediterranei from Food Waste Derived Nutrients for Biodegradable Plastic Applications.

Journal of Microbiology and Biotechnology 31, 338–347. https://doi.org/10.4014/jmb.2008.08057

Wang, K., Zhang, R., 2020. Production of Polyhydroxyalkanoates (PHA) by Haloferax mediterranei from Food Waste Derived Nutrients for Biodegradable Plastic Applications. J Microbiol Biotechnol. https://doi.org/10.4014/jmb.2008.08057

Warnecke, T., Gill, R.T., 2005. Organic acid toxicity, tolerance, and production in Escherichia coli biorefining applications. Microbial Cell Factories 4, 25. https://doi.org/10.1186/1475-2859-4-25

Wolf, M., Gasparin, B.C., Paulino, A.T., 2018. Hydrolysis of lactose using β-d-galactosidase immobilized in a modified Arabic gum-based hydrogel for the production of lactose-free/low-lactose milk. International Journal of Biological Macromolecules 115, 157–164. https://doi.org/10.1016/j.ijbiomac.2018.04.058

Yu, J., Si, Y., Keung, W., Wong, R., 2002. Kinetics modeling of inhibition and utilization of mixed volatile fatty acids in the formation of polyhydroxyalkanoates by Ralstonia eutropha. Process Biochemistry 37, 731–738. https://doi.org/10.1016/S0032-9592(01)00264-3

Zaharia, C., Suteu, D., Muresan, A., Muresan, R., Popescu, A., 2009. Textile wastewater treatment by homogenous oxidation with hydrogen peroxide. Environmental engineering and management journal 8, 1359–1369. https://doi.org/10.30638/eemj.2009.199

Zhang, R., El-Mashad, H.M., Hartman, K., Wang, F., Liu, G., Choate, C., Gamble, P., 2007. Characterization of food waste as feedstock for anaerobic digestion. Bioresource Technology 98, 929–935. https://doi.org/10.1016/j.biortech.2006.02.039

Zhao, Y., Zhuang, X., Ahmad, S., Sung, S., Ni, S.-Q., 2020. Biotreatment of high-salinity wastewater: current methods and future directions. World J Microbiol Biotechnol 36, 37. https://doi.org/10.1007/s11274-020-02815-4

Zhou, M., Yan, B., Wong, J.W.C., Zhang, Y., 2018. Enhanced volatile fatty acids production from anaerobic fermentation of food waste: A mini-review focusing on acidogenic metabolic pathways. Bioresource Technology, Bioconversion of Food Wastes 248, 68–78. https://doi.org/10.1016/j.biortech.2017.06.121

Appendices

Appendix A. Supplemental data in Chapter 5

Table A. 1 Productions of CDM and PHBV using fermented food waste permeate (FWP) with different substrate loadings and aeration rates

Label	Substrate loading (g/L COD)	Aeration (vvm)	CDM ave. (g/L)	CDM std. (g/L)	PHBV ave. (g/L)	PHBV std. (g/L)	HV content ave. (%)	HV content std. (%)	Substrate consumption ave. (%)	Substrate consumption std. (%)
A1	40	0.5	4.00	1.25	2.49	0.81	20.6	2.21	23.5	3.4
A2	40	1.5	6.45	0.34	4.07	0.15	16.9	0.60	42.8	0.0
A3	40	2.5	6.69	0.02	4.32	0.10	17.0	1.28	50.0	4.8
A4	80	0.5	3.33	0.28	1.42	0.04	25.7	2.37	19.9	1.0
A5	80	1.5	3.98	1.02	2.35	0.76	21.5	3.10	21.5	4.6
A6	80	2.5	6.05	0.88	3.63	0.50	17.3	0.64	27.0	2.9

Table A. 2 Short-chain carboxylate consumption using FWP with different substrate loadings and aeration rates

Label	Short-chain carboxylates consumption (g/L)													
	La ave.	La std.	Ac ave.	Ac std.	Pr ave.	Pr std.	Iso-Bu ave.	Iso-Bu std.	Bu ave.	Bu std.	Iso-Va ave.	Iso-Va std.	Va ave.	Va std.
A1	3.21	0.60	-1.31	0.92	2.08	0.36	0.00	0.00	0.14	0.72	0.11	0.00	0.00	0.00
A2	5.38	0.81	-0.10	0.73	6.54	0.39	0.00	0.00	0.84	0.45	0.11	0.00	0.00	0.00
A3	4.83	0.26	0.36	0.06	6.76	0.05	0.00	0.00	0.76	0.03	0.11	0.00	0.00	0.00
A4	3.23	0.65	-3.33	0.17	4.84	0.40	0.00	0.00	1.33	0.57	-0.01	0.00	0.00	0.00
A5	3.29	0.98	-3.51	0.40	4.87	0.01	0.00	0.00	0.80	0.59	0.01	0.01	0.00	0.00
A6	5.22	0.82	-4.78	0.33	3.37	0.33	0.00	0.00	-0.22	0.11	0.15	0.05	0.00	0.00

Table A. 3 Productions of CDM and PHBV using FWP with different substrate types and loadings

Label	Substrate loading (g/L COD)	FWP type	CDM ave. (g/L)	CDM std. (g/L)	PHBV ave. (g/L)	PHBV std. (g/L)	HV content ave. (%)	HV content std. (%)	Substrate consumption ave. (%)	Substrate consumption std. (%)
B1	20	1	3.67	0.03	2.24	0.07	16.1	0.9	26.5	2.1
B2	40	1	6.76	0.08	4.01	0.05	16.5	0.0	37.3	4.6
B3	60	1	5.84	0.77	3.14	0.78	16.3	0.3	29.7	0.5
B4	80	1	5.11	0.07	2.77	0.02	17.5	1.0	21.3	5.3
B5	20	2	1.21	0.17	0.05	0.04	8.2	0.3	23.5	3.5
B6	40	2	2.67	0.86	0.67	0.21	13.0	1.0	43.8	3.9
B7	60	2	4.38	0.47	2.26	0.12	13.0	1.0	39.0	5.2
B8	80	2	3.74	0.16	1.46	0.19	14.9	0.2	33.6	2.7

Table A. 4 Short-chain carboxylate consumption using FWP with different substrate types and loadings

Label	Short-chain carboxylates consumption (g/L)													
	La ave.	La std.	Ac ave.	Ac std.	Pr ave.	Pr std.	Iso-Bu ave.	Iso-Bu std.	Bu ave.	Bu std.	Iso-Va ave.	Iso-Va std.	Va ave.	Va std.
B1	3.09	0.32	0.06	0.02	3.43	0.00	0.00	0.00	0.77	0.07	0.32	0.00	0.19	0.00
B2	3.65	0.10	-0.89	0.14	6.87	0.05	0.00	0.00	1.95	0.05	0.60	0.00	0.82	0.11
B3	3.46	0.35	-2.70	0.70	4.65	0.33	0.00	0.00	2.27	0.29	0.89	0.05	1.21	0.06
B4	2.13	0.35	-2.22	0.21	6.20	0.13	0.00	0.00	4.07	0.11	1.20	0.02	1.66	0.00
B5	2.95	0.46	-0.09	0.20	0.40	1.32	0.00	0.00	1.04	0.15	0.00	0.01	0.89	1.26
B6	4.69	4.96	1.34	1.37	2.25	2.70	0.00	0.00	1.80	0.03	0.00	0.00	3.56	0.07
B7	4.48	1.07	0.38	1.08	1.53	0.21	0.00	0.00	0.30	0.42	0.04	0.06	3.54	0.00
B8	0.69	3.66	-1.51	0.38	2.89	0.16	0.00	0.00	0.54	0.52	0.08	0.11	4.53	0.34

Table A. 5 Time profiles of CDM, PHBV, dissolved oxygen (DO), temperature, pH, sCOD and ammonium of 6-L batch production using FWP with a controlled aeration rate at 2.5 vvm (replicate 1)

Time (h)	CDM (g/L)	PHBV (g/L)	HV content (% PHBV)	HB content (% PHBV)	DO (mg/L)	DO (% sat)	T (degC)	pH	Substrate (g/L COD)	Ammonium (mg/L N)
0	0.79	0.20	10.0	90.0	2.40	98.5	38.4	6.8	39.8	584
12	1.31	0.42	13.7	86.3	2.00	82.9	38.6	6.8	35.0	374
36	2.16	0.77	25.4	74.6	0.30	11.0	39.4	7.0	29.6	252
60	5.30	2.23	19.5	80.5	0.20	9.9	37.9	6.8	26.0	273
84	6.35	3.14	16.9	83.1	0.40	16.5	38.5	6.9	22.0	181
108	7.90	4.12	15.2	84.8	1.70	68.6	37.1	6.9	17.4	95
132	7.85	4.61	15.3	84.7	2.10	86.0	38.5	7.0	13.8	53

Table A. 6 Time profiles of short-chain carboxylates of 6-L batch production using FWP with a controlled aeration rate at 2.5 vvm (replicate 1)

Time	Short-chain carboxylates (g/L)						
(h)	La	Ac	Pr	Iso-Bu	Bu	Iso-Va	Va
0	7.21	2.47	5.41	0.32	3.52	0.82	0.66
12	6.69	2.01	3.88	0.15	3.21	0.49	0.56
36	6.04	2.69	4.24	0.00	1.55	0.30	0.69
60	4.85	2.15	4.14	0.00	1.70	0.11	0.63
84	1.89	1.78	0.99	0.00	2.90	0.01	0.90
108	1.64	0.05	0.63	0.00	2.76	0.00	0.27
132	1.54	0.05	0.74	0.00	3.40	0.00	0.44

Table A. 7 Time profiles of CDM, PHBV, dissolved oxygen (DO), temperature, pH, sCOD and ammonium of 6-L batch production using FWP with a controlled aeration rate at 2.5 vvm (replicate 2)

Time	CDM	PHBV	HV content	HB content	DO	DO	T	pH	Substrate	Ammonium
(h)	(g/L)	(g/L)	(% PHBV)	(% PHBV)	(mg/L)	(% sat)	(degC)		(g/L COD)	(mg/L N)
0	1.52	0.58	10.1	89.9	2.42	95.10	38.7	7.1	35.7	574
12	1.84	0.75	11.7	88.3	2.41	95.10	38.9	7.0	32.0	381
36	1.69	0.60	21.3	78.7	0.41	16.84	38.9	7.0	25.5	256
60	3.47	2.63	26.1	73.9	0.16	6.46	37.7	6.8	23.2	250
84	5.59	4.20	17.9	82.1	0.58	23.52	39.1	6.8	19.8	171
108	6.16	5.54	15.6	84.4	0.93	37.84	39.4	6.9	15.4	96
132	6.34	4.32	15.6	84.4	1.39	56.45	39.1	7.0	12.1	52

Table A. 8 Time profiles of short-chain carboxylates of 6-L batch production using FWP with a controlled aeration rate at 2.5 vvm (replicate 2)

Time	Short-chain carboxylates (g/L)						
(h)	La	Ac	Pr	Iso-Bu	Bu	Iso-Va	Va
0	6.28	1.28	3.13	0.00	0.74	0.26	0.00
12	5.98	1.19	2.77	0.00	0.62	0.28	0.00
36	5.36	1.41	2.66	0.00	1.23	0.25	0.00
60	2.52	1.57	2.52	0.00	1.43	0.14	0.00
84	0.59	1.21	2.43	0.00	1.61	0.07	0.00
108	0.54	0.35	2.23	0.00	1.02	0.01	0.00
132	0.48	0.06	2.16	0.00	0.64	0.01	0.00

Table A. 9 Spent salts recycling experiment using FWP as feedstock

Label	Batch No.	Substrate loading (g/L COD)	H_2O_2 pretreatment	Recycled salts ave. (%)	Recycled salts std. (%)	New salts ave. (%)	New salts std. (%)	Loss of salts ave. (%)	Loss of salts std. (%)
C1	1	20	No	0	0	100	0	0	0
C2	2	20	Yes	80	2	21	2	0	0
C3	3	20	Yes	80	2	20	2	0	0
C4	4	20	Yes	80	1	19	1	0	0
D1	1	20	No	0	0	100	0	0	0
D2	2	20	Yes	93	0.5	8	0.5	0	0
D3	3	20	Yes	90	0.0	10	0.0	0	0
D4	4	20	Yes	90	0.1	10	0.1	0	0

Table A. 10 Productions of CDM and PHBV in spent salts recycling experiments with FWP as feedstock

Label	CDM ave. (g/L)	CDM std. (g/L)	PHBV ave. (g/L)	PHBV std. (g/L)	HV content ave. (% PHBV)	HV content std. (% PHBV)	HB content ave. (% PHBV)	HB content std. (% PHBV)
C1	3.9	0.1	2.6	0.2	16.1	0.3	83.9	0.3
C2	5.6	0.2	3.6	0.3	17.8	1.3	82.2	1.3
C3	5.2	0.4	3.3	0.7	21.5	1.9	78.5	1.9
C4	5.5	0.2	3.2	0.2	20.0	0.3	80.0	0.3
D1	4.1	0.1	2.6	0.1	17.1	0.8	82.9	0.8
D2	3.0	0.1	1.5	0.2	22.8	0.5	77.2	0.5
D3	4.6	0.1	2.2	0.3	22.3	0.5	77.7	0.5
D4	4.4	0.2	2.1	0.0	21.2	0.7	78.8	0.7

Appendix B. Supplemental data in Chapter 6

Table B. 1 Productions of CDM and PHBV using whey sugar hydrolysate with different substrate loadings

Label	Substrate loading (g/L COD)	N source	C/N ratio	CDM ave. (g/L)	CDM std. (g/L)	PHBV ave. (g/L)	PHBV std. (g/L)	HV content ave. (% PHBV)	HV content std. (% PHBV)
A1	12	NH_4Cl	10	4.4	0.3	1.90	0.64	15.4%	0.7%
A2	24	NH_4Cl	10	7.6	0.3	3.85	0.11	17.1%	0.2%
A3	36	NH_4Cl	10	11.8	0.0	5.89	0.65	20.8%	0.2%

Table B. 2 COD consumptions using whey sugar hydrolysate with different substrate loadings

Label	Initial COD ave. (g/L COD)	Initial COD std. (g/L COD)	End COD ave. (g/L COD)	End COD std. (g/L COD)	COD consumption ave. (g/L COD)	COD consumption std. (g/L COD)	COD consumption ave. (%)	COD consumption std. (%)
A1	13.1	0.2	7.7	0.1	5.4	0.1	41.0	0.1
A2	24.7	0.2	15.0	0.0	9.7	0.2	39.2	0.6
A3	36.3	0.1	21.3	0.6	15.0	0.7	41.2	1.9

Table B. 3 Glucose consumptions using whey sugar hydrolysate with different substrate loadings

Label	Initial glucose ave. (g/L)	Initial glucose std. (g/L)	End glucose ave. (g/L)	End glucose std. (g/L)	Glucose consumption ave. (g/L)	Glucose consumption std. (g/L)	Glucose consumption ave. (%)	Glucose consumption std. (%)
A1	6.5	0.06	0.1	0.00	6.4	0.1	98.5	0.1
A2	12.9	0.04	0.3	0.04	12.6	0.0	97.4	0.3
A3	20.2	0.03	1.5	0.09	18.7	0.1	92.6	0.5

Table B. 4 Galactose consumptions using whey sugar hydrolysate with different substrate loadings

Label	Initial galactose ave. (g/L)	Initial galactose std. (g/L)	End galactose ave. (g/L)	End galactose std. (g/L)	Galactose consumption ave. (g/L)	Galactose consumption std. (g/L)	Galactose consumption ave. (%)	Galactose consumption std. (%)
A1	4.2	0.08	1.0	0.18	3.2	0.3	76.4	4.8
A2	8.5	0.03	5.0	0.03	3.4	0.1	40.6	0.6
A3	13.2	0.08	7.0	0.94	6.2	1.0	47.2	7.5

Table B. 5 Lactose consumptions using whey sugar hydrolysate with different substrate loadings

Label	Initial lactose ave. (g/L)	Initial lactose std. (g/L)	End lactose ave. (g/L)	End lactose std. (g/L)	Lactose consumption ave. (g/L)	Lactose consumption std. (g/L)	Lactose consumption ave. (%)	Lactose consumption std. (%)
A1	3.3	0.04	3.3	0.04	0.0	0.0	0.0	0.0
A2	5.2	0.04	5.2	0.22	0.0	0.3	0.1	5.0
A3	10.7	0.16	10.5	0.09	0.1	0.2	1.2	2.3

Table B. 6 Time profiles of CDM, PHBV, dissolved oxygen (DO), temperature, pH, sCOD and ammonium of 6-L batch production using whey sugar hydrolysate with a controlled aeration rate at 2.5 vvm (replicate 1)

Time (h)	CDM (g/L)	PHBV (g/L)	HV content (% PHBV)	HB content (% PHBV)	DO (mg/L)	DO (% sat)	T (degC)	pH	Glucose (g/L)	Galactose (g/L)	Lactose (g/L)	Ammonium (mg/L N)
0	1.67	0.08	9.6	90.4	2.54	100.0	37.9	7.0	13.5	10.4	4.9	604
12	1.30	0.09	10.0	90.0	2.53	90.0	38.4	6.9	12.9	10.2	4.8	410
36	2.36	1.24	16.0	84.0	0.25	10.8	41.1	6.8	11.2	10.2	4.9	322
60	3.74	2.22	25.4	74.6	0.23	8.4	39.4	6.9	8.4	10.3	5.1	279
84	4.86	2.47	26.8	73.2	0.25	9.0	39.7	7.0	5.1	9.9	5.1	220
108	6.85	4.20	23.9	76.1	1.43	58.9	39.8	7.0	0.5	9.3	5.3	191
132	7.01	3.08	23.9	76.1	1.36	55.7	39.8	7.1	0.5	7.1	5.0	127
156	7.13	3.09	23.9	76.1	1.35	53.2	39.8	7.0	0.5	6.1	4.8	89

Table B. 7 Time profiles of short-chain carboxylates of 6-L batch production using whey sugar hydrolysate with a controlled aeration rate at 2.5 vvm (replicate 1)

Time (h)	CDM (g/L)	PHBV (g/L)	HV content (% PHBV)	HB content (% PHBV)	DO (mg/L)	DO (% sat)	T (degC)	pH	Glucose (g/L)	Galactose (g/L)	Lactose (g/L)	Ammonium (mg/L N)
0	1.23	0.34	12.7	87.3	2.48	100.0	37.8	6.9	12.9	10.2	4.9	598
12	1.80	0.70	14.7	85.3	1.86	78.0	38.3	7.0	11.9	10.1	4.9	432
36	3.27	1.12	23.0	77.0	0.09	4.0	41.0	7.1	8.0	9.7	4.4	346
60	4.89	2.07	24.4	75.6	0.18	7.0	39.3	6.8	3.9	9.1	4.4	288
84	6.46	2.69	24.4	75.6	0.11	4.0	39.9	6.9	0.4	8.5	4.8	216
108	6.68	3.11	24.7	75.3	1.63	66.0	39.5	7.0	0.5	6.5	4.8	184
132	6.60	3.26	24.3	75.7	1.53	62.6	39.6	7.0	0.6	5.4	4.7	143
156	6.94	3.10	24.9	75.1	1.64	66.7	39.8	7.0	0.6	4.5	4.6	93

Table B. 8 Time profiles of CDM, PHBV, dissolved oxygen (DO), temperature, pH, sCOD and ammonium of 6-L batch production using whey sugar hydrolysate with a controlled aeration rate at 2.5 vvm (replicate 2)

Time (h)	CDM (g/L)	PHBV (g/L)	HV content (% PHBV)	HB content (% PHBV)	DO (mg/L)	DO (% sat)	T (degC)	pH	Glucose (g/L)	Galactose (g/L)	Lactose (g/L)	Ammonium (mg/L N)
0	1.94	0.51	16.3	83.7	2.63	99.1	37.5	7.0	15.6	12.5	6.1	585
12	3.41	0.67	16.4	83.6	1.36	55.4	37.8	7.0	14.0	12.3	4.1	442
36	4.53	1.38	25.2	74.8	1.78	69.6	39.9	6.9	1.8	8.7	5.0	366
60	6.14	2.24	27.4	72.6	1.21	47.4	39.3	6.8	0.9	8.0	4.0	292
84	7.53	2.19	25.2	74.8	1.67	66.7	39.6	6.8	0.2	6.4	3.9	234
108	7.36	2.02	26.1	73.9	1.91	79.7	39.7	7.1	0.2	4.1	4.2	195
132	7.45	1.94	25.9	74.1	1.54	64.5	38.9	6.9	0.1	2.6	5.3	128
156	7.32	1.72	26.2	73.8	1.73	72.0	39.5	7.0	0.1	1.6	5.1	92

Table B. 9 Time profiles of short-chain carboxylates of 6-L batch production using whey sugar hydrolysate with a controlled aeration rate at 2.5 vvm (replicate 2)

Time (h)	CDM (g/L)	PHBV (g/L)	HV content (% PHBV)	HB content (% PHBV)	DO (mg/L)	DO (% sat)	T (degC)	pH	Glucose (g/L)	Galactose (g/L)	Lactose (g/L)	Ammonium (mg/L N)
0	1.73	0.65	14.8	85.2	2.61	99.0	37.3	6.9	13.5	10.0	4.5	599
12	3.32	0.71	18.0	82.0	1.47	60.4	37.9	7.0	12.9	9.9	5.0	481
36	4.60	1.24	27.0	73.0	1.80	72.4	38.9	6.8	2.3	8.8	4.2	371
60	5.99	2.21	24.4	75.6	1.23	47.0	39.5	6.8	1.3	8.2	4.5	301
84	7.21	2.43	25.4	74.6	2.00	81.6	39.6	7.1	0.5	7.0	4.5	247
108	6.88	2.13	24.7	75.3	1.44	59.5	39.5	7.0	0.3	4.9	4.0	188
132	7.12	2.28	26.3	73.7	1.63	68.0	39.9	6.9	0.1	2.8	4.4	116
156	7.21	2.21	28.0	72.0	1.87	79.0	39.5	6.9	0.1	1.7	4.5	87

Table B. 10 Spent salts recycling experiment using whey sugar hydrolysate as feedstock

Label	Batch No.	Substrate loading (g/L COD)	Recycled salts ave. (%)	Recycled salts std. (%)	New salts ave. (%)	New salts std. (%)	Loss of salts ave. (%)	Loss of salts std. (%)
B1	1	20	0.0	0.0	100.0	0.0	0.0	0.0
B2	2	20	79.0	2.0	21.0	2.0	0.0	0.0
B3	3	20	80.0	2.0	20.0	2.0	0.0	0.0
B4	4	20	81.0	1.0	19.0	1.0	0.0	0.0
C1	1	20	0.0	0.0	100.0	0.0	0.0	0.0
C2	2	20	89.5	0.7	10.5	0.7	0.0	0.0
C3	3	20	90.0	0.0	10.0	0.0	0.0	0.0
C4	4	20	90.0	0.0	10.0	0.0	0.0	0.0
D1	1	40	0.0	0.0	100.0	0.0	0.0	0.0
D2	2	40	90.3	0.4	9.8	0.4	0.0	0.0
D3	3	40	90.5	0.7	9.5	0.7	0.0	0.0
D4	4	40	90.0	0.0	10.0	0.0	0.0	0.0
E1	1	60	0.0	0.0	100.0	0.0	0.0	0.0
E2	2	60	89.8	0.4	10.3	0.4	0.0	0.0
E3	3	60	90.5	0.7	9.5	0.7	0.0	0.0
E4	4	60	90.0	0.0	10.0	0.0	0.0	0.0

Table B. 11 Productions of CDM and PHBV in spent salts recycling experiments with whey sugar hydrolysate as feedstock

Label	CDM ave. (g/L)	CDM std. (g/L)	PHBV ave. (g/L)	PHBV std. (g/L)	HV content ave. (% PHBV)	HV content std. (% PHBV)	HB content ave. (% PHBV)	HB content std. (% PHBV)
B1	3.3	0.7	1.4	0.3	16.9	0.8	83.1	0.8
B2	5.4	0.4	1.9	0.2	20.2	0.3	79.8	0.3
B3	4.8	0.1	2.0	0.4	16.0	0.6	84.0	0.6
B4	4.9	0.2	2.0	0.2	14.1	0.5	85.9	0.5
C1	4.4	0.3	1.7	0.2	18.2	1.0	81.8	1.0
C2	4.4	0.1	1.5	0.0	14.6	0.2	85.4	0.2
C3	4.7	0.2	1.3	0.5	17.7	0.2	82.3	0.2
C4	4.7	0.3	1.3	0.3	17.7	0.1	82.4	0.1
D1	7.6	0.3	3.7	0.1	20.3	0.2	79.7	0.2
D2	7.5	0.1	3.6	0.0	18.7	0.1	81.3	0.1
D3	7.8	0.4	3.1	0.7	20.3	0.4	79.7	0.4
D4	8.0	0.4	3.3	0.4	20.7	0.4	79.4	0.4
E1	11.8	0.0	6.0	0.3	24.2	0.2	75.8	0.2
E2	8.3	0.5	3.2	0.4	21.4	0.6	78.6	0.6
E3	8.5	0.5	4.1	0.4	21.8	0.2	78.2	0.2
E4	8.4	0.6	4.0	0.4	21.1	0.1	78.9	0.1

Appendix C. Statistical analysis reports

Table C. 1 Two-way ANOVA table for PHBV yield (as illustrated in Figure 3.4 a)

	DF	Sum of Squares	Mean Square	F Value	P Value
time	6	0.09255	0.01542	6.61719	3.63413E-4
substrate	1	0.04914	0.04914	21.08162	1.28853E-4
Interaction	6	0.01423	0.00237	1.01777	0.43849
Model	13	0.17107	0.01316	5.64522	1.622E-4
Error	23	0.05361	0.00233		
Corrected Total	36	0.22468			

At the 0.05 level, the population means of **time** are **significantly** different.
At the 0.05 level, the population means of **substrate** are **significantly** different.
At the 0.05 level, the interaction between **time** and **substrate** is **not significant**.

Table C. 2 Two-way ANOVA table for HV content (as illustrated in Figure 3.4 b)

	DF	Sum of Squares	Mean Square	F Value	P Value
time	6	0.0229	0.00382	133.03726	3.83591E-16
substrate	1	0.00379	0.00379	132.08924	9.06638E-11
Interaction	6	0.0157	0.00262	91.21027	2.08444E-14
Model	13	0.03835	0.00295	102.81582	1.3778E-16
Error	22	6.3117E-4	2.86896E-5		
Corrected Total	35	0.03898			

At the 0.05 level, the population means of **time** are **significantly** different.
At the 0.05 level, the population means of **substrate** are **significantly** different.
At the 0.05 level, the interaction between **time** and **substrate** is **significant**.

Table C. 3 One-way ANOVA table for CDM concentration (as demonstrated in Figure 3.7 a)

	DF	Sum of Squares	Mean Square	F Value	Prob>F
Model	3	0.90557	0.30186	22.09832	0.00595
Error	4	0.05464	0.01366		
Total	7	0.96021			

Null Hypothesis: The means of all levels are equal.
Alternative Hypothesis: The means of one or more levels are different.
At the 0.05 level, the population means are significantly different.

Table C. 4 One-way ANOVA table for PHBV concentration (as demonstrated in Figure 3.7 a)

	DF	Sum of Squares	Mean Square	F Value	Prob>F
Model	3	0.27022	0.09007	15.99815	0.01081
Error	4	0.02252	0.00563		
Total	7	0.29274			

Null Hypothesis: The means of all levels are equal.
Alternative Hypothesis: The means of one or more levels are different.
At the 0.05 level, the population means are significantly different.

Table C. 5 One-way ANOVA table for PHBV yield (as demonstrated in Figure 3.7 b)

	DF	Sum of Squares	Mean Square	F Value	Prob>F
Model	3	0.10955	0.03652	5.18398	0.0729
Error	4	0.02818	0.00704		
Total	7	0.13772			

Null Hypothesis: The means of all levels are equal.
Alternative Hypothesis: The means of one or more levels are different.
At the 0.05 level, the population means are not significantly different.

Table C. 6 One-way ANOVA table for HV content (as demonstrated in Figure 3.7 b)

	DF	Sum of Squares	Mean Square	F Value	Prob>F
Model	3	0.00248	8.28065E-4	43.75844	0.00162
Error	4	7.56942E-5	1.89235E-5		
Total	7	0.00256			

Null Hypothesis: The means of all levels are equal.
Alternative Hypothesis: The means of one or more levels are different.
At the 0.05 level, the population means are significantly different.

Table C. 7 One-way ANOVA table for Propionate consumption (as demonstrated in Figure 3.8 b)

	DF	Sum of Squares	Mean Square	F Value	Prob>F
Model	3	0.06236	0.02079	10.33829	0.02352
Error	4	0.00804	0.00201		
Total	7	0.0704			

Null Hypothesis: The means of all levels are equal.
Alternative Hypothesis: The means of one or more levels are different.
At the 0.05 level, the population means are significantly different.

Table C. 8 Two-way ANOVA table for CDM concentration (as demonstrated in Figure 4.10)

	DF	Sum of Squares	Mean Square	F Value	P Value
substrate type	3	3.29921	1.09974	12.04471	0.00246
substrate loading	1	11.44813	11.44813	125.38397	3.62659E-6
Interaction	3	2.66332	0.88777	9.72322	0.0048
Model	7	17.41067	2.48724	27.24111	5.68211E-5
Error	8	0.73044	0.0913		
Corrected Total	15	18.1411			

At the 0.05 level, the population means of **substrate type** are **significantly** different.
At the 0.05 level, the population means of **substrate loading** are **significantly** different.
At the 0.05 level, the interaction between **substrate type** and **substrate loading** is **significant**.

Table C. 9 Two-way ANOVA table for CDM yield (as demonstrated in Figure 4.10)

	DF	Sum of Squares	Mean Square	F Value	P Value
substrate type	3	0.02077	0.00692	8.41882	0.0074
substrate loading	1	0.01412	0.01412	17.166	0.00324
Interaction	3	0.01086	0.00362	4.40228	0.0416
Model	7	0.04575	0.00654	7.94704	0.0045
Error	8	0.00658	8.2236E-4		
Corrected Total	15	0.05233			

At the 0.05 level, the population means of **substrate type** are **significantly** different.
At the 0.05 level, the population means of **substrate loading** are **significantly** different.
At the 0.05 level, the interaction between **substrate type** and **substrate loading** is **significant**.

Table C. 10 Two-way ANOVA table for PHBV concentration (as demonstrated in Figure 4.11)

	DF	Sum of Squares	Mean Square	F Value	P Value
substrate type	3	3.3931	1.13103	44.60412	2.43541E-5
substrate loading	1	9.42118	9.42118	371.5392	5.4436E-8
Interaction	3	0.9408	0.3136	12.36735	0.00226
Model	7	13.75509	1.96501	77.49337	1.01655E-6
Error	8	0.20286	0.02536		
Corrected Total	15	13.95794			

At the 0.05 level, the population means of **substrate type** are **significantly** different.
At the 0.05 level, the population means of **substrate loading** are **significantly** different.
At the 0.05 level, the interaction between **substrate type** and **substrate loading** is **significant**.

Table C. 11 Two-way ANOVA table for PHBV yield (as demonstrated in Figure 4.11)

	DF	Sum of Squares	Mean Square	F Value	P Value
substrate type	3	0.01154	0.00385	19.09693	5.26774E-4
substrate loading	1	0.00218	0.00218	10.80817	0.01106
Interaction	3	0.00158	5.26173E-4	2.61305	0.12335
Model	7	0.01529	0.00218	10.8483	0.00159
Error	8	0.00161	2.01363E-4		
Corrected Total	15	0.0169			

At the 0.05 level, the population means of **substrate type** are **significantly** different.
At the 0.05 level, the population means of **substrate loading** are **significantly** different.
At the 0.05 level, the interaction between **substrate type** and **substrate loading** is **not significant**.

Table C. 12 Two-way ANOVA table for PHBV content (as demonstrated in Figure 4.12)

	DF	Sum of Squares	Mean Square	F Value	P Value
substrate type	3	0.17004	0.05668	27.90601	1.37379E-4
substrate loading	1	0.11985	0.11985	59.00582	5.84307E-5
Interaction	3	0.01501	0.005	2.46409	0.13692
Model	7	0.3049	0.04356	21.44516	1.38676E-4
Error	8	0.01625	0.00203		
Corrected Total	15	0.32115			

At the 0.05 level, the population means of **substrate type** are **significantly** different.
At the 0.05 level, the population means of **substrate loading** are **significantly** different.
At the 0.05 level, the interaction between **substrate type** and **substrate loading** is **not significant**.

Table C. 13 Two-way ANOVA table for HV content (as demonstrated in Figure 4.13)

	DF	Sum of Squares	Mean Square	F Value	P Value
substrate type	3	0.0138	0.0046	37.91761	4.4649E-5
substrate loading	1	0.00162	0.00162	13.33407	0.00648
Interaction	3	0.00469	0.00156	12.89723	0.00197
Model	7	0.0201	0.00287	23.68266	9.59465E-5
Error	8	9.70191E-4	1.21274E-4		
Corrected Total	15	0.02107			

At the 0.05 level, the population means of **substrate type** are **significantly** different.
At the 0.05 level, the population means of **substrate loading** are **significantly** different.
At the 0.05 level, the interaction between **substrate type** and **substrate loading** is **significant**.

Table C. 14 Two-way ANOVA table for CDM concentration (as demonstrated in Figure 5.6)

	DF	Sum of Squares	Mean Square	F Value	P Value
Substrate loading	1	4.77541	4.77541	7.9872	0.03011
Aeration	2	14.73741	7.3687	12.32467	0.0075
Interaction	2	2.17254	1.08627	1.81687	0.24158
Model	5	21.68536	4.33707	7.25406	0.01586
Error	6	3.58729	0.59788		
Corrected Total	11	25.27266			

At the 0.05 level, the population means of **Substrate loading** are **significantly** different.
At the 0.05 level, the population means of **Aeration** are **significantly** different.
At the 0.05 level, the interaction between **Substrate loading** and **Aeration** is **not significant**.

Table C. 15 Two-way ANOVA table for PHBV concentration (as demonstrated in Figure 5.6)

	DF	Sum of Squares	Mean Square	F Value	P Value
Substrate loading	1	4.06013	4.06013	16.00432	0.00711
Aeration	2	8.29681	4.14841	16.35228	0.00373
Interaction	2	0.53902	0.26951	1.06237	0.40274
Model	5	12.89596	2.57919	10.16672	0.00682
Error	6	1.52214	0.25369		
Corrected Total	11	14.4181			

At the 0.05 level, the population means of **Substrate loading** are **significantly** different.
At the 0.05 level, the population means of **Aeration** are **significantly** different.
At the 0.05 level, the interaction between **Substrate loading** and **Aeration** is **not significant**.

Table C. 16 Two-way ANOVA table for cell content of PHBV (as demonstrated in Figure 5.7 a)

	DF	Sum of Squares	Mean Square	F Value	P Value
Substrate loading	1	0.02705	0.02705	36.34597	9.4062E-4
Aeration	2	0.02201	0.01101	14.78958	0.0048
Interaction	2	0.01397	0.00698	9.38388	0.01422
Model	5	0.06303	0.01261	16.93858	0.00176
Error	6	0.00447	7.44236E-4		
Corrected Total	11	0.0675			

At the 0.05 level, the population means of **Substrate loading** are **significantly** different.
At the 0.05 level, the population means of **Aeration** are **significantly** different.
At the 0.05 level, the interaction between **Substrate loading** and **Aeration** is **significant**.

Table C. 17 Two-way ANOVA table for HV content (as demonstrated in Figure 5.7 b)

	DF	Sum of Squares	Mean Square	F Value	P Value
Substrate loading	1	0.00336	0.00336	8.95269	0.02425
Aeration	2	0.00738	0.00369	9.84858	0.01273
Interaction	2	0.00136	6.81732E-4	1.81911	0.24125
Model	5	0.0121	0.00242	6.45762	0.02094
Error	6	0.00225	3.74761E-4		
Corrected Total	11	0.01435			

At the 0.05 level, the population means of **Substrate loading** are **significantly** different.
At the 0.05 level, the population means of **Aeration** are **significantly** different.
At the 0.05 level, the interaction between **Substrate loading** and **Aeration** is **not significant**.

Table C. 18 Two-way ANOVA table for CDM concentration (as demonstrated in Figure 5.9 a)

	DF	Sum of Squares	Mean Square	F Value	P Value
substrate type	1	19.73581	19.73581	151.5907	1.76233E-6
substrate loading	3	15.32746	5.10915	39.24339	3.92963E-5
Interaction	3	5.88503	1.96168	15.06763	0.00118
Model	7	40.94829	5.84976	44.93197	8.44716E-6
Error	8	1.04153	0.13019		
Corrected Total	15	41.98982			

At the 0.05 level, the population means of **substrate type** are **significantly** different.
At the 0.05 level, the population means of **substrate loading** are **significantly** different.
At the 0.05 level, the interaction between **substrate type** and **substrate loading** is **significant**.

Table C. 19 Two-way ANOVA table for PHBV concentration (as demonstrated in Figure 5.9 b)

	DF	Sum of Squares	Mean Square	F Value	P Value
substrate type	1	14.53207	14.53207	765.45815	3.1425E-9
substrate loading	3	5.05762	1.68587	88.80129	1.75701E-6
Interaction	3	3.73241	1.24414	65.53333	5.66154E-6
Model	7	23.3221	3.33173	175.49457	4.05834E-8
Error	8	0.15188	0.01898		
Corrected Total	15	23.47398			

At the 0.05 level, the population means of **substrate type** are **significantly** different.
At the 0.05 level, the population means of **substrate loading** are **significantly** different.
At the 0.05 level, the interaction between **substrate type** and **substrate loading** is **significant**.

Table C. 20 Two-way ANOVA table for cell content of PHBV (as demonstrated in Figure 5.10 a)

	DF	Sum of Squares	Mean Square	F Value	P Value
substrate type	1	0.31212	0.31212	629.77474	6.80361E-9
substrate loading	3	0.09882	0.03294	66.46458	5.36376E-6
Interaction	3	0.15673	0.05224	105.41036	9.0305E-7
Model	7	0.56767	0.0811	163.62851	5.35483E-8
Error	8	0.00396	4.95611E-4		
Corrected Total	15	0.57164			

At the 0.05 level, the population means of **substrate type** are **significantly** different.
At the 0.05 level, the population means of **substrate loading** are **significantly** different.
At the 0.05 level, the interaction between **substrate type** and **substrate loading** is **significant**.

Table C. 21 Two-way ANOVA table for HV content (as demonstrated in Figure 5.10 b)

	DF	Sum of Squares	Mean Square	F Value	P Value
substrate type	1	0.00746	0.00746	146.30531	2.01793E-6
substrate loading	3	0.0033	0.0011	21.56568	3.44637E-4
Interaction	3	0.00175	5.84657E-4	11.46527	0.00287
Model	7	0.01251	0.00179	35.05688	2.18645E-5
Error	8	4.0795E-4	5.09937E-5		
Corrected Total	15	0.01292			

At the 0.05 level, the population means of **substrate type** are **significantly** different.
At the 0.05 level, the population means of **substrate loading** are **significantly** different.
At the 0.05 level, the interaction between **substrate type** and **substrate loading** is **significant**.

Table C. 22 One-way ANOVA table for CDM concentration (as demonstrated in Figure 6.1 b)

	DF	Sum of Squares	Mean Square	F Value	Prob>F
Model	2	54.98556	27.49278	446.64367	1.93647E-4
Error	3	0.18466	0.06155		
Total	5	55.17022			

Null Hypothesis: The means of all levels are equal.
Alternative Hypothesis: The means of one or more levels are different.
At the 0.05 level, the population means are significantly different.

Table C. 23 One-way ANOVA table for PHBV concentration (as demonstrated in Figure 6.1 b)

	DF	Sum of Squares	Mean Square	F Value	Prob>F
Model	2	15.94355	7.97178	28.49952	0.01118
Error	3	0.83915	0.27972		
Total	5	16.7827			

Null Hypothesis: The means of all levels are equal.
Alternative Hypothesis: The means of one or more levels are different.
At the 0.05 level, the population means are significantly different.

Table C. 24 One-way ANOVA table for HV content (as demonstrated in Figure 6.1 c)

	DF	Sum of Squares	Mean Square	F Value	Prob>F
Model	2	0.00304	0.00152	77.13561	0.00263
Error	3	5.90343E-5	1.96781E-5		
Total	5	0.00309			

Null Hypothesis: The means of all levels are equal.
Alternative Hypothesis: The means of one or more levels are different.
At the 0.05 level, the population means are significantly different.

Table C. 25 One-way ANOVA table for PHBV yield (as demonstrated in Figure 6.1 d)

	DF	Sum of Squares	Mean Square	F Value	Prob>F
Model	2	0.00236	0.00118	0.17591	0.84676
Error	3	0.02016	0.00672		
Total	5	0.02253			

Null Hypothesis: The means of all levels are equal.
Alternative Hypothesis: The means of one or more levels are different.
At the 0.05 level, the population means are not significantly different.